THE UNIVERSITY OF WARWICK

Library Declaration and Deposit Agreement

1. STUDENT DETAILS

Please complete the following:

Full name: ……

University ID number: ……

2. THESIS DEPOSIT

2.1 I understand that under my registration at the University, I am required to deposit my thesis with the University in BOTH hard copy and in digital format. The digital version should normally be saved as a single pdf file.

2.2 The hard copy will be housed in the University Library. The digital version will be deposited in the University's Institutional Repository (WRAP). Unless otherwise indicated (see 2.3 below) this will be made openly accessible on the Internet and will be supplied to the British Library to be made available online via its Electronic Theses Online Service (EThOS) service.
[At present, theses submitted for a Master's degree by Research (MA, MSc, LLM, MS or MMedSci) are not being deposited in WRAP and not being made available via EthOS. This may change in future.]

2.3 In exceptional circumstances, the Chair of the Board of Graduate Studies may grant permission for an embargo to be placed on public access to the hard copy thesis for a limited period. It is also possible to apply separately for an embargo on the digital version. (Further information is available in the *Guide to Examinations for Higher Degrees by Research*.)

2.4 *If you are depositing a thesis for a Master's degree by Research, please complete section (a) below. For all other research degrees, please complete both sections (a) and (b) below:*

(a) Hard Copy

I hereby deposit a hard copy of my thesis in the University Library to be made publicly available to readers (please delete as appropriate) EITHER immediately OR after an embargo period of ……..... months/years as agreed by the Chair of the Board of Graduate Studies.

I agree that my thesis may be photocopied. YES / NO (*Please delete as appropriate*)

(b) Digital Copy

I hereby deposit a digital copy of my thesis to be held in WRAP and made available via EThOS.

Please choose one of the following options:

EITHER My thesis can be made publicly available online. YES / NO (*Please delete as appropriate*)

OR My thesis can be made publicly available only after…..[date] (Please give date)
YES / NO (*Please delete as appropriate*)

OR My full thesis cannot be made publicly available online but I am submitting a separately identified additional, abridged version that can be made available online.
YES / NO (*Please delete as appropriate*)

OR My thesis cannot be made publicly available online. YES / NO (*Please delete as appropriate*)

3. GRANTING OF NON-EXCLUSIVE RIGHTS

Whether I deposit my Work personally or through an assistant or other agent, I agree to the following:

Rights granted to the University of Warwick and the British Library and the user of the thesis through this agreement are non-exclusive. I retain all rights in the thesis in its present version or future versions. I agree that the institutional repository administrators and the British Library or their agents may, without changing content, digitise and migrate the thesis to any medium or format for the purpose of future preservation and accessibility.

4. DECLARATIONS

(a) I DECLARE THAT:

- I am the author and owner of the copyright in the thesis and/or I have the authority of the authors and owners of the copyright in the thesis to make this agreement. Reproduction of any part of this thesis for teaching or in academic or other forms of publication is subject to the normal limitations on the use of copyrighted materials and to the proper and full acknowledgement of its source.

- The digital version of the thesis I am supplying is the same version as the final, hard-bound copy submitted in completion of my degree, once any minor corrections have been completed.

- I have exercised reasonable care to ensure that the thesis is original, and does not to the best of my knowledge break any UK law or other Intellectual Property Right, or contain any confidential material.

- I understand that, through the medium of the Internet, files will be available to automated agents, and may be searched and copied by, for example, text mining and plagiarism detection software.

(b) IF I HAVE AGREED (in Section 2 above) TO MAKE MY THESIS PUBLICLY AVAILABLE DIGITALLY, I ALSO DECLARE THAT:

- I grant the University of Warwick and the British Library a licence to make available on the Internet the thesis in digitised format through the Institutional Repository and through the British Library via the EThOS service.

- If my thesis does include any substantial subsidiary material owned by third-party copyright holders, I have sought and obtained permission to include it in any version of my thesis available in digital format and that this permission encompasses the rights that I have granted to the University of Warwick and to the British Library.

5. LEGAL INFRINGEMENTS

I understand that neither the University of Warwick nor the British Library have any obligation to take legal action on behalf of myself, or other rights holders, in the event of infringement of intellectual property rights, breach of contract or of any other right, in the thesis.

Please sign this agreement and return it to the Graduate School Office when you submit your thesis.

Student's signature: .....…… Date: .....

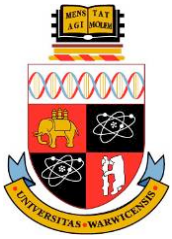

Regulation of Clb1 during meiosis in *Saccharomyces cerevisiae*

By Katherine Louise Tibbles

A thesis submitted to the University of Warwick in partial fulfilment of the requirements of the degree of Doctor of Philosophy

Systems Biology DTC, Warwick University

Submitted: August 2013

Supervisors Dr Prakash Arumugam – Life Sciences, Warwick University

Prof. Bela Novak – Dept of Biochemistry, Oxford University

Table of contents

List of Illustrations

List of Tables

List of Equations

Acknowledgements

First I would like to thank my first supervisor Dr Prakash Arumugam. Prakash has provided advice, encouragement and support as well as scientific training. I am also thankful to the members of the Arumugam Group for the discussions and lab meetings, and the Millar group for assistance and advice especially regarding the microscopy. I would like to thank the members of my thesis committee, Dr Jonathan Millar, Dr Till Bretschneider, and Dr Jacob Dalgaard for their help in improving the project and improving my approach as a scientist.

I am thankful to my second supervisor Prof. Bela Novak and Dr Vinod Palakkad Krishnanunni of Novak's group, for advice and suggestions in dealing with the modelling work. I am thankful to Dr Mirela Domijan for her great patience and helpful discussions in this area.

I would like to thank my friends and housemates for being supportive and understanding as I disappeared into the work. Last but not least, I am hugely indebted to my family for their support and encouragement in this endeavour and in everything else. I would especially like to thank my parents who supported me during the writing up stages and encouraged me at every step.

Declaration of inclusion

All the results presented in this work were obtained by the author, Katherine Tibbles, under the supervision of Dr Prakash Arumugam, unless otherwise stated. None of the work has been submitted for any other degree. Katherine Tibbles was funded by BBSRC and EPSRC via the Warwick University Systems Biology Department.

Parts of this thesis have been published in the following publication:

Part of Chapter 6:

Gary W. Kerr, Sourav Sarkar, Katherine L. Tibbles, Mark Petronczki,
Jonathan B.A. Millar & Prakash Arumugam (2011) Meiotic nuclear divisions in budding yeast require PP2ACdc55-mediated antagonism of Net1 phosphorylation by Cdk, Journal of Cell Biology 193(7): 1157-1166.

Parts of this thesis are submitted for publication in the following report currently under review:

Work in Chapters 3 and 5:

Katherine Louise Tibbles, Bela Novak, and Prakash Arumugam - CDK-dependent nuclear localization of B-cyclin Clb1 promotes FEAR activation during meiosis I in budding yeast.

Abstract

Meiosis is a specialised form of cell division in which diploid cells divide to form four non-identical spores containing half the genetic complement of the parent. During this cell division program, much of the usual machinery regulating cell division is put to alternate use to allow the cells to undergo an extra round of division without an intervening phase of DNA synthesis. In particular, the end of the first division, meiosis I, must be regulated differently than the end of the mitotic division. We used the model organism *Saccharomyces cerevisiae* to determine some of these differences in regulation.

The cell division program is driven by the sequential association of cyclins with the CDK (cyclin dependent kinase), leading to waves of kinase activity. Exit from mitosis requires the downregulation of CDK activity, and is coordinated by two signalling networks, the FEAR (Cdc14 Early Anaphase Release) network and the MEN (Mitotic Exit Network). Both networks initiate the release of the phosphatase Cdc14 from its inhibitor, Net1, to counter CDK activity. Exit from meiosis I similarly relies on Cdc14 activity, but is driven only by the FEAR network.

Experimental results showed that the phosphorylation state and subcellular localisation of the meiotic cyclin, Clb1, are altered in meiosis I. We investigated this relationship and aimed to determine the kinase responsible. We used modelling techniques to explore several rationales for the specific regulation of Clb1. We examined the functional significance of Clb1 localisation, using localisation mutants, and made an investigation into Cdc14 release in meiosis I.

List of Abbreviations

β-ME	β-mercaptoethanol
β-GP	β-glycerophosphate
ACS	ARS consensus sequence
APC	Anaphase promoting complex
ARS	Autonomously replicating sequence
BSA	Bovine serum albumin
CAK	CDK activating kinase
CDK	Cyclin Dependent Kinase
CKI	CDK inhibitor
DAPI	4'-6-diamidino-2-phenylindole
DNA	Deoxyribonucleic acid
EDTA	Ethylene diamine tetraacetic acid
EGTA	Ethylene glycol tetraacetic acid
FEAR	Cdc14 early anaphase release
FITC	Fluorescein isothiocyanate
GFP	Green fluorescent protein
HA	Haemagglutinin
HEPES	4-(2-hydroxylethyl)-1-piperazineethanesulfonic acid
MBF	MCB binding factor
MCB	MluI cell cycle box
MEN	Mitotic exit network
MSE	Middle sporulation element
1-NA-PP1	1-(1,1-dimethylethyl)-3-(1-naphthalenyl)-1H-pyrazolo[3,4-d]pyrimidin-4-amine
1-NM-PP1	1-(1,1-dimethylethyl)-3-(1-naphthalenylmethyl)-1H-pyrazolo[3,4-d]pyrimidin-4-amine
ORC	Origin recognition complex
PBS	Phosphate buffered saline
PCR	Polymerase Chain Reaction
PEI	Poly(ethyleneimine)
RNA	Ribonucleic acid
SAC	Spindle assembly checkpoint
SBF	SCB-binding factor
SCB	Swi4-Swi6 regulated cell cycle boxes
SCE	Sodium citrate EDTA solution
SCF	Skp, Cullin, F-box containing complex
SDS	Sodium dodecyl sulphate
SPOC	Spindle position orientation checkpoint
TAP	Tandem affinity purification
TCA	Trichloroacetic acid
TE	Tris EDTA solution
TEV	Tobacco etch virus
Tris	Tris(hydroxymethyl)aminomethane
YNB	Yeast Nitrogen Base

1 Introduction

1.1 The cell cycle and meiosis

All life depends on the ability of one cell to divide into two cells. To achieve this, the cell must duplicate its contents and partition them into two volumes, which separate to form the daughter cells. In eukaryotes, this is achieved by the mitotic cell cycle. Most cell contents can be approximately doubled over the growth periods. However, the genome must be precisely replicated and split. Missegregated or unreplicated chromosomes would lead to aneuploid cells, which can be lethal to the daughter cells, and is associated with cancer (Nowak et al., 2002; Pellman, 2007).

In sexually reproducing organisms, a specialised cell cycle is required to halve the genetic complement of the cells, forming a haploid cell in preparation for combination with the genome of another haploid cell. This is meiosis. In this process, the chromosomes of a diploid cell are precisely duplicated, reshuffled by crossovers, and split into four haploid nuclei. Disruptions in this process in humans can lead to aneuploidy and are associated with birth defects, such as Down syndrome (Hassold and Hunt, 2001).

1.2 Cell cycle regulation

Cell cycle controls are widely conserved across animal and fungal cells, so insight into the cell cycle from simple organisms, such as yeast, can be applied to mammalian cells (Nurse, 1990). Much of the current knowledge of the mitotic cell cycle has been elucidated from studies in budding and fission yeast, frog embryonic cells and sea urchin embryonic cells, as well as cultured human cells.

These studies have led to detailed working computational models of the mitotic cell cycle.

The meiotic cell cycle is less well understood. It is known that much of the same machinery is used in both mitosis and meiosis, and many meiosis-specific attributes of the regulation have been noted (Perez-Hidalgo et al., 2007). Due to the similarities between the cycles, and the more comprehensive information on mitosis, it is helpful to consider the mitotic cell cycle before moving on to meiosis.

1.2.1 Summary of Mitosis

The mitotic cell cycle results in two daughter cells that are genetically identical to the mother cell. In single celled organisms, mitosis allows proliferation in good conditions; in multicellular organisms, mitotic division produces the majority of the cells that constitute the organism's body.

The cell must first replicate its contents, and then divide them equally into two regions before separating into two cells, genetically identical to the initial cell, to resume the cycle. The molecular machinery to achieve this is complex, but the order of events is conserved. Most cellular components can fluctuate in number and can be multiplied continuously throughout the cycle, but the cell must precisely maintain the chromosomes down the generations, duplicating DNA exactly once per cycle. Mitotically dividing cells must, therefore, strictly alternate DNA synthesis and nuclear division to maintain ploidy (the correct number of sets of chromosomes in the cell). The cell must also divide at the same rate as the doubling of its mass. Otherwise, cells would increase or decrease in size at each division.

The mitotic cycle of eukaryotic cells begins in interphase (Figure 1-1), during which the chromosomes are uncondensed. Interphase consists of three stages. G1 is the first stage, a gap phase in which the cells grow, take account of their conditions and environment, and commit to division. The following stage, S-phase, consists of DNA synthesis. This is followed by G2, a second gap phase. The cell then enters the mitotic division.

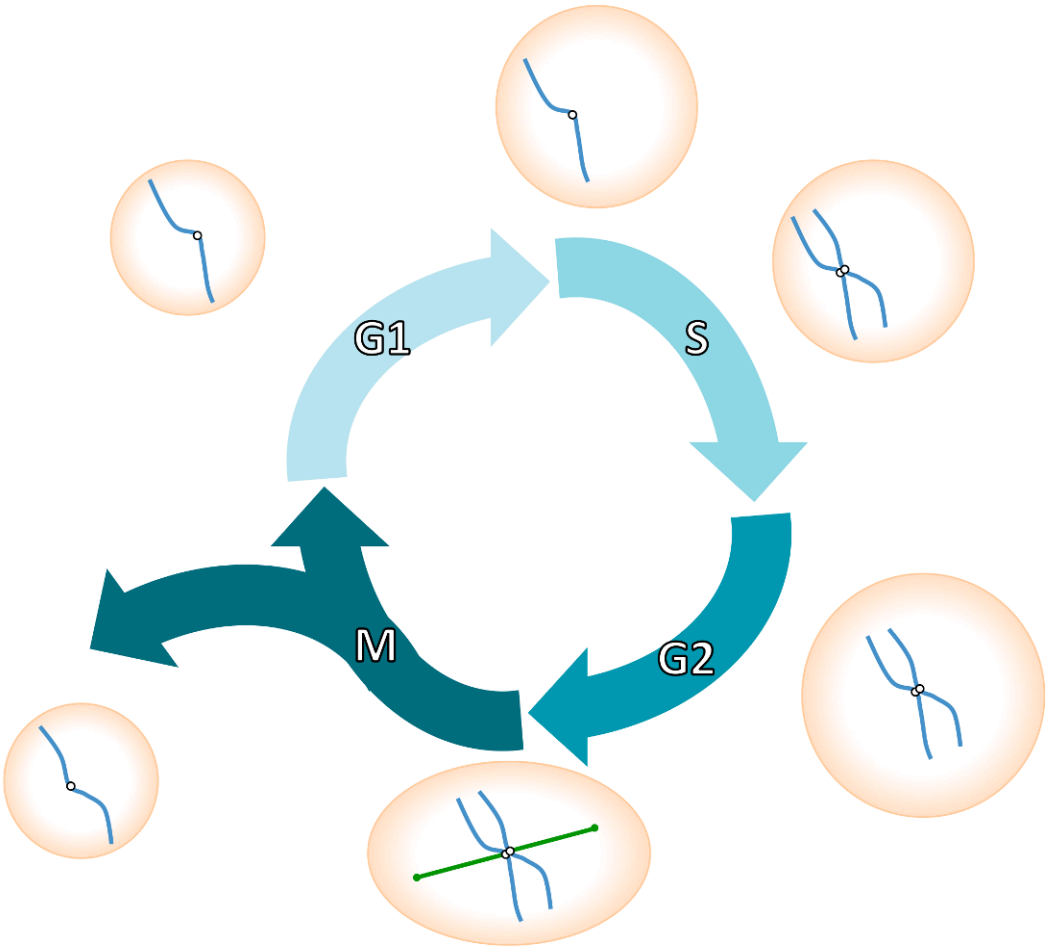

Figure 1-1 ***Summary of eukaryotic mitosis.*** *The cell starts at G1, the first gap stage. During S phase, DNA is replicated. There is a second gap stage, G2, before the cell enters mitosis and divides.*

The stages of the mitotic division were recognised in the late 1800s by Flemming (Paweletz, 2001), using light microscopic viewing of dividing cells and the movement of the condensed, stained chromosomes. Mitosis is named for the "little thread" form that the chromosomes take as they condense in the first stage, prophase. In metaphase, the chromosomes are lined up in the middle of the cell on a structure of microtubules called the spindle. The separation of the chromosomes to opposite sides of the cell is known as anaphase. This is followed by telophase, in which the cell physically divides and the chromosomes decondense. At this point, the two daughter cells re-enter G1, or can enter a dormant state, G0 (Morgan, 2007).

1.2.2 Summary of meiosis

The meiotic program is entered into by diploid cells in response to external signals. In metazoans, the signal is from other cells, coordinating the

production of gametes from progenitor cells in preparation for sexual reproduction. In single-celled organisms, meiotic entry requires environmental signals (Perez-Hidalgo et al., 2007). For example, in budding yeast, a lack of both a nitrogen source and a respirable carbon source triggers meiosis in cells containing both mating type genes (Kassir and Simchen, 1991). The end points of meiosis are resilient spores, which can lie dormant until conditions improve.

The meiotic cell cycle begins in G1, and proceeds in a similar way to mitosis, entering S phase to replicate its DNA. However, in a meiotic cycle, the M phase contains two consecutive rounds of chromosome segregation, resulting in four haploid cells. In budding yeast, meiosis ends in the formation of tough spore coats and the protective ascus of the spores (Figure 1-2).

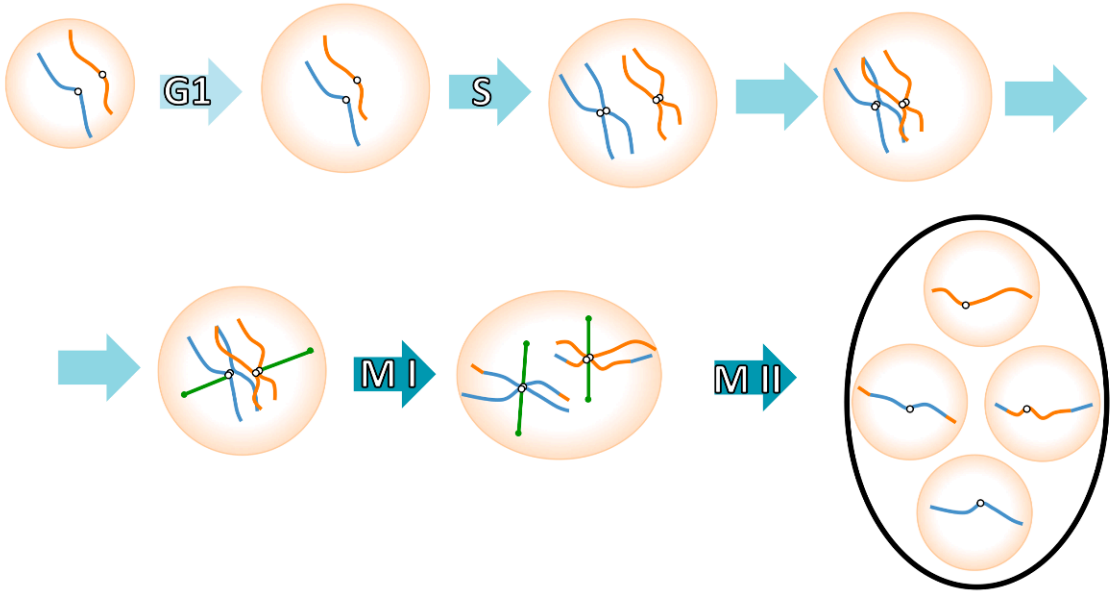

Figure 1-2 ***Summary of meiosis.*** *Cells begin in G1 and then undergo DNA synthesis in S phase as usual. S phase is longer, probably to account for meiosis specific processes that result in crossover formation. Crossover are resolved and the cell undergoes two divisions, one reductional and one equational. In Saccharomyces cerevisiae, this results in four spores, enclosed in an ascus.*

As in mitosis, meiosis requires DNA replication and division. Unlike mitosis, the first division of meiosis must be reductional rather than equational (splitting homologous chromosomes rather than sister chromatids). The cell must then undergo a second round of nuclear division (equational), without an intervening round of DNA replication.

This introduction will explore how the regulation of meiosis achieves these aims, in contrast to the regulation of mitosis.

1.3 Regulation of mitosis in budding yeast

The order of events of the cell cycle must be maintained, despite fluctuations in the environment, stochastic variation, and other confounding factors that a cell may expect throughout growth.

The cell cycle is driven by cyclin-dependent kinase (CDK) activity (Nasmyth, 1993). The importance of this protein in the cycle is conserved across all eukaryotes. The cell cycle initiates from a state of low CDK activity in G1. Through S-phase, G2 and M-phase, CDK activity increases. CDK activity acts as the driving signal, triggering the processes of the mitotic cycle: DNA replication, spindle assembly, and nuclear division. At mitotic exit, CDK activity is sharply reduced, by both inhibition and cyclin degradation, and the cell re-enters the G1 state.

1.3.1 CDK and cyclins

CDK is a serine/threonine kinase, a catalytic subunit whose activity is dependent on the presence of the regulatory subunits called cyclins (Nasmyth, 1993). Originally identified by their distinctive expression profile, cyclins appear and disappear over the cell cycle(Evans et al., 1983). Now sequence identity can be used to classify these proteins (Morgan, 2007). Cyclins control the substrate specificity, localisation and inhibitor-sensitivity of the catalytic subunit.

Cyclin levels are controlled by expression and by the activity of ubiquitin ligases APC (Anaphase Promoting Complex) and SCF (Skp, Cullin, F-box complex), which target the cyclins for degradation (Peters, 1998, 2002). CDK activity is also controlled by regulatory phosphorylation of the catalytic subunit, and by the presence of stoichiometric CDK inhibitors (Morgan, 1995). The apparent CDK activity experienced by the cell can also be altered by the activity of CDK-counteracting phosphatases (Bouchoux and Uhlmann, 2011; Drapkin et al., 2009). This activity is another point of input for regulation of the cycle.

Saccharomyces cerevisiae has nine cyclins, whose role is to activate the cell cycle CDK, Cdc28 (Andrews and Measday, 1998). The G1 cyclins, Cln1-Cln3, are expressed in the G1/S phase. B-type cyclins Clb5 and Clb6 follow, and are responsible for S phase, with roles during mitosis in spindle formation. Clb1,

Clb2, Clb3, and Clb4 dominate through mitosis (Figure 1-3). In higher eukaryotes, there are multiple cyclins and multiple CDK subunits, fulfilling the same roles.

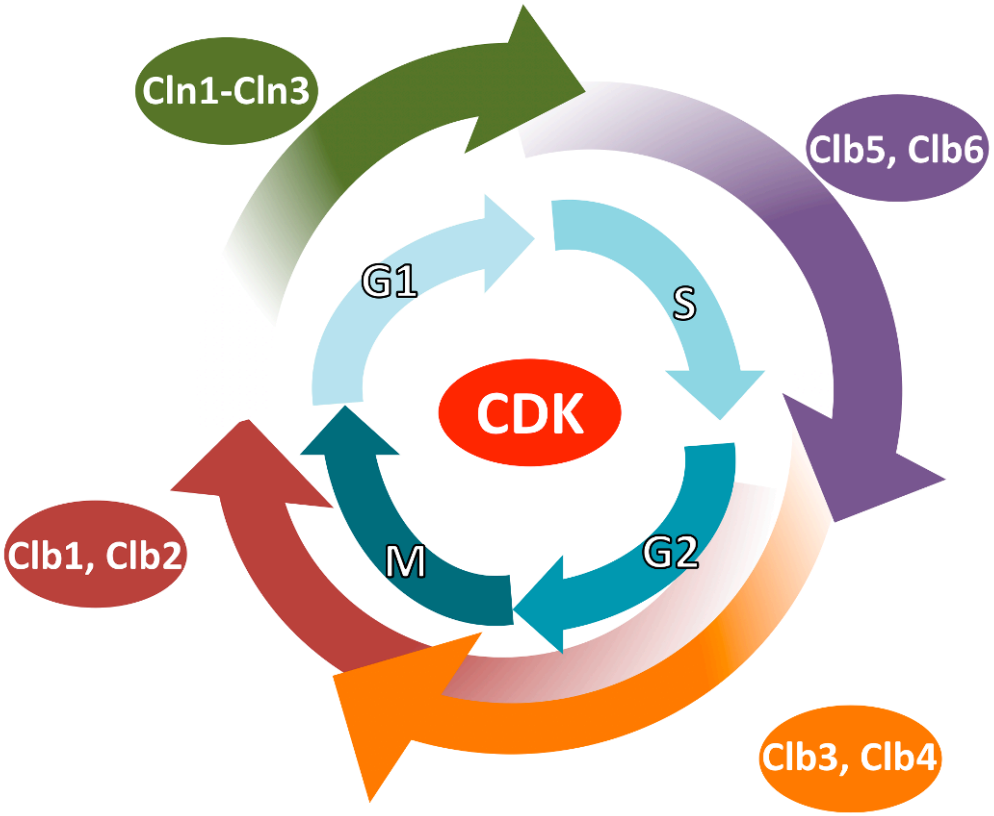

Figure 1-3 ***Cyclin-CDK activity over the mitotic cell cycle in Saccharomyces cerevisiae****. Cln1-Cln3 are expressed during G1, Clb5 and Clb5 expression is triggered at the start of S-phase, and Clb1, Clb2, Clb3 and Clb4 are expressed during mitosis.*

To ensure the success of the cell cycle, advancement can be halted at certain stages by checkpoints (Hartwell and Weinert, 1989). These are surveillance mechanisms that monitor the progress of the cell, and prevent the cell moving to the next stage unless a specific condition is met. The checkpoints police the cell cycle progress in response to incomplete replication during S phase (Weinert et al., 1994), or DNA damage at G2 (Longhese et al., 1998), and the spindle assembly checkpoint and spindle orientation checkpoint ensure that nuclear division would be successful (Caydasi and Pereira, 2012; Rudner and Murray, 1996), more detail in Section 1.3.4.

1.3.2 Initiation of the mitotic cycle in budding yeast

The cycle begins with the cell in a G1 state. At this point, although Cdc28 is present, it is mostly inactive. B-type cyclins are absent due to the activity of the

ubiquitin ligase APC, bound with the activator Cdh1, in targeting them for degradation (Amon et al., 1994). The stoichiometric Clb-CDK inhibiter Sic1 is active and highly expressed, maintaining the cell in a low Clb-CDK state.

To enter the cycle, the cell passes through the first checkpoint, known as START in yeast, and the restriction point in mammals. After passing through START, the cell is committed to S-phase and division, and can no longer be arrested by mating pheromones (Hartwell et al., 1974; Hereford and Hartwell, 1974). Passage through START is cell-size dependent, and is blocked by starvation conditions, or in haploid cells, by the presence of the opposing mating pheromone.

Passage through START is instigated by the G1 cyclin Cln3. Unlike other cyclins, Cln3 is expressed independently of cell cycle stage, and is unstable (Cross and Blake, 1993). This means it can act as a size control mechanism, as its concentration in the nucleus will depend on the rate of translation, which depends, in turn, on the number of ribosomes in the cell. This is a proxy for cell size. As the cell grows and Cln3-CDK activity rises, it activates expression of *CLN1* and *CLN2* by activating the SBF (Swi4,6-dependent Cell-cycle Box (SCB) binding factor) transcription factor (Swi4-Swi6) (Dirick et al., 1995; Stuart and Wittenberg, 1995). This transcription factor also activates *CLN3* expression in a positive feedback loop (Amon et al., 1993; Cross and Tinkelenberg, 1991).

Cln-CDK activity is not inhibited by Cdh1-directed APC or by Sic1, but does result in the phosphorylation of both proteins. The phosphorylation directs Cdh1 nuclear export and Sic1 destruction via the SCF (Jaquenoud et al., 2002; Verma et al., 1997; Zachariae et al., 1998; Zhou et al., 2003). This removes the inhibition that maintains the low CDK G1 state, permitting Clb-CDK activity to emerge. The G1 cyclins remain present until Clb-CDK activity represses their expression in G2 (Amon et al., 1993).

Cln3-CDK activates a second transcription factor, MBF (Mlu1 Cell-cycle Box(MCB) binding factor) (Swi6-Mbp1). MBF targets include the S-phase cyclins CLB5 and CLB5 and a number of DNA replication proteins. Passage through START is characterised by a rapid increase in cyclin-CDK activity, the emergence of the bud (Cvrckova and Nasmyth, 1993), and the expression of genes in the G1/S regulon in preparation for S-phase (Cross, 1995).

1.3.3 S-phase and DNA replication

Once Clb-CDK activity is established, Cln-CDK activity decreases (Amon et al., 1993), but Clb-CDK activity is sufficient to maintain the inhibition of Sic1. Rising Clb5- and Clb6-CDK activity initiates DNA replication at a series of points on the chromosomes, known as origins of replication. In *Saccharomyces cerevisiae*, the ORC is found at the origins throughout the cycle (Diffley et al., 1994), while other components, Cdc6, Cdt1 and the helicase complex Mcm2-7, are recruited to the ORC during G1 (Diffley, 2004). The assembly of these components means the complex is licensed for replication, and is now referred to as the pre-replicative complex (pre-RC). Further components are recruited at the start of S-phase to form the initiation complex (IC). This further assembly is dependent on both CDK and DDK (Cdc7-Dbf4) (Sheu and Stillman, 2006; Zou and Stillman, 1998). DNA replication is activated by S-phase cyclin phosphorylation of the proteins of the IC (Epstein and Cross, 1992; Kuhne and Linder, 1993; Schwob and Nasmyth, 1993). This initiates DNA unwinding and DNA replication then begins, known as origin firing.

1.3.4 M-phase

Of the four mitotic cyclins, Clb3 and Clb4 are expressed first, Clb1 and Clb2 are expressed later (Fitch et al., 1992). The mitotic cyclins control entry into mitosis, and are required for Spindle Pole Body (SPB) separation, changes in chromosomal structure, spindle assembly, spindle elongation and control of metaphase-anaphase transition (Andrews and Measday, 1998; Rahal and Amon, 2008a).

In mammalian cells, the nuclear envelope breaks down on entry to mitosis, allowing the spindle access to the chromosomes. The spindle microtubules emanate from the centrosomes and bind to kinetochores. In budding yeast, the spindle is constructed inside the nucleus, emanating from SPBs embedded in the nuclear membrane (Winey and O'Toole, 2001) and there is a single microtubule attachment site per kinetochore (Peterson and Ris, 1976). The duplicated chromatids are still held in pairs by cohesin, a ring-like protein complex (Michaelis et al., 1997; Morgan, 2007). As paired kinetochores become bound by microtubules from opposing SPBs, they are held under tension. At this

point the cell is in metaphase, with short spindles and condensed chromosomes. Progress through anaphase requires two checkpoints to be passed: the spindle assembly checkpoint (SAC) and the spindle position orientation checkpoint (SPOC).

The SAC ensures that all kinetochores are bound and tension (Biggins and Murray, 2001; Nicklas and Koch, 1969; Varetti and Musacchio, 2008), confirming that paired chromosomes are attached to opposite poles. This amphitelic attachment (Figure 1-4) is required to ensure that the chromatids are separated appropriately once the cohesin is degraded, one of each pair going to each daughter cell.

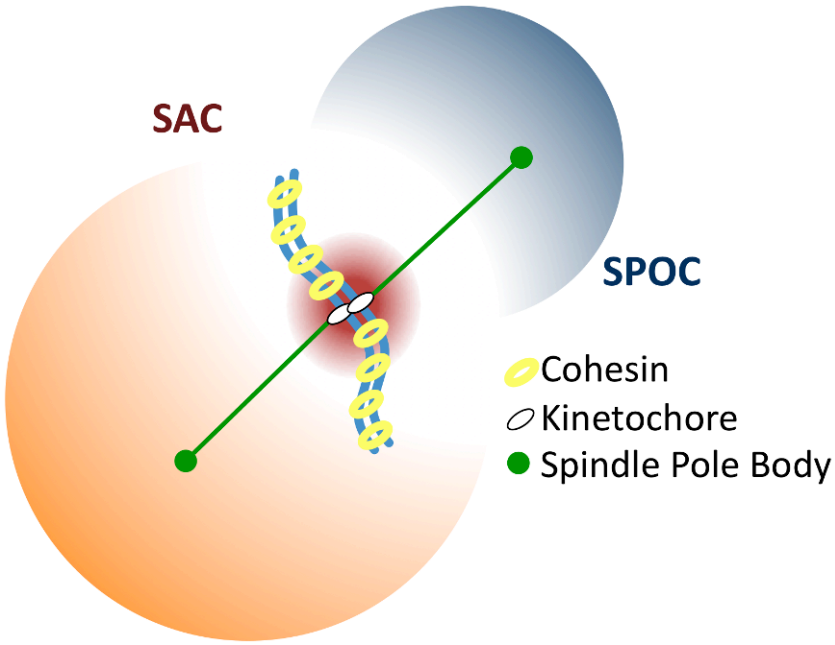

Figure 1-4 ***Spindle Assembly Checkpoint and Spindle Position Orientation Checkpoint in budding yeast.*** *The SAC detects the attachment and tension of kinetochores to microtubules, ensuring that the microtubules are attached to opposing spindle pole bodies. The SPOC ensures that the daughter SPB has entered the daughter cell. These conditions have to be met before the cell enters anaphase.*

The SAC senses kinetochores that are unbound or not under tension, and acts to inhibit Cdc20, preventing the activation of the APC (Hwang et al., 1998; Rudner and Murray, 1996). Once the SAC is satisfied, Cdc20 is able to activate the APC. This triggers activation of Esp1 (separase) via degradation of its inhibitor, Pds1 (securin). Esp1 is a protease whose role is to proteolyse a subunit of the cohesin ring, allowing the chromatids to separate (Uhlmann et al., 1999; Uhlmann et al., 2000). The newly detached chromatids are separated by the

elongating spindle, into two separate nucleic masses in anaphase. The SPOC acts to ensure that each cell resulting from the division has one of the new nuclei (Bardin et al., 2000). In budding yeast, this means that one of the nuclei ends up in the bud. The SPOC requires that an SPB enter the daughter cell, making certain that the two nuclei will end up separated in the two resulting cells. Once this occurs, the SPOC triggers the activation of the Mitotic Exit Network (MEN), which causes sustained, cytoplasmic Cdc14 release, promoting activation of the APC and completing mitotic exit (Smeets and Segal, 2002). The role of the SPOC in MEN activation is described in more detail in the following section.

1.3.5 Mitotic exit and resetting to G1

During mitosis, CDK activity reaches a maximum due to high levels of the B-type cyclins. This state is self-sustaining as the inhibitors of CDK, Cdh1 and Sic1, are themselves inhibited by CDK phosphorylation (Jaquenoud et al., 2002; Knapp et al., 1996; Verma et al., 1997; Zachariae et al., 1998). This is the second stable state of the CDK system. The same mutual inhibition would maintain the first stable state, the low Clb-CDK activity of G1, without the intervention of the Clns. Transition from one state to the other requires an intervention to break the feedback loops (Figure 1-5). In mitotic exit, the abrupt decrease in CDK activity must be instigated by the Exit Phosphatase, Cdc14 (Stegmeier et al., 2004; Visintin et al., 1998). Cdc14 allows the G1 stable state to assert itself.

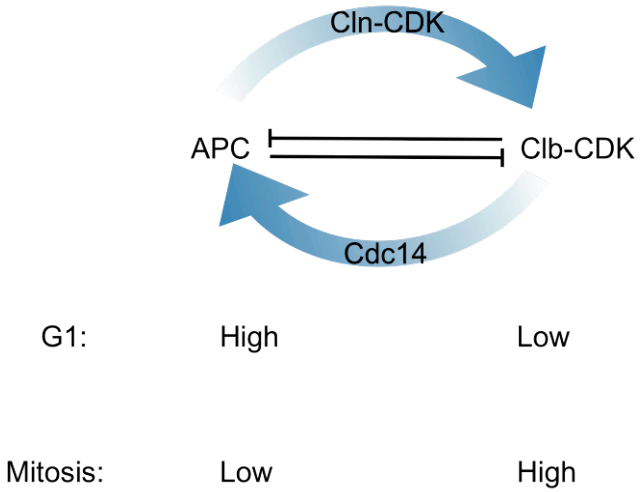

Figure 1-5 ***Mutual inhibition of inhibitors/APC and CDK activity.*** *The mutual inhibition creates a system with two stable states. Intervention is required to move between them. To break the inhibition of CDK by the CKIs (APC^{Cdh1}) and allow Clb-CDK activity to rise, Starter Kinase Cln-CDK is*

required. To break the inhibition of CKI by the high Clb-CDK levels, Exit Phosphatase Cdc14 is required.

Cdc14 is sequestered in the nucleolus for most of the cell cycle by its inhibitor Net1 (also referred to as Cfi1) (Visintin et al., 1999). Release is initiated during anaphase by the phosphorylation of Net1 by Clb-CDK (Azzam et al., 2004), and countered by the phosphatase $PP2A^{Cdc55}$, which maintains Net1 in a dephosphorylated state (Wang and Ng, 2006; Yellman and Burke, 2006). Cdc14 release during mitotic exit is coordinated by two regulatory networks, known as the Cdc14 Early Anaphase Release network (FEAR) (Stegmeier et al., 2002) and the Mitotic Exit Network (MEN) (Jaspersen et al., 1998).

1.3.5.1 Triggering Anaphase

Cdc20 is activated by CDK phosphorylation (Rudner and Murray, 2000) and goes on to bind and activate the APC, and trigger anaphase (Visintin et al., 1997). Cdc20 is also inhibited by an active SAC (Figure 1-4). The active APC^{Cdc20} triggers anaphase. Cdc20 targets the APC to two important substrates, the Esp1-inhibitor Pds1 and the cyclins (Shirayama et al., 1999; Thornton and Toczyski, 2003). Esp1, released from inhibition, triggers chromosome separation by its protease activity on cohesin. Cdc20 initiates the cyclin degradation that leads to mitotic exit, but is activated itself by CDK phosphorylation. Cdc20 therefore leads to its own inactivation and cannot maintain inhibition of CDK. In order to complete mitotic exit, CDK inhibition by the CKIs (in particular Sic1) must be triggered to initiate the mutual inhibition that maintains the lower CDK state (Lopez-Aviles et al., 2009).

1.3.5.2 The FEAR pathway

The FEAR network involves a group of parallel signalling pathways converging on Cdc14 release from Net1 (Figure 1-6). Esp1 has a non-proteolytic function to trigger the FEAR network. Esp1 acts with Slk19, via Zds1 and Zds2, to inhibit $PP2A^{Cdc55}$ (Lu and Cross, 2009; Queralt and Uhlmann, 2008; Sullivan and Uhlmann, 2003). $PP2A^{Cdc55}$ dephosphorylates Net1, countering phosphorylation by Clb-CDK (Queralt et al., 2006). Cdc5 activity, triggered by CDK (Lowery et al., 2004; Mortensen et al., 2005), contributes to phosphorylation of Net1 (Yoshida and Toh-e, 2002). Downstream of Esp1 and Slk19, phosphorylation of FEAR

component Spo12 inhibits Fob1, a negative regulator of Cdc14 release (Stegmeier et al., 2004; Tomson et al., 2009).

The combined activities of the parallel FEAR pathways, all triggered by Clb-CDK activity, serve to increase the phosphorylation status of Net1 and reduce its ability to bind Cdc14. The result is a nuclear release of Cdc14 (Stegmeier et al., 2002), which, by its dependence on Esp1 activation, occurs simultaneously with chromatid division and the initial APC targeting of cyclins.

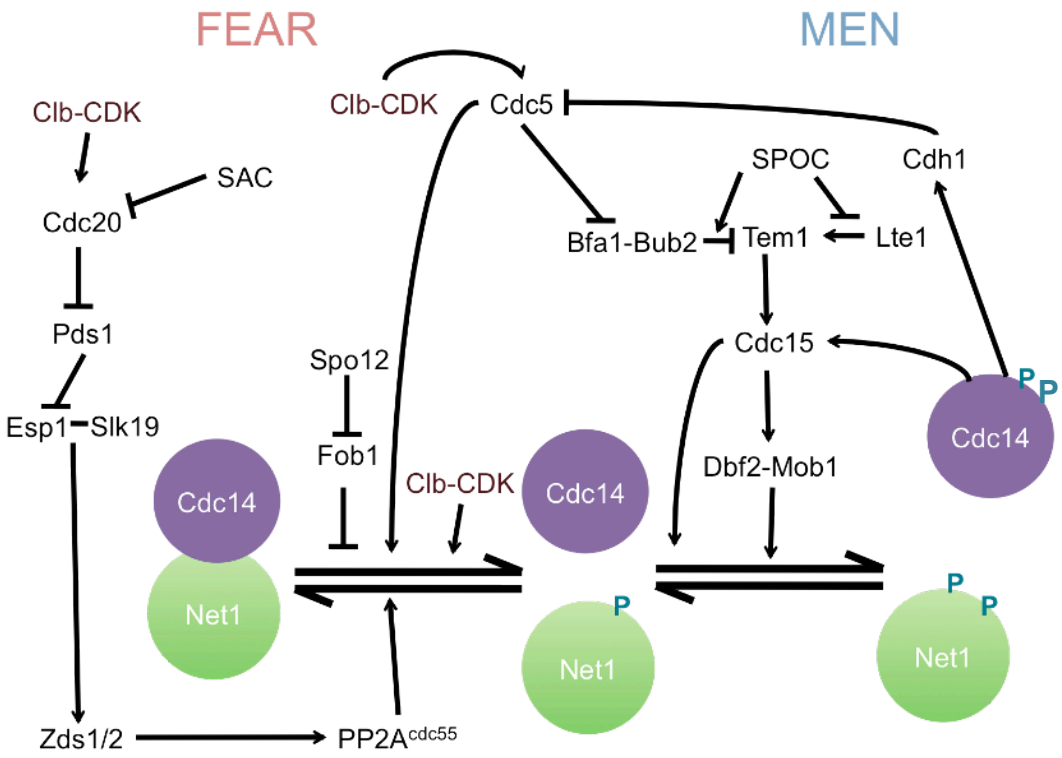

Figure 1-6 ***FEAR and MEN networks*** *The FEAR and MEN networks drive Cdc14 release during anaphase*

However, the FEAR network is incapable of sustaining sufficient Cdc14 release to enter the G1 state. The activation of the FEAR network and phosphorylation of Net1 relies on Clb-CDK activity, which the Cdc14 release and Cdc20 activation begins to counter. Complete downregulation of the Clb-CDK activity requires the MEN (Geymonat et al., 2002a).

1.3.5.3 The Mitotic Exit Network

The Mitotic Exit Network (Figure 1-6) consists of a G-protein activating a kinase cascade leading to the sustained release and nuclear export of the phosphatase Cdc14. The G-protein Tem1 is inhibited by the GTPase Activating

Protein Bub2-Bfa1 (Bardin et al., 2000; Geymonat et al., 2002b), and activated by proximity with the spatially regulated Lte1 (Low Temperature Essential), which may act as the Guanine Exchange Factor (GEF). Lte1 is restricted to the bud cortex, and Tem1 is localised to the daughter SPB (Valerio-Santiago and Monje-Casas, 2011), along with the majority of MEN proteins. This ensures that the network only becomes active when Tem1 and Lte1 are brought into proximity by the movement of the daughter SPB into the bud (Bardin et al., 2000).

There is some doubt as to whether the Lte1 has the function of a G-protein exchange factor, due to results suggesting it does not act as G-protein, and may be involved in determining localisation instead (Geymonat et al., 2009). The G-protein/GAP relationship is still assumed in some literature (Hancioglu and Tyson, 2012). This may be because a role in activating the natural catalytic activity of Tem1 would explain the loss of requirement for Lte1 at warmer temperatures; the innate GTPase activity of Tem1 may be sufficient at these temperatures. Alternatively, Lte1 has been shown to alter localisation of Kin4 (Bertazzi et al., 2011; Falk et al., 2011). Kin4 is a kinase that inhibits MEN function, and is concentrated in the mother cell (Chan and Amon, 2010). Daughter-cell-concentrated Lte1 would prevent Kin4 activity from inhibiting the MEN once the daughter SPB enters the bud. This role of Lte1 has also been incorporated in models (Caydasi et al., 2012).

Activation of Tem1 leads to the activation of a kinase cascade, consisting of Cdc15 (Asakawa et al., 2001) and the Dbf2-Mob1 complex (Mah et al., 2001; Visintin and Amon, 2001). Cdc15 activates the Dbf2-Mob1 complex, which phosphorylates Net1 and Cdc14 (Mohl et al., 2009) (Figure 1-6). Cdc15 is activated by increasingly released Cdc14 in a positive feedback loop (Jaspersen and Morgan, 2000), giving the FEAR-driven Cdc14 release a means to contribute to MEN activation. Dbf2-Mob1 phosphorylation of Cdc14 inactivates the nuclear localisation sequence (NLS) allowing Cdc14 to be exported from the nucleus altogether (Mohl et al., 2009). Phosphorylated Cdc14 can now reach cytoplasmic targets, such as the APC-activator Cdh1, which is cytoplasmic due to phosphorylation-induced export (Jaquenoud et al., 2002; Jaspersen et al., 1999). The polo kinase Cdc5 also has a role in MEN activation, driving Tem1 activation by phosphorylating and inhibiting Bfa1 (Hu et al., 2001). Components of the

MEN: Bub2, Bfa1, Tem1, Cdc15, Dbf2 and Mob1, (Bardin et al., 2000; Cenamor et al., 1999; Pereira et al., 2000; Yoshida and Toh-e, 2001) are found on the daughter SPB. The last essential component of the MEN, the scaffold protein Nud1, is responsible for locating these proteins to the SPB, which is also necessary for the action of MEN in mitotic exit (Valerio-Santiago and Monje-Casas, 2011).

The MEN only becomes active when the daughter SPB enters the bud, and Tem1 on the SPB and Lte1 on the bud cortex are brought into proximity (Bardin et al., 2000). MEN activation is further restricted to the daughter SPB by the kinase Kin4, which is located to the mother cell. Kin4 phosphorylates Bfa1 and inhibits its phosphorylation by Cdc5 (D'Aquino et al., 2005; Maekawa et al., 2007). This restriction of the Mitotic Exit Network is referred to as the Spindle position orientation checkpoint, or SPOC.

1.3.5.4 The roles of FEAR- and MEN- driven Cdc14 release

Dephosphorylation by Cdc14 contributes to the requirements of anaphase and telophase. Cdc14 released by FEAR and by MEN accomplish different tasks. FEAR driven Cdc14 release is sufficient to accomplish rDNA separation (Geil et al., 2008; Stegmeier and Amon, 2004; Sullivan et al., 2004), stabilise the spindle during elongation against spindle breakage (Higuchi and Uhlmann, 2005; Pereira and Schiebel, 2003), and contributes to the activation of MEN, by Cdc15 dephosphorylation (Jaspersen and Morgan, 2000).

FEAR-based Cdc14 release is transient and insufficient for mitotic exit. This Cdc14 release depends on CDK activity, to drive Cdc20 activity to activate Esp1, and to phosphorylate Net1. When CDK activity begins to fall in response to the released phosphatase, the drive to continue the release is lost. Mutants in which the MEN is inactivated, and which therefore rely only on FEAR for Cdc14 release, arrest in mitosis with elongated spindles (Stegmeier et al., 2002).

MEN driven Cdc14 release is required for completion of telophase and mitotic exit, completing the inhibition of Clb-CDK. MEN and Cdc14 have roles in cytokinesis that are independent of CDK regulation. Cdc14 also counters the Cdc5 phosphorylation of Bub2-Bfa1 leading to the eventual termination of the MEN signal (Pereira et al., 2002). In contrast to the FEAR pathway, the MEN

alone is capable of sufficient Cdc14 release to drive a successful mitotic exit. Mutants of the FEAR network will undergo mitosis with only a slight delay (Jensen et al., 2002). Therefore the FEAR network is neither necessary nor sufficient for a successful mitotic exit, whereas the MEN is both.

In its role as the Exit Phosphatase, Cdc14 needs to instigate sustained inhibition of Clb-CDK activity, permitting the cell to enter G1 phase. To fulfil this role, Cdc14 dephosphorylates Clb-CDK inhibitor Sic1 and its transcription factor Swi5, and the APC activator, Cdh1, (Visintin et al., 1998) that targets B-type cyclins for destruction (Zachariae et al., 1998). As these CDK inhibitors (CKIs) escape CDK inhibition and rise, they reduce Clb-CDK activity and establish the initial stable state of the system (Figure 1-5). The CKIs are now dominant and Clb-CDK activity is low. Thus, Cdc14 release is required to trigger the M/G1 transition, but not to maintain it.

Cdc14 has an order of preference in which it removes CDK phosphorylation (Bouchoux and Uhlmann; Bremmer et al., 2012). As the phosphatase activity increases, the ratio of CDK and Cdc14 activities and Cdc14's site preferences lead to sites becoming dephosphorylated in a reproducible order (Bouchoux and Uhlmann, 2011). The order given in Bremmer *et al.* (Bremmer et al., 2012) indicates that proteins involved in spindle stabilisation are dephosphorylated at a lower phosphatase activity than DNA replication proteins and CKIs, whose release from inhibition waits for MEN. This relates to the separate roles of FEAR and MEN driven Cdc14 release.

1.4 Meiosis in budding yeast

The meiotic cell cycle re-uses much of the machinery from mitosis. However, the cell has a different aim to achieve during meiosis: halving of ploidy by an extra division. Specialised regulation and meiosis-specific components exist to achieve this.

1.4.1 Specialised requirements of meiosis

A diploid cell undergoes meiosis to produce four haploid non-identical spores. This has several specialised requirements, summarised below and in Figure 1-7.

1 – recombination – crossovers between homologous chromosomes reshuffle the DNA and maintain tension in kinetochore-mitochondrial attachments despite monopolar attachments (Section **Error! Reference source not found.**)

2 – monopolar attachment – homologous chromosomes are separated in meiosis I rather than sister chromatids. This means the kinetochores on paired sister chromatids must attach to microtubules from the same spindle pole body (Section 1.5.3.4).

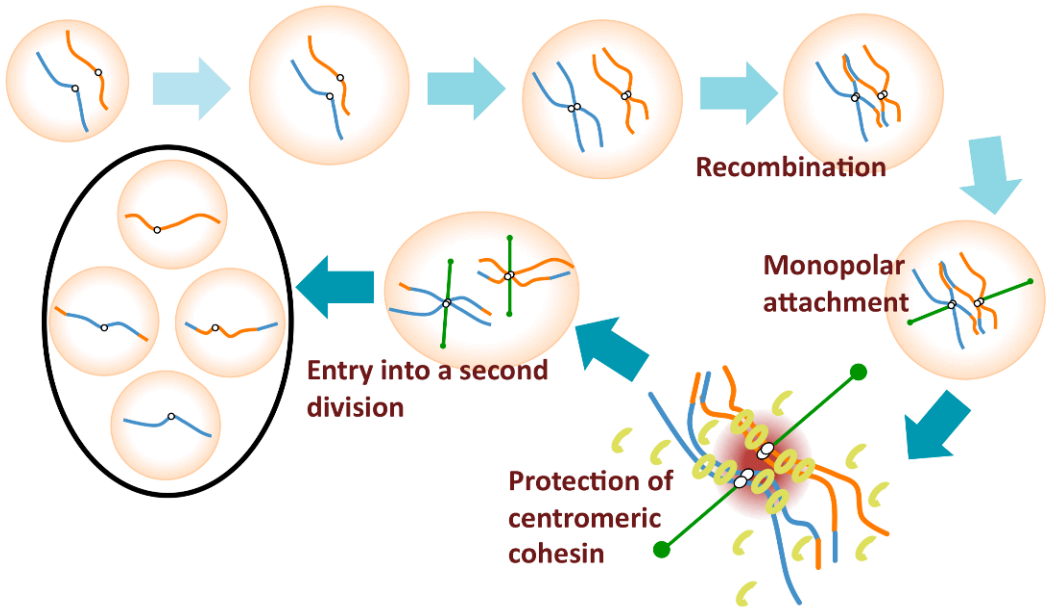

Figure 1-7 ***Four special features of meiosis.*** *The four features highlighted are recombination, monopolar attachment and protection of centromeric cohesin during meiosis I, and the second division, meiosis II.*

3 – protection of cohesin – during meiosis I, pericentromeric cohesin is protected from degradation, maintaining the attachment of paired sister chromatids for the second division (Section 1.5.3.5).

4 – second division – the cell goes on to meiosis II without entering DNA replication (Section 1.5.4.1).

1.5 Regulation of meiosis

1.5.1 Initiation of meiosis

The initiation of the meiotic program occurs before entry into S-phase, when the cell is in the G1 state. For entry into meiosis in *Saccharomyces cerevisiae*, the following genetic and environmental conditions must be met. The

cell must bear both *MATa* and *MATα* alleles, which restricts meiosis to diploid cells. The products of the genes form a dimer whose role is to inhibit the protein Rme1, which is responsible for inhibiting meiosis and promoting mitosis (Covitz et al., 1991). The environment must be depleted of nitrogen and respirable carbon sources, particularly glucose (Honigberg and Purnapatre, 2003), though unfermentable carbon sources are still required as respiration is necessary (Jambhekar and Amon, 2008).

Under these conditions, *IME1* (*i*nitiator of *me*iosis) gene is expressed, encoding a transcription factor responsible for activating expression of early meiosis-specific genes (Kassir et al., 2003). This notably includes Ime2, a CDK-like kinase both specific to, and necessary for, meiosis (Foiani et al., 1996). Therefore, Ime1 initiates the transcriptional program of meiosis. In mitosis, the Cln-CDKs are responsible for initiation of the cycle. However, they are not necessary for meiosis, and in fact suppress it (Colomina et al., 1999). The role of starter kinase is undertaken instead by Ime2, which in turn suppresses the G1 cyclins (Dirick et al., 1998). Ime2 is a Ser/Thr kinase with homology to CDK, but is independent of cyclins for its activity. By phosphorylating Sic1 and Cdh1 (Dirick et al., 1998; Holt et al., 2007), the inhibitors of Clb-CDK activity, Ime2 allows CDK activity to rise and promote entry into meiosis and meiotic S phase.

1.5.2 Premeiotic DNA replication

Pre-meiotic DNA synthesis is initiated in a similar way to that of mitosis and uses the same machinery (Lindner et al., 2002; Ofir et al., 2004) and origins of replication (Collins and Newlon, 1994). However, pre-meiotic S-phase is longer than pre-mitotic S-phase (Williamson et al., 1983) and does not seem to bear the same redundancy in cyclin requirements (See Section1.6).

1.5.3 Meiosis I

Pre-meiotic S-phase and prophase of meiosis take longer than the pre-mitotic equivalents (Williamson et al., 1983). During this time, a number of meiosis-specific processes take place. A meiosis specific cohesin subunit, Rec8, replaces the mitotic cohesin subunit Scc1 during S phase, (Klein et al., 1999) and during prophase, the synaptonemal complex, a protein structure binding

homologous chromosomes, forms between the chromosomes (Smith et al., 2001).

Prophase of meiosis I can be described in four stages: leptotene, zygotene, pachytene and diplotene. In leptotene, chromosomes become more condensed but do not yet associate with homologues. Axial elements form along the sisters (Kim et al., 2010), and in zygotene, chromosomes pair off. The axial elements form the lateral elements of the synaptonemal complex, connected by a central element of transverse filaments.

1.5.3.1 Recombination during prophase

Recombination, the formation of crossovers between homologous chromosomes, is specific to meiosis. This process contributes to the reshuffling of the genetic information, allowing formation of non-identical haploid spores, and also provides tension during first division, permitting accurate reductional division. Recombination requires both CDK and DDK, similarly to DNA replication (Henderson et al., 2006; Wan et al., 2008).

Recombination begins in early prophase, in leptotene (Andersen and Sekelsky, 2010; Karpenshif and Bernstein, 2012). Double- stranded breaks (DSBs) are introduced by Spo11 (Keeney et al., 1997) and the MRX complex (Keeney and Neale, 2006). The breaks then undergo resection and processing by endonucleases to produce 3' overhangs (Manfrini et al., 2010). One of the ssDNA ends can invade the homologous chromosome, annealing to the homologous sequence. This displaces a single-stranded loop of the homologous chromosome. The invading 3' end is extended along the homologous chromosome. The other 3' overhang from the DSB is captured to form a double Holliday Junction (dHJ). On exit from pachytene, the dHJs can be resolved by resolvases forming a crossover (CO) (Figure 1-8) (Allers and Lichten, 2001; Ashton et al., 2011; Cromie and Smith, 2007; Neale and Keeney, 2006; Schwartz and Heyer, 2011).

Not every DSB becomes a crossover. DSBs can also be repaired before resecting happens. Later in the process, the 3' end can be displaced after being extended along the homologous chromosome, leading to synthesis-dependent strand annealing (SDSA) (Allers and Lichten, 2001; Andersen and Sekelsky, 2010; Karpenshif and Bernstein, 2012).

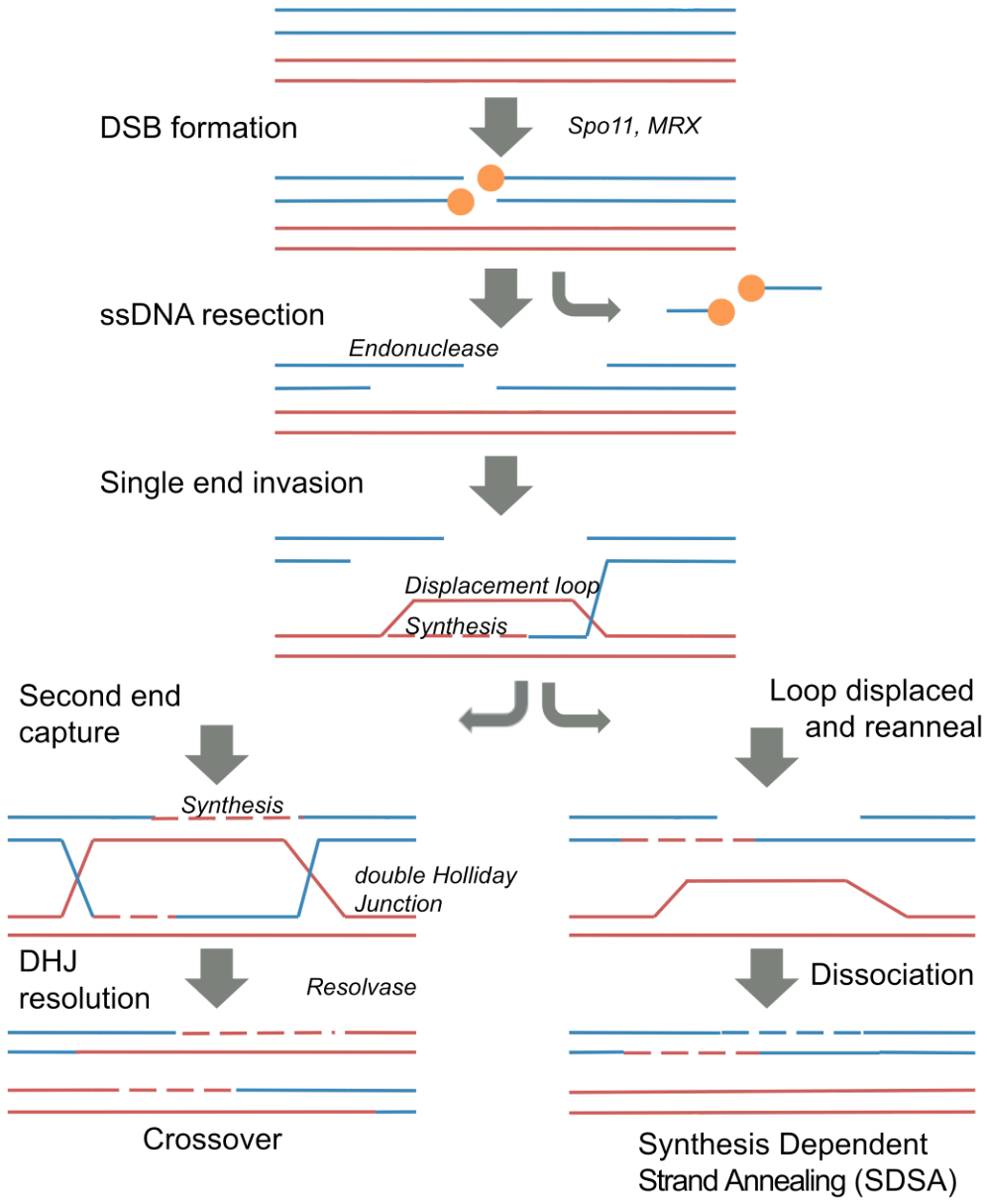

Figure 1-8 ***Meiotic recombination*** *(adapted from Neale and Keeney 2006 (Neale and Keeney, 2006) and Karpenshif and Bernstein 2012(Karpenshif and Bernstein, 2012))*

1.5.3.2 Exit from pachytene

In pachytene, DSBs have been processed into dHJs, and the spindle pole bodies have duplicated, but not been separated. The meiosis-specific recombination checkpoint can arrest the cell in pachytene if recombination is incomplete, by inhibiting the transcription factor Ndt80 (Allers and Lichten, 2001; Hepworth et al., 1998; Lydall et al., 1996; Roeder and Bailis, 2000). As the checkpoint lifts, Ndt80 triggers a wave of gene expression that drives exit from pachytene.

Ndt80 is required for exit from pachytene (Xu et al., 1995); it recognises the Middle Sporulation Element (MSE), triggering the expression of middle meiotic genes, including the cyclins Clb1, Clb3 and Clb4, driving up CDK activity. Ndt80 is opposed by Sum1, a competing transcription factor, with an overlapping footprint to that of Ndt80, but an opposing effect on transcription. Sum1 inhibits the genes Ndt80 would induce. Since the *NDT80* promoter contains the MSE, Sum1 activity directly reduces Ndt80 levels (Marston and Amon, 2004; Pak and Segall, 2002b; Pierce et al., 2003). However, Ime2 inhibits Sum1, allowing Ndt80 to gain ascendancy in meiosis (Shin et al., 2010).

Ndt80 activation triggers the expression of middle meiotic genes (Chu et al., 1998; Hepworth et al., 1998). This is required for the events that signal exit from pachytene and entry into the final stage, diplotene. These are DHJ resolution into COs, synaptonemal complex disassembly, and separation of the spindle pole bodies (Xu et al., 1995). Important Ndt80 targets are Cdc5 and B-type cyclins. Cdc5 seems sufficient for the completion of recombination and the synaptonemal complex disassembly (Sourirajan and Lichten, 2008), and Clbs 1, 3 and 4 undertake to regulate the meiotic divisions (Dahmann and Futcher, 1995; Grandin and Reed, 1993).

1.5.3.3 Commitment to meiosis

At earlier stages of meiosis, resuspension in rich media will allow the cell to return to the mitotic cycle. However, after a certain stage, the cell will continue to complete the process of sporulation despite environmental signals of the availability of nutrients (Friedlander et al., 2006; Ganesan et al., 1958; Simchen, 2009). Cells are able to return to growth after DNA replication and recombination; this is in contrast to commitment to mitosis: cells are committed to mitosis before DNA replication (Hirschberg and Simchen, 1977; Simchen, 2009). Commitment to both meiosis and mitosis coincides with the timing of SPB separation in these processes (Simchen, 2009). Exit from pachytene is an important transition in the regulation of meiotic progression. The expression and activation of Ndt80, and the separation of SPBs, is associated with the commitment to complete meiosis in budding yeast (Winter, 2012).

1.5.3.4 Monopolar attachment

As Clb-CDK activity rises, the spindle forms and another requirement of meiosis must then be fulfilled. The first division of meiosis is reductional. The homologous chromosomes separate, instead of the sister chromatids splitting. To achieve this, the chromosomes must attach to the kinetochore in a monopolar fashion (interacting only with microtubules from one spindle pole body). A protein complex, known as monopolin, is responsible for this arrangement (Petronczki et al., 2006Corbett, 2010 #10257; Rabitsch et al., 2003; Toth et al., 2000). In *Schizosaccharomyces pombe* (fission yeast) this depends on a protein called Moa1 (Yokobayashi and Watanabe, 2005). Crossovers established in prophase between the homologues align them correctly on the meiosis I spindle, and maintain the tension that stabilises kinetochore-microtubule attachment (Marston and Amon, 2004). The spindle assembly checkpoint acts to ensure all kinetochores are bound under tension to microtubules (Malmanche et al., 2006). Then APC/Cdc20 activity is triggered and the cells enter anaphase I.

1.5.3.5 The meiosis I divisions – Protection of pericentromeric cohesin

As in mitosis, the cohesin holding the chromatids together must be proteolysed by the protease Esp1, in order to divide (Buonomo et al., 2000). In anaphase I, however, the cohesin removal does not go to completion. The division is reductional, so the centromeres of the sister chromatids are not separated. The cohesin subunits on the chromosome arms are preferentially targeted for degradation.

During S-phase, the subunit of cohesin that Esp1 targets in mitosis, Scc1, is replaced by the meiosis-specific subunit, Rec8. This substitution is required for the maintenance of centromeric cohesin in anaphase I (Toth et al., 2000). Rec8 degradation by Esp1 is dependent on phosphorylation by Casein Kinase and DDK (Katis et al., 2010). Centromeric cohesin is protected from proteolysis by Esp1 by dephosphorylation. This protection requires Sgo1 (Katis et al., 2004a; Kitajima et al., 2004) and Spo13 (Katis et al., 2004b). Sgo1 recruits $PP2A^{Rts1}$ (Riedel et al., 2006) to maintain dephosphorylation of pericentromeric cohesin, allowing it to resist proteolytic cleavage by Esp1. Retaining centromeric cohesin through this

division allows the sister chromatids to remain paired until the second, equational division.

1.5.4 Meiosis II

1.5.4.1 Entry into a second cycle

Exit from meiosis I requires a drop in Clb-CDK activity comparable to the exit from mitosis, to allow the spindle to disassemble. However, the cell must not exit the cell cycle entirely, resetting to G1 and relicensing DNA replication origins. The cell must now enter meiosis II. The exit from meiosis I is controlled by the FEAR network (Buonomo et al., 2003), triggered by Cdc20-bound APC. However, in contrast to exit from mitosis, the MEN is not necessary, and MEN proteins are downregulated (Kamieniecki et al., 2005).

1.5.4.2 Regulation of FEAR in meiosis I

Cdc14 release due to the FEAR network in meiosis I is sufficient to bring about disassembly of the meiotic spindle, whereas the mitotic FEAR-dependent Cdc14 release is not sufficient. In observing the exit from mitosis in mutants in which MEN is inactivated, it is seen that the cells arrest with intact spindles (Stegmeier et al., 2002). In meiosis, in the MEN-independent exit from meiosis I, the cells complete the division by disassembling their spindles ready to assemble two new ones for the second meiotic division. This is dependent on the FEAR network, as mutants in which FEAR is inactivated cannot disassemble their spindles and instead undergo two divisions on one spindle. This leads to dyads with irregular segregation (Buonomo et al., 2003; Marston et al., 2003).

1.5.4.3 Prevention of DNA rereplication

DNA replication must be prevented between the divisions to allow the cell to halve ploidy. Due to the drop in CDK activity permitting the exit from meiosis I, DNA replication origins could potentially become relicensed, and permit the initiation of DNA replication when CDK levels rise for meiosis II.

Cdc6 and MCM2-7 are controlled in meiosis in a similar way to mitosis, although Ime2 may also be involved (Lindner et al., 2002; Ofir et al., 2004). Rereplication before entry into the meiosis I division is noted in some cases: those in which Cdc28 regulation is compromised, Clb1 is overexpressed, or

uninhibitable Sic1 is expressed (Rice et al., 2005; Sawarynski et al., 2009; Strich et al., 2004). However, rereplication during the MI to MII transition is not observed.

Cdc14 dephosphorylation may be limited by the reduced, solely FEAR-driven release (Buonomo et al., 2003; Marston et al., 2003) and the continued presence of Ime2, whose phosphorylation sites are resistant to Cdc14 dephosphorylation (Holt et al., 2007).

A recent report suggests that MCM binding is one of the points of inhibition of rereplication, providing redundant and robust inhibition of rereplication at this stage (in fission yeast) (Hua et al., 2013).

1.5.5 Meiosis II

The spindle is disassembled after separation, but the cell now enters a second division rather than the G1 state. Spindle pole bodies are re-duplicated, and two spindles are then formed. Chromosomes align with bipolar attachments and are divided equationally in anaphase II.

Exit from meiosis II requires Cdc14 release as before. The MEN is active here, but is not regulated in the same way as in mitosis. Spore coats will form around the nuclei from the spindle pole bodies, enveloping the DNA (Neiman, 2011), so the spindle does not have to reach a certain location as in mitotic exit. Consequently, the function of MEN in meiosis II does not appear to depend on SPB localisation (Attner and Amon, 2012). The MEN appears to be involved in the timing of Cdc14 release, but to be dispensable for successful division: MEN component Cdc15 is not required for the second division, but is involved in spore morphogenesis (Pablo-Hernando et al., 2007).

At the end of meiosis II, spore coats form and the individual haploid spores enter dormancy.

1.6 Cyclin specificity in budding yeast

Sequence similarity suggests cyclins arose from a common ancestor by gene duplication. The original cyclin may have had full control of all the functions of the cell cycle (Nasmyth, 1995). When multiple versions accumulated by gene duplication, diversification would allow them to specialise. Cyclin specificity can

be due to specific interaction with substrates, timing of accumulation, sub-cellular localisation and resistance to inhibitors.

The nine cyclins of *Saccharomyces cerevisiae* can be split into two groups: the G1 cyclins (Cln1-3) and the B-type cyclins (Clb1-6). There is a lot of evidence for a high level of functional overlap between the cyclins within those two groups. Most significantly, no single cyclin deletion results in inviability (Fitch et al., 1992; Grandin and Reed, 1993; Tyers et al., 1991).

The G1 cyclins initiate the cycle, trigger budding and cause polarised growth (Dirick et al., 1995; Lew and Reed, 1993; Richardson et al., 1989). Cells containing any single G1 cyclin are viable, though a triple deletion is inviable. Cells in which *CLN1* and *CLN2* are deleted are delayed in growth and passing start, and the further deletion of two more genes, *PCL1* and *PCL2,* prevents bud formation, although Cln3 alone can cause Sic1 degradation and trigger DNA replication, but not budding (Moffat and Andrews, 2004). Cells in which *CLN3* is deleted are larger, with an extended G1 period (Cross, 1988; Dirick et al., 1995; Mendenhall and Hodge, 1998). The function of Cln1-Cln3 as Starter Kinases requires immunity to the Clb-CDK inhibitors that maintain the G1 state. This is demonstrated in that a *SIC1* deletion can compensate for the otherwise lethal *cln1Δ cln2Δ cln3Δ* mutants (Tyers, 1996).

Clbs 5 and 6 trigger DNA synthesis, and are expressed in late G1 and S-phase (Epstein and Cross, 1992; Schwob and Nasmyth, 1993). Clb5 and 6 are necessary for timely firing of replication origins but in their absence, firing can be accomplished by the mitotic cyclins, albeit with a delay(Epstein and Cross, 1992; Schwob and Nasmyth, 1993). This implies that the timing of expression rather than substrate specificity determines their specific roles. However, *clb5Δ* cells with early-induced expression of *CLB2* are still delayed to undergo replication (Cross et al., 1999; Hu and Aparicio, 2005). A hydrophobic patch specific to Clb5 seems to be required for its biological role, though not its associated kinase activity(Cross et al., 1999), and series of proteins involved in S-phase functions are specifically phosphorylated in a manner dependent on the hydrophobic patch(Loog and Morgan, 2005). Clb5 and Clb6 substrate specificity could explain the inability of early expression of *CLB2* to trigger timely DNA replication.

Initially, experiments found that Clb5 and Clb6 were required for pre-meiotic DNA replication (Stuart and Wittenberg, 1998). Temperature sensitive *cdc28* experiments found that either Cdc28 or Ime2 activity was sufficient for pre-meiotic DNA replication (Guttmann-Raviv et al., 2001), implying that the Clb5 and Clb6 were not necessary. However, the heat inhibition may have been incomplete, due to the sensitivity of meiosis to temperature. Recent studies enquired as to the redundancy of cyclins for DNA replication, focusing on the hydrophobic patch identified as important for Clb5 substrate specificity (Loog and Morgan, 2005; Takeda et al., 2001). It was found that the hydrophobic patch did not confer the ability to initiate DNA replication during meiosis on to Clb3 but that an N-terminal region of Clb5 could do so(DeCesare and Stuart, 2012).

Clb1-Clb4 are required for the mitotic division and promoting unpolarised growth (Richardson et al., 1992). Clb3 and Clb4 are expressed first during S-phase, and Clb1 and Clb2 expression arises during G2 (Richardson et al., 1992). Of these four mitotic cyclins Clb2 seems to be the most important: of the triple cyclin deletions only *clb1Δ,clb3Δ,clb4Δ* cells are viable (and, in fact, have only a slight phenotype), while the lethal double cyclin deletions invariably include *clb2Δ* (Fitch et al., 1992; Grandin and Reed, 1993; Richardson et al., 1992).

Clb3 and Clb4 are not essential, the double deletion completes mitosis successfully. However, in a *clb1Δ clb2Δ* mutant they are capable of driving spindle formation, before mitotic arrest, whereas *clb1Δ clb2Δ clb3Δ clb4Δ* cells arrest without spindles (Dahmann and Futcher, 1995). Additionally, *clb3Δ clb4Δ clb5Δ* cells arrest and fail to make spindles (Schwob and Nasmyth, 1993). Clb3, Clb4 and Clb5 are necessary for the formation of the spindle.

Cyclin localisation is likely to be a factor in determining their roles. Clb2 in particular is shown to localise to different cellular compartments (Bailly et al., 2003). Clb2 pools in different localisations were found to have different functions: nuclear Clb2 appears to control cell cycle progression while cytoplasmic Clb2 regulates cell morphology and the shift from polarised growth (Eluere et al., 2007). The different localisation of Cln2 and Cln3 also appears to contribute to their substrate specificity (Edgington and Futcher, 2001; Miller and Cross, 2000).

Substrate preference has been shown to vary between cyclins; Clb2 and Clb5 have been shown to have differing substrate preferences *in vitro,* which could explain the inability of early *CLB2* expression to rescue *clb5Δ* (Archambault et al., 2004; Loog and Morgan, 2005). Similarly Clb3 and Clb5 substrate specificities have been found to differ (Archambault et al., 2004; Koivomagi et al., 2011). High levels of cyclins Clb1-Clb4 during mitosis presumably can phosphorylate even the non-preferred substrates to initiate delayed DNA replication in *clb5Δ clb6Δ* mutants.

Differences in the non-specific kinase activity of different cyclin-CDK complexes have been noted (Loog and Morgan, 2005), which may suggest another mechanism of driving the cell cycle, by increasing the level of kinase activity. S-phase may require an intermediate level of kinase activity and thus be driven by the less effective Clb5, whereas mitosis required higher level of kinase activity driven by Clb2. In fission yeast, Coudreuse *et al* demonstrate that a single cyclin-CDK fusion protein can drive a successful cell cycle (Coudreuse and Nurse, 2010). The authors link this to the predicted single cyclin that controlled the primitive cell cycle.

Cyclins have diversified to have specific roles in the cell cycle, and lost the ability to perform other roles. However, most of the specialised roles can be undertaken by other cyclins in the case of deletion or mutation. In fact, overexpression of either *CLB1* or *CLB2* can compensate for the deletion of all other B-type cyclins (Haase and Reed, 1999; Hu and Aparicio, 2005) allowing a successful cell cycle, and *CLB5* overexpression can compensate for *cln1Δ cln2Δ cln3Δ* mutants (Epstein and Cross, 1992). This implies that overexpression can counter factors that contribute to specificity, such as localisation or stoichiometric inhibitors, and increase kinase activity towards non-preferred substrates sufficiently to compensate for the deleted cyclins.

In higher eukaryotes, the system becomes more complicated, with multiple CDKs and different cyclins, which can be expressed in different cells as well as in different stages of the cell cycle (Satyanarayana and Kaldis, 2009). The overall logic of the transitions remains the same, in which Starter Kinases and Exit Phosphatases are required to move the system between two stable states

established by mutual inhibition of CDK and the CKIs (Cross et al., 2011; Kapuy et al., 2009).

1.7 Modelling the cell cycle

1.7.1 Modelling mitosis

Mathematical approaches have been used to study the cell cycle for decades. Early work described the behaviour of the system with no reference to precise molecular mechanisms, as these were unknown (Johnston et al., 1977). Experiments with fusion of cells undergoing mitosis indicated that there was a diffusible factor whose presence drove mitosis, and that progress through mitosis was irreversible. Observations were compatible with two theories. One theory proposed an independently oscillating factor whose peak levels would trigger mitosis. An alternative theory was that simple accumulation of the factor triggered mitosis at high levels, and mitosis was required to reset levels to the beginning of the cycle (Murray and Kirschner, 1989).

More details of the molecular mechanisms were elucidated. *Xenopus* oocytes provided evidence of cycling kinase activity of CDK (Evans et al., 1983; Labbe et al., 1989; Lohka et al., 1988; Masui and Markert, 1971). Genetic studies in yeast identified further regulatory interactions (Hartwell et al., 1974; Nurse et al., 1976). This prompted models that described the cycle as a series of ordinary differential equations (ODEs) (Goldbeter, 1991; Novak and Tyson, 1993). Analysis of the properties of the models found bistability and hysteresis (Novak and Tyson, 1993). Bistability and hysteresis are system-level properties of the models. Bistability means that there are two stable states the system can be in at one value of the input (e.g. CDK activity) and hysteresis is a consequence of that and means that the system's state depends on its history as well as the level of CDK activity it is experiencing. These properties predict that higher levels of CDK activity would be required to enter the mitotic state than would be needed to maintain it. This was verified experimentally ten years later (Pomerening et al., 2003; Sha et al., 2003). Cross *et al.* (Cross et al., 2002) also demonstrated bistability.

The construction of a working model of the complete cell cycle was made possible as increasing molecular detail became available in the literature (Chen

et al., 2000). Theoretical work, combined with experimental approaches, produced an increasingly complex model, which could accurately reproduce more observations than the previous models (Chen et al., 2004; Cross et al., 2002). The later model proved to have predictive value, anticipating the role of the $PP2A^{Cdc55}$ in countering Net1 phosphorylation (Queralt et al., 2006).

Further models have been proposed, focusing on elements of the mitotic cycle (He et al., 2011; Lopez-Aviles et al., 2009; Queralt et al., 2006; Vinod et al., 2011). Analysis of these models found systems-level explanations for irreversibility of transitions (Lopez-Aviles et al., 2009), and for such recent observations such as endocycles of Cdc14 activity (Lu and Cross, 2010; Vinod et al., 2011).

A more recent model of the mitotic exit (Hancioglu and Tyson, 2012) has been published. This model featured an altered role of Cdc5 in Cdc14 release. This alteration improved the model's ability to predict some results, but the model was no longer consistent with other observations, in particular the endocycles mentioned above (Lu and Cross, 2010). However, the existing models predict many mutant phenotypes, and have provided some insight into the regulation of mitosis. Modelling allows insight into facets of regulation that may not be apparent intuitively, and provides predictions that can be tested by experiment.

1.7.2 Insight from modelling

1.7.2.1 Systems level feedback in the transitions of the cell cycle

Cell cycle transitions must be irreversible and sharp, despite stochastic fluctuations and slow relative changes in the driving signal (for example, growth). Fluctuations of the driving signal must not trigger early responses or permit return to a previous state. These properties are achieved at a systems level, as a consequence of the network structure.

1.7.2.2 Negative feedback contributes to irreversible transitions

Mitotic exit had been proposed to be irreversible due to thermodynamic irreversibility of cyclin degradation (Potapova et al., 2006; Reed, 2003). However, it was contended that continued cyclin synthesis would effectively

reverse cyclin degradation and that cyclin degradation would therefore be insufficient for irreversibility (Novak et al., 2007). This was demonstrated experimentally (Lopez-Aviles et al., 2009). Irreversibility can be provided by feedback, which can make a system bistable (Ferrell, 2002; Tyson et al., 2003). A bistable system can rest in one of two states, but not in any state between them. In particular, a bistable system can exhibit hysteresis, in which the state of the system depends on its history, as well as the amount of signal that is present (Figure 1-9).

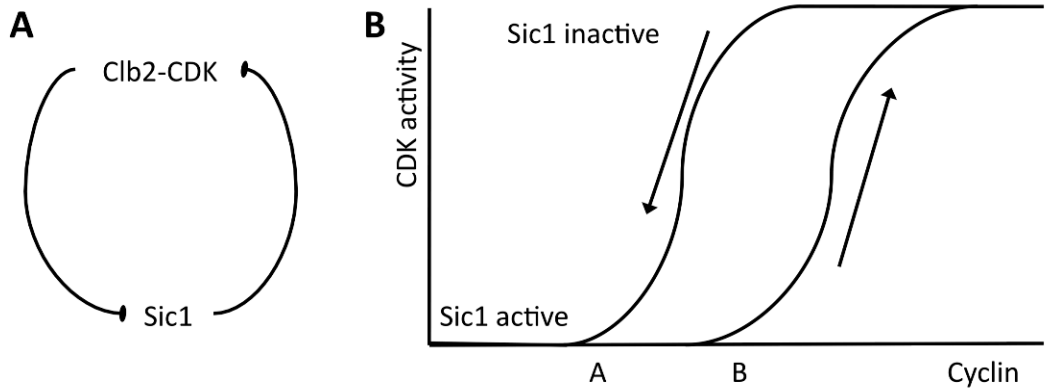

Figure 1-9 ***Double negative feedback in mitotic exit A*** *Double negative feedback loop imparting irreversibility to mitotic exit (Lopez-Aviles et al., 2009; Pomerening et al., 2003)* ***B*** *Illustration of hysteresis. Between Cyclin levels A and B, CDK activity could have two values depending on the history of the system. As cyclin levels rise, Sic1 inhibits cyclin-CDK complexes so CDK activity doesn't rise until cyclin levels reach B. Once cyclin levels have inactivated Sic1, CDK activity is high, and cell undergoes mitosis, reaches anaphase and cyclin levels are decreased by degradation. Sic1 is inactive so as cyclin levels drop, CDK activity doesn't decrease until cyclin levels are closer to A.*

Hysteresis prevents the system from returning to a previous state in the case of a slight decrease or fluctuation in the signal. The cell cycle exhibits hysteresis in that the amount of cyclin required to enter the mitotic state is higher than the amount required to maintain it (Novak and Tyson, 1993; Pomerening et al., 2003; Sha et al., 2003). Hysteresis and mutual inhibition can also result in a robust, irreversible transition. In the case of mitotic exit, the double negative feedback between CDK activity and Sic1 was found to be required for the irreversibility of mitotic exit (Lopez-Aviles et al., 2009): when cyclins were simply degraded, mitotic exit was found to be reversible: stopping the degradation led the cell to re enter the mitotic state. The transition was only irreversible if Sic1 had become active.

1.7.2.3 Positive feedback contributes to switch-like transitions

The slow continuous process of growth must trigger the sharp, discontinuous initiation of the mitotic program in order to pass START. This requires a small relative change in cell size to cause an abrupt change in expression. This is achieved by an ultrasensitive switch in expression of Clns (Carey et al., 2008; Charvin et al., 2010; Goulev and Charvin, 2011). Cln3 is expressed continuously and the levels in the nucleus are proportional to the cell size. Cln3 induces the expression of Clns 1 and 2. These cyclins amplify their own expression in a positive feedback loop. Consequently, a small change in cell size can trigger a rapid increase in cyclin synthesis and CDK activation, leading to a coordinated activation of G1/S gene expression (Skotheim et al., 2008) (Figure 1-10).

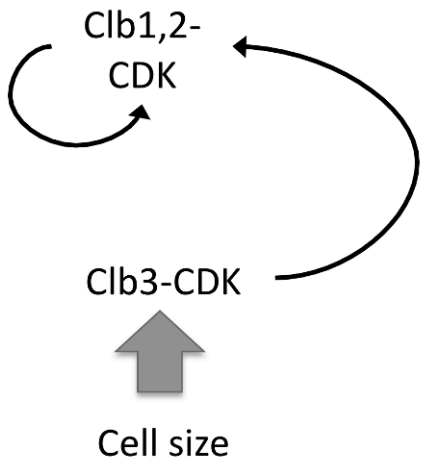

Figure 1-10 ***Positive feedback in G1 cyclin activation*** *as described in (Skotheim et al., 2008). Cln1 and Cln2 are under the control of the SBF promoter, whose activity is increased by Cln-CDK phosphorylation, leading to positive feedback in Cln-CDK activity and rapid expression of genes under the SBF and MBF promoters.*

Another situation in which positive feedback contributes to a sharp, irreversible switch is the commitment to meiosis, and the induction of the transcription factor Ndt80 at exit from pachytene in meiosis. Ndt80 expression is triggered once the cell passes the recombination checkpoint (Hepworth et al., 1998). Ndt80 triggers expression of the middle meiotic genes, and is associated with commitment to meiosis (Winter, 2012). There is positive feedback in the expression of Ndt80: there is a binding site for Ndt80 in it's own promoter (Pak and Segall, 2002a), and downstream targets of Ndt80 increase activity of Ndt80

(Acosta et al., 2011). This produced a switch-like effect (Winter, 2012) and the cell can continue with the sporulation program even if the environmental trigger driving Ndt80 expression is removed and Ndt80 expression is repressed by rich media (Friedlander et al., 2006).

Unlike mitotic exit, anaphase is irreversible due to thermodynamic considerations. Once cohesin is degraded, tension pulls chromatids apart and resynthesis of cohesin would not return them to the metaphase state. However, positive feedback allows the anaphase transition to be rapid and switch-like (Holt et al., 2008), as required to allow rapid cohesin degradation. This permits chromosomes to segregate almost simultaneously, reducing the risk that the loss of tension at the kinetochores that segregate earliest may trigger the SAC before the last chromatids are separated. Pds1 (securin) degradation activates Es1p (Separase), which in turn triggers the release of Cdc14. Pds1 degradation is inhibited by CDK phosphorylation and therefore accelerated by dephosphorylation of Pds1 by Cdc14 (Holt et al., 2008) (Figure 1-11).

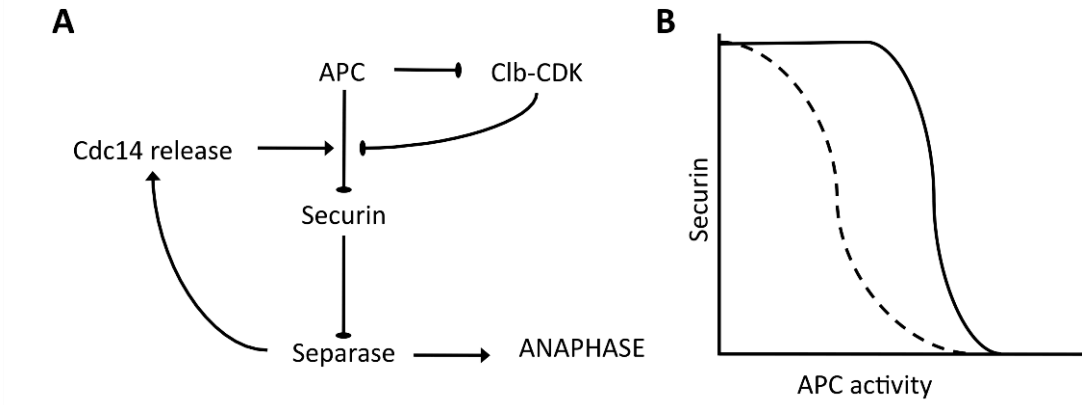

Figure 1-11 ***Positive feedback in securin degradation A*** *Feedback loop in securin degradation: as securin (Pds1) begins to be targeted for degradation by Clb-CDK activation of Cdc20, separase (Esp1) is released from inhibition. Separase leads to increased Cdc14 release by FEAR activation, leading to dephosphorylation of securin, which accelerates its degradation.* ***B*** *Securin degradation in presence (solid line) and absence (dashed line) of the inhibition of securin degradation by phosphorylation. In absence of the inhibition, the feedback loop is inactive. Securin begins to be degraded earlier but less steeply. Both adapted from Holt. et al 2008 (Holt et al., 2008)*

When the feedback loop was removed by mutation of securin, the synchrony of chromosome segregation was reduced (Holt et al., 2008).

1.7.2.4 Cell cycle as phase-locked oscillators

Feedback loops may also indicate the presence of autonomously oscillating systems. Studies using sustained endogenous levels of cyclin noted that although these cyclin levels altered the timing of many cell cycle events, they did not delay Cdc14 release (Drapkin et al., 2009). In fact, where mitotic exit was delayed after Cdc14 release, additional cycles of Cdc14 release could be observed. Further examination of Cdc14 endocycles attempted to determine their cause and function (Lu and Cross, 2010). Cyclin levels were found to alter the frequency of the endocycles, independently of Net1 phosphorylation by the cyclins. The essential interactions comprised a negative feedback loop in which Cdc5 releases Cdc14, activating Cdh1. This causes Cdc5 proteolysis and subsequent resequestration of Cdc14, in turn deactivating Cdh1 and allowing Cdc5 to build up again. (Figure 1-12)

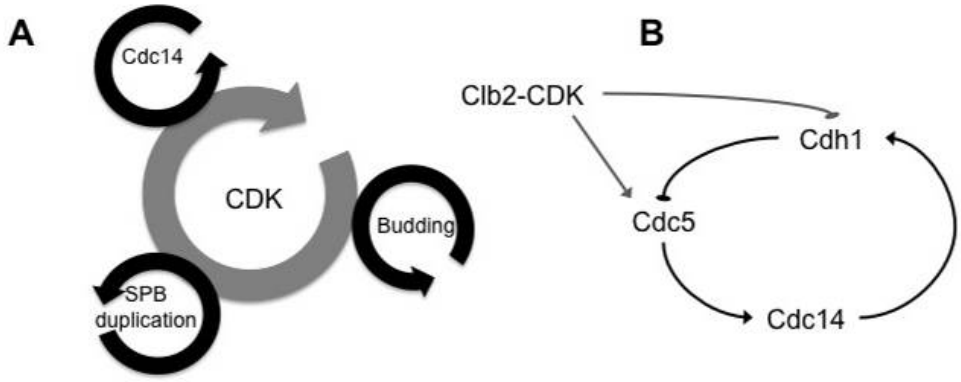

Figure 1-12 ***Phase locking in the cell cycle A*** *CDK oscillator and entrained oscillating modules.* ***B*** *Feedback loop creating the independent Cdc14 oscillator, accelerated by Clb2-CDK activity (grey arrows), both adapted from Lu et al 2010 (Lu and Cross, 2010)*

Cdc5 expression and Cdh1 degradation both depend on Clb-CDK activity, which accounts for the acceleration of the endocycles by raised Clb2. A time delay or non-linear response would be required to prevent the system reaching a steady state, such as the sustained Cdc14 release caused by very high undegradable Clb2 levels. The authors (Lu and Cross, 2010) proposed that the Cdc14 endocycle is an example of an autonomous cell-cycle oscillator, which is phase-locked by its interaction with CDK, but is not dependent on it, and they relate this to the evolution of the cell cycle.

Other reports have found evidence of the potential for the networks in the cell to oscillate independently of CDK (Haase and Reed, 1999; Orlando et al., 2008). The ability for the cell cycle to be phase locked was predicted theoretically (Cross and Siggia, 2005), and demonstrated experimentally by periodic expression of G1 genes, which caused dividing cells to synchronise (Charvin et al., 2009). This method can shorten the phase of the cell cycle but not lengthen it.

1.7.2.5 Convergent evolution of network structure

The behaviour and robustness of the model depends on its structure. Optimal and robust structures that generate the required behaviour are more likely to be found by evolution (Conant and Wagner, 2003). The prokaryotic cell cycle controls have been modelled, and although the proteins involved are not related, structural similarities to eukaryotic cell cycle control are seen in the network (Brazhnik and Tyson, 2006), suggesting that the structure of the cell cycle network is optimal.

1.7.2.6 Modelling meiosis

A functional mathematical model of meiosis has not been published, although partial models covering some of the transitions in meiosis in detail do exist (Okaz et al., 2012; Ray et al., 2013). Okaz *et al.* describe the prophase to metaphase transition and the role of Ama1 in regulating it. Mutual inhibition between Ama1 and Clb1-CDK produce bistable behaviour, with the transition controlled by Ndt80 expression (Okaz et al., 2012). Ray *et al.* describes the earlier stage of the initiation of the meiotic developmental pathway and highlights the feedback loops involved in the regulation of Ime1 and Ime2 (Ray et al., 2013).

In discussing the bifurcation analysis of mitosis, Novak and Tyson considered what a conceptual model of meiosis would have to achieve, in terms of the behaviour of CDK and its inhibitors (Tyson and Novak, 2008). This is described in differential equations in Chapter 4 and is used to explore possible mechanisms of regulation, and how my results may have relevance towards meiotic regulation in *Saccharomyces cerevisiae*.

1.8 Introduction to the project

This project aims to consider the meiosis I to II transition, MEN activation during meiosis I, and the specific regulation of cyclins. Meiosis I is controlled by Clb1, which is seen to have a modification inducing a gel shift at this stage (Carlile and Amon, 2008). Clb1 is the major meiotic cyclin, whose deletion has the greatest phenotype (Dahmann and Futcher, 1995; Grandin and Reed, 1993), so this project focussed on the regulation of meiosis.

The meiosis-specific regulation of Clb1 is investigated in Chapters 3 and 4. We discovered the nature of the modification, and identified some requirements for the modification to occur. We clarified the causal relationship between the meiosis-specific modification and the meiosis-specific localisation of Clb1. In Chapter 5, we carried out an investigation into the functional significance of the meiosis-specific localisation of Clb1.

The results are considered alongside a preliminary model of meiosis in Chapters 4 and 5, in which the observed regulation of Clb1 is incorporated, and used to explain observations and make predictions.

In Chapter 6, the amplification of FEAR release is explored during meiosis I, through attempts to activate MEN or increase Cdc14 release. These findings are considered in relation to the specific requirements of meiosis I.

2 Materials and Methods

2.1 Materials

All chemicals were purchased from Fisher Scientific, Sigma Aldrich, Formedium or Difco. Solutions were sterilised by filtration (0.45µM Sartorius filter). Media was sterilised by autoclaving.

2.1.1 Yeast and bacterial growth media

2XYT: 1.6% bactotryptone, 1% bacto yeast extract, 0.5% NaCl.

-MET media: 0.8% YNB, 55mg/L Tyrosine, 55mg/L Adenine, 55mg/L Uracil, 2% glucose, 10ml/L of –MET dropout solution.

Minimal media: 0.8% Yeast Nitrogen Base without amino acids (YNB), 2.2% agar, 2% glucose.

SPO (SPS) media: 0.3% Potassium Acetate, 0.02% raffinose, 0.02% Sigma antifoam.

SPO (YEPA1) media: 2% Potassium Acetate.

SPO (YEPA3) media: 0.3% Potassium Acetate, 0.02% Sigma antifoam.

SPO plates: 0.82% Sodium Acetate, 0.19% KCl, 0.12% NaCl, 0.35g/L Mg_2SO_4, 1.5% Agar.

SPS liquid media: 0.05% Yeast Extract, 1% Bactopeptone, 1% Potassium Acetate, 0.5% Ammonium Sulphate, 0.05M Potassium Hydrogen pthalate, 0.17% Yeast Nitrogen Base, 1x amino acid solution (no dropout).

YEPA liquid media: 2% Bactopeptone, 1% Yeast Extract, 1% Potassium Acetate, 55mg/L Adenine (YEPA3 method only).

YEPD liquid media: 2.2% Bactopeptone, 1.1% Yeast Extract, 2% glucose**,** 55mg/L Adenine.

YEPD plates: 2.2% Bactopeptone, 1.1% Yeast Extract, 2% glucose**,** 55mg/L Adenine, 2.2% Agar.

YEPD+MET: 2.2% Bactopeptone, 1.1% Yeast Extract, 0.15% Methionine, 2% glucose**,** 55mg/L Adenine, 2.2% Agar.

YEPG plates: 2.2% Bactopeptone, 1.1% Yeast Extract, 2% Glycerol**,** 55mg/L Adenine, 2.2% Agar.

YEP Raff/Gal plates: 2.2% Bactopeptone, 1.1% Yeast Extract, 2% Galactose, 2% Raffinose**,** 55mg/L Adenine, 2.2% Agar.

Antibiotic selection plates YEPD plates plus:

G418: added to 100µg/ml, selects for KanMX.

Hygromycin: added to 50µg/ml, selects for hphMX.

Clonat: 100µg/ml, selects for NatMX

Ampicillin: added to 100µg/ml, added to prevent bacterial growth.

Auxotrophic selection plates:

-URA: 0.8% YNB, 2.2% agar, 55mg/L Tyrosine, 55mg/L Adenine, 11g/L C.A.A vitamin assay, 2% glucose, 10ml/L of 0.5% tryptophan, 10ml/L of 0.5% Leucine.

-TRP: 0.8% YNB, 2.2% agar, 55mg/L Tyrosine, 55mg/L Adenine, 55mg/L Uracil, 11g/L C.A.A vitamin assay, 2% glucose, 10ml/L of 0.5% Leucine.

-HIS: 0.8% YNB, 2.2% agar, 55mg/L Tyrosine, 55mg/L Adenine, 55mg/L Uracil, 2% glucose, 10ml/L of –HIS dropout solution.

-LEU: 0.8% YNB, 2.2% agar, 55mg/L Tyrosine, 55mg/L Adenine, 55mg/L Uracil, 2% glucose, 10ml/L of –LEU dropout solution.

-MET: 0.8% YNB, 2.2% agar, 55mg/L Tyrosine, 55mg/L Adenine, 55mg/L Uracil, 2% glucose, 10ml/L of –MET dropout solution.

2.1.2 Solutions and Buffers

Amino Acid dropout solution (per litre, minus amino acid for dropout): 2.0g Arginine, 1.0g Histidine, 6.0g Leucine, 4.0g Lysine, 1.0g Methionine, 6.0g Phenylalanine, 5.0g Threonine, 4.0g Tryptophan.

Calmodulin Binding Buffer: (*added immediately before use) 10mM Tris-Cl pH8, 300mM NaCl, 1mM MgAc, 2mM $CaCl_2$, 10mM β-mercaptoethanol*. NP40 to 0.1%, later 0.02%.

Calmodulin Elution Buffer: (*added immediately before use) 10mM Tris-Cl pH8, 300mM NaCl, 1mM MgAc, 20mM EGTA, 10mM β-mercaptoethanol*, 0.02% NP40.

Developer Solution: (prepared fresh) 3% sodium carbonate , 0.05% formaldehyde.

Electrophoresis Buffer 5X: (1L) 15.1g Tris, 72.0g Glycine, 5g SDS in water.

In Situ Buffer 1: 0.1 Potassium Phosphate pH 6.4, 0.5mM Magnesium Chloride.

In Situ Buffer 2: 0.1 Potassium Phosphate pH 7.4, 0.5mM Magnesium Chloride,1.2M Sorbitol.

Inoue Buffer: 5mM $MnCl_2$, 15mM $CaCl_2$, 250mM KCl, 10mM PIPES pH6.7, 0.075% DMSO.

IPP50: (*added immediately before use) 10mM Tris-Cl pH8, 30mM NaCl, 0.1%NP40, 1mM PMSF*.

Kinase Assay Buffer: 50 mM Tris-Cl pH 7.5, 10 mM MgCl2, 1mM DTT, 5mM β-glycerophosphate.

Laemmli Buffer (5x): (*added immediately before use or aliquots at -20˚C) 60mM Tris-Cl pH6.8, 2% SDS, 10% glycerol, 5% β-mercaptoethanol*, 0.01% bromophenol blue.

Lysis Buffer (*omitted when phosphatase inhibitors aren't required †added immediately before use): 50mM Hepes pH7.6, 75mM KCl, 1mM $MgCl_2$, 1mM EGTA*, 0.1% NP40, 50mM NaF*, 1mM Na Vanadate*, 60mM β-glycerophosphate*, 1mM pefabloc*, 1mM PMSF†, 15mM nitrophenylphosphate*†, 5x protease inhibitors.

Lysis Buffer 2 (*omitted when phosphatase inhibitors aren't required): 50mM Hepes pH7.6, 75mM KCl, 1mM MgCl2, 1mM EGTA*, 0.1% NP40, 50mM NaF*, 1mM Na Vanadate*, 60mM β-glycerophosphate*, 1mM pefabloc*, 1x protease inhibitors.

NP40 Buffer: (*added immediately before use) 15mM Na_2HPO_4, 10mM NaH_2PO4, 1% Non-idet (Igepal), 150mM NaCl, 2mM EDTA, 0.1M $NaVO_4$, 1mM PMSF*1xRoche protease inhibitor cocktail, 50mM NaF, 60mM β-glycerophosphate, 15mM nitrophenyl phosphate*.

Pd-DAPI: 100mg/100mL p-phenylenediamine, 10ml/100mL PBS,90% Glycerol, 0.05µg/mL DAPI, pH8.0.

Stacking Buffer: (500mL) dissolve 30.35g Tris Base, pH to 6.8 with HCl, 20ml 10% SDS.

Separating Buffer: (500mL) dissolve 91g Tris Base, pH to 8.8 with HCl, 20ml 10% SDS.

SCE Solution: 1M Sorbitol, 0.1M Sodium Citrate, 0.06M EDTA.

SDS Solution: 2% SDS, 0.1M Tris-Cl pH9, 0.05M EDTA.

Silver Nitrate Solution: (prepared fresh) 0.1% silver nitrate.

Stripping buffer: 62.5mM Tris-Cl pH6.8 10.05% SDS, 0.7% β-mercaptoethanol.

TE Solution: 10mM Tris-Cl pH 7.5, 1mM EDTA.

TEV cleavage buffer: (*added immediately before use) 10mM Tris-Cl pH8, 300mM NaCl, 0.1% NP40, 0.5mM EDTA, 10mM DTT*.

Transfer Buffer: 39mM Glycine, 48mM Tris Base, 0.037% SDS, 20% methanol.

2.1.3 Kits

For PCR, Taq polymerase kit and dNTPs from Invitrogen were used. For PCR product or digested plasmid purification from gels, a QIAgen QIAquick Gel Extraction kit was used. For plasmid extraction from *E. coli*, a QIAgen MiniPrep kit was used.

2.2 Methods

2.2.1 Yeast Culture Methods

2.2.1.1 Transformation

Yeast cells were taken from YEPD plates, inoculated into 50mL YEPD media and grown in a 30°C shaker, 170-180 rpm for ~16 hours. At the end of this time, the OD_{600} was measured and the starter culture was used to inoculate a second culture to an OD_{600} of 0.2.

After 3-4 hours growth, cells reached an OD_{600} of 0.8. Cultures were spun down at 1300rpm for 5 minutes. Supernatant was removed and cells washed in 20mL water. After being spun down again and the water removed, cells were resuspended in 1mL of 1M Lithium Acetate and transferred to a 1.5mL Eppendorf. Cells were spun at 5000rpm and supernatant removed. Cells were resuspended in 150µL of 1M Lithium Acetate.

For a transformation mix, 24µL of the cells were transferred to a fresh Eppendorf tube. 8µL of carrier DNA (heated to 95˚C and chilled briefly on ice) was added, then 8µL of transforming DNA. 90µL of 50% Poly Ethylene Glycol was added finally. The transformation mixes were vortexed for 1 minute then left for 30 minutes at room temperature. 20µL of 50% Glycerol was added to each mix, followed by briefly vortexing then leaving at room temperature a further 30 minutes. Transformation mixes were then incubated at 42°C for 20 minutes.

If the selective marker was antibody resistance, cells were then grown in non-selective YEPD media at 30°C for an hour.

Cells were spun down at 5000 rpm for 1 minute, then resuspended in 150µL sterile water. 20µL of suspended cells was spread on one plate and the remainder on a second plate of selective media, and plates were incubated at 30°C for 2-3 days.

2.2.1.2 Sporulation protocol

YEPA3: Yeast cells were taken from -80°C storage and patched onto YEPD plates, which were kept at 30°C for 8-16 hours to allow cells to recover before being streaked out for single colonies. These were allowed to grow for 1½ to 2 days before six single colonies from each strain were patched onto fresh YEPD plates and returned to 30°C.

After 24 hours the patches were moved onto fresh YEPD plates, YPG plates and Sporulation plates and returned to 30°C. After 24 hours, the sporulation efficiency on Sporulation plates of the patches whose equivalents had grown on YPG was examined under a light microscope and one or two patches with high efficiency were used to inoculate 50mL of YEPD media (from the equivalents on the YEPD plates).

After 24 hours, the OD_{600} was measured, and found to be at around 8-10. Cells were inoculated into YEPA media to obtain cultures of a range of OD_{600} of between 0.05 and 0.2,in a flask of 5-10x the media volume. These were grown overnight at 30°C shaking at 250-270 rpm.

16 hours after inoculation, the OD_{600} of these cultures was tested and should be selected between 1.4 – 2, with few/no budded cells. These cultures

were spun down at room temperature, washed in pre-warmed SPO (YEPA3) media, and resuspended in pre-warmed SPO (YEPA3) media at OD_{600} 3 in flasks of 10x culture volume. These cultures were returned to the shaker at 30°C shaking at 270rpm.

The YEPA3 method was used for the work in Chapters 3, 4 and 5. In Appendix Section 9.3.1, three different methods of producing high efficiency, reliable and relatively synchronous sporulation were discussed and method YEPA1 was used for the work in Chapter 6.

YEPA1: Yeast cells were taken from -80°C storage and streaked out for single colonies on YPG plates. These were kept at 30°C for 48 hours to grow single colonies. Six single colonies of each strain were patched onto fresh YEPD plates and returned to 30°C.

After 24 hours the patches were moved onto fresh YEPD plates, and Sporulation plates and returned to 30°C. After 24 hours, the sporulation efficiency on Sporulation plates was examined under a light microscope and one or two patches with high efficiency were used to inoculate 50mL of YEPD media (from the equivalent patches on the YEPD plates).

After ~12 hours, the OD_{600} was measured, and should be at around 1.2-1.5. Cells were inoculated into YEPA media to obtain cultures of an OD_{600} of between 0.05 and 0.2, in a flask of 5-10x the media volume. These were grown for ~12 hours at 30°C shaking at 270 rpm. 12 hours after inoculation, the OD_{600} of these cultures was tested and cultures whose OD_{600} had reached 1.3 – 1.8 selected, with few/no budded cells. These cultures were spun down at room temperature, washed in pre-warmed sporulation media, and resuspended in pre-warmed sporulation media at OD_{600} 3 in flasks of 10x culture volume. These cultures were returned to the shaker at 30°C shaking at 270rpm.

SPS2: Yeast cells were taken from -80°C storage and streaked out onto YPG plates, which were kept at 30°C for 48 hours to grow single colonies. Six single colonies of each strain were patched onto fresh YEPD plates and returned to 30°C.

After 24 hours the patches were moved onto fresh YEPD plates, and Sporulation plates and returned to 30°C. After 24 hours, the sporulation efficiency on Sporulation plates was examined under a light microscope and one

or two patches with high efficiency were used to inoculate 50mL of YEPD media (from the equivalent patches on the YEPD plates). These were grown at 30˚C shaking at 180 rpm to an OD_{600} of around 6-7.

These cells were then inoculated into SPS liquid media to form cultures with an OD_{600} of between 0.05 and 0.2 and grown overnight at 30˚C shaking at 180 rpm. After 12-14 hours the OD_{600} of the cultures should have reached ~1.4 with few/no budded cells. Cells were spun down and washed in pre-warmed SPO (SPS) media antifoam, then resuspended in SPO (SPS) media to an OD_{600} of 3 in flasks of 10x culture volume. These cultures were returned to the shaker at 30°C shaking at 270rpm.

2.2.1.3 Mitotic Metaphase Arrest

P_{MET}*CDC20* strains were arrested in metaphase by growth in +MET media in which the P_{MET} promoter is not expressed: Cells were taken out of -80˚C storage, streaked out on –MET plates. Single cultures were inoculated into YEPD –MET media and grown to an OD of 3 (overnight at 30˚C). This was diluted to an OD of 0.2 and grown a further 5 hours to achieve an OD of around 0.8.

Cells were spun down and resuspended in YEPD +MET media and returned to the shaker.

2.2.1.4 Tetrad Dissection

Sporulated cells were scraped from a Sporulation plate and suspended using a toothpick in 100µL of 1M sorbitol and 2.5mg/mL zymolyase, before incubating at 30°C for 10 minutes. 10µL was pipetted onto a dried YEPD or Met+ plate. Single colonies were dissected and the spores separated using a Singer Instruments MSM400 tetrad dissection microscope. Plates were then incubated at 30°C for 2-3 days.

2.2.1.5 Random Sporulation

Two mutations were sufficiently close that linkage effects meant that it was unlikely to find a spore combining them by tetrad dissection (Clb1-HA ChrVII: 703636 to 705051 and esp1-1 ChrVII: 687458 to 682566)

Sporulated yeast cells incubated in 100µL of 1M sorbitol and 2.5mg/mL zymolyase for 30 minutes at 30°C. The digested cells were diluted by 1/1000 in

water and spread on 6 -His plates, progressively diluting by 1/10. His plates were incubated at 25˚C. This identified spores carrying the His marker, positive for Clb1-HA. To identify the spores bearing esp1-1, the plates were replicated onto YEPD plates and incubated at 35˚C. Replica colonies that did not grow were positive for esp1-1 as well.

2.2.2 DNA Methods

2.2.2.1 Transformation of *E. coli*

Competent *E. coli* cells in Inoue Buffer were thawed on ice. 1μL of DNA was added per 150μL aliquot. Cells were kept on ice for 30 minutes, with shaking at 15 minutes.

Cells were heat-shocked at 42˚C for 20 seconds then returned to ice for 2 minutes. 800μL of pre-warmed 2xYT buffer was added to each aliquot and cells were incubated in a shaker at 37˚C for 1 hour.

Cells were spun down and resuspended in ~500μL of 2xYT, before being split unevenly between selective Agar plates (10μL and 500μL). Plates were incubated in 37˚C overnight.

2.2.2.2 PCR

PCR was performed using a Taq polymerase kit (Invitrogen). The PCR mix was assembled to the following proportions

1xBuffer, 2.5μM $MgCl_2$, 0.2mM each dNTPs, 0.5μM Primer1, 0.5μM Primer2, Template DNA 1-2μL, 1μL/50μL reaction Taq Polymerase, H_20 to final volume. Typical cycle for a standard PCR reaction follows:

Initial denaturing - 95˚C (5 minutes)

Cycle - 95˚C (1 minute), 50˚C (1 minute), 72˚C (1min per kb) x 30

Final Extension - 72˚C (10 minutes) then 4˚C (hold)

Reactions were performed on a BioRad Thermal Cycler.

Primers used in this project are listed in the Appendix Section 9.5.

2.2.2.3 Colony PCR

Small amounts of a yeast colony was scraped up by toothpick and mixed into 15 μL of 0.1M potassium phosphate (pH7.4) with 3mg/mL zymolyase. These mixes were incubated at 25°C for 20 minutes, 35°C for 5 minutes, 95°C for 5

minutes. 60µL of sterile water was added to dilute, then 2.5µL was used as template in a 25µL PCR reaction as above.

In some cases, when the above method proved unsuccessful, the colony was inoculated into YEPD media and the culture subjected to genomic DNA extraction to provide a more reliable template.

2.2.2.4 Genomic DNA extraction

10mL of yeast cells at stationary phase (OD_{600} of 6-7) were spun down for 2 minutes at 3000rpm. The cell pellet was resuspended in 1mL water and transfer to 1.5mL Eppendorf tube. The tubes were spun for 30 seconds at 13000 rpm and the water poured off.

The cells were resuspended in 0.2mL of SCE Solution plus 2mg/mL zymolyase plus 8µL /mL βME and incubated at 37°C with shaking for up to one hour, checking spheroplasting at intervals after half an hour.

Once spheroplasting was complete, 0.2mL of SDS Solution was added, the cells were vortexed briefly and incubated at 65°C for 5 minutes. 0.2mL of 5M potassium acetate was added, the mix was vortexed briefly and left on ice for 20 minutes.

The tubes were spun at 13000rpm for 5 minutes and 0.4-0.5mL of the supernatant was transferred using a cut off P1000 tip to a fresh 1.5mL Eppendorf tube. 0.2mL 5M ammonium acetate and 1 mL of isopropanol were added and mixed.

The tubes were spun twice at 500rpm for 30 seconds and the supernatant removed. The pellet was dissolved in 90µL TE Solution. 10 µL of 5M ammonium acetate and 200µL of isopropanol were added and mixed. DNA precipitate forms and tubes were spun to push it to the bottom of the tube. Supernatant was removed carefully and pellets rinsed in 80% ethanol. Once ethanol was removed, pellets were resuspended in 50µL of TE Solution.

2.2.2.5 Restriction digests

Restriction enzymes were purchased from NEB, and digests were completed following the instructions.

2.2.2.6 Ligation

Ligations were performed using a DNA Ligation Kit (Roche). For greater success, Shrimp alkaline phosphatase (New England Biolabs) was used to prevent self-ligation of the vector in the construction of the NLS6A mutant (Section 5.4.1)

2.2.2.7 DNA gels

DNA samples were analysed by agarose gel electrophoresis using ethidium bromide for detection. 0.8% agarose gels were made by dissolving agarose in TAE buffer. Ethidium bromide was added to 0.5μg/ml. Samples were loaded in sample buffer (Fermentas) and band size markers provided by the Fermentas 1kb ladder. Gels were run at 120V and DNA detected using a transilluminator.

2.2.3 Cell Visualisation

2.2.3.1 In situ immunofluorescent imaging

Sample preparation

At the point of taking the sample, 900μL of cells were added to 100μL of formaldehyde (37% stock solution). The cells were shaken with formaldehyde at 25°C for 15 minutes then spun down 13000 rpm for 2 minutes. The supernatant was removed and the cells resuspended in In Situ Buffer 1 plus 3.7% formaldehyde, and incubated at 4°C overnight.

The following day, samples were spun 13000 rpm resuspended in 1mL In Situ Buffer 1 without formaldehyde. This wash was repeated twice with 500μL of In Situ Buffer 1 and once with 500μL In Situ Buffer 2.

Cells were resuspended in 200μL In Situ Buffer 2 plus 4μL /mL βME and incubated at 25°C with shaking for 15 minutes. Zymolyase was added to each sample to 0.1mg/mL and samples were incubated at 37°C with shaking. Spheroplasting was checked at 5-minute intervals.

Once spheroplasting has occurred, 500μL of In Situ Buffer 2 was added to each sample. The samples were spun at 2500rpm for 5 minutes. Supernatant was removed and cells were washed with a further 500μL In Situ Buffer 2, before

being resuspended in 150-300µL In Situ Buffer 2. These samples were then stored at -20°C until use.

Preparing Slides

Thermoscientific 21-well slides were prepared by adding 5µL 0.1% polylysine to each well and leaving at room temperature for 10 minutes. The slides were rinsed with water and dried by aspiration. 15µL of cell samples were added to each well. Cells were left 5 minutes on the slide then aspirated off. Slides were then plunged into -20°C methanol for 3 minutes and -20°C acetone for 10 seconds. Slides were left on the bench to warm up and acetone evaporate. 5µL of BSA-PBS (PBS plus 10g/L BSA) was added to each well, before leaving at room temperature for 30 minutes. BSA-PBS was aspirated off and replaced with 5µL Primary Antibody Solution. Slides were placed in a humidity chamber for 2 hours. The wells were washed four times by pipetting 5µL of BSA-PBS onto each well, leaving for 5 minutes, then aspirating off the solution. 5µL Secondary Antibody Solution was added to each well and slides were placed into the humidity chamber for 2 hours.

The wells were washed four times by pipetting 5µL of BSA-PBS onto each well, leaving for 5 minutes, then aspirating off the solution. 5µL pd-DAPI was added to each well and the slides were covered with a cover slip and sealed with clear nail varnish. Antibody solutions were comprised of the required antibodies at the following dilutions in BSA-PBS.

Primary		**Secondary**	
Antibody	**Dilution**	**Antibody**	**Dilution**
Rat anti tubulin (Serotec)	1/100	Anti Rat Cy5	1/100
Rat anti-HA (Roche)	1/500	Anti-Rat Cy3	1/500
Mouse Anti Nop1 (ThermoFisher Scientific)	1/500	Anti-Mouse FITC	1/500
Mouse Anti Myc (Cambridge Bioscience)	1/500	Anti Mouse Cy3	1/500
Rabbit Anti Cdc14 (SantaCruz)	1/500	Anti Rabbit Cy3	1/500
Rabbit Anti TAP (ThermoScientific)	1/500	Anti Rabbit Cy3	1/500

Table 2-1 Antibodies for in situ fluorescence imaging

Taking images

Images were taken using a Photometrics system comprising a Photometrics CoolSnapHQ2 camera, Nikon TE2000E inverted microscope with

100X 1.49NA objective. Images were taken with a Z series of 16 steps using a 0.2μm step size for a total range of 3μm. For Cy5, Cy3 and FITC exposures of 1 second were used, for DAPI exposure of 300ms and for transparent, exposure of 5ms.

2.2.3.2 Live cell imaging of meiosis

PEI prep: PEI slides were made using cover slips and gaskets to maintain space between them. Lower cover slips were prepared as below and cells were covered with agarose pads. The gasket forms a chamber between the upper and lower cover slips to hold SPO media and prevent drying over the duration of the imaging.

To prepare the cover slips, PEI was dissolved in water to 0.5% and 10μL placed on the cover slip. The cover slips were rinsed in sterile water and allowed to dry. Agarose pads were made by pipetting 1% agarose in PBS between two slides held apart by cover slips. Once set, these were cut into pads with razor and stored in PBS at 4˚C.

In strains undergoing wild type meiosis, 5mL aliquots of cells were taken from cultures 3.5 hours into sporulation media (YEPA1). In strains in which the P_{GAL}*NDT80 GAL4ER* system was used to synchronise meiosis, aliquots were taken at 6 hours into sporulation media, immediately after induction. Aliquots were spun down and resuspended in 1/3 the original volume fresh pre-warmed SPO media to concentrate the cells.

Agarose pads were soaked briefly in pre-warmed SPO media and dried by touching with filter paper. ~1mL of the cell suspension was pipetted on to the prepared cover slip surfaces. Agarose pad was placed over the top of the cells. The gasket was placed on the cover slip and a little SPO media was dropped onto the cover slip. The cover slip was transferred to microscope, or incubator kept at 30˚C.

Concanavalin prep: Concanavalin Type IV dissolved in water at 2mg/mL. 50μL of the solution was placed onto Glass bottom culture dishes (35mm diameter 10mm deep, Microwell, MatTek Co) in the cover slip region and allowed to dry for 2 hours before washing with 70% ethanol and drying again.

Aliquots of the cultures were prepared as above. Cell suspension was pipetted onto the concanavalin and left for 10 minutes, before two washes in pre-warmed SPO media and 0.5mL SPO media was pipetted on top of the cells. The dish was then transferred to the microscope or incubator at 30˚C.

Image acquisition: Cells were viewed in a Nikon Eclipse TE2000-E motorised inverted microscope. Temperature of the stage is set at 30°C using an objective heater. Images were recorded 6hours performing Z-stacks of 8 sections (step size= 1µm) and images are acquired using a Cool Snap HQ2 high speed monochrome CCD camera. Exposure timings and intervals were varied during optimisation, see chapter 6 for more details

2.2.4 Protein extraction, assays, and detection

2.2.4.1 Whole cell extracts using TCA

5-10mL of yeast cells from a culture with OD600 were spun down at 2000rpm for 5 minutes. The cell pellet was washed in 500µL 20% TCA and transferred to a 1.5mL Eppendorf tube. The samples were spun at 13000 rpm for 2 minutes and the TCA removed by pipetting. The pellets were frozen in liquid nitrogen and stored -80°C.

Pellets were thawed on ice and resuspended in chilled 250µL 20% TCA. The suspended pellets were transferred to chilled 2mL Costar tubes containing 250µL glass beads. These tubes were shaken in a bead beater at 4°C for 10 minutes. Heated needles were used to pierce the bottom of the Costar tube and they were placed into a clean Eppendorf with lid cut off. The tubes were spun at 6000rpm, for 2 minutes at 4°C to push lysate and precipitate from beads. The beads were washed with 300µL chilled 5% TCA followed by a second spin.

Costar tubes and beads were discarded and 700µL chilled 5% TCA was added to each Eppendorf tube. The samples were spun at 14000rpm for 10 minutes at 4°C. The supernatant was removed and the pellet was resuspended in 40-80µL 1M Tris-Cl pH8. Twice the Tris-volume was added of 2x Laemmli buffer and BME 40µL /ml

Samples were then heated to 95˚C for 5 minutes at 95°C before freezing at -20°C until running on a gel. Samples were heated again and spun 14000rpm for 5 minutes before being run on a gel.

2.2.4.2 Running polyacrylamide gel

Samples were run on 8% polyacrylamide gels, except in Section 5.5.2.5, where the detection of the Net1 gel shift required the use of 5% gels, and in Section 5.5, where the detection of phosphorylated histone required the use of 15% gels.

Making gels

	Separating gel			Stacking Gel
	5%	8%	15%	
Stacking Buffer	2.5mL	2.5mL	2.5mL	-
Stacking Buffer	-	-	-	1.25mL
Protogel Mix	1.56mL	2.3mL	4.31mL	0.825mL
Water	5.79mL	5.05mL	3.04mL	2.95mL
APS*	100µL	100µL	100µL	50µL
Temed*	50µL	50µL	50µL	25µL

Table 2-2 Polyacrylamide gel recipes

Gels were made in 1.5mm or 1.0mm protein gel cassettes (Invitrogen). Recipes are given below. Separating gel was made first and poured into the cassette. The gel was allowed to set for ten minutes, topped with isopropanol and left a further 5 minutes. The isopropanol was poured off and wicked out with filter paper. Stacking gel was then prepared and poured in on top, fitted with a comb and left to set for 10 minutes. After setting, the comb was removed.

Running gels

Samples were taken from -20˚C, heated to 95˚C for 5 minutes, and spun 14000rpm for 5 minutes before being run on a gel. Gels were placed into Invitrogen gel running apparatus with Electrophoresis Buffer and samples loaded with PageRuler Prestained Ladder (Fermentas) or Spectra Prestained Ladder (ThermoScientific) as ladders. Gels were run at 25mA for the required time, or at 20mA for stacking gel and 30mA for separating gel for the required time.

2.2.4.3 Western blot Transfer

Gels were transferred to a nitrocellulose membrane (Whatman) using a wet transfer method. The transfer was run in a Bio-Rad western transfer tank using Transfer Buffer, running at 120V, 230mA for 90 minutes at room temperature

2.2.4.4 Antibody Detection

After transfer, membranes were rinsed in PBS and blocked in PBS plus 0.01% Tween plus 5% powdered milk for 30 minutes, shaking at room temperature. The membranes were shaken in primary antibody mix in PBS/Tween/Milk for 1 hour room temperature or overnight at 4°C, then washed in PBS/Tween four times. The membranes were shaken in secondary antibody mix.

Primary		Secondary	
Antibody	Dilution	Antibody	Dilution
Rat anti tubulin (Serotec)	1/1000	Anti Rat HRP (Invitrogen)	1/1000
Rat anti HA (Roche)	1/5000		
Mouse anti-Myc (Cambridge Bioscience)	1/5000	Anti Mouse HRP (Promega)	1/1000
Mouse anti-HA (Santa Cruz Biotechnology)	1/5000		
Goat anti Cdc5 (Santa Cruz Biotechnology)	1/5000	Anti Goat HRP (Promega)	1/1000
Goat anti Cdc28 (Santa Cruz Biotechnology)	1/5000		
Rabbit anti TAP (Cambridge Bioscience)	1/5000	Anti Rabbit HRP (New England Biolabs)	1/1000

Table 2-3 Antibodies for western blot protein detection

The membrane is then washed of in PBS-Tween four times for 5 minutes each. Developing solution was added (Amersham ECL Plus) for one minute. The membrane was touch dried by touching to tissue paper and wrapped in cling film. To detect fluorescence, Kodak Bio-Max light film or Amersham Hyperfilm ECL were exposed to the membrane, and developed.

2.2.4.5 Membrane stripping

Membranes were incubated in Stripping Buffer for 30 minutes at 50˚C before being washed 6x in PBS/Tween. The membrane could then be reprobed for a new antigen, starting at the blocking step.

Some epitopes were unable to be detected after stripping by the previous method, while others may be fainter. To allow the sequential detection of such sensitive epitopes, a second method of clearing previous detection was used.

The membrane was incubated with PBS/Tween/Milk plus 0.1% sodium azide for 2 hours to overnight on a shaker at room temperature. The sodium

azide inactivates the HRP enzyme. The membrane was then rinsed 6x5min in PBS/Tween to remove the high azide and could be reprobed from the 1˚ antibody step. This method was gentler but sometimes left visible bands if the previous signal had been very strong and short stripping times were used.

2.2.4.6 Silver staining gels

For a normal 10mL gel, wash volumes were 200mL and washes were performed on a rocker at room temperature unless otherwise stated.

Polyacrylamide gels were fixed in 50% ethanol, 5% acetic acid for between 20 minutes and overnight at 4˚C. The gel was washed in 50% methanol for 10 minutes, and water for 10 minutes, then sensitised in 0.02% sodium thiosulphate for 1 minute. The gel was washed in water for 1 minute.

The gel was then incubated for 20 minutes in Silver Nitrate Solution in a dark container, then washed in water for one minute, ensuring Silver Nitrate Solution was washed away thoroughly.

To develop the gel, it was incubated in Developer Solution and must be watched until staining was optimum. Developer Solution goes yellow and should be replaced. Staining was stopped by washing twice in 5% acetic acid. Gel was stored in 1% acetic acid and photographed in the transilluminator.

2.2.4.7 Immunoprecipitation

20mL samples taken from sporulation cultures (with an OD600 of 3) and spun down at 2000 rpm for 5 minutes. Resuspended in 1mL sporulation media, transferred to a 1.5mL Eppendorf tube and spun at 13000 rpm for 2 minutes. Supernatant was removed and cell pellets frozen in liquid nitrogen, stored at -80°C until use.

Cells were thawed on ice and 300µL of Lysis Buffer added. Cells were added to a 2mL Costar tube with ~300µL of acid washed glass beads. Samples were shaken in a bead beater at 4°C for 3 second then placed on ice for 30 seconds, for a total of 10 times (adding up to 5 minutes bead beating altogether).

The Costar tube was pierced with a heated needle, and placed into second 1.5mL Eppendorf tube then spun at 6000rpm for 2 minutes at 4°C. The Costar tube was then discarded and the Eppendorfs were spun at 13000rpm for 15min

at 4°C. The supernatant was transferred to fresh Eppendorf tubes and the spin repeated.

DTT was added to each sample to 1mM and the primary antibody was added (Covance anti Myc mouse antibody 9E10). The sample was incubated on a turner in the cold room for 1hour 20 minutes. 100µL sepharose beads per sample were prepared by spinning at 800rpm for 2 minutes at 4°C, washing in Lysis Buffer and resuspending in Lysis Buffer.

Beads were added to the samples, 100µL beads per 300µL sample, then the samples were incubated on a turner at 4°C for 2 hours. Samples were spun at 800rpm, 2 minutes, 4°C and washed three times in 250µL Lysis Buffer without phosphatase inhibitors. These samples can were used immediately for the phosphatase assay.

2.2.4.8 Phosphatase Assay

Phosphatase assay used the Lambda Protein Phosphatase kit from New England Biolabs. Samples were spun at 800rpm, 2 minutes, 4°C,and washed once with 250µL 1x NEB buffer for Lambda protein phosphatase. Samples was resuspended in 100µL 1x NEB buffer and divided between two 1.5mL Eppendorfs. 2µL of Lambda Protein Phosphatase was added to one of the two vials each sample. Samples were placed on the shaker for 30 minutes at 30°C.

Samples were spun at 800rpm, 2min, 4°C to remove supernatant, 60µL 4x Laemmli buffer was added to each, then samples were heated to 95°C for 5 minutes and spun for 5 minutes at 13000 rpm before further analysis.

2.2.4.9 Kinase Assay

For the kinase assay, 75mL mitotic cultures were grown to an OD_{600} of ~1 before cell harvesting. Cell pellets were flash frozen in nitrogen and stored at -80°C. Cells were thawed on ice and resuspended in 300µL of Lysis Buffer 2 before transfer to a pre-chilled Costar tube with ~300µL acid washed beads. The tubes were shaken in a bead beater at 4°C for 30 second then placed on ice for 30 seconds, for a total of 10 times (adding up to 5 minutes bead beating altogether). Lysis was confirmed by light microscope.

The Costar tube was pierced with a heated needle, and placed into second 1.5mL Eppendorf tube then spun at 6000rpm for 2 minutes at 4°C. The Costar

tube was then discarded and the Eppendorfs were spun at 13000rpm for 15min at 4°C. The supernatant was transferred to fresh Eppendorf tubes and the spin repeated. The protein content was checked by Bradford assay. The primary antibody was added, 1µL of antibody for 1mg protein, plus DTT to 1mM. The sample was incubated on a turner in the cold room for 1hour. Protein A Dynabeads were prepared by spinning at 800rpm for 2 minutes at 4°C, washing in Lysis Buffer 2 and resuspending in Lysis Buffer 250µL of Dynabead slurry was added to each sample before returning to the rotator for a further hour at 4˚C Beads were spun down at 800rpm for 2 minutes and washed three times with 1mL of Lysis Buffer 2. Gel samples were taken now. The remaining bead slurry was washed twice more with Kinase Assay Buffer then resuspended in Kinase Assay Buffer and kept on ice.

Kinase assay mixes of 40µL were as follows: 30.5µL beads in kinase buffer, 50µM ATP, 0.25µCi/µL γ-32-ATP, 35µM or 3.5µM histone. The beads and histone were mixed first and the ATP solutions added at T0. Reactions were incubated at 30˚C for the duration. Reactions were stopped by the adding to 4x Laemmli buffer, and frozen at -20˚C.

Samples were run on a 15% polyacrylamide gel according to the above protocol. The gel was rinsed in water an soaked in 10% glycerol for 5 minutes, then dried in a gel drier for an hour. The gel was exposed overnight at -80˚C to FujiFilm Imaging Plate Phosphor Screen and the result analysed using a phosphoimager.

2.2.4.10 Tandem Affinity Purification

To provide a large enough culture for TAP preparations, the mitotic cells from which Clb1TAP was extracted were grown to an OD_{600} of 1-1.5 in a total volume of 4 litres.

To achieve a similar amount of arrested meiotic cells in attempts to purify modified Clb1, a 2L culture with an OD_{600} of 3 was prepared following the YEPA3 method and incubated in sporulation media for 8 hours before cell harvesting. This required a 4L volume of YEPA culture, which entailed the use of a media to air ratio of 1/5 rather than 1/10 and a slower shaking speed of 250rpm rather than the 270rpm typical for this stage in the method, to prevent the heavier flasks falling. Otherwise the YEPA3 method was simply scaled up. Cells were

harvested by spinning 6500rpm for 12 minutes at 4˚C and were rinsed in cold water and flash frozen in liquid nitrogen before storage in -80˚C.

Cell pellets were thawed on ice and resuspended in ice-cold Lysis Buffer. Cells were broken in bead beater in around 70mL of ice-cold lysis buffer – enough to fill the bead-beater chamber and leave no air. The bead beater was packed in ice and pre-chilled to maintain a cold temperature. The bead beater was run for 30 seconds and stopped for 30 seconds a total of 10 times to break the cells. Lysis was assessed by light microscope. Lysate was cleared by spinning at 15,000rpm for 10 minutes at 4˚C, then decanting the supernatant into a clean tube and spinning again. Protein content was checked using the Bradford assay before continuing.

IgG beads were pre-equilibrated in Lysis Buffer. 750µL IgG beads were added to each sample, which were then rotated at 4˚C for one hour. Beads were spun down at 300rpm, 4˚C for 2 minutes and washed twice with IPP50 and once with TEV Cleavage Buffer. Beads were resuspended in 1mL TEV Cleavage Buffer + 30µL of TEV protease. Returned to 4˚C shaker for 16 hours.

IgG beads were spun at 800rpm for 2 minutes at 4˚C. Eluate was decanted into a 15mL Falcon tube and beads were washed with 1mL TCB, into the Falcon tube. Per 2mL of the sample the sample, 6mL of ice cold Calmodulin Binding Buffer (CBB), 6µL 1M $CaCl_2$ were added, with a total of how 300µL Calmodulin beads, pre-equilibrated in ice cold Calmodulin Binding Buffer (CBB). The beads and sample were returned to the rotator for 1 hour at 4˚C.

Beads were spun down at 800rpm for 2 minutes at 4˚C and washed twice with 10mL CBB (0.1%NP40), then once with 10mL CBB (0.02%NP40). Bound protein was eluted from the beads with 2x1mL Calmodulin Elution Buffer. (To determine if any protein was present at low concentrations, 1mL sample was mixed with 1mL 100% TCA to cause protein precipitation, and rotated at 4˚C overnight before being spun down at 15,000rpm, 4˚C for 30 minutes and resuspended in Laemmli buffer). Later attempts at this protocol used Bio-Rad Econo Pac Columns to improve elutions.

2.3 Strains

2.3.1 Yeast Strains

Strains used in this study are from SK1 background. All strains were stored in 20% glycerol solution at -80˚C for long term storage.

Number	Genotype	Strain	Chapter
Strains to investigate cyclin requirements, Clb1 modifications and requirements. *CLB1-MYC* and *CLB1-TAP*			
2564	*MATa/alpha ura3 lys2 ho::LYS2 arg4Δ(eco47III-hpa1), clb3::natMX4*	*clb3Δ*	3 5
2570	*MATa/alpha ura3 lys2 ho::LYS2 arg4Δ(eco47III-hpa1) clb4::hphMX4*	*clb4Δ*	3 5
2603	*SK1 MATalpha/a, lys2:arg4Δ(eco47III-hpa1),LYS2,ADE2,his3::hisG,trp1::hisG,leu2::hisG,ura3, clb1::His*	*clb1Δ*	3 5
2623	*"SK1 MATa/alpha, ho::LYS2,ura3,leu2::hisG,his3::hisG,trp1::hisG clb1-del:His,clb3::natMX4*	*clb1Δ clb3Δ*	3 5
2620	*"SK1 MATa/alpha, ho::LYS2,ura3,leu2::hisG,his3::hisG,trp1::hisG clb1::his,clb4::hphMX4*	*clb1Δ clb4Δ*	3
2567	*MATa/alpha ura3 lys2 ho::LYS2 arg4Δ(eco47III-hpa1) clb3::natMX4 clb4::hphMX4*	*clb3Δ clb4Δ*	3
2618	*"SK1 MATa/alpha, ho::LYS2,ura3, leu2::hisG, his3::hisG, trp1::hisG clb1::His,clb3::natMX4,clb4::hphMX4*	*clb1Δ clb3Δ clb4Δ*	3
2027	*SK1 MATa/MAT alpha, ho::LYS2,his3::hisG,trp1::hisG,ura3::hisG,leu2::hisG, CLB1-myc9::klTRP1,REC8-HA3::URA3*	*CLB1-MYC Rec8-HA*	3
2028	*SK1 MATa /MATalpha, ho::LYS2,his3::hisG,trp1::hisG,ura3::hisG,leu2::hisG, CLB1-myc9::klTRP1, REC8-HA3::URA3, cdc55:pClb2-Cdc55:KanMX6*	p_{CLB2}*CDC55 CLB1-MYC Rec8-HA*	3
3067	*SK1 MATa/alpha, ho::LYS2,his3::hisG,trp1::hisG,ura3::hisG,leu2::hisG, CLB1-myc9::klTRP1, cdc20::pCLB2-CDC20::kanMX6", ama1:HIS3(S.pombe)*	p_{CLB2}*CDC20 ama1Δ CLB1-MYC*	3
2311	*"SK1 MATa/alpha,ho::LYS2,ura3,leu2::hisG,his3::hisG,trp1::hisG cdc20::pCLB2-CDC20::kanMX6",CLB1-myc9::klTRP1*	p_{CLB2}*CDC20 CLB1-MYC*	3
2312	*"SK1 MATa/alpha,ho::LYS2,ura3,leu2::hisG,his3::hisG, trp1::hisG cdc20::pCLB2-CDC20::kanMX6", CLB1-myc9::klTRP1,cdc55:pClb2-Cdc55:KanMX6*	p_{CLB2}*CDC20* p_{CLB2}*CDC55 CLB1-MYC*	3
2348	*SK1 MATalpha/a,ho::LYS2, leu2::hisG,his3::hisG, ura3::hisG,trp1::hisG, CLB1-myc9::klTRP1,cdc55:pClb2-Cdc55:KanMX6*	p_{CLB2}*CDC55 CLB1-MYC*	3
2350	*SK1 MATalpha/ahis3::hisG, trp1::hisG, ura3::hisG, leu2::hisG, ho::LYS2 CLB1-myc9::klTRP1*	*CLB1-MYC*	3
2378	*SK1 MATa his3::hisG, trp1::hisG, ura3::hisG, leu2::hisG, ho::LYS2 CLB1-myc9::klTRP1,cdc20::pMET3-CDC20::TRP1*	P_{MET}*CDC20 CLB1-MYC*	3
2579	*"SK1 MATa/Alpha, ho::LYS2,ADE2,ura3,leu2::hisG,trp1::hisG,his3::hisG,?lys2?" ime2-as1-myc::TRP1(M146G)*	*ime2-as*	3
2452	*"SK1 MATa/alpha, LYS2,ADE2,ura3,leu2::hisG,trp1::hisG,his3::hisG,?lys2?"*	*ime2-as* P_{CLB2}*CDC20*	3

	Clb1-TAP::TRP1,cdc20::pCLB2-CDC20::kanMX6,ime2-as1-myc::TRP1(M146G)	*CLB1-TAP*	
2366	*"SK1 MATa/alpha, LYS2,ADE2,ura3,leu2::hisG,trp1::hisG,his3::hisG,?lys2?" Clb1-TAP::TRP,cdc20::pCLB2-CDC20::kanMX6*	P_{CLB2}*CDC20 CLB1-TAP*	3
2597	*"SK1 MATa/alpha LYS2,ura3,leu2::hisG,his3::hisG,trp1::hisG x ura3,lys2,LYS2,leu2::hisG,his3-11,15trp1ΔFA::hisG CLB1-myc9::klTRP1,cdc20::pCLB2-CDC20::kanMX6"*	P_{MET}*CDC20 CLB1-MYC*	3
2600	*"SK1 MATa/alpha, LYS2,ura3,leu2::hisG,his3::hisG,trp1::hisG x ura3,lys2,LYS2,leu2::hisG,his3-11,15trp1ΔFA::hisG cdc28-as1,CLB1-myc9::klTRP1,cdc20::pCLB2-CDC20::kanMX6"*	*cdc28-as* P_{MET}*CDC20 CLB1-MYC*	3 5
2893	*SK1 MATa/alpha his3::hisG, trp1::hisG, ura3::hisG, leu2::hisG, ho::LYS2 CLB1-myc9::klTRP1,pClb2-Cdc5::His,cdc20::pCLB2-CDC20::kanMX6*	p_{CLB2}*CDC20* p_{CLB2}*CDC5 CLB1-MYC*	3
	P_{GAL}CLB1 P_{GAL}CDC5 P_{CUP1}NDT80		
2895	*SK1 MATa/alpha, ho::LYS2, ADE2, ura3, leu2::hisG, trp1::hisG, his3::hisG,lys2 ndt80:pCUP1-Ndt80::KanMX6, pGPD1-GAL4(848).ER::URA3 Estrogen Receptor-GAL4TF (URA3), pGal-CLB1 (His)*	P_{CUP1}*NDT80 GAL4-ER* P_{GAL}*CLB1*	3
2907	*SK1 MATa/alpha, ho::LYS2, ADE2, ura3, leu2::hisG, trp1::hisG, his3::hisG,lys2 ndt80:pCUP1-Ndt80::KanMX6, pGPD1-GAL4(848).ER::URA3 Estrogen Receptor-GAL4TF (URA3) heterozygous:pGal-CLB1 (His)*	P_{CUP1}*NDT80 GAL4-ER het:* P_{GAL}*CLB1*	3
3013	*SK1 MATa/alpha, ho::LYS2, ADE2, ura3, leu2::hisG, trp1::hisG, his3::hisG,lys2 ndt80:pCUP1-Ndt80::KanMX6, pGPD1-GAL4(848).ER::URA3 Estrogen Receptor-GAL4TF (URA3) heterozygous:pGal-CLB1 (His),pGal Cdc5*	P_{CUP1}*NDT80 PGPD1GAL4-ER het:* P_{GAL}*CLB1* P_{GAL}*CDC5*	3
	Strains for effects of localisation, *CLB1-HA*		
2567	*MATa/alpha ura3 lys2 ho::LYS2 arg4Δ(eco47III-hpa1) clb3::natMX4 clb4::hphMX4*	*clb3Δ clb4Δ*	5
2615	*"SK1 MATa/alpha, ho::LYS2,ura3,leu2::hisG,his3::hisG,trp1::hisG clb1-del:His*	*clb1Δ*	5
3078	*"SK1 MATa/alpha, LYS2ura3,leu2::hisG,his3::hisG,trp1::hisG x ura3,lys2,LYS2,leu2::hisG,his3-11,15,trp1ΔFA::hisG cdc28-as1,Clb1-NLS,NLS-HA::His,cdc20::pCLB2-CDC20::kanMX6"*	*cdc28-as* p_{CLB2}*CDC20 CLB1-NLS*$_2$*-HA*	5
3073	*"SK1 MATa/alpha, LYS2ura3,leu2::hisG,his3::hisG,trp1::hisG x ura3,lys2,LYS2,leu2::hisG,his3-11,15,trp1ΔFA::hisG cdc28-as1,CLB1-HA6:HIS3,cdc20::pCLB2-CDC20::kanMX6"*	*cdc28-as* p_{CLB2}*CDC20 CLB1-HA*	5
3081	*"SK1 MATa/alpha, LYS2ura3,leu2::hisG,his3::hisG,trp1::hisG x ura3,lys2,LYS2,leu2::hisG,his3-11,15,trp1ΔFA::hisG cdc28-as1,Clb1-NES,NES-HA::HIS3,cdc20::pCLB2-CDC20::kanMX6"*	*cdc28-as* p_{CLB2}*CDC20 CLB1-NES*$_2$*-HA*	5
2858	*SK1 MATa/alpha, ho::LYS2, ADE2,his3::hisG,trp1::hisG,leu2::hisG,ura3, PDS1-myc18::TRP(K.lactis),Clb1-NLS,NLS-HA::His*	*PDS1-MYC CLB1-NLS*$_2$*-HA*	5
2542	*SK1 MATa/alpha, ho::LYS2,ADE2,his3::hisG,trp1::hisG,leu2::hisG,ura3, PDS1-myc18::TRP(K.lactis),CLB1-HA6:HIS3*	*PDS1-MYC CLB1-HA*	5
2550	*SK1 MATa/alpha, ho::LYS2,ADE2,his3::hisG,trp1::hisG,leu2::hisG,ura3, PDS1-myc18::TRP(K.lactis),Clb1-NES,NES-HA::HIS3*	*PDS1-MYC CLB1-NES*$_2$*-HA*	5
2881	*SK1 MATa/alpha, ho::LYS2,ADE2,his3::hisG,trp1::hisG,leu2::hisG,ura3, PDS1-myc18::TRP(K.lactis),Clb1-NLS,NLS-HA::His,cdc20::pCLB2-*	p_{CLB2}*CDC20 CLB1-NLS*$_2$*-HA*	5

	CDC20::kanMX6"		
2674	*SK1 MATa/alpha, ho::LYS2,ADE2,his3::hisG,trp1::hisG,leu2::hisG,ura3, CLB1-HA6:HIS3,cdc20::pCLB2-CDC20::kanMX6*	p_{CLB2}*CDC20 CLB1-HA*	5
2640	*"SK1 MATa/alpha, ho::LYS2,ura3,leu2::hisG,his3::hisG,trp1::hisG cdc20::pCLB2-CDC20::kanMX6",Clb1-NES,NES-HA::HIS3*	p_{CLB2}*CDC20 CLB1-NES*$_2$*-HA*	5
2272	*"SK1 MAT a /MAT alpha his3::hisG, trp1::hisG, ura3::hisG, leu2::hisG, del spo12::KanMX*	*spo12Δ*	5, 6
2952	*"SK1 Mat a/alpha his3::hisG,trp1::hisG,ura3::hisG,leu2::hisG del spo12::KanMX,Clb1-NLS,NLS-HA::His*	*Spo12Δ CLB1-NLS*$_2$*-HA*	5
2946	*"SK1 Mat alpha/a his3::hisG,trp1::hisG,ura3::hisG,leu2::hisG del-spo12::KanMX,CLB1-HA6:HIS3*	*spo12Δ CLB1-HA*	5
2949	*"SK1 Mat a/alpha his3::hisG,trp1::hisG,ura3::hisG,leu2::hisG del-spo12::KanMX,Clb1-NES,NES-HA::HIS3*	*spo12Δ CLB1-NES*$_2$*-HA*	5
2237	*SK1 MATa / MAT alpha, ho::LYS2, lys2, ADE2, his3::hisG, trp1::hisG, ura3, leu2::hisG, esp1-2*	*esp1-ts*	5, 6
3007	*SK1 MATa/alpha, ho::LYS2,lys2,ADE2,his3::hisG,trp1::hisG,ura3,leu2::hisG, esp1-2,Clb1-NLS-HA:His*	*esp1-ts CLB1-NLS*$_2$*-HA*	5
3006	*SK1 MATa/alpha, ho::LYS2,lys2,ADE2,his3::hisG,trp1::hisG, ura3,leu2::hisG, esp1-2,CLB1-HA6:HIS3*	*esp1-ts CLB1-HA*	5
3008	*SK1 MATalpha/a, ho::LYS2,lys2,ADE2,his3::hisG,trp1::hisG,ura3,leu2::hisG, esp1-2,Clb1-NES,NES-HA::HIS3*	*esp1-ts CLB1-NES*$_2$*-HA*	5
2267	*SK1 MATa / MAT alpha, ho::LYS2,ura3,leu2::hisG,trp1::hisG,his3::hisG,?lys2? slk19::HIS3MX6*	*slk19*	5, 6
2937	*SK1 MATalpha/a, ho::LYS2,ADE2,his3::hisG,trp1::hisG,leu2::hisG,ura3, Clb1-NLS,NLS-HA::His,slk19::HIS3MX6*	*slk19 CLB1-NLS*$_2$*-HA*	5
2943	*SK1 MATa, ho::LYS2,ura3,leu2::hisG,trp1::hisG,his3::hisG,?lys2? slk19::HIS3MX6, CLB1-HA6:HIS3*	*slk19 CLB1-HA*	5
2926	*SK1 MATa/alpha, ho::LYS2,ura3,leu2::hisG,trp1::hisG,his3::hisG,?lys2? slk19::HIS3MX6, Clb1-NES,NES-HA : HIS3*	*slk19 CLB1-NES*$_2$*-HA*	5
2119	*SK1 MATa/alpha ho::LYS2,lys2,ADE2,his3::hisG,trp1::hisG,ura3,leu2::hisG, net1Δ::HIS5,trp1::NET1-TEV-myc9::TRP1,ccdc20:pClb2-Cdc20-KanMx6*	p_{CLB2}*CDC20 net1Δ NET1-TEV-MYC*	5
2120	*SK1 MATa/alpha ho::LYS2,lys2,ADE2,his3::hisG,trp1::hisG,ura3,leu2::hisG, net1Δ::HIS5,trp1::NET1-TEV-myc9::TRP1,cdc55:pClb2-Cdc55-KanMX6,cdc20:pClb2-Cdc20-KanMx6,*	p_{CLB2}*CDC20* p_{CLB2}*CDC55 net1Δ NET1-TEV-MYC*	5
3057	*SK1 MATa/alpha ho::LYS2,lys2,ADE2,his3::hisG,trp1::hisG,ura3,leu2::hisG, net1Δ::HIS5,trp1::NET1-TEV-myc9::TRP1,cdc55:pClb2-Cdc55-KanMX6,cdc20:pClb2-Cdc20-KanMx6,CLB1-NLS,NLS-HA6:HIS3*	p_{CLB2}*CDC20* p_{CLB2}*CDC55 net1Δ NET1-TEV-MYC CLB1-NLS*$_2$*-HA*	5
3015	*SK1 MATa/alpha ho::LYS2,lys2,ADE2,his3::hisG,trp1::hisG,ura3,leu2::hisG, net1Δ::HIS5,trp1::NET1-TEV-myc9::TRP1,cdc55:pClb2-Cdc55-KanMX6,cdc20:pClb2-Cdc20-KanMx6,CLB1-HA6:HIS3*	p_{CLB2}*CDC20* p_{CLB2}*CDC55 net1Δ NET1-TEV-MYC CLB1-HA*	5
3016	*SK1 MATa/alpha ho::LYS2,lys2,ADE2,his3::hisG,trp1::hisG,ura3,leu2::hisG, net1Δ::HIS5,trp1::NET1-TEV-myc9::TRP1,cdc55:pClb2-Cdc55-KanMX6,cdc20:pClb2-Cdc20-KanMx6,CLB1-NES,NES-HA6:HIS3 NET1-*	p_{CLB2}*CDC20* p_{CLB2}*CDC55 net1Δ NET1-TEV-MYC CLB1-*	5

	TEV-myc9::TRP1	*NES_2-HA*	
Wild type and synchronised strains, strains tagged for live cell imaging			
1738	*SK1 MATa/ MAT alpha, ho::LYS2,ura3, leu2::hisG,trp1::hisG,his3::hisG,lys2*	*Wild type*	35
1904	*SK1 MATa/MAT alpha, ho::LYS2, ADE2, ura3, leu2::hisG, trp1::hisG, his3::hisG,?lys2?" ura3::pGPD1-GAL4(848).ER::URA3 Estrogen Receptor-GAL4TF (URA3), proGAL1-NDT80 (TRP1)*	*PGPD1GAL4-ER P_{GAL}NDT80*	6
1983	*"SK1 MATa / MAT alpha, ho::LYS2, ADE2, ura3, leu2::hisG, trp1::hisG, his3::hisG,lys2 ndt80:pCUP1-Ndt80::KanMX6*	*P_{CUP1}NDT80*	6
2007	*SK1 MATa/alpha, ho::LYS2, ADE2, ura3, leu2::hisG, trp1::hisG, his3::hisG,?lys2?" ura3::pGPD1-GAL4(848).ER::URA3 Estrogen Receptor-GAL4TF (URA3), proGAL1-NDT80 (TRP1), his3::HIS3p-GFP-TUB1-HIS3 Het::CDC14-GFP-LEU2, leu2:URA3p-tetR-td-Tomato::LEU2, ura3::tetOx224-URA3*	*CDC14-GFP TUBULIN-GFP TetR-Tomato TetOx(het)* *PGPD1GAL4-ER P_{GAL}NDT80*	6
***CDC15* mutants**			
2050	*SK1 MATa/alpha, ho::LYS2, ADE2, ura3, leu2::hisG, trp1::hisG, his3::hisG,?lys2?" ura3::pGPD1-GAL4(848).ER::URA3 Estrogen Receptor-GAL4TF (URA3), TRP1: gal CDC15HA-7A*	*PGPD1GAL4-ER cdc15-7A-HA*	6
2161	*SK1 MATa / MATalpha, ho::LYS2, ADE2, ura3, leu2::hisG, trp1::hisG, his3::hisG,?lys2?" ura3::pGPD1-GAL4(848).ER::URA3 Estrogen Receptor-GAL4TF (URA3)*	*PGPD1GAL4-ER*	6
2053	*SK1 MATa/alpha, ho::LYS2, ADE2, ura3, leu2::hisG, trp1::hisG, his3::hisG,?lys2?" ura3::pGPD1-GAL4(848).ER::URA3 Estrogen Receptor-GAL4TF (URA3), proGAL1-NDT80 (TRP1), TRP1: gal CDC15HA-7A*	*PGPD1GAL4-ER P_{GAL}cdc15-7A-HA P_{GAL}NDT80*	6
***CDC14* mutants**			
2178	*SK1 MATa/alpha, ho::LYS2,ADE2,ura3,leu2::hisG,trp1::hisG,his3::hisG,?lys2?" ura3::pGPD1-GAL4(848).ER::URA3 Estrogen Receptor-GAL4TF (URA3), his3::pGal-cdc14-TAB6*	*PGPD1GAL4-ER P_{GAL}cdc14TAB6*	6
2210	*SK1 MATa/alpha, ho::LYS2, ADE2, ura3, leu2::hisG, trp1::hisG, his3::hisG,?lys2?" Homozygous::his3: pGal-cdc14-TAB6, ura3::pGPD1-GAL4(848).ER::URA3 Estrogen Receptor-GAL4TF (URA3)*	*ho:PGPD1GAL4-ER P_{GAL}cdc14TAB6*	6
2212	*SK1 MATa/alpha, ho::LYS2, ADE2, ura3, leu2::hisG, trp1::hisG, ,?lys2?" Ho::pGPD1-GAL4(848).ER::URA3 Estrogen Receptor-GAL4TF (URA3) Het::his3: pGal-cdc14-TAB6*	*ho:PGPD1GAL4-ER het:P_{GAL}cdc14TAB6*	6
2214	*SK1 MATa/alpha, ho::LYS2, ADE2, ura3, leu2::hisG, trp1::hisG, ,?lys2?" heterozygous for his3: pGal-cdc14-TAB6, ura3::pGPD1-GAL4(848). pGPD1-GAL4(848).ER::URA3 Estrogen Receptor-GAL4TF (URA3)*	*het:PGPD1GAL4-ER P_{GAL}cdc14TAB6*	6
2285	*" SK1 MATa/alpha, ho::LYS2, ADE2, ura3, leu2::hisG, trp1::hisG, ,?lys2?" cdc20::Pclb2-CDC20::kanMX6, ura3::Pgpd-GAL4(484).ER::URA3, heterozygous for his3;pGAL-cdc14 (TAB6)-HIS3*	*P_{CLB2}CDC20 PGPD1GAL4-ER het:P_{GAL}cdc14TAB6*	6
2288	*" SK1 MATa/alpha, ho::LYS2, ADE2, ura3, leu2::hisG, trp1::hisG, ,?lys2?"*	*P_{CLB2}CDC20 PGPD1GAL4-ER*	6

	cdc20::Pclb2-CDC20::kanMX6, ura3::Pgpd-GAL4(484).ER::URA3		
2314	*"SK1 MATa/alpha, ho::LYS2, ADE2, ura3, leu2::hisG, trp1::hisG, his3::hisG,?lys2?" cdc14-BP12A-GFP::HIS3*	*cdc14-BP12A*	6
2353	*"SK1 MATa/alpha, ho::LYS2, ADE2, ura3, leu2::hisG, trp1::hisG, his3::hisG,?lys2?" cdc14-BP12A-GFP::HIS3,cdc14:pCLB2-CDC14::HIS3 (S.pombe)*	*cdc14-BP12A* P_{CLB2}*CDC14*	6
2300	*SK1 MATa/alpha, ho::LYS2, ADE2, ura3, leu2::hisG, trp1::hisG, his3::hisG,?lys2?" cdc14-PS12E-GFP::HIS3*	*cdc14-PS12E*	6
2341	*"SK1 MATalpha, ho::LYS2, ADE2, ura3, leu2::hisG, trp1::hisG, his3::hisG,?lys2?" cdc14-PS12E-GFP::HIS3, cdc14:pCLB2-CDC14::HIS3 (S.pombe)*	*cdc14-PS12E* P_{CLB2}*CDC14*	6
Remaining FEAR and *ime2-as* mutants			
	ime2-as alone	*ime2-as*	6
2362	*"SK1 MATa/alpha, ho::LYS2, ADE2, ura3, leu2::hisG, trp1::hisG, his3::hisG,?lys2?" ime2-as1-myc::TRP1(M146G),esp1-2*	*esp1-2 ime2-as*	6
2320	*SK1 MATa/alpha, ho::LYS2,ura3,leu2::hisG,trp1::hisG,his3::hisG,?lys2? slk19::HIS3MX6, ime2-as1-myc::TRP1(M146G)*	*slk19 ime2-as*	6
2343	*"SK1 MATa/alpha, ho::LYS2, ADE2, ura3, leu2::hisG, trp1::hisG, his3::hisG,?lys2?" net1-6CDK-TEV-myc9::TRP1,net1Δ::his5, ime2-as1-myc::TRP1(M146G)*	*net1-6CDK-MYC net1Δ ime20-as-MYC*	6
2518	*"SK1 MATa/alpha, ho::LYS2, ADE2, ura3, leu2::hisG, trp1::hisG, his3::hisG,?lys2?"*	*net1-6CDK-MYC net1Δ*	6
2345	*"SK1 MATa/alpha, ho::LYS2,ADE2,ura3,leu2::hisG,trp1::hisG,his3::hisG,?lys2?" ime2-as1-myc::TRP1(M146G), net1Δ::HIS5, trp1::NET1-TEV-myc9::TRP1*	*NET1-MYC net1Δ ime2-as-MYCΔ*	6

Table 2-4 Yeast strains used in this project

2.3.2 Bacterial strains

Escherichia coli strain DH5α was used for plasmid construction and amplification.

3 Meiosis-specific regulation of Clb1

3.1 Cyclin Clb1 is located in the nucleus and modified by phosphorylation specifically during metaphase I

Clb1 is the most important B-cyclin for meiosis: the deletion of Clb1 produces the most severe effect on sporulation and only those double deletions that include *clb1Δ* cause a substantial decrease in tetrads (Dahmann et al., 1995; Grandin and Reed, 1993). Reports differ in the exact phenotype of Clb1 deletion: Grandin *et al.* reported a result of 70% of one-spored asci with a few dyads, triads and tetrads, while Dahman *et al*. indicated that a similar proportion of their *clb1Δ* strain failed to form an ascus at all. However, the importance of Clb1 over Clb3 and Clb4 is consistent. We have also observed that Clb1 deletion had a greater effect on sporulation compared to deletion of the other B-type cyclins (Figure 3-1 A, B). Around 18% of *clb1Δ* cells still formed tetranucleates, so it seems that no individual cyclin is entirely essential for successful meiosis, but rather that cyclin redundancy operates during meiosis as well as mitosis. We found that only double cyclin deletions that included *clb1Δ* had a great effect on sporulation (Figure 3-1 A, C), although even in those cases some tetrads were produced. In the quadruple deletion, *clb1Δ*, *clb6Δ*, *clb3Δ clb4Δ* no tetrads were produced (Figure 3-1 A, B).

Of particular interest in understanding meiosis is the regulation of cyclins during the transition between meiosis I and meiosis II, in comparison to the end of mitosis. During the meiosis I-II transition, CDK activity must be reduced sufficiently to disassemble the meiosis I spindle and complete exit from meiosis I. DNA replication is not reinitiated during the second Clb-CDK activity peak, suggesting that the drop in Clb-CDK activity does not allow replication origin

relicensing. The two meiotic divisions are directed by two different cyclins, Clb1 in meiosis I and Clb3 in meiosis II (Carlile and Amon, 2008).

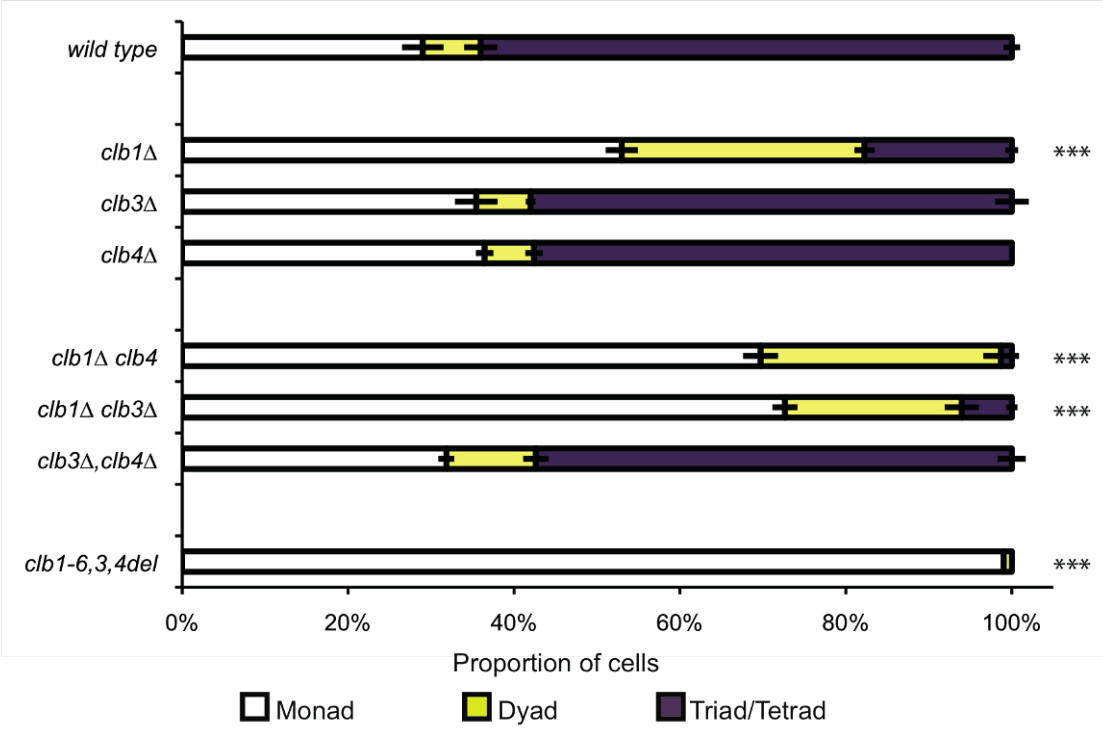

Figure 3-1 ***Sporulation efficiency of cyclin deletion strains.*** *Strains bearing cyclin deletions were allowed to sporulate on SPOVB plates at 30˚C for 48 hours.* ***A*** *Wild type strain.* ***B*** *Single deletions of cyclins.* ***C*** *Double deletions of cyclins.* ***D*** *Quadruple deletion of cyclins. In each case, three sets of 100 cells were examined for nuclear divisions. Percentage of cells forming dyads, tetrads and monads or mononucleates were calculated. Asterisks show significance calculated using Mann Whitney U test (***p<0.001) in comparison to the wild type.*

Clb1 showed an unidentified gel shift during its active period in meiosis I (Carlile and Amon, 2008), and has also been observed to localise to the nucleus during meiosis I (Buonomo et al., 2003; Carlile and Amon, 2008; Marston et al., 2003). Clb1 was present but inactive during meiosis II (Carlile and Amon, 2008). The functional significance of Clb1 modification and nuclear localisation during meiosis is unknown. In other species, cyclin import depends on phosphorylation, for example in *Xenopus* and human cells (Hagting et al., 1999; Li et al., 1997). The modification of Clb1 may also be phosphorylation and may drive nuclear import.

Export of Clb1 towards the end of meiosis I was found to depend on the genes of the FEAR network, suggesting that Cdc14 drove the export of Clb1 from the nucleus (Buonomo et al., 2003). If, as suggested above, the gel shift is due to a

phosphorylation that directs nuclear import, Cdc14 phosphatase may inactivate the nuclear localisation signal and cause Clb1 export by dephosphorylating Clb1.

It is, therefore, worthwhile to determine the effect of ectopic Cdc14 release during meiosis I on Clb1 localisation and modification. Cells in which Cdc55 is depleted during meiosis ectopically release Cdc14, preventing them from forming spindles and completing nuclear divisions (Kerr et al., 2011). Cdc55 depletion was used to examine the effect of ectopic Cdc14 release on Clb1 modification and nuclear localisation.

In this chapter, we examined the effect of premature activation of FEAR and of a metaphase arrest on the modification and localisation of Clb1 during meiosis (Sections 3.2 and 3.3). We identified the nature of the modification as phosphorylation (Section 3.4).

3.2 Clb1-Myc modification and nuclear localisation during meiosis and in Cdc55 meiotic-null arrest

To deplete a protein essential for mitosis during meiosis, the relevant gene can be placed under the control of the mitosis-specific *CLB2* promoter. Clb2 is not expressed during meiosis (Grandin and Reed, 1993) but is expressed in mitosis, so cells are viable.

CLB1-MYC$_9$ and *CLB1-MYC*$_9$ P_{CLB2}*CDC55* cultures were induced to enter meiosis and samples were taken hourly for in situ immunofluorescent imaging and bi hourly for western blot analysis of whole cell extracts. Cells expressing *CDC55* under the mitosis-specific *CLB2* promoter failed to undergo meiotic divisions (Figure 3-2 A). Clb1 is expressed in both strains (Figure 3-2 B) suggesting both have passed through pachytene and entered metaphase I.

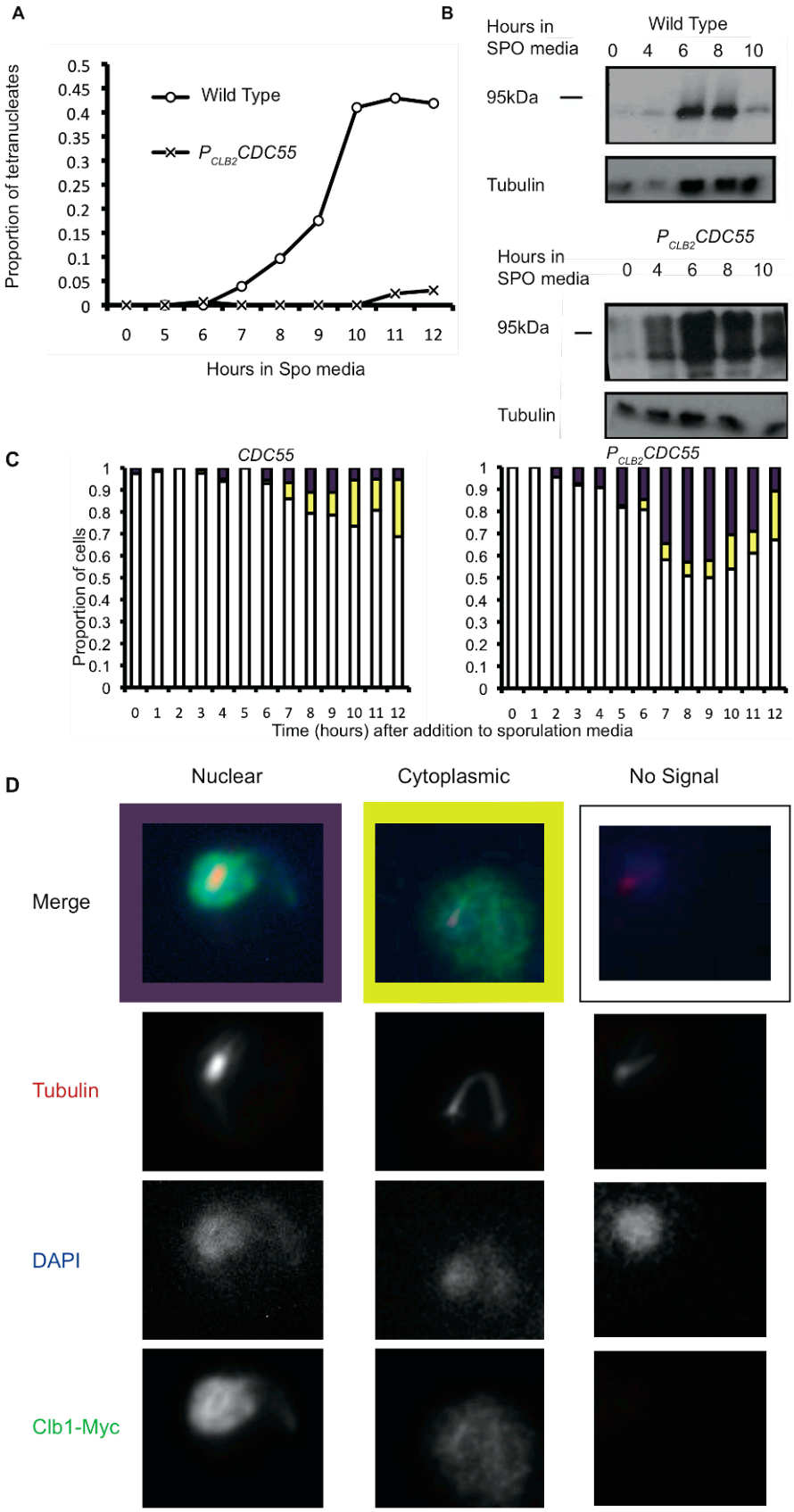

Figure 3-2 ***Clb1 localisation and modification in Cdc55-depleted strains.*** *Cultures of* CDC55 *and* P_{CLB2}CDC55 *cultures were induced to undergo meiosis by resuspension in sporulation media (SPO media). Hourly aliquots of sporulating cells were taken after transfer to SPM for* in situ

immunofluorescence. ***A****: nuclear division was scored by DAPI staining.* ***B****: Gel mobility of Clb1-Myc$_9$ was assayed by subjecting whole cell extracts to SDS-PAGE on an 0.8% gel followed by western blot analysis using anti-myc. Blots were also probed with anti-tubulin.* ***C:*** *Cells were examined for Clb1-Myc$_9$ localisation by* in situ *immunofluorescence. Proportion of cells with Clb1 concentrated in the nucleus (purple), Clb1 distributed in the cytoplasm (yellow) and no detectable Clb1 (white) are indicated. 100 cells were counted for each time point.*

Clb1 in the wild type control samples showed no clear gel shift (Figure 3-2 B). Since samples were taken for TCA extracts every two hours, the gel shift may have been missed due to the sparse sampling. However, smearing and higher Clb1-Myc$_9$ levels were observed at 6 and 8 hour samples (Figure 3-2 B). In contrast, *CLB1-MYC$_9$ P$_{CLB2}$CDC55* cells showed a sustained gel shift. The gel shift appeared as two distinct bands; the lower (unmodified) protein band did not disappear, indicating that only a proportion of the protein was modified in such a way as to produce the gel shift. The gel shift was also present in the *P$_{CLB2}$CDC55* samples an hour earlier than the smearing appeared in wild-type strain. This may show that Cdc55 countered the modification and in absence of Cdc55, the modification could arise earlier. Alternatively, cells lacking Cdc55 may have entered meiosis early in comparison to wild type cells.

The localisation of Clb1 was examined over the time course by immunofluorescent imaging of fixed cells (Figure 3-2 C, D). In the control strain, Clb1-Myc$_9$ was initially nuclear, with nuclear localisation peaking at 8 hours. Clb1 was then increasingly cytoplasmic up to the 12 hour end point, though at each time point most cells showed no signal. This is possibly due to poor synchrony of the culture. In *CLB1-MYC$_9$ P$_{CLB2}$CDC55* cells, all time points up to 11 hours had a greater proportion of nuclear than cytoplasmic Clb1 bearing cells. However, both nuclear localisation, and proportion of cells bearing any Clb1 signal at all, diminished after 9 hours. Nuclear localisation of Clb1, therefore, appeared to be related to the modification causing the gel shift; both were sustained in the case of a *P$_{CLB2}$CDC55* metaphase I arrest, despite the associated Cdc14 release (Kerr et al., 2011). These results suggest that Cdc14 might not be sufficient for the loss of the modification or for nuclear export of Clb1 following meiosis I. These localisation results, and others in this chapter, have to be considered with the fact that a control to detect non-specific binding of the antibodies was not performed on the fixed cells.

P_{CLB2}CDC55 strains arrest in a metaphase I-like state, after DNA replication; however, spindles do not form and Clb3 is also expressed at a later stage (Kerr et al., 2011). This indicated that depleting Cdc55 in meiosis does not result in a simple metaphase arrest, as seen in Cdc20 depletion. Instead, the nuclear divisions and biochemical regulatory networks of meiosis are decoupled, leading to the prevention of some cell cycle events and the permitting of others. The sustained modification in the metaphase I–like arrest raises the question of what happens to Clb1 in a metaphase arrest.

In the case of Cdc20 depletion in meiosis, the APC is not activated even though the spindle assembly checkpoint may be inactive, and the cell can't enter anaphase. In this case, $PP2A^{Cdc55}$ would not be inactivated by the FEAR network. With respect to $PP2A^{Cdc55}$ activity, cells arrested in metaphase I by Cdc20 depletion would show the opposite result to those arrested by Cdc55 depletion. The following experiment also considers the possibility that the above results indicate that Clb1 modification is a phosphorylation that is removed by $PP2A^{Cdc55}$, and thus retained in *P_{CLB2}CDC55* cells.

We assessed the Clb1-Myc_9 behaviour in *P_{CLB2}CDC20* cells and *P_{CLB2}CDC20 P_{CLB2}CDC55* cells.

3.3 Clb1-Myc modification and nuclear localisation during metaphase I arrest

Four strains were assessed here: *CDC20 CDC55, P_{CLB2}CDC20 CDC55, CDC20 P_{CLB2}CDC55,* and *P_{CLB2}CDC20 P_{CLB2}CDC55,* all bearing *CLB1-MYC_9*. Strains were induced to enter meiosis and samples were taken for *in situ* immunofluorescent imaging and western blot analysis hourly.

Cdc20 depletion arrests cells in metaphase I, preventing the onset of anaphase through the prevention of both spindle elongation and cyclin down-regulation. We found that *P_{CLB2}CDC20* cells were healthier than *P_{CLB2}CDC55* cells, forming largely monads, and a few dyads (Figure 3-3 A). Both strains in which Cdc55 was depleted did not form dyads or tetrads.

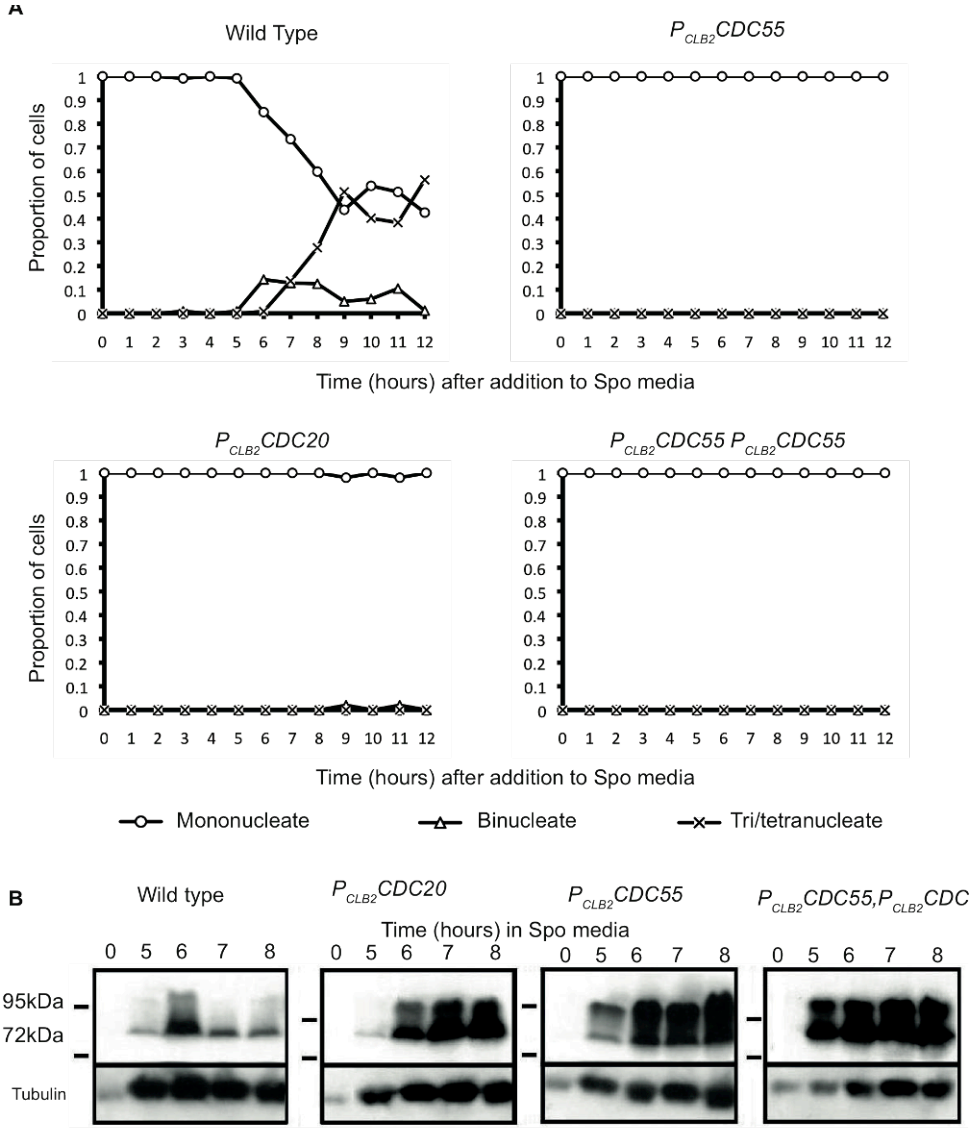

Figure 3-3 ***Clb1 modification in cells undergoing meiosis, depleted of Cdc20 and Cdc55.*** *Cultures of wild type,* P_{CLB2}CDC55, P_{CLB2}CDC20 *and* P_{CLB2}CDC55 P_{CLB2}CDC20 *cells were induced to undergo meiosis by resuspension in SPO media. Samples were taken for* in situ *immunofluorescence hourly.* ***A:*** *Nuclear division was scored by DAPI staining. 100 cells were counted for each time point.* ***B:*** *Gel mobility of Clb1-Myc*$_9$ *was assayed by subjecting whole cell extracts to SDS-PAGE followed by western blot analysis using anti-myc. Blots were also probed with anti-tubulin.*

The presence of the sustained gel shift was confirmed in $P_{CLB2}CDC20$ cells, and in $P_{CLB2}CDC20$ $P_{CLB2}CDC55$ cells, showing that the retention of the modification was independent of $PP2A^{Cdc55}$ inactivity. The tighter sampling allowed us to see the gel shift in the wild type cells, which occurred at the 6 hour time point (Figure 3-3 B).

Samples of fixed cells from the same time course were probed for Clb1-Myc$_9$. The results showed that the Clb1-Myc$_9$ nuclear localisation was also sustained in *P_{CLB2}CDC20* cells, and in *P_{CLB2}CDC20 P_{CLB2}CDC55* cells (Figure 3-4).

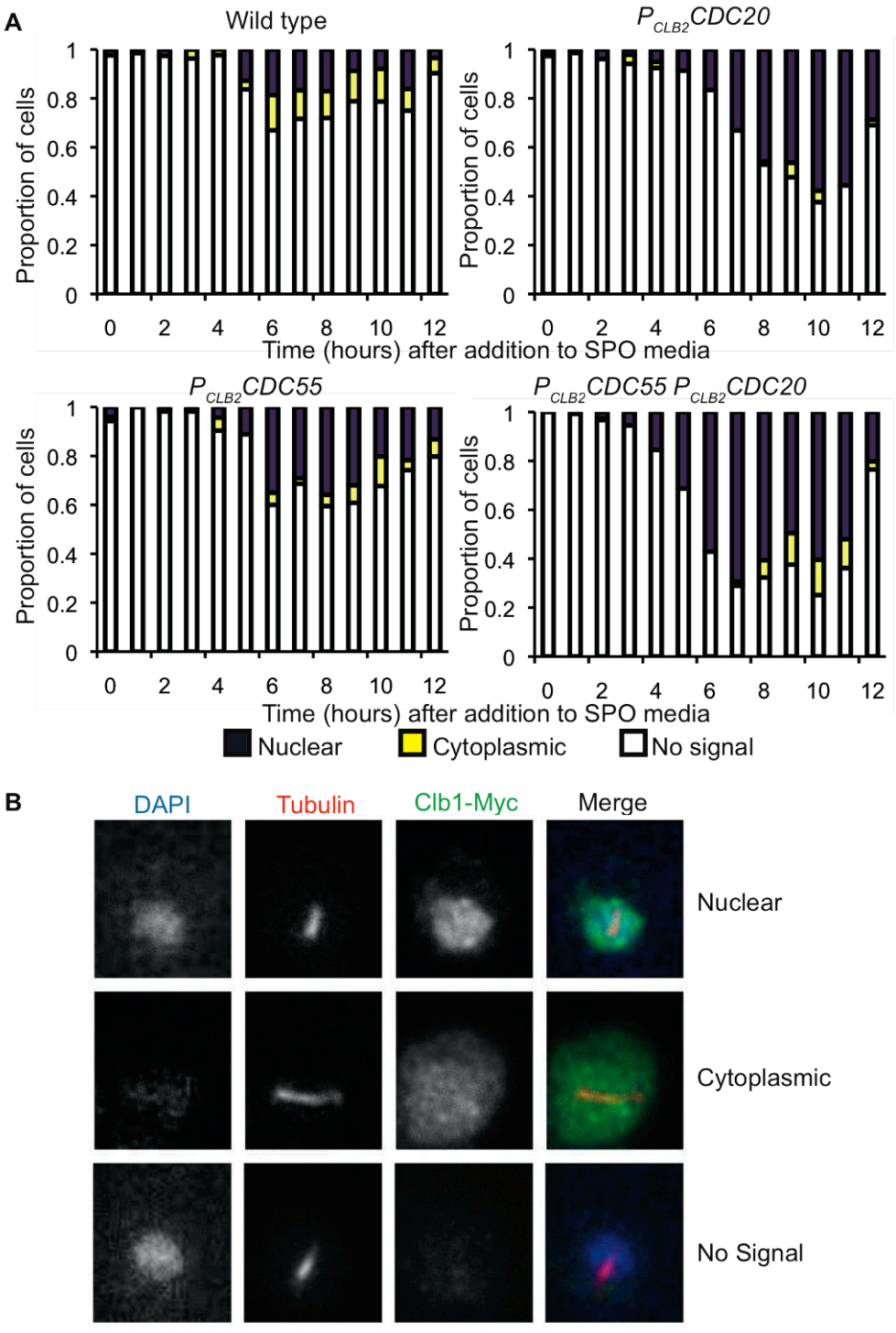

Figure 3-4 ***Clb1 localisation in cells undergoing meiosis, depleted of Cdc20 and Cdc55 A:*** *Cells were examined for Clb1-Myc$_9$ localisation by* in situ *immunofluorescence. Proportion of cells with Clb1 concentrated in the nucleus (purple), Clb1 distributed in the cytoplasm (yellow) and no Clb1*

signals (white) are indicated. 100 cells were counted for each time point. ***B:*** *Example images from these strains. These cells are from the same time course as in Figure 3-3.*

Closer sampling times allowed us to detect the Clb1 gel shift in the wild-type cells, evident at 6 hours. Wild type Clb1 nuclear localisation peaked at 6-7 hours, which coincided with the point at which a distinct upper band indicated the presence of the modification. The timing of the gel shift in the control strain coincided with the greatest number of cells being in metaphase I, as judged by nuclear division (Figure 3-3).

The ability to reliably maintain Clb1 in a modified state gave us the opportunity to study it at further length. Cells undergoing a normal meiosis are not well synchronised. The Clb1 gel shift may be apparent on the gel for two or three time points, or may be missed between them, due to day-to-day variance in the timing and synchronicity of cultures undergoing meiosis.

Cdc55 has roles in mitosis and stress responses (Wang and Burke, 1997), and P_{CLB2}*CDC55* cells, despite being healthier than the *cdc55Δ* cells, are less successful in entering meiosis than wild-type cells or P_{CLB2}*CDC20* cells. Therefore, further work requiring a sustained Clb1 gel shift was done in P_{CLB2}*CDC20* rather than P_{CLB2}*CDC55* cells.

3.4 The gel shift of Clb1 is caused by its phosphorylation

Clb1-Myc$_9$ was purified from metaphase I-arrested cells and subjected to a phosphatase assay. Cell extracts from cultures bearing P_{CLB2}*CDC20* were taken 7 hours into sporulation medium and then subjected to an optimised immunoprecipitation protocol to extract modified Clb1 (Section 2.2.4.7). The protein was then incubated in the presence or absence of alkaline protein phosphatase.

After immunoprecipitation, the modification appeared as a smear between the upper and lower bands, as seen in the IP lane (pre-incubation, Figure 3-5). This could be due to partial loss of the modification during the immunoprecipitation protocol. After incubation in phosphatase buffer with no phosphatase, the sample showed no change in the smeared gel shift. In contrast, after incubation with phosphatase, the smear disappeared and the lower band appeared heavier, indicating that the slower running forms had contracted into one faster running band (Figure 3-5).

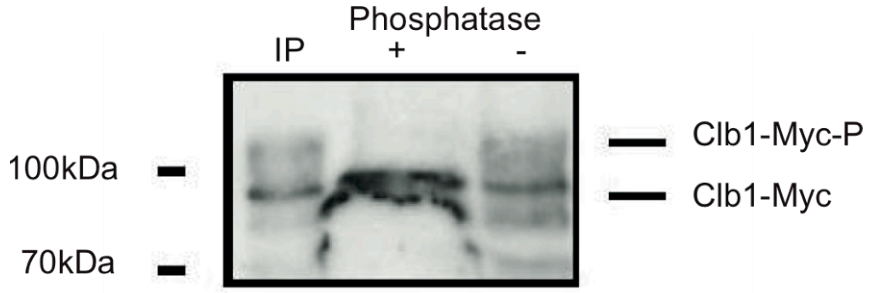

Figure 3-5 ***Clb1 modification is phosphorylation.*** *Modified Clb1-Myc$_9$ was immunoprecipitated from* P_{CLB2}CDC20 *cells 7 hours into sporulation media (IP lane). Precipitated Clb1-Myc$_9$ was incubated with (+) or without (-) lambda protein phosphatase for 45 minutes. Gel mobility of Clb1-Myc$_9$ was assayed by subjecting whole cell extracts to SDS-PAGE followed by western blot analysis using anti-myc.*

This is a definite indication that the modification is a phosphorylation. There may be phosphorylation at multiple sites, if the smearing after immunoprecipitation indicates partial dephosphorylation during the protocol.

3.5 Meiosis-specificity of the phosphorylation and nuclear localisation of Clb1

We have found a phosphorylation of Clb1 during metaphase of meiosis, which appears to correlate with its nuclear localisation. Nuclear localisation has been reported in mitotic cells in a different strain (Bailly et al., 2003). We investigated the meiosis-specificity of both the nuclear localisation and phosphorylation of Clb1, using a mitotic metaphase arrest time course was performed to determine the meiosis-specificity of both Clb1 phosphorylation and the nuclear localisation.

P_{MET}CDC20 CLB1-MYC$_9$ cells were arrested in mitotic metaphase by resuspension in YEPD media supplemented with methionine, preventing *CLB2* expression (Section 2.2.1.3). Fixed cells were analysed by immunofluorescent imaging and whole cell extracts by western blot analysis to examine Clb1-Myc$_9$ location and gel mobility. Mitotic metaphase arrest was confirmed by the increase in metaphase spindles (Figure 3-6 A).

Cells were examined for localisation of Clb1-Myc$_9$ localisation (Figure 3-6 B, C]. Clb1-Myc$_9$ appeared to be present in the cytoplasm during the metaphase

arrest. However, the nucleus was not seen as a darker patch so Clb1 was not excluded from the nucleus during mitosis. Clb1-Myc$_9$ gel mobility was examined using whole cell extracts. Clb1-Myc$_9$ did not acquire the gel shift seen in metaphase I (Figure 3-6 D).

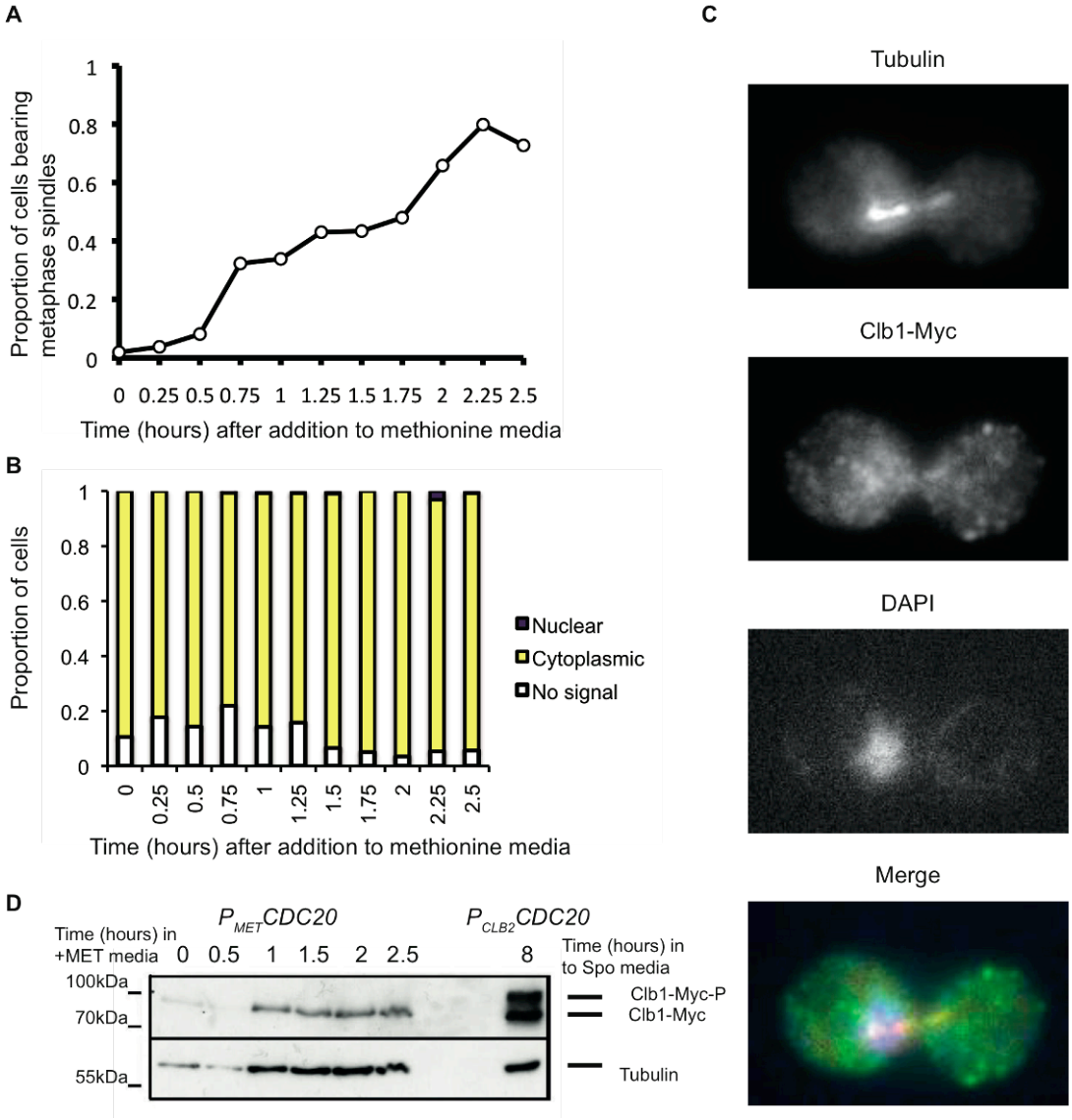

Figure 3-6 ***Clb1 is not modified or concentrated in the nucleus in metaphase of mitosis.*** *A culture of* P$_{MET}$CDC20 *cells was arrested in metaphase by resuspension in high methionine media. Hourly samples of cells were fixed for analysis by* in situ *immunofluorescence.* ***A*** *Fixed cells were probed for tubulin and metaphase spindles were counted. 100 cells were counted at each time point.* ***B*** *Fixed cells were probed for Myc antibody to determine Clb1-Myc$_9$ localisation. Proportion of cells with Clb1 concentrated in the nucleus (purple), Clb1 distributed in the cytoplasm (yellow) and no Clb1 signals (white) are indicated.* ***C*** *Example image of mitotic cell* ***D*** *Gel mobility of Clb1-Myc$_9$ was assayed by subjecting whole cell extracts to SDS-PAGE followed by western blot analysis using anti-myc. Blots were also probed with anti-tubulin. A sample 8 hours into a meiotic metaphase arrest* ***(****Figure 3-3****)*** *is shown as a control.*

3.6 Summary

Reports show that Clb1 undergoes a meiosis-specific nuclear import around metaphase I. Clb1 also shows a meiosis-specific gel shift at the same time (Buonomo et al., 2003; Carlile and Amon, 2008; Marston et al., 2003).

Our earlier results (Section 3.1) indicated that both the gel shift and nuclear localisation of Clb1 were retained in metaphase I-arrested cells and in Cdc55-depleted cells. In addition, we have shown that the gel shift is phosphorylation, and that both phosphorylation and nuclear localisation are meiosis-specific.

Possible reasons for cyclin phosphorylation could be to alter the activity, localisation, substrate specificity, or stability of the target protein, or to create or disguise recognition sites for further modification or interactions. In particular, the change in location correlated with the phosphorylation. In *Xenopus* and human cells, there are examples of cyclin localisation being controlled by phosphorylation (Hagting et al., 1999; Li et al., 1997). The phosphorylation and nuclear localisation appeared to be related, but no information on a causal relationship could be determined from these results.

It has been shown that Clb1 protein remains present but inactive after meiosis I (Carlile and Amon, 2008). Previous results indicated a decline in Clb1 after the first division (Buonomo et al., 2003; Marston et al., 2003). Two possible explanations could account for this discrepancy. The tag used in the earlier results may have led to degradation due to instability. This is suggested as a mechanism by which Clb1-Myc$_9$ could partially rescue the *spo12Δ* phenotype (Buonomo et al., 2003). However, the Myc tag was used by Carlile *et al.* so this may not be a complete explanation. Secondly, in the earlier reports, Clb1 presence was measured by immunofluorescence. Clb1 may be present in the cytoplasm after anaphase I, but may be difficult to detect by *in situ* immunofluorescence, due to increased dispersal.

In our expression of Clb1-Myc, the gel shift occurred at around 6 hours into SPO media, and the continued presence of Clb1-Myc$_9$ was seen in the following two hours (Figure 3-3 B). Our strain did not include the Ndt80 expression system to increase synchrony, but the progress of meiosis could be followed. Between 6 – 8 hours into sporulation, wild type cells were entering

meiosis II, as judged by nuclear division (Figure 3-3 A). This seemed to agree with the report that Clb1 continues to be present in meiosis II, but does not bear the modification (Carlile and Amon, 2008).

To identify modified sites on Clb1, we attempted to purify Clb1 for mass spectrometric analysis (Appendix Section 9.1.1). TAP purification was unsuccessful. In the following chapter we consider kinases that may be responsible for Clb1 phosphorylation, and the roles that Clb1 phosphorylation may play in the regulation of meiosis.

4 Clb1 phosphorylation and models of meiosis

4.1 Introduction

In Chapter 3, the modification of Clb1 during meiosis I has been identified as meiosis-specific phosphorylation. The specificity of this modification and import suggests that it may have a role in the regulation of meiosis I. In this chapter, we investigated the possibility that Clb1 phosphorylation is involved in regulating progress through meiosis, using a simple model of meiosis.

4.1.1 Chapter Outline

The Initial model of meiosis is described in Section 4.2. This model uses information from the literature, and some hypothetical relationships, to reproduce the behaviour of meiosis. The initial model has two hypothetical functions inserted. The Intermediate enzyme (IE) introduces a time delay to Cdc20 activation, and the hypothetical protein Y protects the activity of the Starter Kinase, permitting the Clb-CDK activity to peak twice before the high-CKI state stabilises (Figure 4-1). In this chapter, we considered ways in which the meiosis-specific regulation of Clb1 may accomplish, or contribute to, the former of these functions.

In Section 4.3 we investigated whether the Clb1 phosphorylation could be incorporated into the initial model in place of the hypothetical IE. We considered three scenarios: Clb1 phosphorylation may be accomplished by the Starter Kinase, by Clb1 itself in autophosphorylation, or by a kinase not yet incorporated in the model (which is proposed to be Cdc5). We experimentally examined the results of depleting or inhibiting the kinases during meiosis,

In Section 4.4 we considered an alternative model structure that could reproduce the behaviour of the initial model. In this model, Y had a different role

than that of protecting the activity of the Starter Kinase; instead, Y limits the activity of the CKI. This permitted a different role for Clb1 phosphorylation.

4.2 A provisional model of meiosis

All of the models described in this chapter originate from the following model, referred to as the Initial model. This is a phenomenological model meaning that the behaviour of meiosis is represented, but the precise biochemical relationships are not all represented. For example, the FEAR network is covered in a single interaction. This is in contrast to a mechanistic model, which would precisely represent the biochemical reactions of the participating proteins. The model is shown in (Figure 4-1). This decision simplified the model, while allowing its capabilities and requirements with respect to meiosis I-specific regulation to be examined. The model uses information in the literature and analogy to mitosis, and incorporates some hypothetical interactions.

4.2.1 Description of the model

The network structure (Figure 4-1) was suggested by Novak and Tyson (Tyson and Novak, 2008) and the model is mentioned in the introductory chapter (Section 1.7.2.6). The behaviour produced is an oscillation between two stable states, characterised by either low or high CDK activity. Low CDK activity, the G1 state, is maintained by CKIs (CDK inhibitors). In the high CDK state, CDK activity represses the CKIs, and the cell goes through S and G2 phases and enters the M phase. The transitions between the states are driven by Exit Phosphatases or Starter Kinases (Nasmyth, 1996). The requirements of meiosis have been considered in terms of this view of the cell cycle (Tyson and Novak, 2008). It was suggested that maintenance of the Starter Kinase activity would permit the cell to undergo multiple cycles without entering the high-CKI stable state. To achieve meiosis, the starter kinase activity would be maintained for two cycles. Once the high-CKI stable state arises at the end of the second cycle, the starter kinase remains inactive, precluding further cycles. The wiring diagram for this Initial model is given in Figure 4-1.

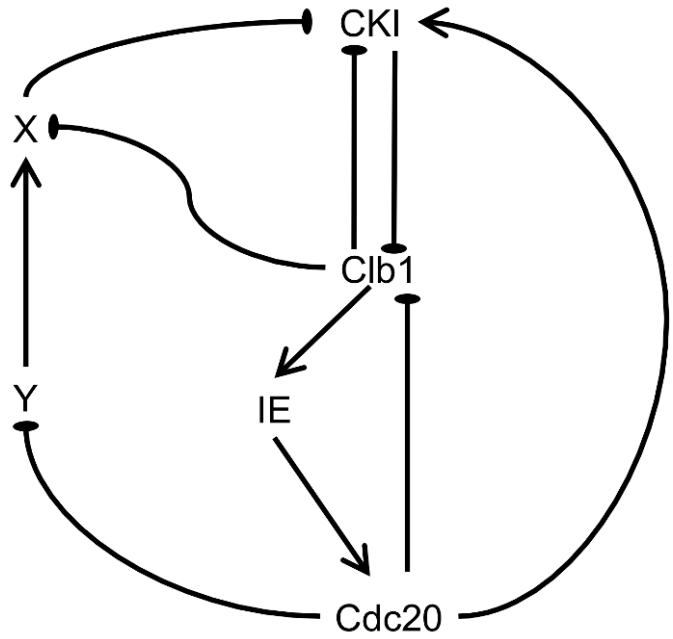

Figure 4-1 ***Proposed wiring diagram of the initial model for meiosis.*** *The reactions are described below. Justification of this diagram with references is in Section 1.2.2, and Section 1.2.3 describes the reactions in more detail. Arrow-headed interactions are positive interactions e.g. activation. Flat-ended interactions are negative interactions e.g. inhibition. Interacting partners of Clb1 and Cdc20, Cdc28 and APC, are not shown.*

The Starter Kinase, X, drives down CKI activity so that Clb1-CDK can rise. The characteristics of X can be attributed to Ime2 (Dirick et al., 1998). Once X is inactivated, it does not re-accumulate. The regulation of X leads to the behaviour of the model. Without X, the Initial model would fail to initiate a cycle, but remain in the high-CKI state. If X is inactivated during the first cycle, the Initial model does not initiate a second cycle, but remains in the high-CKI state. If re-accumulation of X is permitted, the model would produce multiple cycles. The Exit Phosphatase of *Saccharomyces cerevisiae* is Cdc14. In the Initial Model, Cdc14 is encapsulated in the link between Cdc20 and CKI (Figure 4-1) and Cdc20 can be assumed to play the Exit Phosphatase role in activating the CKI variable and triggering the transition. Without Cdc20, the Initial model would accumulate Clb1-CDK and remain in a high-CDK stable state. The Initial model also requires a hypothetical protein, Y, to prevent the inhibition of Starter Kinase X during the first cycle, a role for which Spo13 is proposed (Tyson and Novak, 2008).

4.2.2 Assumptions and literature contributions to the initial model

Much of the literature discussed below refers to mitosis but is applied to meiosis where pertinent.

1. In a typical simplification, stochastic variation and spatial diffusion are not accounted for; instead the model represents the cell as a well-stirred system.
2. The variables represent the relative concentration of the protein.
3. Time is given in an arbitrary unit.
4. Ordinary differential equations (ODEs) describe the rate of change of the variables given in the wiring diagram. Each differential equation is of the form:

   $$dA/dt = production\ terms - removal\ terms$$

   in which A is a variable in the model and its rate of change over time (dA/dt, or A' in model files) is given by the interactions on the right hand side of the equation. Each interaction is depicted by an arrow in the wiring diagram, and depends on the molecular concentrations of the participants at that point in time, and on fixed rate constants given by the parameters.
5. Post-translational modification of proteins and complex formation are assumed to be rapid compared to synthesis and degradation rates.
6. Synthesis and degradation rates of proteins are described by mass action kinetics.
7. Rates of phosphorylation and dephosphorylation reactions are described by Michaelis-Menten kinetics (MM).
8. The levels of Cdc28 and core APC complex are not considered as they are generally assumed to be constant over the cycle, and their activity controlled by their interacting partners (Mendenhall and Hodge, 1998; Zachariae and Nasmyth, 1999). The variable annotated as Clb1 represents the Cdc28/Clb1 complexes. Cdc20 represents active Cdc20/APC complexes.
9. The model does not have multiple cyclins. This means there is no difference in CDK activation between the first and second division in the initial model, or in the following models, despite the experimental evidence that Clb1 and Clb3 are responsible for separate divisions (Carlile and Amon, 2008). This

is a simplification, as the role of Clb1 regulation in meiosis I is the focus of this chapter.

10 The total amount of Cdc20 is assumed to be constant, as the limiting step of Cdc20 activation is its phosphorylation, controlled by Clb1-CDK (Kramer et al., 2000; Rudner and Murray, 2000).

11 Clb1 indirectly activates Cdc20 (Rahal and Amon, 2008a) via a hypothetical Intermediate Enzyme (IE) (Figure 4-1). This introduces a delay in Cdc20 activation, which is required for the negative feedback loop between Clb-CDK and Cdc20 to generate cell cycle oscillations (Ferrell et al., 2011; Pomerening et al., 2003; Tyson et al., 2003).

12 APC/Cdc20 activity triggers the FEAR pathway, leading to Cdc14 release. Cdc14 triggers the activation of the inhibitors of Clb1-CDK that are in turn inhibited by phosphorylation (CKIs) (Jaspersen et al., 1999; Queralt et al., 2006; Shirayama et al., 1999; Stegmeier et al., 2002). This is summarised in one reaction, represented as one arrow, by which Cdc20 activates CKI (Figure 4-1). Also, it is worth noting that the other roles of FEAR – such as nuclear separation, are not included in the model, due to simplification.

13 The variable CKI refers to Sic1 (Verma et al., 1997), Ama1 (Cooper et al., 2000), CKI (Jaspersen et al., 1999; Zachariae et al., 1998). Since they have the same interactions in the logic of the model, they are summed up under the single variable CKI. This simplification will lead the model to differ in the case of some mutants like *cdh1Δ*.

14 The total amount of CKI is assumed to be constant. This is a simplification based on the assumption that phosphorylation is the limiting step for control of activity and that protein levels change slowly in comparison.

15 CKI and Cdc20 cause a decrease in Clb1 activity by causing degradation of Clb1 (Schwab et al., 1997; Shirayama et al., 1999; Tyers, 1996)

16 CDK activity is required to have two peaks during meiosis, before resetting to a stable G1 state (Marston and Amon, 2004).

17 The inhibitors summed up under CKI must not gain ascendancy over Clb/CDK activity during the first cycle. They are assumed to be inhibited by the Starter Kinase X activity. The Starter Kinase candidate Ime2 is known to be active during meiosis and to cause phosphorylation of the inhibitors

(Bolte et al., 2002; Sedgwick et al., 2006), although it is not always sufficient to inhibit them (Sedgwick et al., 2006).

18 CDK activity causes phosphorylation of Starter Kinase X (Figure 4-1). This interaction is suggested by analogy with Clb-CDK inhibition of Clns, as Starter Kinase X takes the role of Clns in meiosis. The Starter Kinase X candidate, Ime2, undergoes hyperphosphorylation during meiosis (Schindler and Winter, 2006); and mutants of phosphorylation sites sporulate less efficiently. Interaction of Ime2 phosphorylation site mutants with FEAR mutants suggests a role for Ime2 phosphorylation regulation of the meiosis I transition.

19 Hypothetical gene Y inhibits CDK action on Starter Kinase X for the first cycle and is degraded by Cdc20 (Figure 4-1). A candidate for this role would be Spo13 (Tyson and Novak, 2008), whose deletion phenotype is the production of dyads during meiosis (Klapholz and Esposito, 1980a, b). This is the expected phenotype of the model lacking Y.

4.2.2.1 Starter Kinase X and Ime2

The Ime2 protein is present for both divisions of meiosis (Schindler and Winter, 2006), but does not inhibit the CDK inhibitors that instigate meiotic exit at meiosis II. Ime2 is involved in driving the cell out of the G1 (inhibitor-dominated) state in initiation of meiosis (Dirick et al., 1998). Progressive phosphorylation of Ime2 is noted through meiosis (Schindler and Winter, 2006). This information led us to consider that phosphorylation of Ime2, driven (possibly indirectly) by the CDK activity, leads to alterations in the activity of Ime2 that end the starter kinase role. This would produce a meiotic analogue of the relationship between Clb-CDK and Cln-CDK activities in mitosis (Amon et al., 1993). Alternative routes for the prevention of Ime2 activity as a result of CDK activity may be possible, such as induction of a specific inhibitor. However, direct phosphorylation is the simplest route to implement in the model, as it avoids the introduction of further variables. Hypothetically, Y then acts to dephosphorylate X and prevent the phosphorylation from inhibiting X activity over the first cycle.

4.2.3 Reactions of the model

(1) The wiring diagram repeated in Figure 4-2 is described by the ODEs in the following

$$\frac{d[Clb1]}{dt} = ks_{Clb1} - (kd_{Clb1} + kd_{Clb1CKI} \cdot [CKIa] + kd_{Clb1Cdc20} \cdot [Cdc20a]) \cdot [Clb1]$$

(2)
$$\frac{d[CKIa]}{dt} = \frac{(ka_{CKI} + ka_{CKICdc20} \cdot [Cdc20a]) \cdot ([CKI_t] - [CKIa])}{Ja_{CKI} + (CKI_t - CKIa)} - \frac{(ki_{CKIX} \cdot [X] + ki_{CKIClb1} \cdot [Clb1]) \cdot [CKIa]}{Ji_{CKI} + [CKIa]}$$

(3)
$$\frac{d[IEa]}{dt} = \frac{ka_{IEClb1} \cdot [Clb1] \cdot ([IE_t] - [IEa])}{Ja_{IE} + ([IE_t] - [IEa])} - \frac{ki_{IE} \cdot [IEa]}{Ji_{IE} + [IEa]}$$

(4)
$$\frac{d[Cdc20A]}{dt} = \frac{ka_{Cdc20IE} \cdot [IE] \cdot ([Cdc20_t] - [Cdc20a])}{Ja_{Cdc20} + ([Cdc20_t] - [Cdc20a])} - \frac{ki_{Cdc20} \cdot [Cdc20a]}{Ji_{Cdc20} + [Cdc20a]}$$

(5)
$$\frac{d[X]}{dt} = \frac{kdp_X \cdot [Y] \cdot ([X_0] - [X])}{Jdp_X + ([X_0] - [X])} - \frac{kp_X \cdot [Clb1] \cdot [X]}{Jp_X + [X]}$$

(6)
$$\frac{d[Y]}{dt} = -kd_Y \cdot [Cdc20A] \cdot [Y]$$

Equation System 4-1, using the following conventions:

Clb1 indicates the active form of Clb1-CDK. X and Y indicate the amounts of those proteins. Cdc20a indicates the amount of active APCCdc20. Active forms are indicated by an appended “a” and inactive forms by an appended “i”: this applies to Cdc20, IE and CKI. Phosphorylated forms of Clb1 and X are indicated by addition of a “P”. Initial or total amounts of proteins are indicated by a subscript “0” or “T”, respectively. Parameter names begin with k (for rates) or J (for the Michaelis constant) followed by “a” for activation, “i” for inhibition, “p” for phosphorylation, “dp” for dephosphorylation, “s” for synthesis, or “d” for degradation. This is followed in subscript by the protein undergoing the reaction, then the protein catalysing it. For example, $ka_{Cdc20IE}$ indicates the rate of activation of Cdc20 by IE.

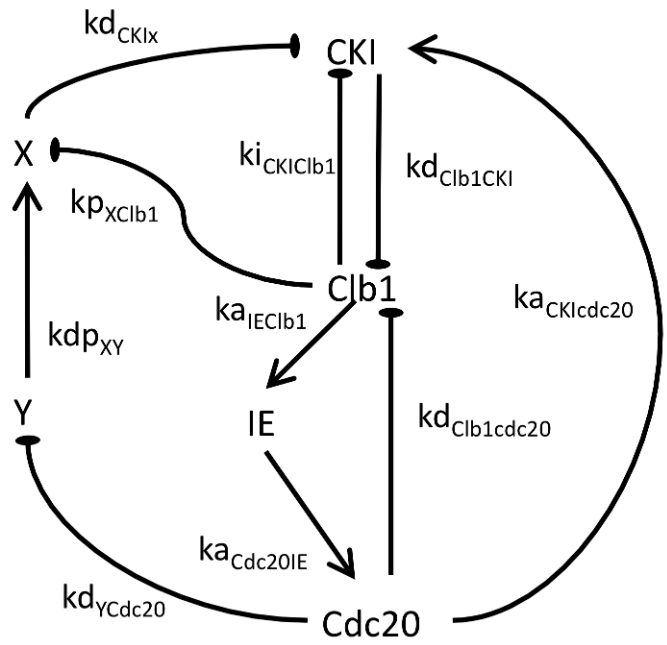

Figure 4-2 ***Wiring diagram of the initial model****. As seen in Figure 4-1. Parameters controlling the interactions are shown next to the arrows indicating the interaction. Parameter naming conventions are described above.*

Synthesis and degradation are described using mass action kinetics. The synthesis of Clb1 is of zero order, meaning the rate is constant and independent of the current level of Clb1. The background rate of degradation of Clb1 is first order, meaning it depends only on Clb1 levels. Regulated degradation of Clb1 is second order, meaning that Cdc20 and CKI each catalyse this reaction. Degradation of Y is second order and catalysed by Cdc20.

Phosphorylation and dephosphorylation of X is described using Michaelis-Menten (MM) kinetics. X is phosphorylated by Clb1 and dephosphorylated by Y. Activation and inactivation of Cdc20, IE and CKI are described using MM kinetics. IE is activated by Clb1 and Cdc20 is activated by IE; both have a constant inactivation rate. Cdc20 catalyses CKI activation, and CKI inactivation is catalysed by Clb1 and X.

The total amounts of the inactive and active forms of CKI, Cdc20 and IE are assumed to be constant. The sum of X and XP is assumed to be constant and equal to X_0. These follow from the assumption that the total amount of each protein changes slowly compared to the post-translational modifications altering the activity status. The reactions following the inactive forms of each protein are

omitted: the amount of inactive form can be calculated by subtracting the amount of active form from the total amount.

4.2.3.1 Reactions of the initial model

The reactions of the model are summarised in the following table. Figure 4-2 gives the wiring diagram for the initial model, with parameters controlling the interactions between the variables shown in place.

Reactions	Contributing	Parameters
→ Clb1		$ks_{clb1,}$
Clb1 →	CKI, Cdc20	kdclb1, $kd_{clb1CKI}$,$kd_{clb1cdc20}$
CKI (active) → CKI (inactive)	X, Clb1-P, Clb3	ki_{CKIx}, Ji_{CKI} ka_{CKI}, $ka_{CKIcdc20}$, Ja_{CKI}
CKI (inactive) → CKI (active)	Cdc20,	ka_{CKI}, $ka_{CKIcdc20}$, Ja_{CKI}
Cdc20 (active)→ Cdc20(inactive)	IE	ki_{cdc20}, Ji_{cdc20}
Cdc20 (inactive)→ Cdc20(active)		$ka_{cdc20ie}$, Ja_{cdc20}
IE (active) → IE (inactive)	Clb1	ka_{ieclb1}, Ja_{ie}
IE (inactive) → IE (active)		ki_{ieclb1}, Ji_{ie}
X→XP	Clb1	kp_{x}, $Jp_{x,}$
XP→X	Y	kdp_{xp}, Jdp_{xp}
Y→	Cdc20, X	kd_{y}

Table 4-1 ***Reactions of the model.*** *Table of reactions for the model depicted in Figure 4-1 listed with parameters and variables that affect the rates.*

4.2.3.2 Initial Model in ODE form

The model is described below in ordinary differential equations. Model files that can be run on XPP are given in Section 9.2.

(7) $$\frac{d[Clb1]}{dt} = ks_{Clb1} - (kd_{Clb1} + kd_{Clb1CKI}\cdot [CKIa] + kd_{Clb1Cdc20}\cdot [Cdc20a])\cdot [Clb1]$$

(8) $$\frac{d[CKIa]}{dt} = \frac{(ka_{CKI} + ka_{CKICdc20}\cdot [Cdc20a])\cdot ([CKI_t] - [CKIa])}{Ja_{CKI} + (CKI_t - CKIa)} - \frac{(ki_{CKIX}\cdot [X] + ki_{CKIClb1}\cdot [Clb1])\cdot [CKIa]}{Ji_{CKI} + [CKIa]}$$

(9) $$\frac{d[IEa]}{dt} = \frac{ka_{IEClb1}\cdot [Clb1]\cdot ([IE_t] - [IEa])}{Ja_{IE} + ([IE_t] - [IEa])} - \frac{ki_{IE}\cdot [IEa]}{Ji_{IE} + [IEa]}$$

(10) $$\frac{d[Cdc20A]}{dt} = \frac{ka_{Cdc20IE}\cdot [IE]\cdot ([Cdc20_t] - [Cdc20a])}{Ja_{Cdc20} + ([Cdc20_t] - [Cdc20a])} - \frac{ki_{Cdc20}\cdot [Cdc20a]}{Ji_{Cdc20} + [Cdc20a]}$$

(11) $$\frac{d[X]}{dt} = \frac{kdp_X \cdot [Y] \cdot ([X_0] - [X])}{Jdp_X + ([X_0] - [X])} - \frac{kp_X \cdot [Clb1] \cdot [X]}{Jp_X + [X]}$$

(12) $$\frac{d[Y]}{dt} = -kd_Y \cdot [Cdc20A] \cdot [Y]$$

Equation System 4-1 ***System of ODEs describing the initial model****. The model described in Figure 4-1 and Figure 4-2 is described above ordinary differential equations suitable for simulating in XPP.*

4.2.3.3 Parameter Selection and time series

Parameters were chosen so that the simulations would demonstrate two peaks of Clb1-CDK activity, with two peaks of Cdc20 controlling each division, before CKI achieved the stable state (Marston and Amon, 2004). CKI was slightly active at the first cycle in this time series, but this is not a strict criterion. Later models were not fitted using a program, instead parameters were chosen by trial and error, aiming to reproduce the behaviour. This method was chosen due to the qualitative nature of the criteria and the lack of time course data for the active levels of the variables over meiosis. Parameters are given in Table 4-2 and the time series is displayed in Figure 4-3.

Parameter	Value	Initial Conditions	
ks_{clb1}	0.01	Clb1=0	CKI=1
kd_{clb1}	0.01	IE=0	Y=1
$kd_{clb1CKI}$	1	Cdc20=0	X=1
$kd_{clb1cdc20}$	0.2		
ka_{CKI}	0.2		
$ka_{CKIcdc20}$	0.8		
ki_{CKIx}	2		
$ki_{CKIclb1}$	15		
Ja_{CKI}	0.04		
Ji_{CKI}	0.02		
$ka_{cdc20ie}$	1		
ki_{cdc20}	0.5		
Ja_{cdc20}	0.001		
Ji_{cdc20}	0.001		
ka_{ieclb1}	0.1		
ki_{ie}	0.02		
kp_x	0.2		
Jp_x	0.04		
kdp_{xp}	0.1		
Jdp_{xp}	0.04		
kd_y	0.2		
CKI_t	1		

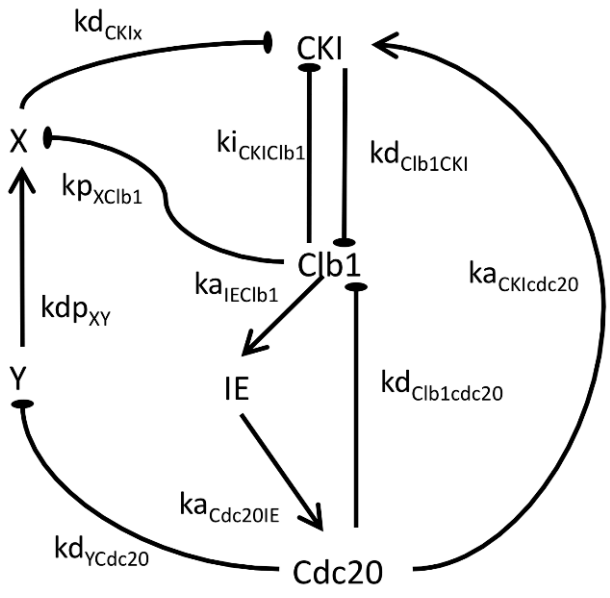

$Cdc20_t$	1

Table 4-2 ***Parameters for initial model****. Parameters for the initial model, which result in the time series in Figure 4-3. The wiring diagram in Figure 4-2 is reproduced for reference.*

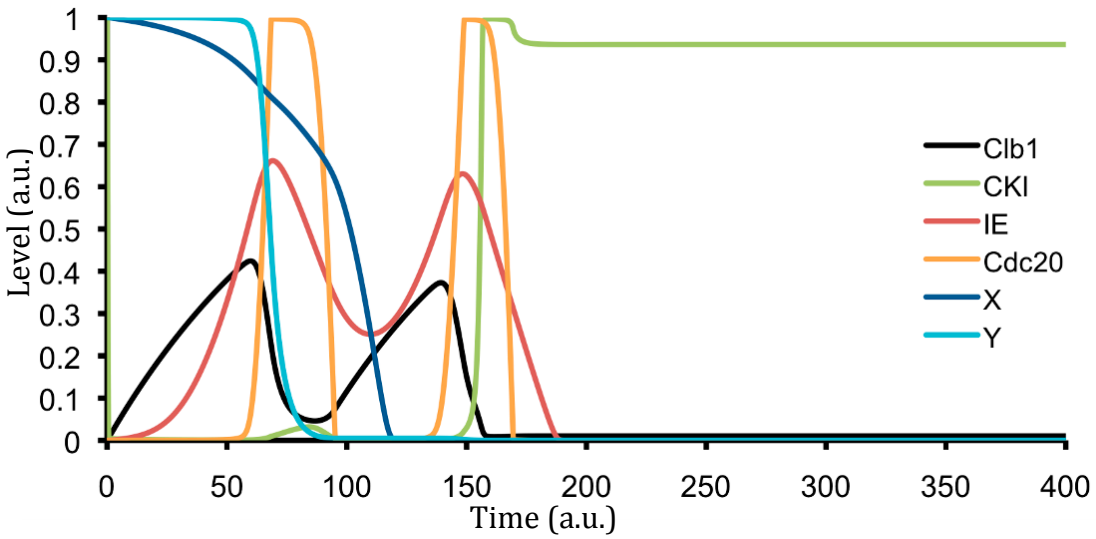

Figure 4-3 ***Numerical simulation of the initial model*** *Time series produced using the initial model and the parameters given in Table 4-2. The model produces two peaks of Cdc20 and CDK activity before CKI activity rises and holds the model in the low CDK state.*

This time series emulated the two cycles of meiosis. The variables of interest are Cdc20, CKI, and Clb1. Clb1 levels signified CDK activity driving each meiotic division, while Cdc20 peaks indicated the point that the two divisions occurred. Cdc20, IE and Clb1 form a negative feedback oscillator to drive the cycles. CKIa levels increased after the second division, signifying the entry into the low-CDK stable state. The following mutant phenotypes were simulated using the model to demonstrate its behaviour and the limitations introduced by the simplifications listed above.

Mutant	Experimental Phenotype	Model phenotype
cdc20Δ	Mitotic arrest, high CDK	CDK activity remains high
cdh1Δ	No effect	Sustained cycles – The CKI variable covers several inhibitors so differs from a single CKI deletions. The negative feedback loop is capable of sustained oscillations.
yΔ	Y is unidentified, but *SPO13* is suggested as a gene whose deletion leads to one cycle	Single cycle

Table 4-3 ***Table of phenotypes in the model****. The model is able to reproduce the phenotype of* cdc20Δ*, but is oversimplified to accurately produce* cdh1Δ*. The phenotype of* yΔ *is predicted as Y is unidentified.*

4.3 Clb1 phosphorylation and Clb1 activity

Clb1 was found to be present for both meiosis I and meiosis II divisions, though only active during meiosis I (Carlile and Amon, 2008). A gel-shift was seen in meiosis I that appears to coincide with Clb1 activity (Carlile and Amon, 2008).

We have shown that a meiosis-specific Clb1 phosphorylation coincided with a nuclear localisation, and that $P_{CLB2}CDC20$ and $P_{CLB2}CDC55$ conditions both caused the phosphorylated state and nuclear localisation to be sustained (Chapter 3). In $P_{CLB2}CDC20$ strains undergoing meiosis, $PP2A^{Cdc55}$ remains active as the FEAR network is not triggered (Queralt et al., 2006) whilst in $P_{CLB2}CDC55$ strains undergoing meiosis, Cdc14 is ectopically active (Kerr et al., 2011). Sustained Clb1 phosphorylation in these backgrounds indicated that Clb1 phosphorylation is resistant to both Cdc14 and $PP2A^{Cdc55}$ dephosphorylation.

The previously noted correlation of Clb1 activity and gel shift (Carlile and Amon, 2008) raised the possibility that Clb1 phosphorylation is required for its activity in meiosis I. For example, the phosphorylation may be altering a recognition site and allowing Clb1 to escape the effect of a specific inhibitor, whose existence is implied by the presence and inactivity of Clb1 in meiosis II (Carlile and Amon, 2008).

4.4 Phosphorylated state of Clb1 replacing IE

In the Initial model, described in Section **4.2**, a delay was introduced by the Intermediate Enzyme (IE). Clb1 causes the activation of IE, which in turn activates Cdc20. In light of the phosphorylation of Clb1 being concurrent with its activity, we considered the possibility that the delay is provided by Clb1 activation by phosphorylation. In the Initial model, Cdc20a acts only on Clb1, not on its own immediate activator, IE, which supplies the delay. However, in these cases, Cdc20a acts on Clb1P directly. A pool of Clb1 still undergoing phosphorylation at a sufficient rate would counter Cdc20a degradation until Clb1 levels decrease, effectively delaying Cdc20a's action on Clb1P. In this case, we would expect to see the Clb1P peak to be delayed relative to the unphosphorylated Clb1 peak in the time series, as Clb1P continues to increase even as unphosphorylated Clb1 decreases.

In the subsequent models incorporating Clb1 phosphorylation in place of IE, Clb1 phosphorylation was not proposed to affect Clb1 degradation. This was chosen as a simplification of the model, and also because our results in Chapter 3 showed that the lower band of unphosphorylated Clb1 remained present during normal meiosis I, along with an upper phosphorylated band (Section 3.1), although this could be due to poor synchrony. Degradation parameters for Clb1 are assumed the same as those for Clb1P.

Including Clb1 phosphorylation as a prerequisite for Cdc20 activation raises the question of whether (Clb1 + Clb1P), or only Clb1P, can accomplish the other tasks of CDK (*i.e.* X phosphorylation and CKI inactivation). Assuming the relationship suggested above, in which phosphorylation of Clb1 engenders resistance to specific inhibition, it is likely that all tasks of CDK must be accomplished by Clb1P. In the case of another mechanism, such as an effect on substrate recognition, this does not necessarily follow. We have assumed that the former relationship is the case.

Three candidate kinases are considered in the following work for the dependence of the phosphorylation and nuclear localisation of Clb1. Two of these proteins are already represented in the model: Ime2 as the Starter Kinase X, and CDK activity as Clb1 and Clb1P. The following models consider the plausibility of Clb1 phosphorylation as a method of delaying Cdc20 activation, when each of these three different kinases is responsible for the phosphorylation. The model predictions are tested by inhibiting or depleting the kinases.

Ime2 has multiple consensus sequences (Moore et al., 2007), one complete site and four minimal ones, among the Clb sequence (Figure 4-4). There is a single minimal CDK site in the sequence. Another candidate is Cdc5, a polo kinase whose consensus sequence is usually paired with a polo box binding site primed by CDK phosphorylation, Ser-(PSer/PThr)-(Pro/X) (Lowery et al., 2004). Although, *CLB1* has no polo box part of the binding sequence, Cdc5 has been implicated in binding non-consensus sequences (Chen and Weinreich, 2010), indicating that there is potentially another binding mechanism. In *CLB1*, there is a sequence that matches the polo kinase region consensus site (Shou et al., 2002).

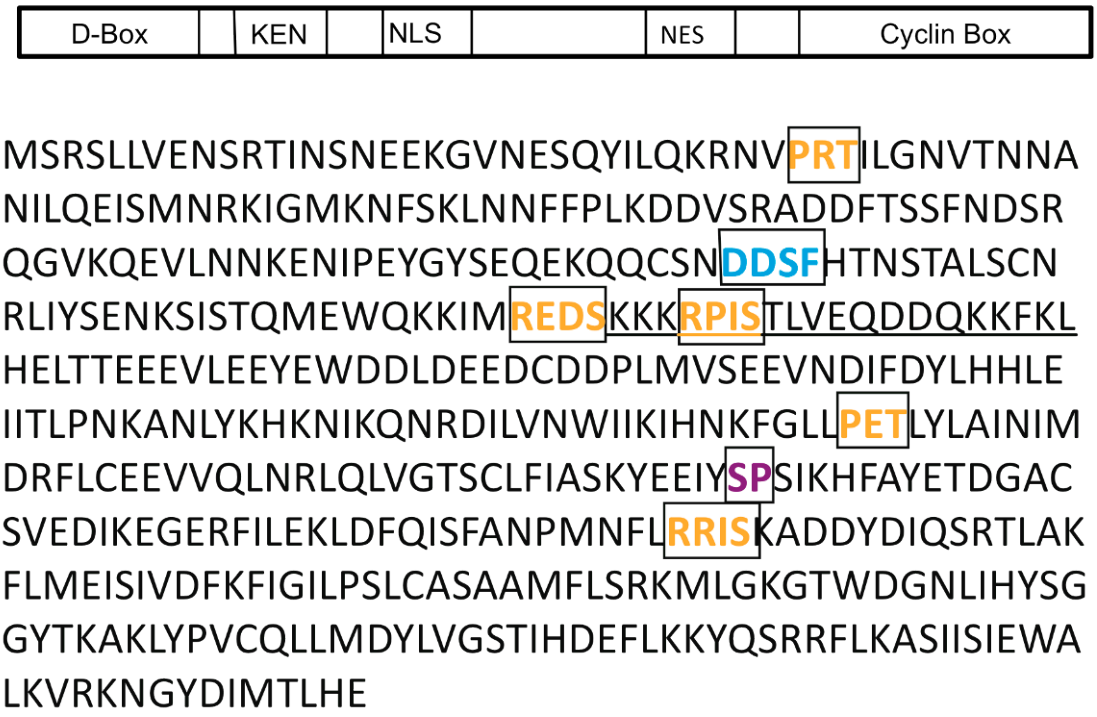

Figure 4-4 ***Sequence data for CLB1.*** *Sequence of Clb1 open reading frame as taken from SGD (Engel et al., 2013). The consensus sites are shown for Ime2 (R-X-X-S/T or X-P-X-S/T, Yellow), Cdc28 (SP, Purple) and Cdc5 kinase domain (D/E-X-S/T-hydrophobic, Blue) are shown in relation to the identified nuclear localisation site (Cherry et al., 1998; Gladfelter et al., 2006).*

4.4.1 Model 1: Phosphorylation by Ime2

We first considered Ime2 as a possibility for the kinase responsible for phosphorylating Clb1. The Clb1 sequence has multiple Ime2 consensus sites, including a strong Ime2 consensus site overlapping the nuclear localisation sequence (Sequence Figure). Ime2 is expressed during meiosis (Foiani et al., 1996), which would explain the meiosis-specificity of the phosphorylation. In addition, Ime2 phosphorylation shows resistance to Cdc14 dephosphorylation (Holt et al., 2007). Ime2 is incorporated in the model as the Starter Kinase denoted by X. The wiring diagram for the X driven model is given in Figure 4-5.

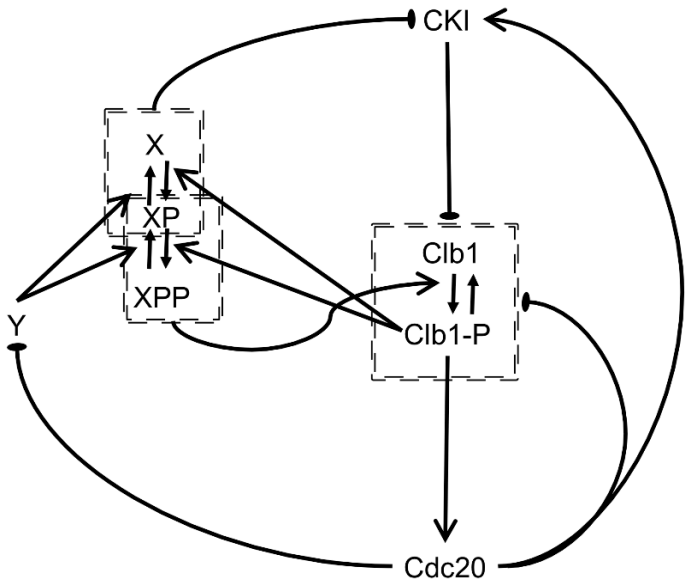

Figure 4-5 ***Proposed wiring diagram of model incorporating Ime2-driven Clb1 phosphorylation in the place of IE.*** *The altered reactions are described below. Clb1 phosphorylation is required for Cdc20 activation. Ime2 is responsible for Clb1 phosphorylation. In this model and all subsequent models, open-headed arrows indicate positive interactions such activation, flat ended arrows indicate negative interactions such as inhibition, and solid-headed arrows indicate transition of proteins between two states i.e. phosphorylation.*

Phosphorylation of X by Clb1 triggers the phosphorylation of Clb1 during the first cycle. However, phosphorylated X retains an inhibitory effect on CKI until the completion of the second cycle. This is achieved by assuming that X undergoes multi-site modification, and that its activity alters towards its substrates with the number of phosphorylations. Here, XP2 has decreased activity towards CKI, whilst X has lower activity towards Clb1 than either phosphorylated state. This is represented with overlapping brackets in the wiring diagram (Figure 4-5). Cdc20 and CKI catalyse both Clb1 and Clb1P destruction.

Reactions	Contributing	Parameters
→ Clb1		$ks_{clb1,}$
Clb1 →	CKI, Cdc20	kdclb1, $kd_{clb1CKI}$,$kd_{clb1cdc20}$
Clb1P →	CKI, Cdc20	kdclb1, $kd_{clb1CKI}$,$kd_{clb1cdc20}$
Clb1→ Clb1P	XP, XP2	$kp_{clb1x,}$ Jp_{clb1}
Clb1P →Clb1	CKI, Cdc20	kdp_{clb1}, Jdp_{clb1}
CKI (active) → CKI (inactive)	X, Clb1-P, Clb3	$ki_{CKIx,}$ Ji_{CKI} ka_{CKI}, $ka_{CKIcdc20}$, Ja_{CKI}
CKI (inactive) → CKI (active)	Cdc20,	ka_{CKI}, $ka_{CKIcdc20}$, Ja_{CKI}
Cdc20 (active)→ Cdc20(inactive)	IE	ki_{cdc20}, Ji_{cdc20}
Cdc20 (inactive)→ Cdc20(active)		$ka_{cdc20ie}$, Ja_{cdc20}
X→XP	Clb1	kp_{x}, $Jp_{x,}$
XP→X	Y	kdp_{xp}, Jdp_{xp}
XP→XP2	Clb1	kp_{x}, $Jp_{x,}$
XP2→XP	Y	kdp_{xp}, Jdp_{xp}

Y→		Cdc20, X, XP	kd_y

Table 4-4 ***Reactions of model 1.*** *Table of reactions for the model incorporating Ime2 phosphorylation of Clb1,* listed with parameters and variables that affect the rates.

The total concentration of X follows the conservation relationship:

(13) $$[X] + [XP] + [XP2] = [X]_0$$

Equation 4-2 ***Conservation relationship of X.*** *The sum of the different forms of X is conserved, meaning that to model can be simplified by removing the equation for XP2, and calculating it by subtracting X and XP from* X_T

The Ime2-driven model is described in

(14) $$\frac{d[Clb1]}{dt} = ks_{Clb1} + \frac{kdp_{Clb1}\cdot [Clb1P]}{Jdp_{Clb1} + [Clb1P]} - (kd_{Clb1} + kd_{Clb1CKI}\cdot [CKIa] + kd_{Clb1Cdc20}\cdot [Cdc20a] + \frac{kp_{Clb1X}\cdot ([X_0] + [X])}{Jp_{Clb1} + [Clb1]})\cdot [Clb1]$$

(15) $$\frac{d[Clb1P]}{dt} = \frac{kp_{Clb1X}\cdot ([X_0] - [X])}{Jp_{Clb1} + [Clb1]})\cdot [Clb1] - (kd_{Clb1} + kd_{Clb1CKI}\cdot [CKIa] + kd_{Clb1Cdc20}\cdot [Cdc20a] + \frac{kdp_{Clb1}}{Jdp_{Clb1} + [Clb1P]})\cdot [Clb1P]$$

(16) $$\frac{d[CKIa]}{dt} = \frac{(ka_{CKI} + ka_{CKICdc20}\cdot [Cdc20a])\cdot ([CKI_t] - [CKIa])}{Ja_{CKI} + ([CKI_t] - [CKIa])} - \frac{(ki_{CKIX}\cdot ([X] + [XP]) + ki_{CKIClb1}\cdot [Clb1P])\cdot [CKIa]}{Ji_{CKI} + [CKIa]}$$

(17) $$\frac{d[Cdc20A]}{dt} = \frac{ka_{Cdc20IE}\cdot [Clb1P]\cdot ([Cdc20_t] - [Cdc20a])}{Ja_{Cdc20} + ([Cdc20_t] - [Cdc20a])} - \frac{ki_{Cdc20}\cdot [Cdc20a]}{Ji_{Cdc20} + [Cdc20a]}$$

(18) $$\frac{d[X]}{dt} = \frac{kdp_X\cdot [Y]\cdot [XP]}{Jdp_X + [XP]} - \frac{kp_X\cdot ([Clb1] + [Clb1P])\cdot [X]}{Jp_X + [X]}$$

(19) $$\frac{d[Y]}{dt} = -kd_Y\cdot [Cdc20A]\cdot [Y]$$

Equation System 4-3:

(20) $$\frac{d[Clb1]}{dt} = ks_{Clb1} + \frac{kdp_{Clb1}\cdot [Clb1P]}{Jdp_{Clb1} + [Clb1P]} - (kd_{Clb1} + kd_{Clb1CKI}\cdot [CKIa] + kd_{Clb1Cdc20}\cdot [Cdc20a] + \frac{kp_{Clb1X}\cdot ([X_0] + [X])}{Jp_{Clb1} + [Clb1]})\cdot [Clb1]$$

(21) $$\frac{d[Clb1P]}{dt} = \frac{kp_{Clb1X} \cdot ([X_0] - [X])}{Jp_{Clb1} + [Clb1]} \cdot [Clb1] - (kd_{Clb1} + kd_{Clb1CKI} \cdot [CKIa] + kd_{Clb1Cdc20} \cdot [Cdc20a] + \frac{kdp_{Clb1}}{Jdp_{Clb1} + [Clb1P]}) \cdot [Clb1P]$$

(22) $$\frac{d[CKIa]}{dt} = \frac{(ka_{CKI} + ka_{CKICdc20} \cdot [Cdc20a]) \cdot ([CKI_t] - [CKIa])}{Ja_{CKI} + ([CKI_t] - [CKIa])} - \frac{(ki_{CKIX} \cdot ([X] + [XP]) + ki_{CKIClb1} \cdot [Clb1P]) \cdot [CKIa]}{Ji_{CKI} + [CKIa]}$$

(23) $$\frac{d[Cdc20A]}{dt} = \frac{ka_{Cdc20IE} \cdot [Clb1P] \cdot ([Cdc20_t] - [Cdc20a])}{Ja_{Cdc20} + ([Cdc20_t] - [Cdc20a])} - \frac{ki_{Cdc20} \cdot [Cdc20a]}{Ji_{Cdc20} + [Cdc20a]}$$

(24) $$\frac{d[X]}{dt} = \frac{kdp_X \cdot [Y] \cdot [XP]}{Jdp_X + [XP]} - \frac{kp_X \cdot ([Clb1] + [Clb1P]) \cdot [X]}{Jp_X + [X]}$$

(25) $$\frac{d[Y]}{dt} = -kd_Y \cdot [Cdc20A] \cdot [Y]$$

Equation System 4-3 ***System of ODEs describing Model 1:*** *incorporating Ime2-driven Clb1 regulation. The model described in Figure 4-5 is converted into ordinary differential equations suitable for simulating in XPP.*

Parameters were selected to match the following criteria, as in Section 4.2.3.3: Clb1P activity produces two peaks, followed by Cdc20 activity. CKI activity does not increase significantly until the second peak of Clb1P. Selected parameters are given in Table 4-5 and the time series in Figure 4-6.

Parameter	Value	Initial conditions	
ks_{clb1}	0.015	Clb1=0	Clb1P=0
kd_{clb1}	0.001	Cdc20A=0	XP=0
$kd_{clb1CKI}$	0.1	CKI=1	X=1
$kd_{clb1cdc20}$	0.1	Y=1	XP2=0
kdp_{clb1}	0.5		
Jdp_{clb1}	0.01		
kp_{clb1x}	0.7		
Jp_{clb1}	0.01		
ka_{CKI}	0.8		
$ka_{CKIcdc20}$	2		
ki_{CKIx}	20		
$ki_{CKIclb1}$	3		
Ja_{CKI}	0.04		
Ji_{CKI}	0.04		
$ka_{cdc20clb1p}$	0.25		
ki_{cdc20}	0.1		
Ja_{cdc20}	0.001		
Ji_{cdc20}	0.001		
kp_{xclb1}	0.1		
Jp_{x}	0.2		
kdp_{xpy}	0.05		
Jdp_{xp}	0.04		
kp_{xpclb1}	0.2		
Jp_{xp}	0.04		
kdp_{xp2y}	3.5		
Jdp_{xp2}	0.04		
kd_{ycdc20}	0.2		
CKI_t	1		
$Cdc20_t$	1		
X_t	1		

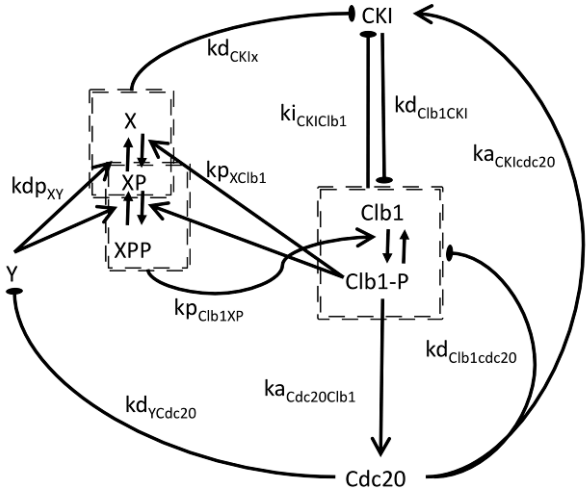

Table 4-5 ***Parameters for Model I incorporating Clb1 phosphorylation by Ime2.*** *Parameters for the model in which Clb1 phosphorylation is dependent on Ime2. The wiring diagram from Figure 4-5 is included for reference, with parameters controlling the interactions shown next to the arrows indicating the interaction.*

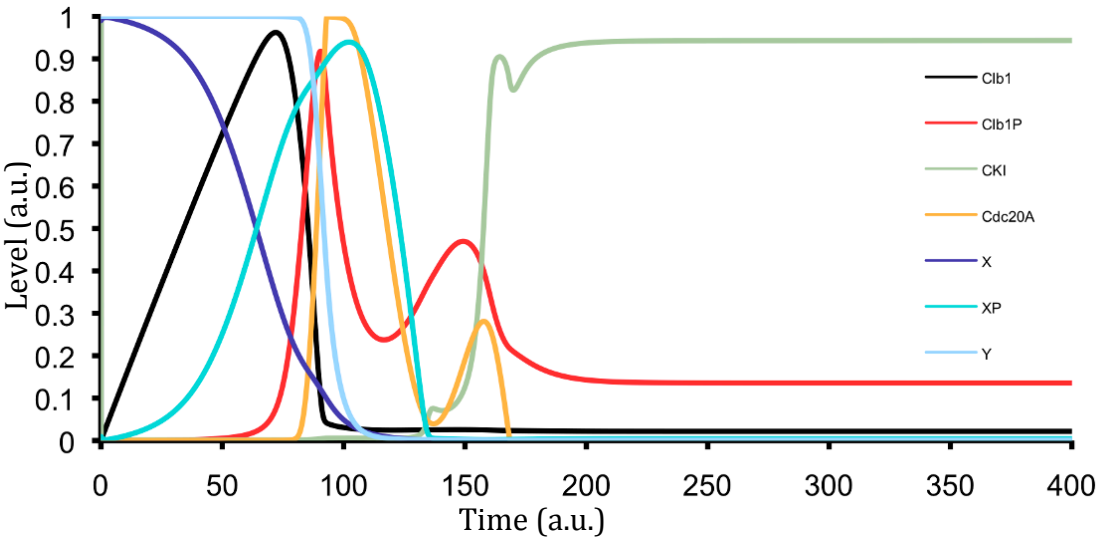

Figure 4-6 ***Numerical simulation of Model 1.*** *Time series produced for Model 1 incorporating Ime2 phosphorylation of Clb1, using the above parameters. The model produces two indistinct peaks of Clb1P-CDK activity before CKI activity rises and the system reaches a steady state.*

Model 1 was able to give two cycles of Clb1P-CDK activity, but they were not well separated. Clb1 had only one peak, before Clb1 phosphorylation increased. Clb1P formed the two peaks of Clb-CDK activity, and did not entirely disappear between cycles. However, there is some evidence from *Xenopus* that CDK activity is maintained at the end of meiosis I (Iwabuchi et al., 2000). In the first cycle, the Clb1P was delayed relative to the Clb1 peak. Clb1P was still rising as Clb1 began to decline, showing that the continued phosphorylation acted to delay Clb1 activity on Cdc20 in the first cycle, as suggested above. The second peak of Cdc20 was reduced, in contrast with the initial model. The ascendance of CKI depended more on the decrease of X and XP, than on activation by Cdc20. Therefore the Clb1P peak was also reduced.

4.4.2 Requirement of Ime2 kinase activity for Clb1 phosphorylation and nuclear localisation

If the above model were true, inhibition of Ime2 would prevent Clb1 phosphorylation, which would be detectable in the P_{CLB2}CDC20 as a loss of the gel shift. To selectively inhibit Ime2 activity, an analogue-sensitive allele of *IME2* was used. *ime2-as* is sensitive to an ATP analogue, 1-NA-PP1 (Benjamin et al., 2003). The *ime2-as-MYC*$_9$ allele was combined with P_{CLB2}*CDC20* to cause the modification to be retained and more easily detectable if it occurred, and *CLB1-TAP* to allow detection of Clb1.

4.4.2.1 *ime2-as* allele: Proof of efficacy

IME2 and *ime2-as-Myc*$_9$ strains of yeast were induced to enter sporulation by resuspension in SPO media containing the analogue 1-NA-PP1 at 20μM, 100μM and 200μM or an equivalent volume of DMSO. Samples were taken hourly and fixed in ethanol for DAPI staining. The analogue-sensitive strain completely failed to form tetrads in the presence of the analogue (Figure 4-7) whereas the wild-type strain formed tetrads. However, the wild type appeared to be delayed by higher concentrations of 1-NA-PP1, when compared to the time course profile as exhibited by the negative control, in which only DMSO was added. 1-NA-PP1 may have some non-specific effect at higher concentrations. However, the *ime2-as-MYC*$_9$ strain was completely incapable of sporulation in the presence of the inhibitor, confirming that the allele is sensitive.

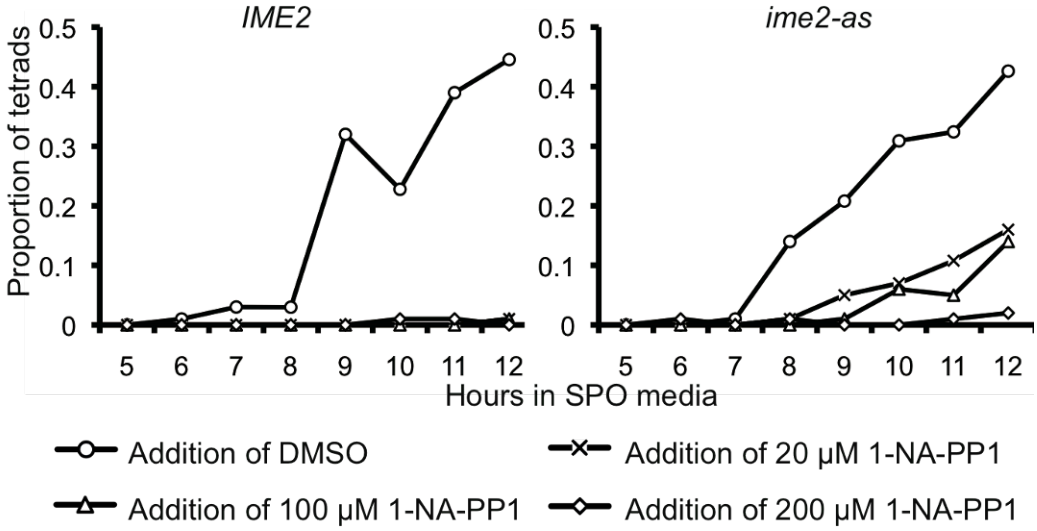

Figure 4-7 ***Inhibition of ime2-as prevents progress through meiosis.*** *Cultures of cells bearing* IME2 *or* ime2-as *were induced to undergo meiosis by resuspension in SPO media. 1-NM-PP1 or the solvent, DMSO, was added as indicated at the time of resuspension. Samples were taken for* in situ *immunofluorescence hourly and nuclear division was scored by DAPI staining. Proportion of tetranucleates is shown. 100 cells were counted for each time point.*

4.4.2.2 *ime2-as* allele: Effects on Clb1 gel shift

IME2 P$_{CLB2}$*CDC20 CLB1-TAP* and *ime2-as P*$_{CLB2}$*CDC20 CLB1-TAP* strains of yeast were induced to enter sporulation by resuspension in SPO media. Samples were taken for *in situ* immunofluorescence and for TCA-prepared cell extracts. The ATP analogue 1-NA-PP1 was added at a final concentration of 20μM to separate sporulating cultures at 5, 6, 7 or 8 hours after the time of resuspension

in sporulation media. An equivalent amount of DMSO was added to the negative control cultures at 5 hours. Samples were taken for *in situ* immunofluorescence and TCA-prepared cell extracts.

The modification of Clb1-TAP was seen in both *IME2* and *ime2-as* strains in the negative controls, confirming that both DMSO and the TAP tag on Clb1 had no effect on Clb1 modification (Figure 4-8). The modification was also seen in the *IME2* cultures with addition of 1-NA-PP1 at 6, 7 and 8 hours (Figure 4-8).

In the cultures with addition of 1-NA-PP1 at 5 hours, the *IME2* strain showed Clb1 expression and modification similar to the controls, whereas the *ime2-as* strain showed a strong attenuation of Clb1 (Figure 4-8). This might be expected, considering the role Ime2 plays in the establishment of Clb-CDK activity (Brush et al., 2012). Clb1 bands could be seen very faintly and appeared to show the presence of the modification. It is not possible to conclude from this whether Ime2 is required for the initial phosphorylation of Clb1 as the appearance and phosphorylation of the protein are closely coincident.

The gel shift was still present though Ime2 activity had been depleted; therefore Ime2 activity is not required for the maintenance of the phosphorylation of Clb1.

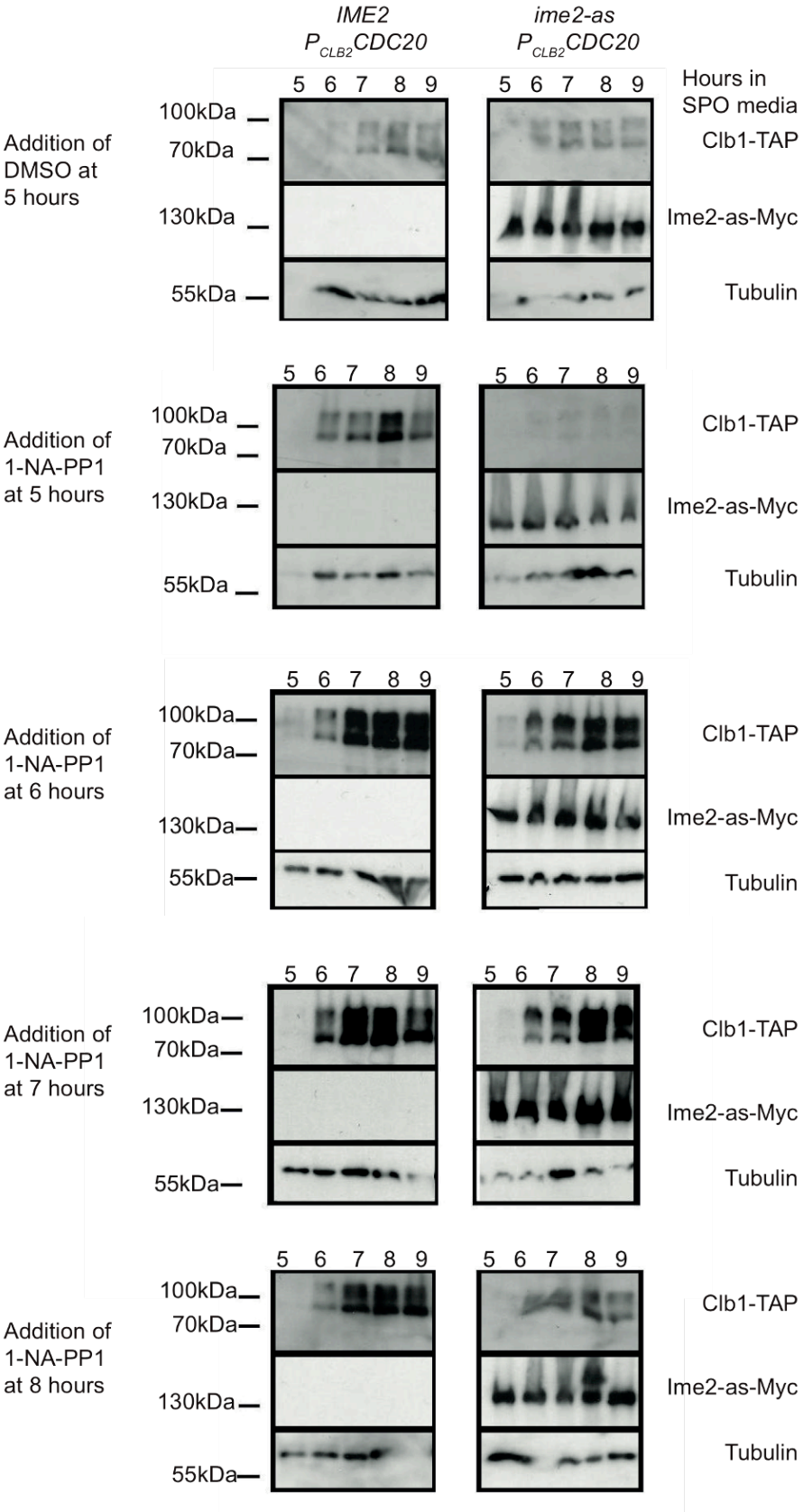

Figure 4-8 ***Inhibition of ime2-as does not prevent Clb1 modification during metaphase I arrest.*** *Cultures of* P_{CLB2}CDC20 CLB1-TAP IME2 *and* P_{CLB2}CDC20 CLB1-TAP ime2-as-MYC_9 *cells were induced to undergo meiosis by resuspension in SPO media. Cultures were treated by addition of*

1-NA-PP1 to 20μM to separate cultures at 5, 6, 7, or 8 hours, or an equivalent volume of the solvent, DMSO, at 5 hours. Gel mobility of Clb1-TAP was assayed by subjecting whole cell extracts to SDS-PAGE followed by western blot analysis using anti-myc. Blots were also probed with anti-tubulin and anti-myc to detect Ime2-as-Myc$_9$.

4.4.2.3 *ime2-as* allele: Effects on Clb1 gel localisation

Phosphorylation contributing to the gel shift of Clb1 may not be the only modification. There is a single strong Ime2 site near the nuclear localisation sequence, so it is possible that Ime2 may contribute to the localisation of Clb1. A single phosphorylation near the NLS may alter the protein's localisation without noticeably affecting the gel mobility. Fixed cell samples from the above cultures were probed for Clb1-TAP to determine the Clb1 localisation (Figure 4-9).

The presence of *ime2-as-Myc*$_9$ seemed to have some effect on Clb1. The number of cells bearing nuclear Clb1-TAP appeared to be lower than in the *IME2* control. However, this effect appeared independently of the addition of the inhibitor, occurring also in the uninhibited control culture, and seemed to reflect a generally lower expression of *CLB1-TAP*. Instead, the reduction of nuclear Clb1-TAP seemed to depend on the presence of the *ime2-as-MYC*$_9$ allele. The decreased Clb1-TAP levels were corroborated by the decreasing intensity of Clb1-TAP bands seen in the western blots. These localisation results, and others in this chapter, have to be considered with the fact that a control to detect non-specific binding of the antibodies was not performed.

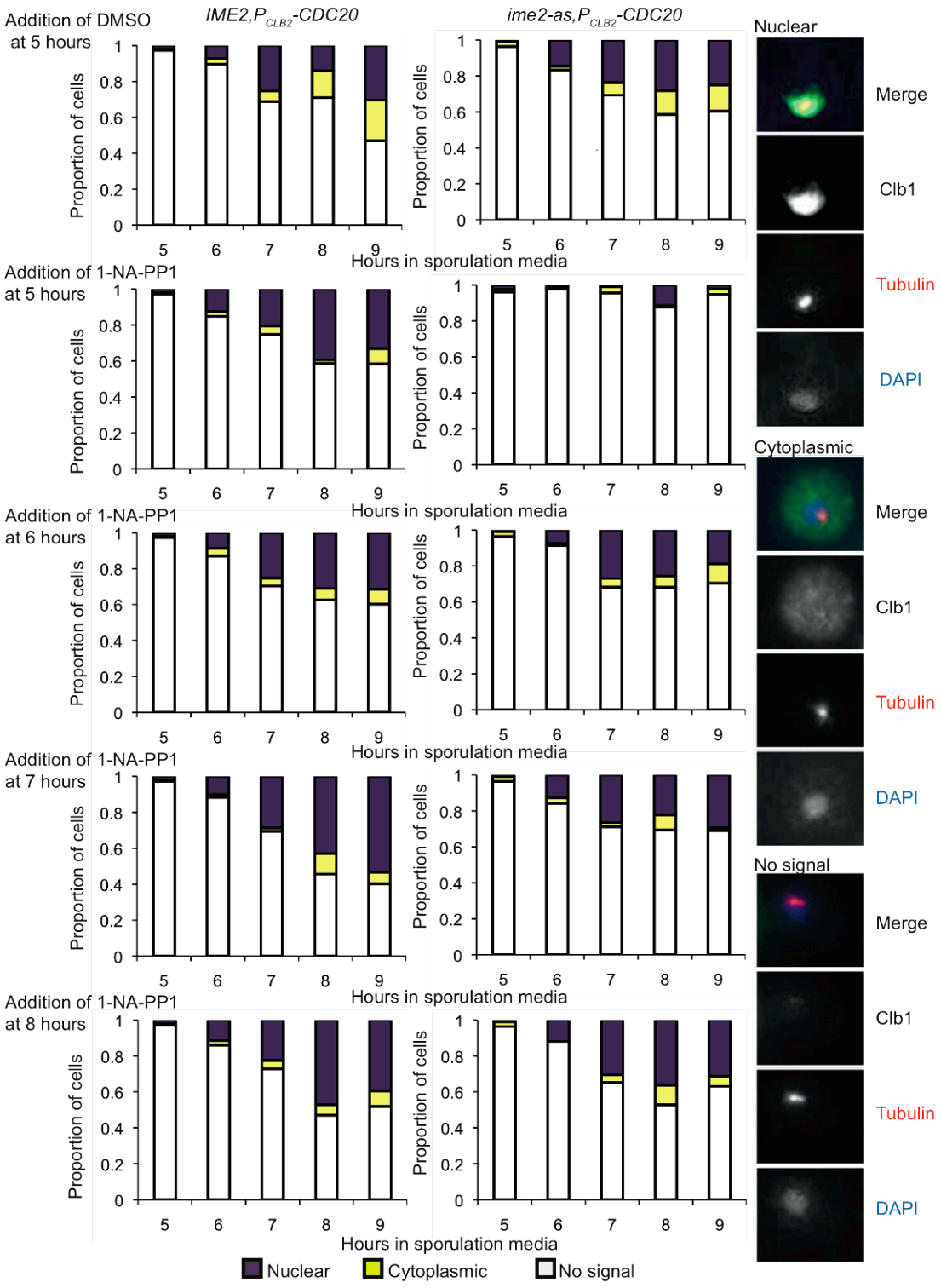

Figure 4-9 ***Inhibition of ime2-as does not prevent Clb1 nuclear concentration in cells arrested in metaphase I.*** *Cultures of cells bearing* P_{CLB2}CDC20 CLB1-TAP IME2 *and* P_{CLB2}CDC20 CLB1-TAP ime2-as-MYC_9 *were induced to undergo meiosis by resuspension in SPO media. Cultures were treated by addition of 1-NA-PP1 to 20μM to separate cultures at 5, 6, 7, or 8 hours, or an equivalent volume of the solvent, DMSO, at 5 hours. Cells were fixed and examined for Clb1-TAP localisation by* in situ *immunofluorescence. Proportion of cells with nuclear-concentrated Clb1 (Purple),*

cytoplasmic or dispersed Clb1 (yellow) and no detectable Clb1 signals (white) are indicated. 100 cells were counted for each time point.

Ime2-as inhibition did not prevent phosphorylation of Clb1, and did not appear to have an inhibitor-dependent effect on Clb1 location, though the *ime2-as-MYC*$_9$ allele may have had an effect on Clb1 levels. We concluded that Ime2 activity is not necessary for the meiosis-specific phosphorylation or localisation of Clb1.

4.4.3 Model 2: Autophosphorylation

Ime2 has been ruled out as a kinase required for the modification and nuclear localisation of Clb1. Another possible kinase is Cdc28 itself, directed by Clb1 or by another cyclin. There is a single Cdc28 consensus site in the Clb1 sequence (Figure 4-4). Although the Clb-CDK complexes are not meiosis-specific, the cyclins undergo alternative regulation compared to that of mitosis (Carlile and Amon, 2008; Grandin and Reed, 1993). Additionally, there is the possibility of meiosis-specific presence or absence of other regulatory proteins.

We investigated the case that Clb1P-CDK activity amplifies itself in a feedback loop (Pomerening et al., 2003). The wiring diagram for the model in which Clb1P phosphorylates Clb1 is shown in Figure 4-10.

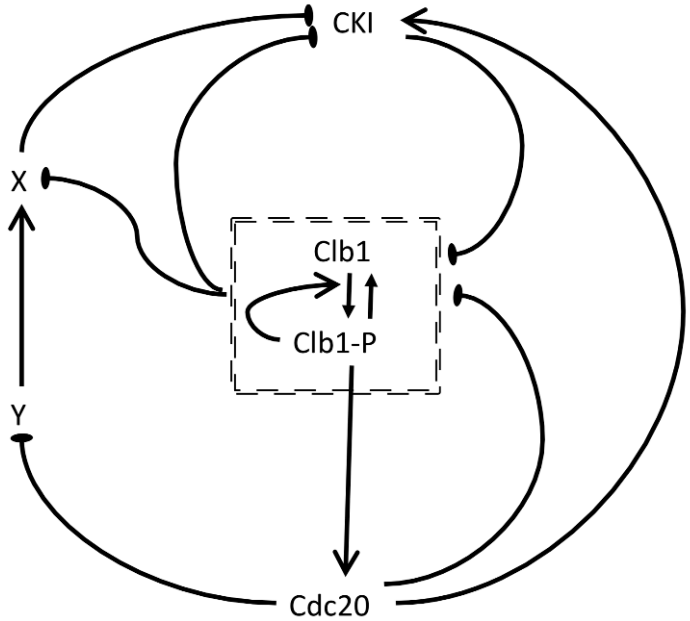

Figure 4-10 ***Proposed wiring diagram for the model incorporating Clb1 autophosphorylation.*** *In this model, Clb1 phosphorylates itself in a feedback loop and Clb1 phosphorylation is required for Cdc20 activation. Open-headed arrows indicate positive interactions such activation, flat ended arrows indicate negative interactions such as inhibition, and solid-headed arrows indicate*

transition of proteins between two states i.e. phosphorylation. The reactions that are altered for this model are described in more detail below.

The reactions are similar to the initial model with the following exceptions. Clb1P replaces Clb1 in the inactivation of CKI and the phosphorylation of X, and replaces IE in the activation of Cdc20. Clb1 phosphorylation and dephosphorylation are described by MM kinetics. Clb1P catalyses phosphorylation, whilst dephosphorylation occurs at a background rate. Clb1P undergoes degradation at the same rate as Clb1. A low basal rate of phosphorylation of Clb1, kp_{Clb1}, is taken into consideration to initiate the feedback loop.

Reactions	Contributing	Parameters
→ Clb1		$ks_{clb1,}$
Clb1 →	CKI, Cdc20	kdclb1, $kd_{clb1CKI}$,$kd_{clb1cdc20}$
Clb1P →	CKI, Cdc20	kdclb1, $kd_{clb1CKI}$,$kd_{clb1cdc20}$
Clb1→ Clb1P	Clb1P	$kp_{clb1clb1p}$ Jp_{clb1}
Clb1P →Clb1	CKI, Cdc20	kdp_{clb1}, Jdp_{clb1}
CKI (active) → CKI (inactive)	X, Clb1-P, Clb3	$ki_{CKIx,}$ Ji_{CKI} ka_{CKI}, $ka_{CKIcdc20}$, Ja_{CKI}
CKI (inactive) → CKI (active)	Cdc20,	ka_{CKI}, $ka_{CKIcdc20}$, Ja_{CKI}
Cdc20 (active)→ Cdc20(inactive)	IE	ki_{cdc20}, Ji_{cdc20}
Cdc20 (inactive)→ Cdc20(active)		$ka_{cdc20ie}$, Ja_{cdc20}
X→XP	Clb1	kp_{x}, $Jp_{x,}$
XP→X	Y	kdp_{xp}, Jdp_{xp}
Y→	Cdc20, X, XP	kd_{y}

Table 4-6 ***Reactions of model 2.*** *Table of reactions for the model incorporating Cdc28 phosphorylation of Clb1 listed with parameters and variables that contribute to the rates.*

Once again, Cdc20, CKI and X reactions are under conservation relationships. The model is described by Equation System 4-4:

$$\frac{d[Clb1]}{dt} = ks_{Clb1} + \frac{kdp_{Clb1P}\cdot [Clb1P]}{Jdp_{Clb1P} + [Clb1P]} - (kd_{Clb1} + kd_{Clb1CKI}\cdot [CKIa] + kd_{Clb1Cdc20}\cdot [Cdc20a] + \frac{kp_{Clb1} + kp_{Clb1Clb}\cdot [Clb1P]}{Jp_{Clb1} + [Clb1]})\cdot [Clb1] \quad (26)$$

$$\frac{d[Clb1P]}{dt} = (kp_{Clb1} + \frac{kp_{Clb1Clb}\cdot [Clb1P]}{Jp_{Clb1} + [Clb1]})\cdot [Clb1] - (kd_{Clb1} + kd_{Clb1CKI}\cdot [CKIa] + kd_{Clb1Cdc20}\cdot [Cdc20a] + \frac{kdp_{Clb1P}}{Jdp_{Clb1P} + [Clb1P]})\cdot [Clb1P] \quad (27)$$

$$\frac{d[CKIa]}{dt} = \frac{(ka_{CKI1} + ka_{CKICdc20}\cdot [Cdc20a])\cdot ([CKI_t] - [CKIa])}{Ja_{Cdh1} + ([CKI_t] - [CKIa])} - \frac{(ki_{CKIX}\cdot [X] + ki_{CKIClb1}\cdot [Clb1P])\cdot [CKIa]}{Ji_{CKI} + [CKIa]} \quad (28)$$

(29) $$\frac{d[Cdc20A]}{dt} = \frac{ka_{Cdc20IE} \cdot [Clb1P] \cdot ([Cdc20_t] - [Cdc20a])}{Ja_{Cdc20} + ([Cdc20_t] - [Cdc20a])} - \frac{ki_{Cdc20} \cdot [Cdc20a]}{Ji_{Cdc20} + [Cdc20a]}$$

(30) $$\frac{d[X]}{dt} = \frac{kdp_X \cdot [Y] \cdot [XP]}{Jdp_X + [XP]} - \frac{kp_X \cdot ([Clb1] + [Clb1P]) \cdot [X]}{Jp_X + [X]}$$

(31) $$\frac{d[Y]}{dt} = -kd_Y \cdot [Cdc20A] \cdot [Y]$$

Equation System 4-4 ***System of ODEs describing Model 2*** *The model described in Figure 4-10, incorporating Clb1 Autophosphorylation, is converted into ordinary differential equations, suitable for simulating in XPP*

Parameter	Value	Initial conditions	
ks_{clb1}	0.015	X=1	Y=1
kd_{clb1}	0.001	Cdc20A=0	Clb1P=0
$kd_{clb1CKI}$	0.08	Clb1=0	CKI=1
$kd_{clb1cdc20}$	0.08		
kdp_{clb1}	0.01		
Jdp_{clb1}	0.01		
kp_{clb1}	0.01		
$kp_{clb1clb1}$	0.08		
Jp_{clb1}	0.01		
ka_{CKI}	0.4		
$ka_{CKIcdc20}$	0.1		
ki_{CKIx}	6		
$ki_{CKIclb1}$	0.2		
Ja_{CKI}	0.01		
Ji_{CKI}	0.01		
$ka_{cdc20clb1p}$	0.5		
ki_{cdc20}	0.2		
Ja_{cdc20}	0.001		
Ji_{cdc20}	0.001		
kp_{xpclb1}	0.07		
Jp_x	0.05		
Kdp_{xy}	0.1		
Jdp_x	0.04		
kd_{ycdc20}	0.8		
CKI_t	1		
$Cdc20_t$	1		
X_t	1		

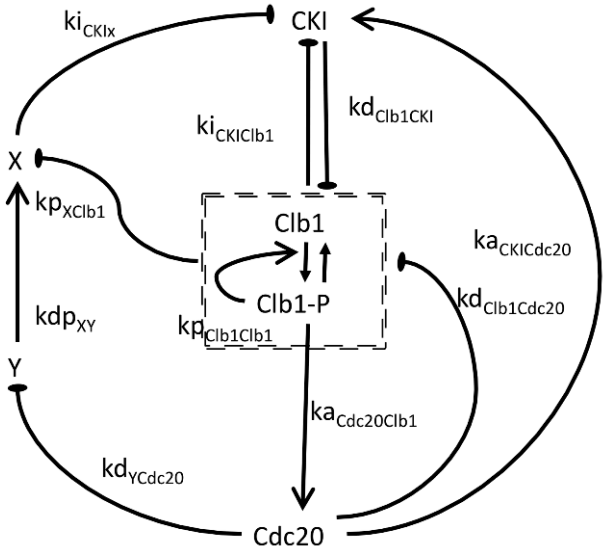

Table 4-7 ***Parameters for the Autophosphorylation-driven Model 2****. Parameters and initial conditions for the model in which Clb1 phosphorylation is dependent on autophosphorylation. The*

wiring diagram in Figure 1-2 is reproduced for reference. Parameters controlling the interactions are shown next to the arrows indicating the interaction.

Parameters were selected to fit the same criteria as the Initial model (Section 4.2.3.3) and are given in Table 4-7. The resulting time series is shown in Figure 4-11.

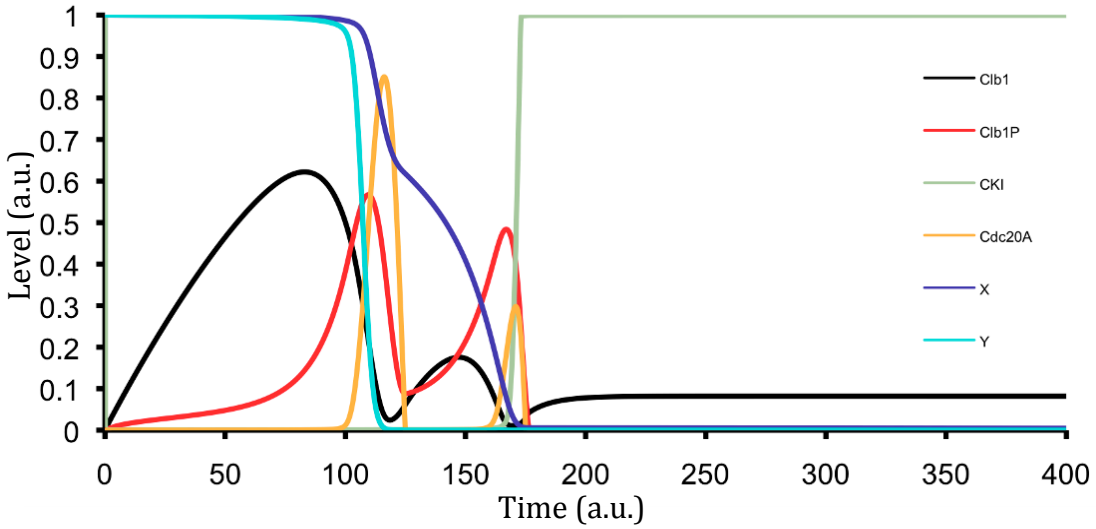

Figure 4-11 ***Numerical simulation of Model 2.*** *Time series for the Autophosphorylation-driven Model 2 as described in Equation System 4-4 using the parameters listed in Table 4-7. Two distinct peaks of Clb1-CDK and Clb1P-CDK activity, before CKI activity rises to induce the low CDK steady state.*

The oscillations are driven by a relaxation oscillator formed of Clb1-CDK and Cdc20. The separation of the first and second peaks was greater with the Autophosphorylation-driven Model 2 than with Ime2-driven Model 1 (Section 4.4.1). Clb1 began to decline while Clb1P was still increasing, even before Cdc20A made an appearance. High phosphorylation rates, as well as Cdc20A, depleted the Clb1 pool. Unphosphorylated Clb1 formed two peaks due to the decrease in Clb1P, reducing the phosphorylation rate and allowing unphosphorylated Clb1 to accumulate.

4.4.4 Requirement of Cdc28 kinase activity for Clb1 phosphorylation and nuclear localisation

The above model predicts that Cdc28 activity would be required for the phosphorylation of Clb1. The analogue sensitive *cdc28-as* allele can be used to determine whether Cdc28 activity is required for the modification of Clb1. Cdc28-as, but not Cdc28, is sensitive to the ATP analogue 1-NM-PP1 (Benjamin et al., 2003; Bishop et al., 2000).

4.4.4.1 *cdc28-as* allele: effects on Clb1 modification

CDC28 P_{CLB2}*CDC20 CLB1-Myc*$_9$ and *cdc28-as* P_{CLB2}*CDC20 CLB1-Myc*$_9$ strains of yeast were induced to enter sporulation by resuspension in SPO media. The analogue 1-NM-PP1 was added to sporulating cultures to a final concentration of 10μM at 5, 6, 7 and 8 hours after the time of resuspension in sporulation media. An equivalent amount of the solvent DMSO was added to the negative control cultures at the 5 hour time point. Samples were taken for *in situ* immunofluorescence and TCA-prepared cell extracts.

The negative controls both showed Clb1-Myc$_9$ modification, which indicated that both DMSO and the *cdc28-as* allele had no effect. The wild-type strain expressed Clb1 an hour later than the *cdc28-as* strain (Figure 4-12).

Clb1-Myc$_9$, though still expressed, showed no gel shift when the inhibitor was added at 5 hours (Figure 4-12). In the following gels, showing later additions of 1-NM-PP1, the phosphorylation arose, but was lost at the time point following the addition of the inhibitor. CDK activity is therefore required for the phosphorylation of Clb1 and for maintenance of the phosphorylated state.

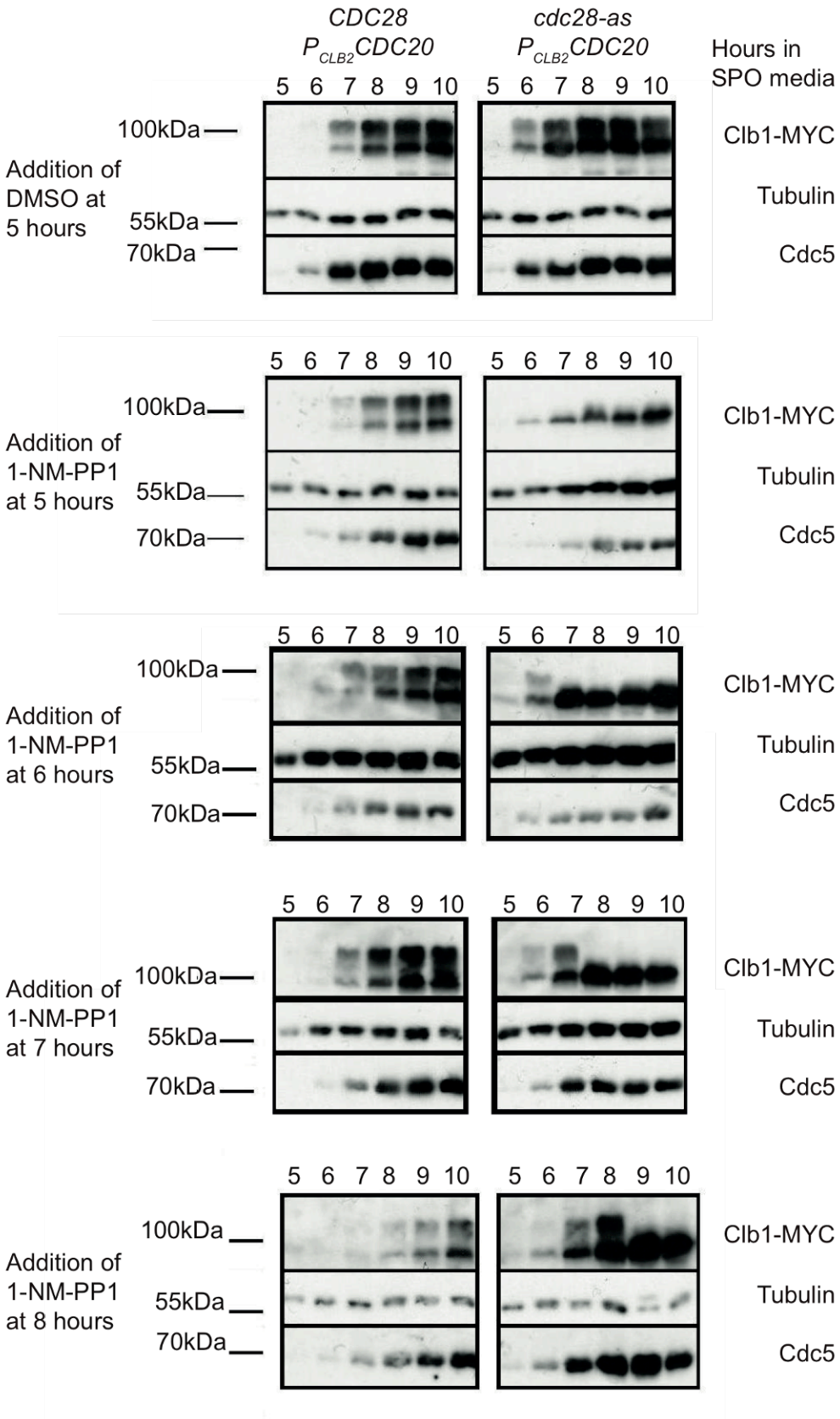

Figure 4-12 ***Inhibition of Cdc28-as in cells arrested in metaphase I prevents Clb1 modification.*** *Cultures of cells bearing* P_{CLB2}CDC20 CLB1-MYC$_9$ CDC28 *and* P_{CLB2}CDC20 CLB1-MYC$_9$ cdc28-as *were induced to undergo meiosis by resuspension in SPO media. Cultures were*

treated by addition of 1-NM-PP1 to 20μM to separate cultures at 5, 6, 7, or 8 hours, or an equivalent volume of the solvent, DMSO, at 5 hours. Gel mobility of Clb1-Myc$_9$ was assayed by subjecting whole cell extracts to SDS-PAGE followed by western blot analysis using anti-myc. Blots were also probed with anti-tubulin and anti-Cdc5. Asterisks show significance calculated using Chi Squared test (p<0.05, ** p<0.01, ***p<0.001).*

Cdc5 expression in the *cdc28-as* strain showed a similar difference in timing to Clb1, arising an hour later compared to the *CDC28* strain. Addition of the inhibitor at 5 hours led to a further delay in expression of Cdc5.

The gel shift is seen to disappear after addition of CDK activity, which suggests that CDK activity is required for the phosphorylation of Clb1. There is one CDK consensus site in Clb1. A single phosphorylation is unlikely to cause a large gel shift, although the effect of a phosphorylation on gel mobility is dependent on the surrounding sequence. The size of the gel shift can be accounted for, if CDK phosphorylation of Clb1 signals for further phosphorylation by other kinases, or CDK may phosphorylate other proteins to indirectly cause Clb1 phosphorylation.

4.4.4.2 *cdc28-as* allele: effects on Clb1 localisation

Cdc28 activity is required for the phosphorylation of Clb1, and may also be required for Clb1 nuclear localisation. To examine this possibility, fixed cell samples from the cultures in 4.4.4.1 were subjected to immunofluorescent imaging to determine Clb1-Myc$_9$ localisation. Clb1-Myc$_9$ localised to the nucleus in both of the control cultures, with DMSO addition at 5 hours (Figure 4-13). The *cdc28-as* allele seemed to have some inhibitor-independent effect, reducing detectable Clb1 and slightly reducing nuclear localisation.

Addition of the inhibitor led to reduced nuclear localisation of Clb1 in the *cdc28-as* strain (Figure 4-13). Nuclear concentration of Clb1 was not entirely prohibited, but was reduced after inhibitor addition, compared to the *CDC28* strain. The clearest demonstration of this is the comparison of the 7 hour additions of DMSO and 1-NM-PP1. Therefore, Cdc28 activity is required for both the nuclear localisation and phosphorylation of Clb1. These localisation results, and others in this chapter, have to be considered with the fact that a control to detect non-specific binding of the antibodies was not performed.

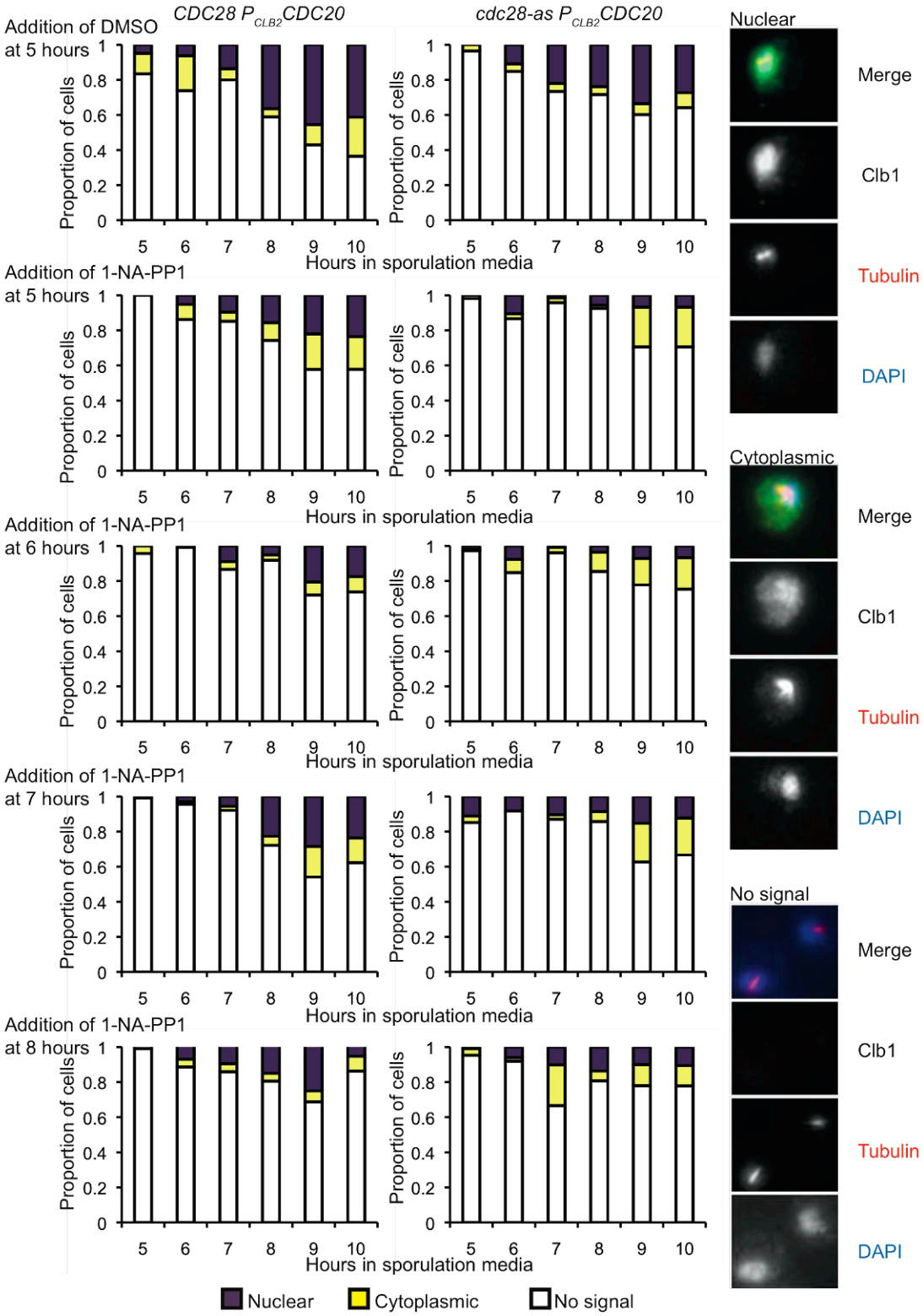

Figure 4-13 ***Inhibition of cdc28-as in cells arrested in metaphase I reduces Clb1 concentration in the nucleus.*** *Cultures of cells bearing* P_{CLB2}CDC20 CLB1-MYC_9 CDC28 *and* P_{CLB2}CDC20 CLB1-MYC_9 cdc28-as *were induced to undergo meiosis by resuspension in SPO media. Cultures were treated by addition of 1-NM-PP1 to 20μM to separate cultures at 5, 6, 7, or 8 hours, or an equivalent volume of the solvent, DMSO at 5 hours. Cells were fixed and examined for Clb1-*Myc_9 *localisation by* in situ *immunofluorescence. Proportion of cells with nuclear-concentrated Clb1 (purple),*

cytoplasmic or dispersed Clb1 (yellow) and no detectable Clb1 signals (white) are indicated. 100 cells were counted for each time point.

Strain	Addition	P_{CLB2}*CDC20 CLB1-MYC₉ CDC28* Mock addition 5	6	7	8	9	10	P_{CLB2}*CDC20 CLB1-MYC₉ cdc28-as* 5 hour addition 5	6	7	8	9	10	6 hour addition 5	6	7	8	9	10
P_{CLB2}*CDC20 CLB1-MYC₉ CDC28* / P_{CLB2}*CDC20 CLB1-MYC₉ cdc28-as*	Mock	0	***		**	***	***	***	**		***	***	***	***	***		***	***	***
	5								***	***		***	***						
	6													***	***	***	*	***	***
	7																		
	8																		

Strain	Addition	P_{CLB2}*CDC20 CLB1-MYC₉ cdc28-as* 7 hour addition 5	6	7	8	9	10	8 hour addition 5	6	7	8	9	10
P_{CLB2}*CDC20 CLB1-MYC₉ CDC28* / P_{CLB2}*CDC20 CLB1-MYC₉ cdc28-as*	Mock	***	***	***	*	***	***	***	***		***	***	***
	5												
	6												
	7	***			***	***	***						
	8									***		***	***

Table 4-8 ***Significance of Clb1 location*** *Table shows significance of Clb1 localisation changes between* P_{CLB2}CDC20 CLB1-MYC₉ cdc28-as *cultures with and without addition of estradiol, and between* P_{CLB2}CDC20 CLB1-MYC₉ cdc28-as and P_{CLB2}CDC20 CLB1-MYC₉ CDC28 *cultures with addition of estradiol. Asterisks show significance calculated using Chi Squared test (* p<0.05, ** p<0.01, ***p<0.001).*

Significant differences in Clb1 localisation are seen using the Chi Squared test between the mock-treated *P_{CLB2}CDC20 CLB1-MYC₉ cdc28-as* and *P_{CLB2}CDC20 CLB1-MYC₉ CDC28* cultures, so it is not possible to say for sure that the inhibition of Cdc28 causes the significant differences between the estradiol-treated *P_{CLB2}CDC20 CLB1-MYC₉ cdc28-as* and *P_{CLB2}CDC20 CLB1-MYC₉ CDC28* cultures.

4.4.5 Model 3: Alternative Kinase

An alternative, CDK-dependent kinase was also considered for phosphorylating Clb1. This kinase is not already incorporated in the model, but its activity would depend on activation by CDK. One possibility, Cdc5, a polo-like kinase, is involved in both entry to and exit from meiosis, and is a candidate kinase for phosphorylating Clb1 (Kamieniecki et al., 2005; Sourirajan and Lichten, 2008). Cdc5 recognises a Polo Box binding sequence (S-pS/pT-P/X) and on binding to this, phosphorylates a consensus sequence elsewhere in the protein (Elia et al., 2003; Lowery et al., 2004). The Polo-Box binding sequence

includes a phosphorylated serine residue, often phosphorylated by CDK. Although the Clb1 sequence includes a consensus for CDK phosphorylation, it does not have a recognisable Polo-Box domain. Cdc5 may be yet be involved in Clb1 phosphorylation, binding to an as-yet unrecognised sequence or directed to Clb1 by an interacting protein. Alternatively, Cdc5 may indirectly cause Clb1 phosphorylation, activating a second kinase. CDK activates Cdc5 (Mortensen et al., 2005), providing the delay.

The model was altered to include an alternative kinase Z, which is activated by Clb1-CDK and in turn activates Clb1 to trigger Cdc20 activation. The model does not include all of the functions of Cdc5 (which has known roles in meiotic entry (Sourirajan and Lichten, 2008) and FEAR (Rahal and Amon, 2008b; Shou et al., 2002)). The only characteristics of Cdc5 described in the model are the activation by Clb1 and the proposed phosphorylation of Clb1. The model could therefore consider any kinase that covered these roles. The model is referred to as Alternative Kinase or Model 3 (Figure 4-14).

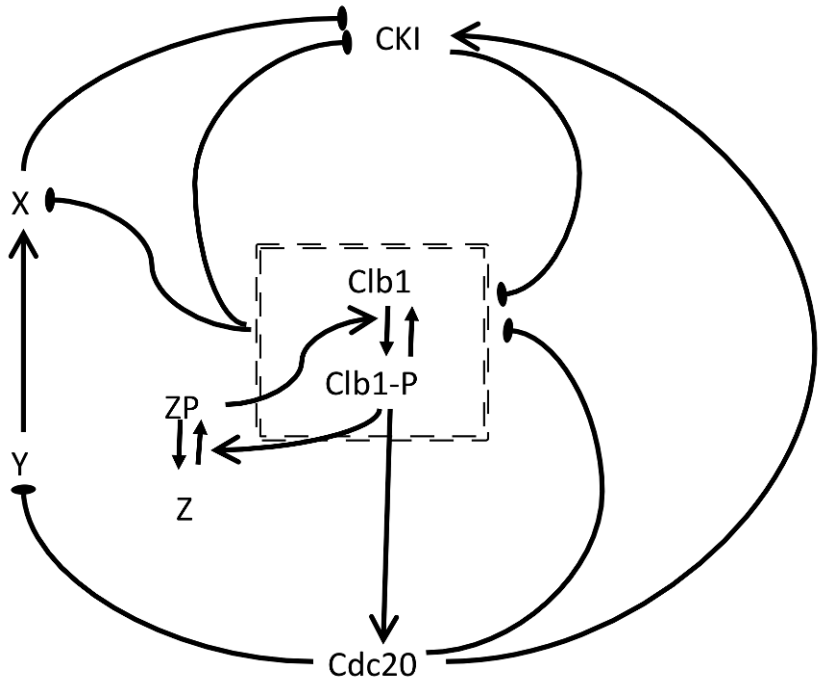

Figure 4-14 ***Proposed Wiring diagram for model 3.*** *This model incorporates an Alternative Kinase to drive Clb1 phosphorylation. Clb1 is required for activation of the alternative kinase. Open-headed arrows indicate positive interactions such activation, flat ended arrows indicate negative interactions such as inhibition, and solid-headed arrows indicate transition of proteins between two states i.e. phosphorylation. The altered reactions are described below.*

Many reactions were taken from the Initial model (Section 4.2.3.2), except for the following: Clb1P replaces Clb1 in the inactivation of CKI and phosphorylation of X, and IE in the activation of Cdc20. Clb1 and Z phosphorylation and dephosphorylation are described by MM kinetics. Phosphorylation of Clb1 is catalyzed by Z, while dephosphorylation is not catalysed. Clb1P undergoes degradation at the same rate as Clb1. Phosphorylation of Z is catalysed by Clb1P and dephosphorylation is not catalysed. A low basal rate of phosphorylation, kp_Z, of Z, initiates the feedback loop on Clb1.

Reactions	Contributing	Parameters
→ Clb1		$ks_{clb1,}$
Clb1 →	CKI, Cdc20	kdclb1, $kd_{clb1CKI}$,$kd_{clb1cdc20}$
Clb1P →	CKI, Cdc20	kdclb1, $kd_{clb1CKI}$,$kd_{clb1cdc20}$
Clb1→ Clb1P	ZP	kp_{clb1zp} Jp_{clb1}
Clb1P →Clb1	CKI, Cdc20	kdp_{clb1}, Jdp_{clb1}
CKI (active) → CKI (inactive)	X, Clb1-P, Clb3	$ki_{CKIx,}$ Ji_{CKI} ka_{CKI}, $ka_{CKIcdc20}$, Ja_{CKI}
CKI (inactive) → CKI (active)	Cdc20,	ka_{CKI}, $ka_{CKIcdc20}$, Ja_{CKI}
Cdc20 (active)→ Cdc20(inactive)	IE	ki_{cdc20}, Ji_{cdc20}
Cdc20 (inactive)→ Cdc20(active)		$ka_{cdc20ie}$, Ja_{cdc20}
X→XP	Clb1	kp_x, $Jp_{x,}$
XP→X	Y	kdp_{xp}, Jdp_{xp}
Y→	Cdc20, X, XP	kd_y
Z→ZP	Clb1P	kp_{zClb1}, kp_z, $Jp_{x,}$
ZP→Z		kdp_{zp}, Jdp_{zp}

Table 4-9 ***Reactions of model 1.*** *Table of reactions for the model incorporating phosphorylation of Clb1 by an alternative kinase, listed with parameters and variables that affect the rates.*

Cdc20, CKI, X and Z reactions are under conservation relationships. Incorporating the above, the alternative kinase-driven model can be described by the ODEs in Equation System 4-5:

$$\frac{d[Clb1]}{dt} = ks_{Clb1} + \frac{kdp_{Clb1P}\cdot [Clb1P]}{Jdp_{Clb1P} + [Clb1P]} - (kd_{Clb1} + kd_{Clb1CKI}\cdot [CKI] + kd_{Clb1Cdc20}\cdot [Cdc20a] + \frac{kp_{Clb1Z}\cdot [ZP]}{Jp_{Clb1} + [Clb1]})\cdot [Clb1] \quad (32)$$

$$\frac{d[Clb1P]}{dt} = (\frac{kp_{Clb1Z}\cdot [[Z]}{Jp_{Clb1} + [Clb1]})\cdot [Clb1] - (kd_{Clb1} + kd_{Clb1CKI}\cdot [CKI] + kd_{Clb1Cdc20}\cdot [Cdc20a] + \frac{kdp_{Clb1P}}{Jdp_{Clb1P} + [Clb1P]})\cdot [Clb1P] \quad (33)$$

$$\frac{d[CKIa]}{dt} = \frac{(ka_{CKI} + ka_{CKICdc20}\cdot [Cdc20a])\cdot ([CKI_t] - [CKIa])}{Ja_{Cdh1} + ([CKI_t] - [CKIa])} - \frac{(ki_{CKIX}\cdot [X] + ki_{CKIClb1}\cdot [Clb1P])\cdot [CKIa]}{Ji_{CKI} + [CKIa]} \quad (34)$$

(35) $$\frac{d[Cdc20A]}{dt} = \frac{ka_{Cdc20IE}[Clb1P]\cdot([Cdc20_t]-[Cdc20a])}{Ja_{Cdc20}+([Cdc20_t]-[Cdc20a])} - \frac{ki_{Cdc20}[Cdc20a]}{Ji_{Cdc20}+[Cdc20a]}$$

(36) $$\frac{d[X]}{dt} = \frac{kdp_X\cdot[Y]\cdot([X_0]-[X])}{Jdp_X+([X_0]-[X])} - \frac{kp_X\cdot[Clb1P]\cdot[X]}{Jp_X+[X]}$$

(37) $$\frac{d[Y]}{dt} = -kd_Y\cdot[Cdc20A]\cdot[Y]$$

(38) $$\frac{d[ZP]}{dt} = \frac{kp_Z+kp_{ZClb1}\cdot[Clb1P]\cdot([Z_0]-[ZP])}{Jp_z+([Z_0]-[ZP])} - \frac{kdp_Z\cdot[ZP]}{Jdp_Z+[ZP]}$$

Equation System 4-5 ***System of ODEs describing Model 3*** *The model in which Alternative Kinase driven Clb1 phosphorylation replaces IE, is converted into ordinary differential equations.*

Parameters (Table 4-10) were chosen to match the previous criteria (Section 4.2.3.3) and the resulting time series is shown in Figure 4-15.

Parameter	Value	Initial conditions	
ks_{clb1}	0.01	Clb1=0	CKI=1
kd_{clb1}	0.005	Cdc20=0	X=0
$kd_{clb1CKI}$	0.1	Clb1P=0	Y=0
$kd_{clb1cdc20}$	0.06	Z=1	ZP=0
kdp_{clb1}	0.12		
Jdp_{clb1}	0.01		
kp_{clb1zp}	0.6		
Jp_{clb1}	0.01		
ka_{CKI}	0.3		
$ka_{CKIcdc20}$	0.8		
ki_{CKIx}	10		
$ki_{CKIclb1}$	4.4		
Ja_{CKI}	0.04		
Ji_{CKI}	0.04		
$ka_{cdc20clb1p}$	0.5		
ki_{cdc20}	0.12		
Ja_{cdc20}	0.001		
Ji_{cdc20}	0.001		
kp_{xpclb1}	0.2		
Jp_x	0.04		
kdp_{xy}	0.1		
Jdp_x	0.04		
kd_{ycdc20}	0.2		
Kp_{zclb1}	0.13		
Jp_z	0.04		

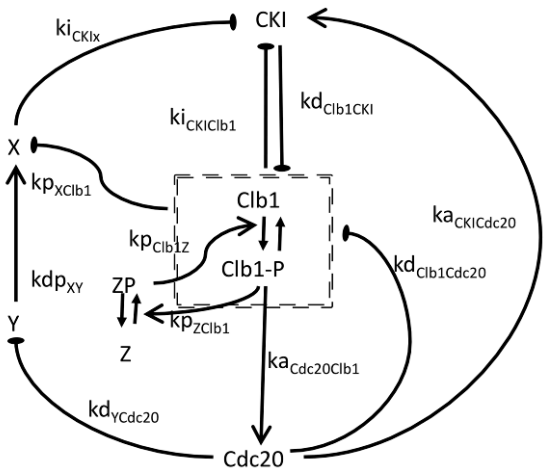

kdp_z	0.06
Jdp_z	0.04
CKI_t	1
$Cdc20_t$	1
X_t	1
Z_t	1
Z_t	1

Table 4-10 ***Parameters for model 3*** *Parameters for the model in which Clb1 phosphorylation is driven by an Alternative Kinase. The wiring diagram in Figure 4-14 is reproduced for reference. Parameters controlling the interactions are shown next to the arrows indicating the interaction.*

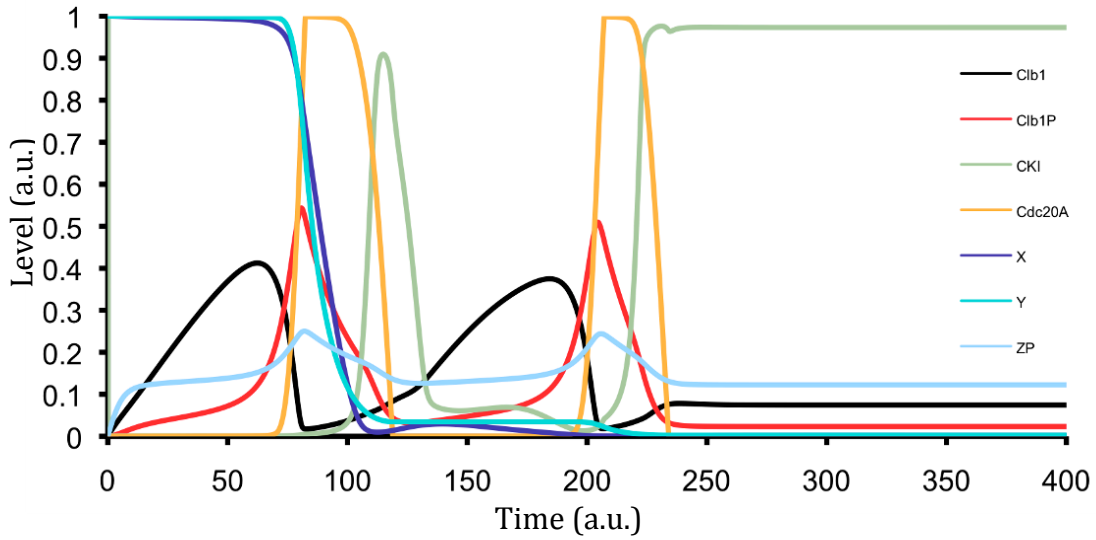

Figure 4-15 ***Numerical simulation of Model 3****. Time series for the Alternative Kinase-driven Model 3 as described in Equation System 4-5 using the parameters listed in Table 4-10.*

The two peaks of Clb1 activity were well separated. Cdc5 levels did not change much beyond small peaks that permitted Clb1 phosphorylation. CKI achieved a transient peak in the first cycle, due to rapid X degradation, but the reappearance of Clb1P prevented CKI from achieving dominance.

4.4.6 Requirement for Cdc5 for Clb1 localisation and modification

A Cdc5 meiotic-null strain was used to determine the requirement for Cdc5 for the modification and nuclear localisation of Clb1. *CDC5* was placed under the control of the *CLB2* promoter.

4.4.6.1 P_{CLB2}*CDC5*: effects on Clb1 modification

CDC5 P_{CLB2}*CDC20 CLB1-MYC*$_9$ and P_{CLB2}*CDC5* P_{CLB2}*CDC20 CLB1-MYC*$_9$ strains of yeast were induced to enter sporulation, and gel mobility of Clb1 was examined. The *CDC5* P_{CLB2}*CDC20* showed modification of Clb1 from 7 hours

(Figure 4-16). In contrast, the $P_{CLB2}CDC5$ $P_{CLB2}CDC20$ strain showed a single Clb1 band. This demonstrates that Cdc5 is required for the modification of Clb1.

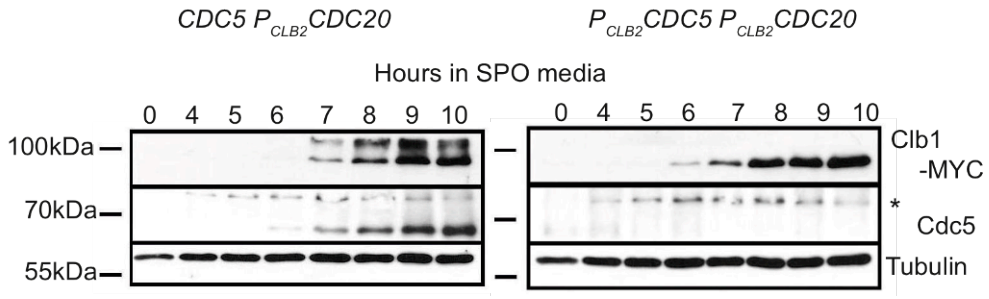

Figure 4-16 ***Clb1 is not modified in Cdc5-depleted cells arrested in metaphase I.*** *Cultures* of CDC5 P_{CLB2}CDC20 CLB1-MYC_9 *and* P_{CLB2}CDC5 P_{CLB2}CDC20 CLB1-MYC_9 *strains of yeast were induced to enter sporulation. Gel mobility of Clb1-*Myc_9 *was assayed by subjecting whole cell extracts to SDS-PAGE followed by western blot analysis using anti-myc. Blots were also probed with anti-tubulin and anti-Cdc5. Asterisk indicates cross-reactive band to the cdc5 antibody.*

Cdc5 is also required for progression into metaphase (Sourirajan and Lichten, 2008), so it is possible progression into metaphase is required for Clb1 phosphorylation to occur, rather than Cdc5 activity directly. This is examined further in Section 4.4.6.3.

4.4.6.2 $P_{CLB2}CDC5$: effects on Clb1 localisation

Cdc5 depletion is sufficient to prevent the phosphorylation of Clb1. Phosphorylation and nuclear localisation of Clb1 have been correlated in previous results so we looked at the localisation of Clb1 in Cdc5-depleted cells undergoing meiosis. Fixed cell samples from the above cultures were imaged to determine Clb1 localisation (Figure 4-17). These localisation results, and others in this chapter, have to be considered with the fact that a control to detect non-specific binding of the antibodies was not performed.

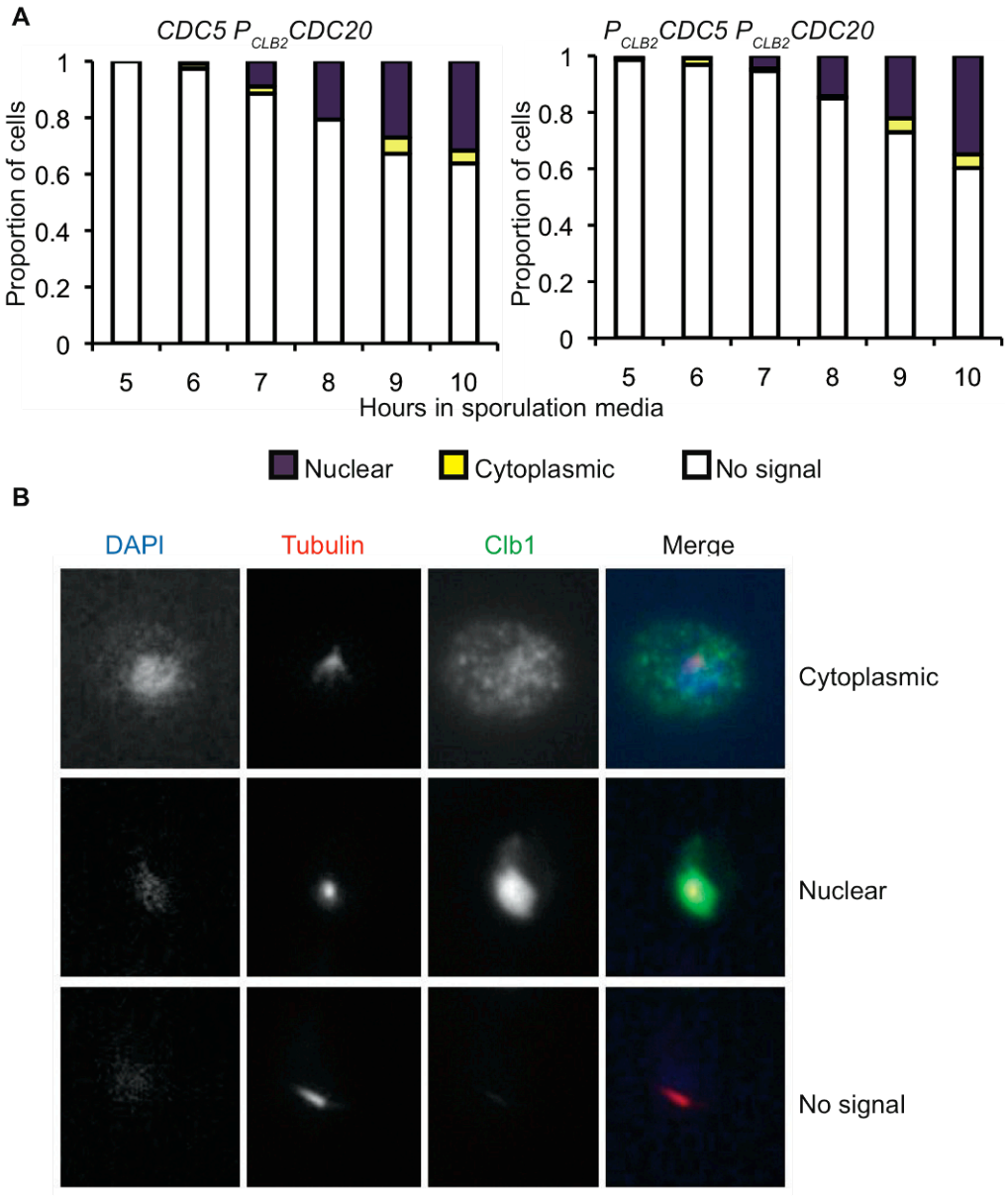

Figure 4-17 ***Clb1 is concentrated in the nucleus in Cdc5-depleted cells arrested in metaphase I*** *Cultures of* CDC5 P_{CLB2}CDC20 CLB1-MYC$_9$ and P_{CLB2}-CDC5 P_{CLB2}CDC20 CLB1-MYC$_9$ *strains of yeast were induced to enter sporulation. Cells were fixed and examined for Clb1-Myc$_9$ localisation by* in situ *immunofluorescence. Proportion of cells with nuclear-concentrated Clb1 (purple), cytoplasmic or dispersed Clb1 (yellow) and no detectable Clb1 signals (white) are indicated. 100 cells were counted for each time point.*

Clb1 nuclear localisation occurred to a similar extent in both *CDC5* and *P_{CLB2}CDC5* strains. Therefore, Cdc5 is not required for the nuclear localisation of Clb1. In addition, these data showed that Clb1 phosphorylation is unnecessary for its nuclear localisation.

4.4.6.3 Is Clb1 phosphorylation dependent on Cdc5 activity or passage into metaphase

The dependence of the phosphorylation on Cdc5 was complicated by the requirement of Cdc5 for passage through pachytene (Sourirajan and Lichten, 2008). The strain we used was depleted in meiosis for Cdc5, and therefore did not pass through pachytene. Passage through pachytene triggers the expression of a wide range of genes by the Ndt80 promoter (Chu and Herskowitz, 1998). Clb1 phosphorylation may, therefore, depend on the passage through pachytene, rather than Cdc5 activity directly. To determine this, we used cells arrested in pachytene using P_{CUP1}*NDT80*. In SPO media without copper, *NDT80* is not expressed and the cell arrests in pachytene (Xu et al., 1995).

Cdc5 was left under its native promoter, or placed under the P_{GAL} promoter to trigger overexpression. Under the native promoter, expression would be expected to be attenuated in the case of Ndt80 depletion. Expression of Cdc5 would be sufficient to trigger the role of Cdc5 in exiting pachytene. Clb1 would also not be expressed in the absence of Ndt80. Clb1 was placed under the P_{GAL} promoter in both strains, and expressed using the P_{GPD1}GAL4-ER system in which addition of estradiol to the media triggers expression. This would determine if Cdc5 activity is sufficient to phosphorylate Clb1 without the rest of the Ndt80 transcriptome. P_{CUP1}*NDT80* P_{GAL}*CLB1-HA*$_6$ P_{GAL}*CDC5* and P_{CUP1}*NDT80* P_{GAL}*CLB1-HA*$_6$ strains were induced to undergo meiosis by resuspension in SPO media. Estradiol or the solvent DMSO was added to each strain at 6 hours into SPO media. Clb1 gel mobility was examined (Figure 4-18).

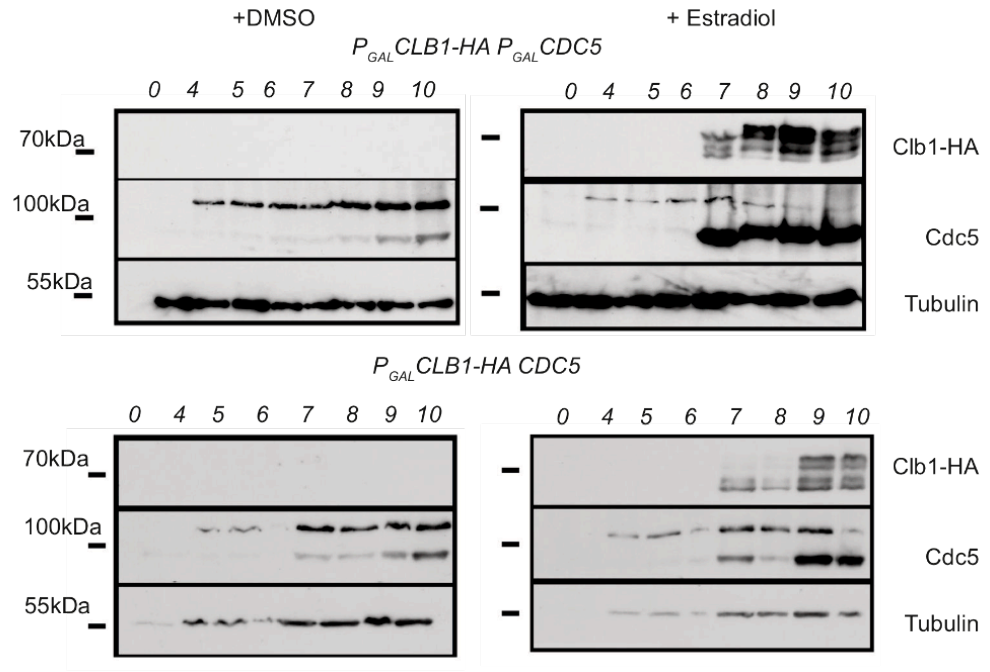

Figure 4-18 ***Cdc5 is sufficient to modify Clb1.*** *Cultures of cells bearing* P_{CUP1}NDT80 P_{GAL}CLB1-HA_6 P_{GAL}CDC5 and P_{CUP1}NDT80 P_{GAL}CLB1-HA_6 *were induced to undergo meiosis by resuspension in SPO media. Estradiol was added to 1 μM, or an equivalent volume of the solvent ethanol, at 6 hours. Gel mobility of Clb1-*HA_6 *was assayed by subjecting whole cell extracts to SDS-PAGE followed by western blot analysis using anti-HA. Blots were also probed with anti-tubulin and anti-Cdc5*

Clb1 was modified in both strains. However, Cdc5 was expressed in the *CDC5* strain, albeit at a lower amount than in the P_{GAL}*CDC5* strain. This indicated that the P_{CUP1}*NDT80* system might be sufficiently leaky to allow some low level induction of middle meiotic genes. An *ndt80Δ* strain may be used to prevent leaky expression of *NDT80*. Alternatively, a *cdc5-as* or P_{CLB2}*CDC5* strain may be used to confirm the Cdc5 activity dependence of the modification. Cdc5 appears to be required to cause Cdc5 phosphorylation.

Unlike the Clb1-Myc gel shift, Clb1-HA_6 and Clb1-NLS_2-HA_6 gel shifts appears to contain intermediate bands between the upper and lower band. In other reports, a Myc tagged version of another protein has shown a reduced ability to display gel shifts in response to phosphorylation (Schindler and Winter, 2006). If this is a trait of the Myc tag, it may explain this disparity between the tags – the intermediate bands don't resolve from the upper and lower bands as well with a Myc tag. The gel-shift seen with Clb1-TAP in Section 4.4.2.2 did not show intermediate bands either. The smaller HA tag may be allowing bands of partially phosphorylated protein to resolve more clearly.

4.5 Incorporating Clb1 phosphorylation as a protection mechanism from degradation

Y, the hypothetical protein, has been proposed to prevent the high CKI and low CDK state from becoming established until the second cycle. In Sections 4.2 and 4.3, Y fulfils this role by inhibiting the action of Clb1 on the Starter Kinase X until after first division. This was preferred because Ime2, proposed to play the role of Starter Kinase X (Dirick et al., 1998), is active during the second division (Schindler and Winter, 2006). However, the phosphorylation may lead to a substrate or localisation change rather than an activity or degradation rate change. Alternatively, Ime2 alone may be insufficient to play the role of Starter Kinase (Sedgwick et al., 2006). In these cases, inactivation of Starter Kinase activity need not require inactivation of Ime2. We considered models in which maintaining Starter Kinase X activity was not the method by which a second cycle was achieved.

4.5.1.1 Model 4: Clb1P acts to prevent Clb1 inactivation

Y may permit the model to achieve a second cycle by inhibiting the action of CKI on Clb1. This rearrangement of the Initial model allows alternative incorporation of Clb1 phosphorylation. In this case, the phosphorylation is proposed to render Clb1 insensitive to the inhibition by the inhibitors designated by CKI. Clb1 phosphorylation coincides with its activity during meiosis I (Carlile and Amon, 2008). However, the lower band did not disappear when the upper band was present, implying that the unphosphorylated portion of Clb1 did not undergo increased degradation (Section 3.2) although this may be the result of poor synchrony in the sporulating culture. Clb1P may be resistant to binding by such stoichiometric inhibitors as Sic1. It is implied, by the persistence of the Clb1 protein and lack of Clb1 activity, that some meiosis-specific inhibitor of Clb1 exists (Carlile and Amon, 2008).

IE is still included, as Clb1P does not act in its place (Figure 4-19). The three kinases proposed in Chapter 3 and in Section 4.4 are not considered for roles as the candidate kinase of Clb1. Instead, Y is considered responsible for Clb1 phosphorylation, with an assumed background dephosphorylation rate.

(Alternatively, Y could have been proposed to inhibit Clb1P dephosphorylation against a constant phosphorylation rate.)

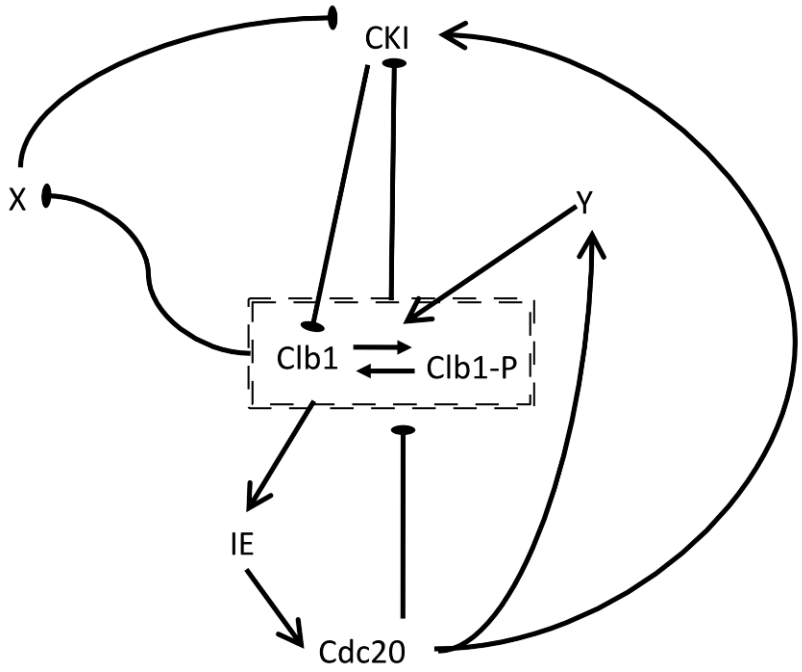

Figure 4-19 ***Proposed wiring diagram of the Degradation model.*** *This model incorporates Clb1 phosphorylation for protection from inactivation at the MI-II transition. Open-headed arrows indicate positive interactions such activation, flat ended arrows indicate negative interactions such as inhibition, and solid-headed arrows indicate transition of proteins between two states i.e. phosphorylation. The reactions are described below.*

Synthesis of Clb1 is described using zero order mass action kinetics. Background rates of degradation of Clb1 and Clb1P are identical, and described using first order mass action kinetics. Regulated degradation of Clb1, Clb1P and Y are described using second order mass action kinetics; all three are degraded by Cdc20, but only Clb1 is degraded by CKI.

Activation and inactivation of CKI, IE and Cdc20 are described using MM kinetics. IE is activated by Clb1 and Clb1P, and inactivation is unregulated. Cdc20 is activated by IE and inactivation is unregulated. CKI undergoes regulated activation by Cdc20, and regulated inactivation by Clb1, Clb1P and X. Phosphorylation and dephosphorylation reactions are described using MM kinetics. X is phosphorylated by Clb1 and Clb1P, and Clb1 is phosphorylated by Y.

Reactions	Contributing	Parameters
→ Clb1		$ks_{clb1,}$
Clb1 →	CKI, Cdc20	kdclb1, $kd_{clb1CKI}$, $kd_{clb1cdc20}$
Clb1→Clb1P	Y	kp_{clb1y}
Clb1P→Clb1		kdp_{clb1}
Clb1P	CKI, Cdc20	kdclb1, $kd_{clb1cdc20}$

CKI (active) → CKI (inactive)	X, Clb1P,	ki_{CKIx}, Ji_{CKI} ka_{CKI}, $ka_{CKIcdc20}$, Ja_{CKI}
CKI (inactive) → CKI (active)	Cdc20,	ka_{CKI}, $ka_{CKIcdc20}$, Ja_{CKI}
Cdc20 (active)→ Cdc20(inactive)	IE	ki_{cdc20}, Ji_{cdc20}
Cdc20 (inactive)→ Cdc20(active)		$ka_{cdc20ie}$, Ja_{cdc20}
IE (active) → IE (inactive)	Clb1	ka_{ieclb1}, Ja_{ie}
IE (inactive) → IE (active)		ki_{ieclb1}, Ji_{ie}
X→XP	Clb1, Clb1P	kp_x, $Jp_{x,}$
Y→	Cdc20, X	kd_y

Table 4-11 ***Reactions of the model.*** *Table of reactions for the model depicted in Figure 4-1. Each reaction is listed with parameters and variables that contribute to the rates.*

The total amounts of CKI, Cdc20 and IE are conserved. The model is described by the ODEs in Equation System 4-6.

$$\frac{d[Clb1]}{dt} = ks_{Clb1} + \frac{kd_{Clb1p}\cdot [Clb1P]}{Jdp_{Clb1p} + [Clb1P]} - (kd_{Clb1} + kd_{Clb1Cdc20}\cdot [Cdc20a] + kd_{Clb1CKI}\cdot [CKI] + \frac{kp_{Clb1Y}\cdot Y}{Jp_{Clb1} + [Clb1]})\cdot [Clb1] \quad (39)$$

$$\frac{d[Clb1P]}{dt} = \frac{kp_{Clb1Y}\cdot Y\cdot [Clb1]}{Jp_{Clb1} + [Clb1]} - (kd_{Clb1} + kd_{Clb1Cdc20}\cdot [Cdc20a] + \frac{kdp_{Clb1p}}{Jdp_{Clb1p} + [Clb1P]})\cdot [Clb1P] \quad (40)$$

$$\frac{d[IEa]}{dt} = \frac{ka_{IEClb1}\cdot ([Clb1] + [Clb1P])\cdot ([IEt] - [IEa])}{Ja_{IE} + ([IEt] - [IEa])} - \frac{ki_{IE}\cdot [IEa]}{Ji_{IE} + [IEa]} \quad (41)$$

$$\frac{d[CKIa]}{dt} = \frac{(ka_{CKI} + ka_{CKICdc20}\cdot [Cdc20a])\cdot ([CKI_t] - [CKIa])}{Ja_{CKI} + (CKI_t - CKIa)} - \frac{(ki_{CKIX}\cdot [X] + ki_{CKIClb1}\cdot ([Clb1] + [Clb1P])\cdot [CKIa]}{Ji_{CKI} + [CKIa]} \quad (42)$$

$$\frac{d[Cdc20A]}{dt} = \frac{ka_{Cdc20IE}\cdot [IE]\cdot ([Cdc20t] - [Cdc20a])}{Ja_{Cdc20} + ([Cdc20t] - [Cdc20a])} - \frac{ki_{Cdc20}\cdot [Cdc20a]}{Ji_{Cdc20} + [Cdc20a]} \quad (43)$$

$$\frac{d[X]}{dt} = -\frac{kp_X\cdot ([Clb1] + [Clb1P])\cdot [X]}{Jp_X + [X]} \quad (44)$$

$$\frac{d[Y]}{dt} = -kd_Y\cdot [Cdc20A]\cdot [Y] \quad (45)$$

Equation System 4-6 ***System of ODE's for Model 4*** *Ordinary differential equations for the model described in Figure 4-19 incorporating Clb1P in resistance to CKI.*

Parameters were selected by the same criteria as before (Section 4.2.3.3). The parameters listed in the following Table 4-12 resulted in the time series shown in Figure 4-20.

Parameter	Value	Initial Conditions	
ks_{clb1}	0.01	Clb1=0	Clb1P=0
kd_{clb1}	0.005	Cdc20A=0	X=1
$kd_{clb1CKI}$	1	CKI=1	IE=1
$kd_{clb1cdc20}$	0.15	Y=1	
kdp_{clb1P}	0.01		
Jdp_{clb1P}	0.04		
kp_{clb1Y}	0.7		
Jp_{clb1}	0.04		
ka_{CKI}	0.4		
$ka_{CKIcdc20}$	0.5		
ki_{CKIx}	2		
$ki_{CKIclb1}$	20		
Ja_{CKI}	0.04		
Ji_{CKI}	0.04		
$ka_{cdc20IE}$	1		
kic_{dc20}	0.5		
Ja_{cdc20}	0.001		
Ji_{cdc20}	0.001		
ka_{IEClb1}	0.1		
ki_{IE}	0.02		
Ja_{IE}	0.01		
Ji_{IE}	0.01		
kp_{XClb1}	0.2		
Jp_{X}	0.04		
kdp_{x}	0.1		
Jdp_{x}	0.04		
kd_{ycdc20}	0.1		
CKI_t	1		
$Cdc20_t$	1		
X_t	1		
Z_t	1		

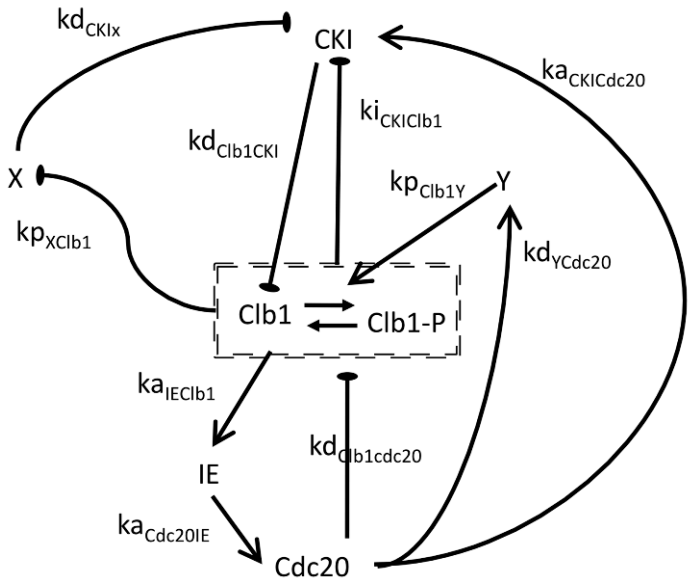

Table 4-12 ***Parameters for Model 4*** *Parameters for the Degradation model including Clb1 phosphorylation in resistance to CKI. The wiring diagram in Figure 4-19 is reproduced for reference. Parameters controlling the interactions are shown next to the arrows indicating the interaction.*

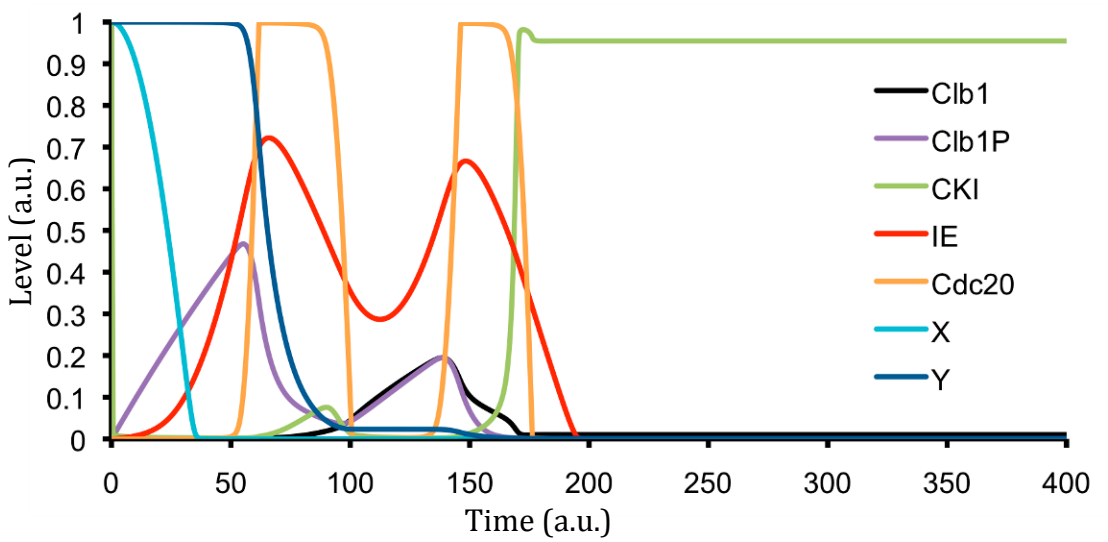

Figure 4-20 ***Numerical simulation of the initial model.*** *Time series of Model 4, Degradation model, incorporating Clb1 phosphorylation in resistance to CKI simulated using Equation System 4-6 and the parameters in Table 4-12.*

Model 4 could reproduce the two-peak representation of meiosis, as with the Initial model. In this time series, Clb1P dominated during the first division, while Clb1P and Clb1 were both present in the second cycle. Clb1 and Clb1P levels decreased between the cycles. However, the phosphorylation of Clb1 was sufficient to maintain low levels of Clb1 activity against the CKIs during the first cycle, and CKI could not achieve dominance until after the second cycle. This implies that Clb1P resistance could feasibly be a method by which CDK activity is partially maintained during the meiosis I to II transition.

In Model 4, if Cdc20 does not become active, Y is not removed and Clb1P will remain phosphorylated, as found in $P_{CLB2}CDC20$ mutants. The effect of $P_{CLB2}CDC55$ mutants cannot be demonstrated, as Cdc55 is not explicit in the model. Here, Y is required to phosphorylate Clb1, imparting resistance to inhibition by the inhibitor placeholder CKI. This is necessary to allow the second cycle. Setting Y_0 to 0 restricts the model to one cycle (Figure 4-21).

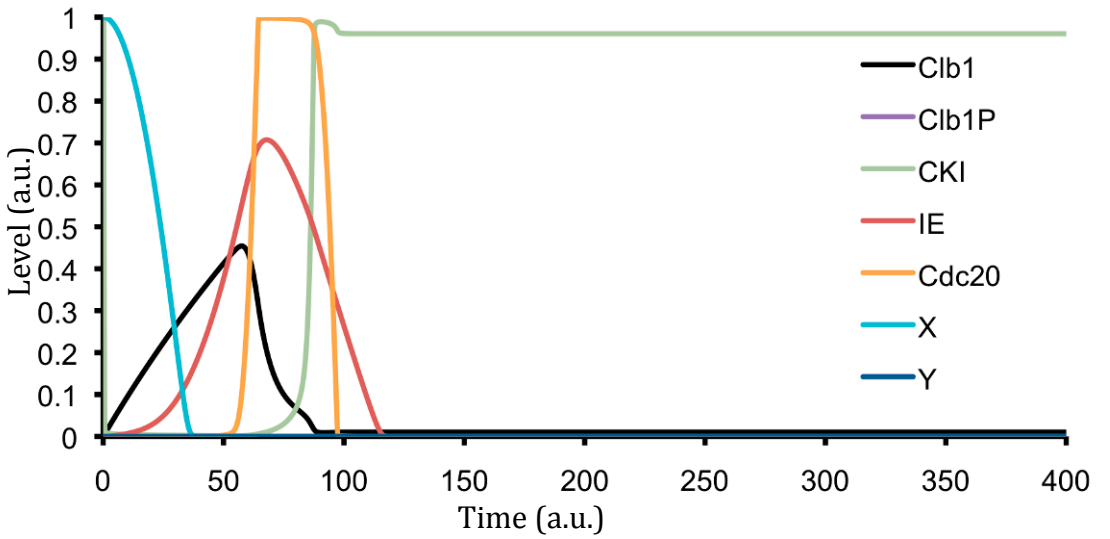

Figure 4-21 ***Numerical simulation of Model 4.*** *Time series for the Degradation model, simulated using Equation System 4-6 and the parameters in Table 4-12 with Y_0 set to 0.*

This model predicts that if Clb1 phosphorylation is prevented, the cell will undergo one cycle successfully, and form a dyad. The phosphorylation was required for the second cycle, but not for Clb1 activity.

4.6 Summary

We considered the possibility that Clb1 phosphorylation is required for Clb1-CDK activity. Using a simple model of meiosis, we investigated this possibility. The model of meiosis included the mutual inhibition of Clb-CDK and CKI. The Starter Kinase is included as X, likely to be Ime2, and Cdc20 as a simplification of the Exit Phosphatase, also inhibiting Clb1-CDK. Intermediate Enzyme (IE) is included as a delay between Clb1-CDK activation and inhibition, and Y is included to prevent X inhibition during the first cycle.

Clb1 phosphorylation was incorporated into the model as a requirement for full Clb1-CDK activity in replacement for IE. The model incorporated two potential kinases for Clb1; we considered both of these and an alternative kinase activated by CDK. The model incorporating Ime2-dependent phosphorylation of Clb1 required that CDK phosphorylation has differing effects on Ime2 activity. This was capable of producing two peaks of CDK activity, though they were indistinct and uneven. Both other models were capable of producing the two CDK activity peaks required for meiosis. A possible kinase suggested for the alternative kinase model was Cdc5.

Each of these models was examined by inhibiting or depleting the kinase considered to rule out its requirement for Clb1 phosphorylation. We discovered that the meiosis-specific Clb1 phosphorylation required the activity of Cdc28 and the presence of Cdc5. Clb1 nuclear localisation appeared to require the activity of Cdc28, but not Cdc5. Neither occurrence required the activity of Ime2, though it is required for Clb1 expression. The requirement for these kinases may be indirect as no site for the modification has been determined. In the case of the experiments involving analogue sensitive Ime2 or analogue sensitive Cdc28 (Sections 4.4.2 and 4.4.4), a better control would have been to compare the effect of adding the inhibitor or solvent only to the mutant at each time point rather adding than adding the inhibitor to the mutant and the wild type. This control would have made the conclusions drawn from each experiment stronger.

CDC5 meiotic null is the first condition in which we have seen an apparent separation of the modification and nuclear localisation of Clb1. This suggests a Cdc28-activity dependent step for nuclear import, and a Cdc5-dependent and possibly Cdc28-dependent step for the modification. Nuclear import may be required to maintain the modification in the case of a cytoplasmic phosphatase, for example. Therefore, the phosphorylation does not cause nuclear localisation, though nuclear localisation may cause phosphorylation. To see if this is the case, we could disrupt nuclear localisation and determine the effect on phosphorylation.

The phosphorylation must have another purpose than to direct the nuclear import of Clb1, possibly substrate selectivity or resistance to an inhibitor. Clb1 continues to be present after anaphase I, but unphosphorylated and inactive. This is proposed to be due to a specific inhibitor of Clb1, as Clb4-CDK and Clb3-CDK are both active (Carlile and Amon, 2008). Phosphorylation could allow Clb1 to escape inhibition during the first cycle of meiosis. Due to the absence of information about modification sites, phosphoinhibitory mutants of Clb1 could not be made. In preference to making speculative mutants of putative sites, it was decided to investigate the function of the localisation of Clb1 in Chapter 5.

5 Clb1 localisation during meiosis I

Meiosis-specific nuclear localisation of Clb1 was observed in Chapter 3. In Section 4.5, we considered the impact of the regulation of Clb1 localisation on FEAR-released Cdc14, and on the CDK/Cdc14 ratio experienced by the cell.

5.1 Model 5: Y prevents full FEAR activation

Y, the hypothetical protein, has been proposed to prevent the high CKI and low CDK state from becoming established until the second cycle. In Chapter 4, Y fulfils this role by inhibiting the action of Clb1 on the Starter Kinase X until after first division. This was chosen because Ime2, proposed to play the role of Starter Kinase X (Dirick et al., 1998), is active during the second division (Schindler and Winter, 2006). However, the phosphorylation may lead to a substrate or localisation change rather than an activity or degradation rate change. Alternatively, Ime2 alone may be insufficient to play the role of Starter Kinase (Sedgwick et al., 2006). In these cases, inactivation of Starter Kinase activity need not require inactivation of Ime2. We considered models in which maintaining Starter Kinase X activity was not the method by which a second cycle was achieved.

In this section, we provide a model in which Y is responsible for preventing the activation of CKI in meiosis I, rather than preventing the inactivation of X. Model 5 extrapolates from mechanistic details in literature that Cdc14 export is a significant step towards exiting the mitotic state and towards establishment of the G1 state (Bembenek et al., 2005; Geymonat et al., 2002a; Mohl et al., 2009; Stegmeier and Amon, 2004). By accessing exported substrates such as Cdh1, exported Cdc14 triggers the transition to the stable state in which

inhibitors dominate. In this case, Y prevents the full activation of CKI by preventing export of Cdc14 from the nucleus until the second cycle (Figure 5-1).

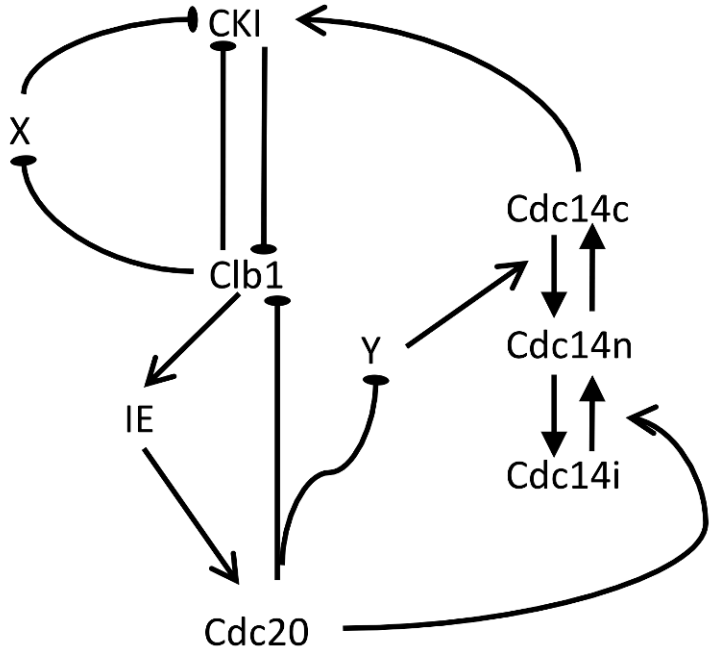

Figure 5-1 ***Proposed wiring diagram for the Model 5 incorporating FEAR.*** *Open-headed arrows indicate positive interactions such activation, flat ended arrows indicate negative interactions such as inhibition, and solid-headed arrows indicate transition of proteins between two states i.e. phosphorylation. Most interactions are similar to those in the models described in Chapter 4. However, CKI is now activated by Cdc14, in turn activated by Cdc20, and Y inhibits this process rather than protecting X. The reactions are described in more detail below.*

Model 5 introduces of three subtypes of Cdc14, only one of which activates CKI. Cdc14 can be inactive, nuclear or cytoplasmic, denoted by a subscript i, n or c, respectively. Cdc14 is initially inactive in the nucleolus. As the transitions between inactive and nuclear, Cdc14i to Cdc14n, are dependent on the phosphorylation reaction of Net1, they were summarised using Michaelis Menten (MM) kinetics. Export and import were described with mass action kinetics. The export of Cdc14 from the nucleus, Cdc14n to Cdc14c, is inhibited or reversed by Y, the hypothetical protein. This could take the role of maintaining inhibition of MEN, against a FEAR-based drive (Jaspersen and Morgan, 2000) to become active. MEN is resistant to activation during meiosis I (Attner and Amon, 2012). CKI activation is now dependent on Cdc14c rather than Cdc20 directly, and is still described by MM kinetics.

Reactions	Contributing	Parameters
→ Clb1		$ks_{clb1,}$
Clb1 →	CKI, Cdc20	kdclb1, $kd_{clb1CKI}$, $kd_{clb1cdc20}$
Clb1→Clb1P	Y	kp_{clb1y}
Clb1P→Clb1		kdp_{clb1}
Clb1P	Cdc14c, Cdc20	kdclb1, $kd_{clb1cdc20}$
CKI (active) → CKI (inactive)	X, Clb1P,	ki_{CKIx}, Ji_{CKI} ka_{CKI}, $ka_{CKIcdc20}$, Ja_{CKI}
CKI (inactive) → CKI (active)	Cdc20,	ka_{CKI}, $ka_{CKIcdc20}$, Ja_{CKI}
Cdc20 (active)→ Cdc20(inactive)	IE	ki_{cdc20}, Ji_{cdc20}
Cdc20 (inactive)→ Cdc20(active)		$ka_{cdc20ie}$, Ja_{cdc20}
Cdc14n→ Cdc14i		ki_{cdc14}, Ji_{cdc14}
Cdc14i→ Cdc14n	Cdc20	$ka_{cdc14nCdc20}$, Ja_{cdc14i}
Cdc14c→ Cdc14n	Y	$kimp_{cdc14c}$, $kimp_{cdc14cY}$
Cdc14n→ Cdc14c		$kexp_{cdc14c}$,
IE (active) → IE (inactive)	Clb1	ka_{ieclb1}, Ja_{ie}
IE (inactive) → IE (active)		ki_{ieclb1}, Ji_{ie}
X→XP	Clb1, Clb1P	kp_x, $Jp_{x,}$
Y→	Cdc20, X	kd_y

Table 5-1 ***Reactions of the model.*** *Table of reactions for the model depicted in Figure 4-1. Each reaction is listed with parameters and variables that contribute to the rates.*

The total amounts of CKI, Cdc20, Cdc14 and IE are conserved. The model is described in Equation System 5-1.

(46) $$\frac{d[Clb1]}{dt} = ks_{Clb1} - (kd_{Clb1} + kd_{Clb1Cdh1}\cdot [CKIa] + kd_{Clb1Cdc20}\cdot [Cdc20a])\cdot [Clb1]$$

(47) $$\frac{d[IEa]}{dt} = \frac{ka_{IEClb1}\cdot [Clb1]\cdot ([IE_T] - [IEa])}{Ja_{IE} + ([IE_T] - [IEa])} - \frac{ki_{IE}\cdot [IEa]}{Ji_{IE} + [IEa]}$$

(48) $$\frac{d[CKIa]}{dt} = \frac{(ka_{CKI} + ka_{CKICdc20}\cdot [Cdc20a])\cdot ([CKI_t] - [CKIa])}{Ja_{CKI} + (CKI_t - CKIa)} - \frac{(ki_{CKIX}\cdot [X] + ki_{CKIClb1}\cdot [Clb1])\cdot [CKIa]}{Ji_{CKI} + [CKIa]}$$

(49) $$\frac{d[Cdc20A]}{dt} = \frac{ka_{Cdc20IE}\cdot [IEa]\cdot ([Cdc20_T] - [Cdc20a])}{Ja_{Cdc20} + ([Cdc20_T] - [Cdc20a])} - \frac{ki_{Cdc20}\cdot [Cdc20a]}{Ji_{Cdc20} + [Cdc20a]}$$

(50) $$\frac{d[X]}{dt} = -\frac{kp_X\cdot [Clb1]\cdot [X]}{Jp_X + [X]}$$

(51) $$\frac{d[Y]}{dt} = -kd_Y\cdot [Cdc20A]\cdot [Y]$$

$$\frac{dCdc14n}{dt} = \frac{ka_{Cdc14n} + ka_{Cdc14nCdc20} \cdot [Cdc20]) \cdot ([Cdc14_0] - [Cdc14n] - [Cdc14c])}{Ja_{Cdc14i} + ([Cdc14_0] - [Cdc14n] - [Cdc14c])}$$
$$+ (kimp_{Cdc14c} + kimp_{Cdc14cY} \cdot [Y]) \cdot [Cdc14c]$$
$$- (\frac{ki_{Cdc14n}}{Ji_{Cdc14n} + [Cdc14n]} + k\exp_{Cdc14n}) \cdot [Cdc14n] \quad (52)$$

$$\frac{dCdc14c}{dt} = k\exp_{Cdc14n} \cdot [Cdc14n] - (kimp_{Cdc14c} + kimp_{Cdc14cY} \cdot [Y]) \cdot [Cdc14c] \quad (53)$$

Equation System 5-1 ***System of ODEs describing the model incorporating Cdc14*** *The model described in Figure 5-1 is converted into ordinary differential equations suitable for simulating in XPP.*

Parameters were selected using the same criteria as before (Section 4.2.3.3). The parameters are listed in Table 5-2. This resulted in the following time series (Figure 5-2).

Parameter	Value	Initial Conditions	
ks_{Clb1}	0.01	Clb1=0	CKI=1
kd_{Clb1}	0.01	Cdc20=0	IE=0
$kd_{Clb1CKI}$	1	Cdc14n=0	X=1
$kd_{Clb1Cdc20}$	0.2	Cdc14c=0	Y=1
ka_{CKI}	0.03		
$ka_{CKICdc14}$	0.5		
Ja_{CKI}	0.001		
ki_{CKIX}	2		
$ki_{CKIClb1}$	2		
Ji_{CKI}	0.001		
ka_{IEClb1}	0.1		
Ja_{IE}	0.01		
ki_{IE}	0.02		
Ji_{IE}	0.01		
$ka_{Cdc20IE}$	1		
Ja_{Cdc20}	0.001		
ki_{Cdc20}	0.5		
Ji_{Cdc20}	0.001		
ka_{Cdc14n}	0.01		
$ka_{Cdc14nCdc20}$	1		
Ja_{Cdc14n}	0.01		
ki_{Cdcd14}	0.1		
ki_{Cdc14Y}	4		
ki_{Cdc14n}	1		
Ji_{Cdc14n}	0.1		
ka_{Cdc14c}	0.1		

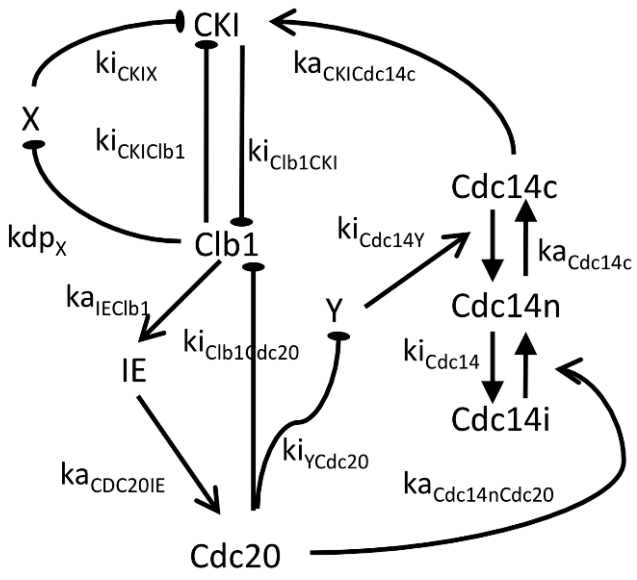

kp_x	0.2
Jp_x	0.04
kdp_x	0.1
Jdp_x	0.04
kd_Y	0.12
CKI_t	1
$Cdc20_t$	1
X_t	1
IE_t	1
$Cdc14_t$	0.5

Table 5-2 ***Parameters for Model 5 incorporating Cdc14 release and export.*** *Parameters for the model, which result in the time series in Figure 5-2. The wiring diagram in Figure 5-1 is reproduced for reference. Parameters controlling the interactions are shown next to the arrows indicating the interaction.*

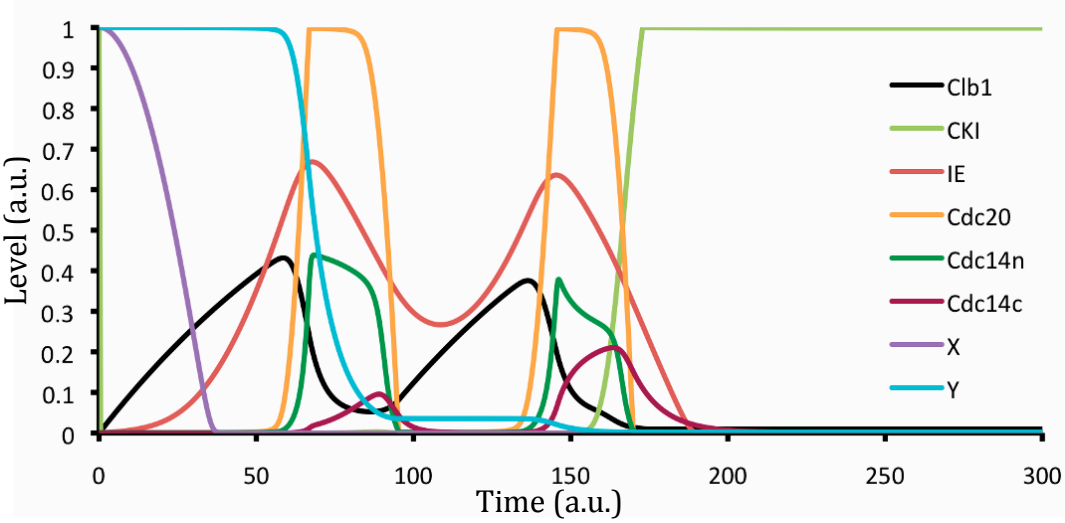

Figure 5-2 ***Numerical simulation for Model 5 incorporating Cdc14 release and export*** *Time series produced by simulating Model 5 using the parameters in Table 5-2. The model produces two peaks of Cdc20 and CDK activity before CKI activity rises and holds the model in the low CDK state.*

Model 5 was capable of reproducing two cycles. Cdc14 release was limited in the first cycle, restricting the activation of CKI to the second cycle, despite the early inactivation of X. This ability is dependent on Y as when Y_0 was set to 0, Cdc14 was exported and CKIs are activated (Figure 5-3).

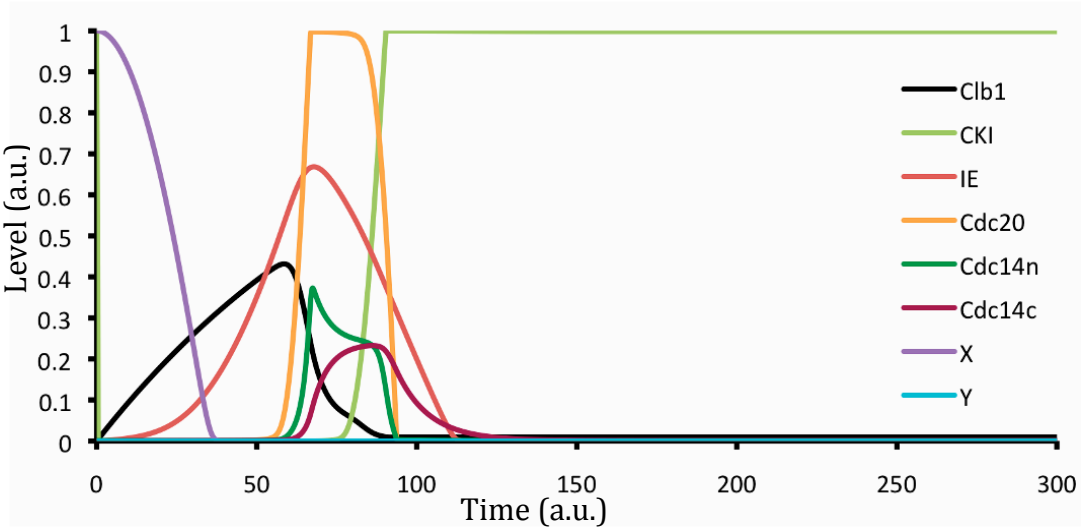

Figure 5-3 ***Numerical simulation for Model 5 when Y_0 is set to 0. Time series produced by*** *simulating Model 5 using the parameters in Table 5-2, with Y_0, the initial value for Y, set to 0. The model produces only one peak, showing that Y is required for the model to give two cycles.*

In mitosis, cytoplasmic localisation of Cdc14 is an important step to drive exit from the high CDK state (Bembenek et al., 2005). If this holds true for meiosis, nuclear retention of Cdc14 during meiosis I, and not during meiosis II, could be enough to prevent the activation of CKI and the establishment of the low CDK stable state. Cdc14 nuclear release may then be amplified sufficiently to establish spindle disassembly.

If this is the case, exporting Cdc14 during meiosis I would be sufficient to establish the CKIs in exit from meiosis I and prevent entry into meiosis II.

5.2 Localisation of Clb1

The FEAR-driven impact on the CDK/Cdc14 ratio must be regulated differently in meiosis from that in mitosis, as discussed in the introduction (Section 1.5.4.2). Spindle disassembly occurs in response to FEAR-driven Cdc14 release during meiosis I, but FEAR-driven Cdc14 release in mitosis is insufficient to cause spindle disassembly. The above model (Section 5.1) included nuclear and cytoplasmic Cdc14 as separate variables. Given the meiosis-specific localisation of Clb1, we were interested to see the effect of this on the Clb-CDK/Cdc14 phosphatase ratio, especially in the nuclear compartment, in which spindle dynamics and DNA relicensing would take place.

5.2.1 Model 6: Clb1 localisation

Model 6 bears similarity to Model 5, but is altered by the addition of Clb1 nuclear import under a constant parameter, and components responsible for increased Net1 phosphorylation are included (Figure 5-4). The new model is referred to as the Clb1 Localisation model.

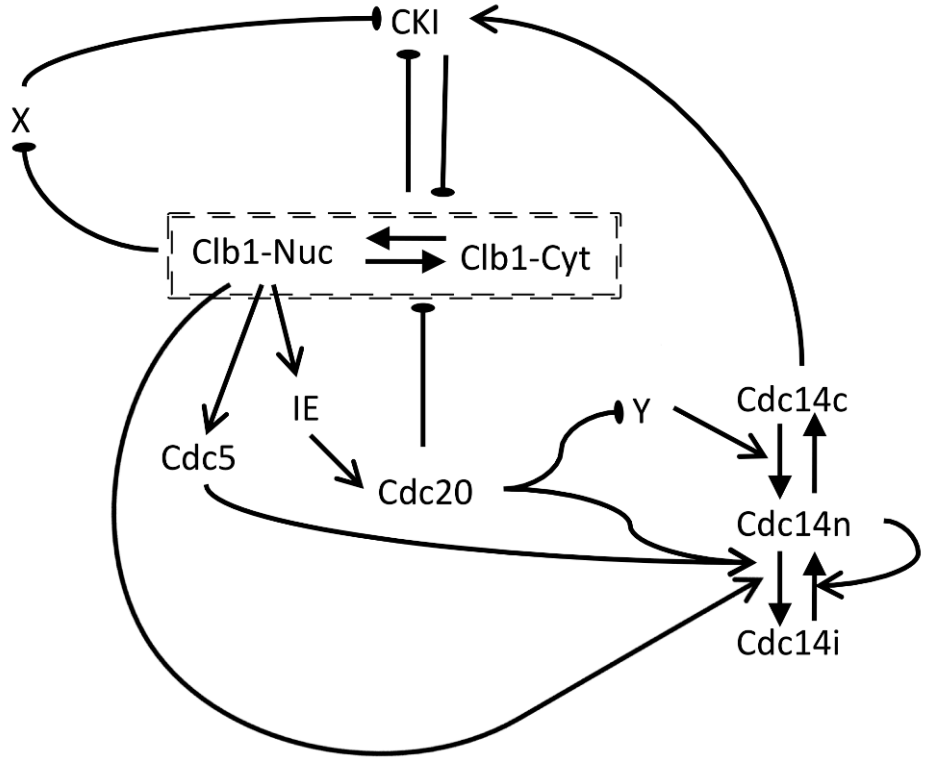

Figure 5-4 ***Proposed wiring diagram for the Clb1 Localisation model.*** *The model is similar to that in Section 5.1. Open-headed arrows indicate positive interactions such activation, flat ended arrows indicate negative interactions such as inhibition, and solid-headed arrows indicate transition of proteins between two states i.e. phosphorylation. However, Cdc14 is activated by parallel pathways from Clb1 activity. Clb1 is split into two subtypes and only nuclear Clb1 activity triggers FEAR activity. The reactions are described in more detail below.*

The synthesis of Clb1Cyt and the degradation of both forms of Clb1, and of Y, are described using mass action kinetics. Synthesis of Clb1Cyt is of zero order, while the background rate of degradation of both forms of Clb1 is first order. Regulated degradation of Clb1Cyt and Clb1Nuc is second order, catalysed by Cdc20 and CKI. Degradation of Y is second order and depends on Cdc20. Clb1 import and export are described using first order mass action kinetics.

Clb1Cyt and Clb1Nuc differ as to which variables they can affect (Figure 5-4). Cdc20, Cdc5, X and Net1 are nuclear, limiting their phosphorylation to Clb1Nuc (Cheng et al., 1998; Jaquenoud et al., 2002; Kominami et al., 1993;

Visintin et al., 1999). CKI includes inhibitors that are degraded and re-synthesised (Sic1)(Verma et al., 1997), or exported from the nucleus by phosphorylation (Cdh1) (Jaquenoud et al., 2002). Therefore, CKI is exposed to both Clb1Cyt and Clb1Nuc.

Phosphorylation of X by Clb1Nuc, and the activation and inactivation of Cdc20, IE and CKI, are all described using MM kinetics. IE is activated by Clb1Nuc and has a constant inactivation rate. Cdc20 is activated by IE and has a constant inactivation rate. CKI activation is catalysed by $Cdc14_{c,}$ and CKI inactivation is catalysed by Clb1Cyt, Clb1Nuc and X.

As before (Section 5.1), Cdc14 can be inactive (Cdc14i), nuclear (Cdc14n) or cytoplasmic (Cdc14c). The transitions between Cdc14i and Cdc14n, are summarised using MM kinetics, being dependent on Net1 phosphorylation. Three proteins contribute to the phosphorylation of Net1 and are included as activators of Cdc14n. These are Cdc5, Cdc20 (via inhibition of Cdc55) and Clb1Nuc (Azzam et al., 2004; Liang et al., 2009; Queralt et al., 2006). Cdc14n is included to catalyse the inactivation of Cdc14n, as it is capable of dephosphorylating Net1 (Shou et al., 1999). Import and export, Cdc14n to Cdc14c, were described with mass action kinetics. The export of Cdc14 is considered to be reversed by Y, the hypothetical protein.

Reactions	Contributing	Parameters
→ Clb1Cyt		$ks_{clb1,}$
Clb1Cyt →	CKI, Cdc20	kd_{clb1}, $kd_{clb1CKI}$, $kd_{clb1cdc20}$
Clb1Cyt→Clb1Nuc	Y	$kimp_{clb1}$
Clb1Nuc→Clb1Cyt		$kexp_{clb1}$
Clb1Nuc→	Cdc14c, Cdc20	kd_{clb1}, $kd_{clb1cdc20}$
CKI (active) → CKI (inactive)	X, Clb1P,	ki_{CKIx}, Ji_{CKI} ka_{CKI}, $ka_{CKIcdc20}$, Ja_{CKI}
CKI (inactive) → CKI (active)	Cdc20,	ka_{CKI}, $ka_{CKIcdc20}$, Ja_{CKI}
Cdc20 (active)→ Cdc20(inactive)	IE	ki_{cdc20}, Ji_{cdc20}
Cdc20 (inactive)→ Cdc20(active)		$ka_{cdc20ie}$, Ja_{cdc20}
Cdc5i→ Cdc5a	Clb1Nuc	ka_{cdc5}, Ja_{cdc5}
Cdc5a→ Cdc5i		ki_{cdc5}, Ji_{cdc5}
Cdc14n→ Cdc14i	Cdc14n	ki_{cdc14}, Ji_{cdc14}
Cdc14i→ Cdc14n	Cdc20, Cdc5, ClbNuc	$ka_{cdc14nCdc20}$,$ka_{cdc14nCdc5}$,$ka_{cdc14nCdc}$, Ja_{cdc14i}
Cdc14c→ Cdc14n	Y	$kimp_{cdc14c}$, $kimp_{cdc14cY}$
Cdc14n→ Cdc14c		$kexp_{cdc14c}$,
IE (active) → IE (inactive)	Clb1Nuc	ka_{ieclb1}, Ja_{ie}
IE (inactive) → IE (active)		ki_{ieclb1}, Ji_{ie}
X→XP	Clb1Nuc	kp_{x}, $Jp_{x,}$
Y→	Cdc20, X	kd_{y}

Table 5-3 ***Reactions of the model.*** *Table of reactions for the model depicted in Figure 4-1. Each reaction is listed with parameters and variables that contribute to the rates.*

The total amounts of CKI, Cdc20, Cdc14, Cdc5 and IE are conserved. Model 6 is demonstrated in ODE form in Equation System 5-2.

(54) $$\frac{d[Clb1Cyt]}{dt} = ks_{Clb1} + k\exp_{Clb1}\cdot[Clb1Nuc] - (kd_{Clb1} + kd_{Clb1CKI}\cdot[CKIa] + kd_{Clb1Cdc20}\cdot[Cdc20a] + kimp_{Clb1})\cdot[Clb1Cyt]$$

(55) $$\frac{d[Clb1Nuc]}{dt} = kimp_{Clb1}\cdot[Clb1Cyt] - (kd_{Clb1} + kd_{Clb1CKI}\cdot[CKIa] + kd_{Clb1Cdc20}\cdot[Cdc20a] + k\exp_{Clb1})\cdot[Clb1Nuc]$$

(56) $$\frac{d[IEa]}{dt} = \frac{ka_{IEClb1}\cdot([IE_t]-[IEa])\cdot[Clb1Nuc]}{Ja_{IE}+([IE_t]-[IEa])} - \frac{ki_{IE}\cdot[IEa]}{Ji_{IE}+[IEa]}$$

(57) $$\frac{d[CKIa]}{dt} = \frac{(ka_{CKI} + ka_{CKICdc20}\cdot[Cdc20a])\cdot([CKI_t]-[CKIa])}{Ja_{Cdh1}+(CKI_t - CKIa)} - \frac{(ki_{CKIX}\cdot[X] + ki_{CKIClb1}\cdot[Clb1])\cdot[CKIa]}{Ji_{CKI}+[CKIa]}$$

(58) $$\frac{d[Cdc20A]}{dt} = \frac{ka_{Cdc20IE}\cdot[IEa]\cdot([Cdc20_t]-[Cdc20a])}{Ja_{Cdc20}+([Cdc20_t]-[Cdc20a])} - \frac{ki_{Cdc20}\cdot[Cdc20a]}{Ji_{Cdc20}+[Cdc20a]}$$

(59) $$\frac{d[Cdc5]}{dt} = \frac{ka_{CdcCdc5Clb1}\cdot[Clb1Nuc]\cdot([Cdc5_t]-[Cdc5])}{Ja_{Cdc5}+([Cdc5_t]-[Cdc5])} - \frac{ki_{Cdc5}\cdot[Cdc5]}{Ji_{Cdc5}+[Cdc5]}$$

(60) $$\frac{d[X]}{dt} = -\frac{kp_X\cdot[Clb1Nuc]\cdot[X]}{Jp_X+[X]}$$

(61) $$\frac{d[Y]}{dt} = -kd_Y\cdot[Cdc20A]\cdot[Y]$$

(62) $$\frac{dCdc14n}{dt} = \frac{(ka_{Cdc14Cdc20}\cdot[Cdc20] + ka_{Cdc14Cdc5}\cdot[Cdc5] + ka_{Cdc14Clb1}\cdot[Clb1Nuc])\cdot([Cdc14_0]-[Cdc14n]-[Cdc14c])}{Ja_{Cdc14i}+([Cdc14_0]-[Cdc14n]-[Cdc14c])} + (kimp_{Cdc14c} + kimp_{Cdc14cY}\cdot[Y])\cdot[Cdc14c] - (\frac{ki_{Cdc14n}}{Ji_{Cdc14n}+[Cdc14n]} + k\exp_{Cdc14n})\cdot[Cdc14n]$$

(63) $$\frac{dCdc14c}{dt} = k\exp_{Cdc14n}\cdot[Cdc14n] - (kimp_{Cdc14c} + kimp_{Cdc14cY}\cdot[Y])\cdot[Cdc14c]$$

Equation System 5-2 ***System of ODEs describing Model 6 incorporating Clb1 localisation.*** *The model described in Figure 5-4 is converted into ordinary differential equations for simulation in XPP.*

Parameters were chosen using the same criteria as above (Section 5.1). Parameters are shown in Table 5-4. The time course is given in Figure 5-5.

Parameter	Value	Initial conditions	
ks_{Clb1}	0.01	Clb1Cyt = 0	Clb1Nuc=0
kd_{Clb1}	0.01	CKI=1	IE=0
$kd_{Clb1Cdc20}$	0.5	Cdc20=0	Cdc14n=0
$kd_{Clb1CKi}$	0.8	Cdc14c=0	Cdc5=0
$kimp_{Clb1}$	0.1	X=1	Y=1
$kexp_{Clb1}$	0.01		
ka_{CKI}	0.08		
$ka_{CKICdc14}$	0.3		
ki_{CKIx}	2		
$ki_{CKIClb1}$	4		
Ja_{CKI}	0.001		
Ji_{CKI}	0.001		
ka_{IEClb1}	0.1		
Ja_{IE}	0.01		
ki_{IE}	0.015		
Ji_{IE}	0.01		
$ka_{Cdc20IE}$	1		
Ja_{Cdc20}	0.01		
ki_{Cdc20}	0.5		
Ji_{Cdc20}	0.001		
Ka_{Cdc14n}	0.01		
$ka_{Cdc14nCdc20}$	0.6		
$ka_{Cdc14nCcd5}$	0.6		
$ka_{Cdc14nClb1}$	0.6		
Ja_{Cdc14n}	0.01		
$kimp_{Cdc14}$	0.1		
$kimp_{Cdc14Y}$	5		
ki_{Cdc14}	0.5		
Ji_{Cdc14n}	0.001		
$kexp_{Cdc14n}$	0.4		
$kp_{Cdc5Clb1}$	1		
Jp_{Cdc5}	0.01		
kdp_{Cdc5}	0.1		
Jdp_{Cdc5}	0.01		
kp_x	0.2		
Jp_x	0.04		
kd_y	0.2		
$Cdh1_t$	1		
IE_t	1		
$Cdc20_t$	1		
$Cdc14_t$	0.5		

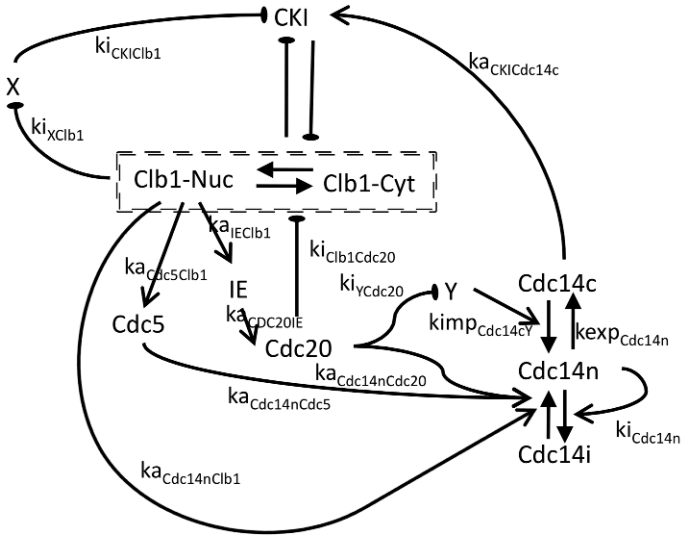

X_t	1
$Cdc5_t$	1

Table 5-4 ***Parameters for Model 6*** *Parameters for the model incorporating Clb1 localisation, which result in the time series in Figure 5-5. The wiring diagram in Figure 5-4 is reproduced for reference. Parameters controlling the interactions are shown next to the arrows indicating the interaction.*

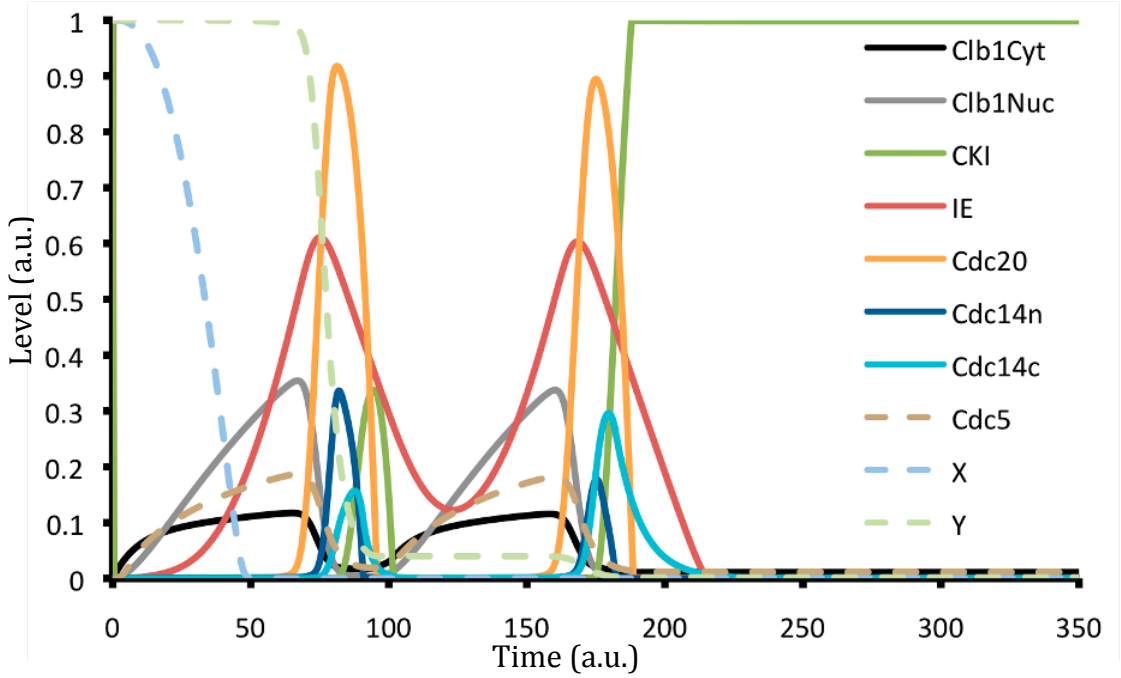

Figure 5-5 ***Numerical simulation for Model 6, incorporating Clb1 localisation*** *Time series produced using Model 6 and the parameters given in Table 5-4. The model produces two peaks of Cdc20 and CDK activity before CKI activity rises and holds the model in the low CDK state.*

Similarly to Model 5, the ability of Model 6 to undergo two cycles is dependent on the presence of Y (Section 5.1). As we now have nuclear and cytoplasmic subtypes for both Cdc14 and Clb1, we can measure the kinase/phosphatase ratio in each region and determine whether Clb1 nuclear import has roles in modulating this quantity. Cdc14n is compared to Clb1Nuc to provide a measure of kinase/ phosphatase ratio experienced by the cell. This is not absolute, but the relative effect on the model of altering Clb1 localisation can be scrutinised. The value of the Clb1/Cdc14 ratio for both nuclear and cytoplasmic compartments is shown (Figure 5-6).

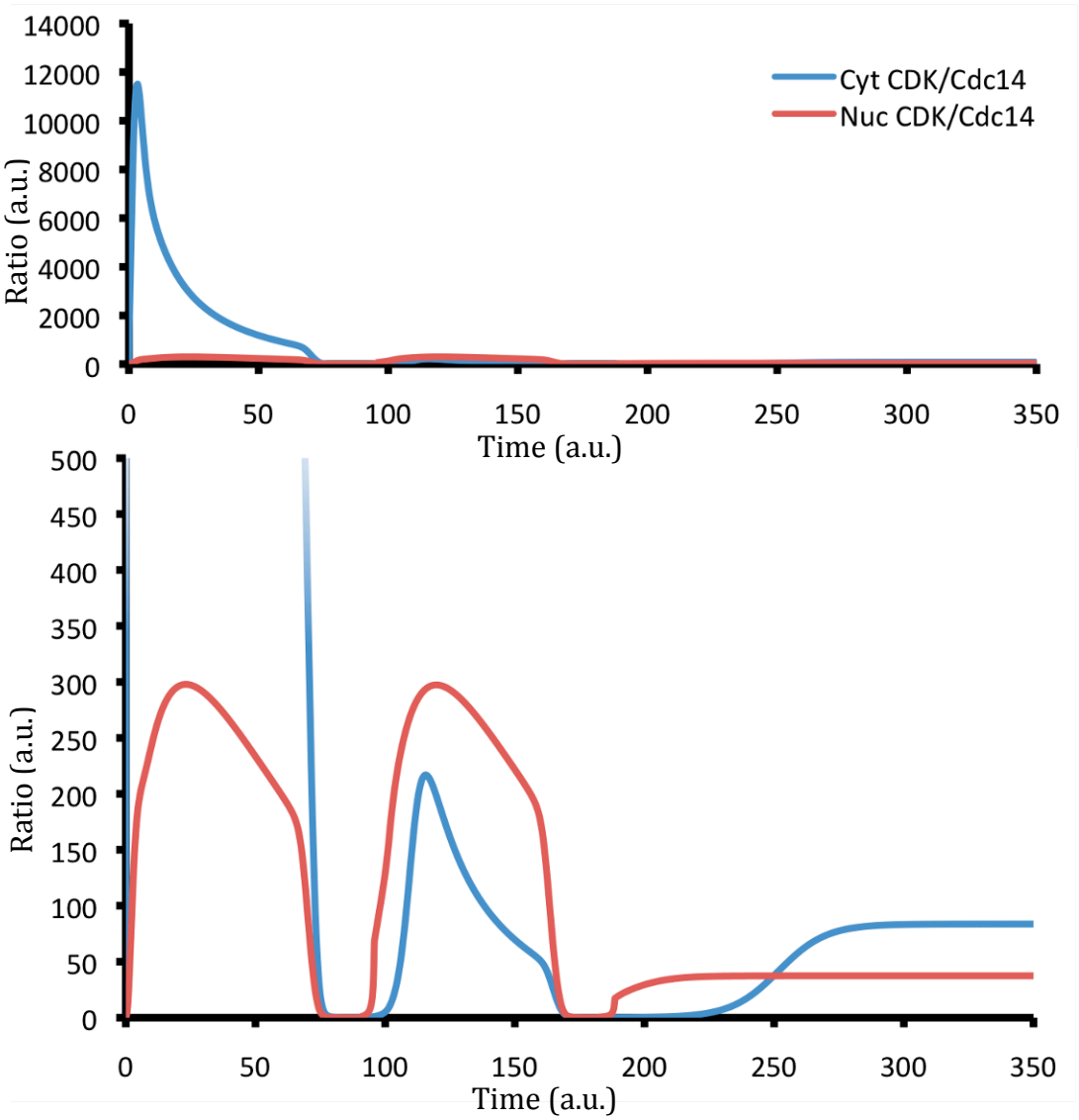

Figure 5-6 ***Clb1-CDK/Cdc14 phosphatase ratios in cytoplasm and nucleus in Model 6.*** *The values of Clb1 and Cdc14 for each compartment derived from the numerical simulation (Figure 5-5) were compared to produce the ratio of Clb1-CDK/Cdc14 phosphatase activity in each compartment. The ratio shows two cycles of CDK activity. CytCDK to Cdc14 ratio is very high in the first cycle before Clb1 import can trigger Cdc14 release.*

The ratio starts at t=0 at a value of 0 as Clb1 has not been expressed, then rises as Clb1 is expressed in the cytoplasm before entering the nucleus to initiate FEAR expression. The cytoplasmic Clb1-CDK ratio reached the highest levels (of around 11,500) during the first cycle, when Cdc14 had not been released to the cytoplasm in a significant amount. The absolute Clb1 level would not be high in these regions, but would not be challenged by Cdc14 activity until Clb1 enters the nucleus. The nuclear Clb-CDK/Cdc14 ratio reached a peak of around 300 for both cycles and was reduced to around 0 in both compartments during the divisions. After t=200, the value for the ratio rose. However, the time series in

Figure 5-5 showed that both absolute values for Clb-CDK and Cdc14 were very low.

5.2.2 Ectopically altering Clb1 localisation

Model 6 can be used to predict the effects of alterations to Clb1 localisation. Ectopically increasing Clb1 nuclear localisation would not be expected to have a huge effect, as Clb1 nuclear localisation is already seen in the first cycle of meiosis. Below, a scenario is considered in which the parameter controlling Clb1 import is tripled, then one in which it is doubled. Tripling nuclear import of Clb1 removed the model's ability to complete two cycles (Figure 5-7).

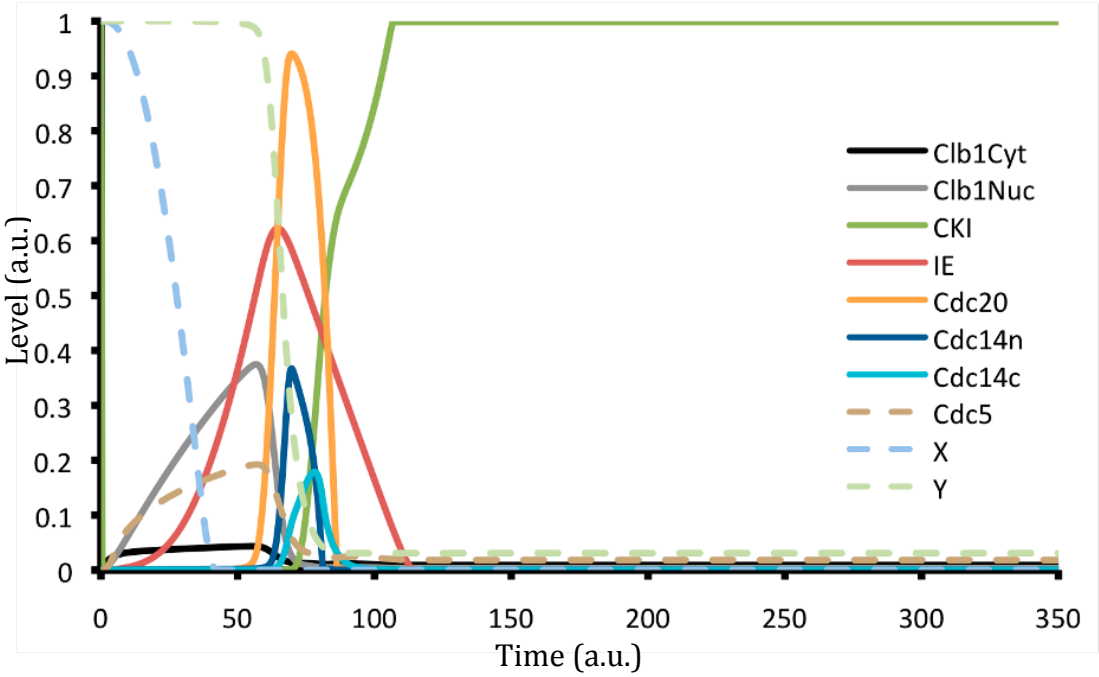

Figure 5-7 ***Numerical simulation of Model 6 in which kimp$_{Clb1}$ = 0.3.*** *Time series produced using Model 6 and the parameters given in Table 5-4, and a value of 0.3 for kimp$_{Clb1}$, the import parameter for Clb1. The model produces a single cycle of CDK activity before CKI activity rises. Increased Clb1 import activates Cdc14 in the first cycle.*

Cytoplasmic Clb1 levels were visibly decreased. FEAR activation occurred slightly earlier. The level of Cdc14 export was similar to the unmodified Model 6, but was sufficient to activate CKI. Nuclear concentration of Clb-CDK activated Cdc14 at a lower total amount of Clb1-CDK, so there was less resistance to consequent CKI activation.

Clb1 is already concentrated in the nucleus in wild type cells undergoing meiosis; so tripling Clb1 import may be an excessive change. As a hypothetical

scenario, however, the above result suggests that increasing the proportion of nuclear Clb1 would hasten the activation of FEAR. When nuclear import of Clb1 is doubled, the model can still achieve two cycles (Figure 5-8).

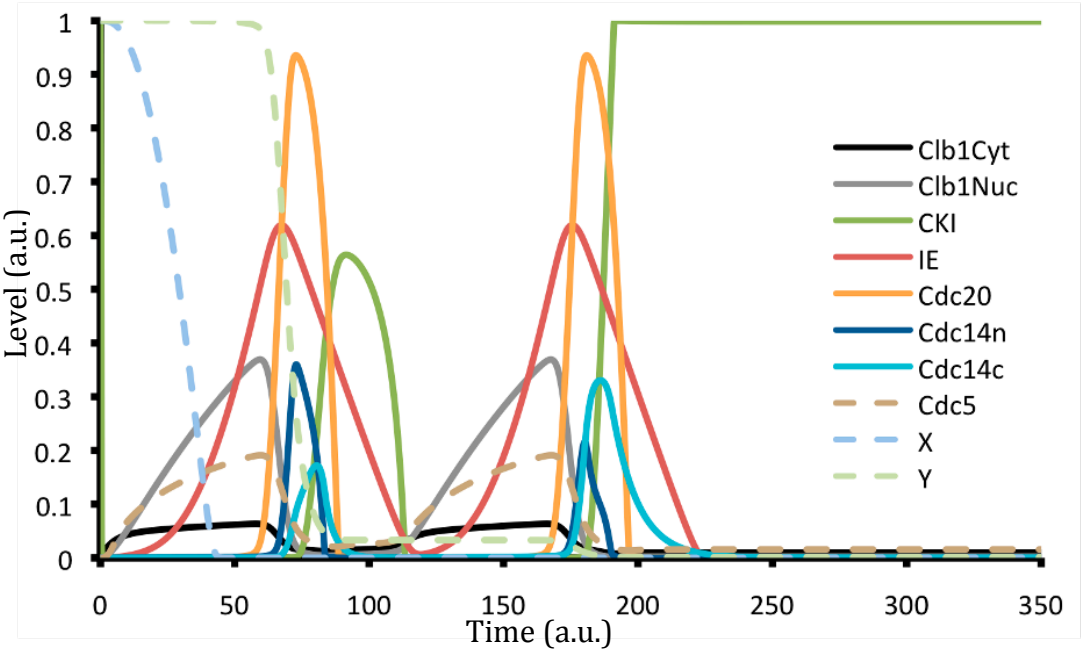

Figure 5-8 ***Numerical simulation for Model 6 in which kimp$_{Clb1}$ = 0.2*** *Time series produced using Model 6 and the parameters given in Table 5-4, and a value of 0.2 for kimp$_{Clb1}$, the import parameter for Clb1. The model can still produce the two cycles of CDK activity before CKI activity reaches its high steady state.*

The ratio of CDK and Cdc14 in each compartment was then considered in comparison to the original Clb1 Localisation model (Figure 5-9).

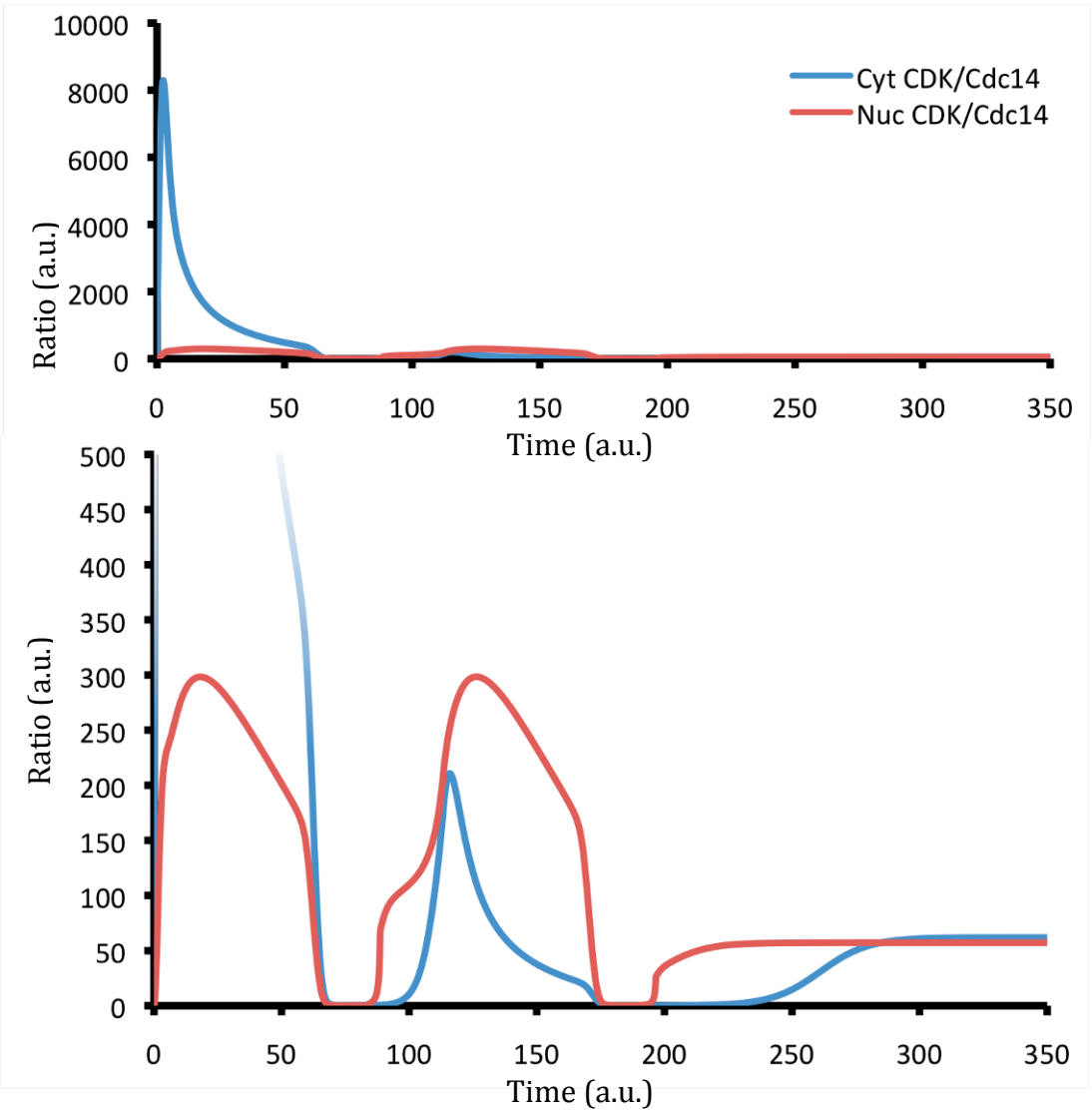

Figure 5-9 ***Clb1-CDK/Cdc14 phosphatase ration in cytoplasm and nucleus as predicted by Model 6 when the kimp$_{Clb1}$ = 0.2.*** *The values of Clb1 and Cdc14 for each compartment derived from the numerical simulation (Figure 5-8) were compared to produce the ratio of Clb1-CDK/Cdc14 phosphatase activity in each compartment. The ratio shows two cycles of CDK activity. CytCDK to Cdc14 ratio is very high in the first cycle before Clb1 import can trigger Cdc14 release.*

We examined how the change in kimp$_{Clb1}$ had affected the ratio of Clb1-CDK and Cdc14 activity. The Clb-CDK/Cdc14 ratio in the nucleus achieved similar peak value of 300. Again, each division is characterised by a very low Clb-CDK/Cdc14 ratio in each compartment. Recovery for the second cycle is delayed; in particular the cytoplasmic ratio does not recover as rapidly. Again, the divisions occur earlier in this scenario. The model suggests that in the case of increased nuclear import of Clb1, both divisions are accelerated. The slow recovery of CDK/Cdc14 ratio may mean that in a non-deterministic system,

where stochastic variation may occur, CKIs become active in the first cycle in some proportion of cells.

Greater increases of the export parameter were also considered. Clb1 is not excluded from the nucleus in cells marked as cytoplasmic, as stated in Chapter 3, so a certain amount of nuclear Clb1 could be tolerated. At 10x nuclear export, Clb1Cyt and Clb1Nuc reached similar levels (Figure 5-10).

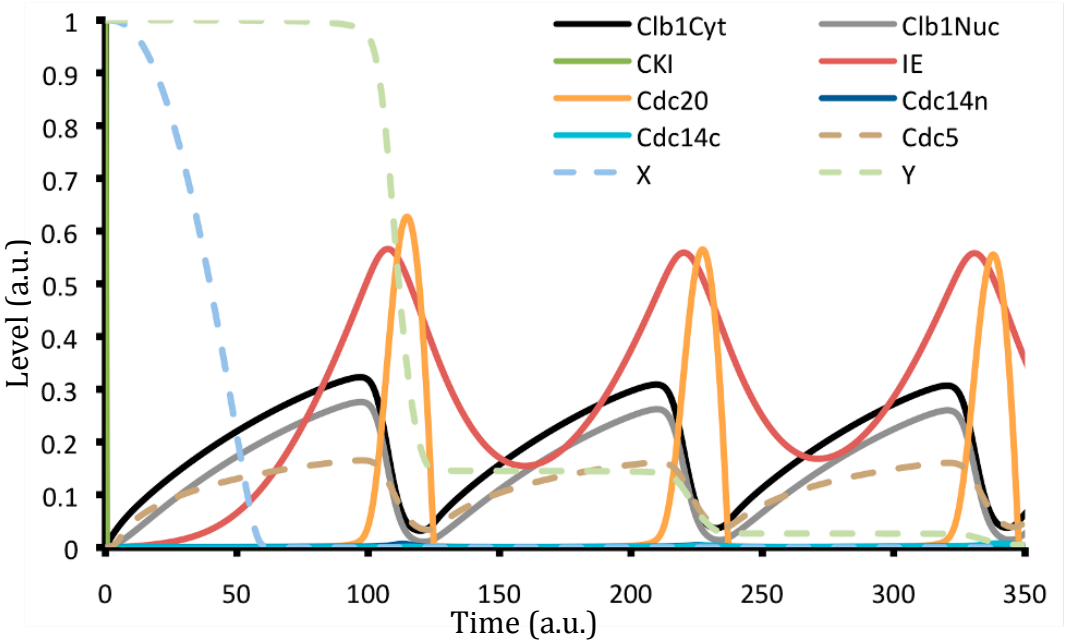

Figure 5-10 ***Numerical simulation for Model 6 in which kexp$_{Clb1}$ =0.1*** *Time series produced using Model 6 and the parameters given in Table 5-4, and a value of 0.1 for kexp$_{Clb1}$, the export parameter for Clb1. The model can still produce the two cycles of CDK activity before CKI activity reaches its high steady state.*

Cdc14 was released and exported. However, due to high levels of Clb1, Cdc14 was no longer capable of activating CKIs. The model behaved like the *CKIΔ* scenario of the Initial model considered in Section 4.2.3.3, cycling indefinitely. Higher Clb1 levels were required to activate the FEAR pathway. The high Clb1 levels continued to resist CKIs while the FEAR pathway was active. We examined how the change in kexp$_{Clb1}$ had affected the ratio of Clb1-CDK and Cdc14 activity. Again, the peak value this ratio reached in the nucleus was 300 (Figure 5-11). This value seems to consistently lead to FEAR activation.

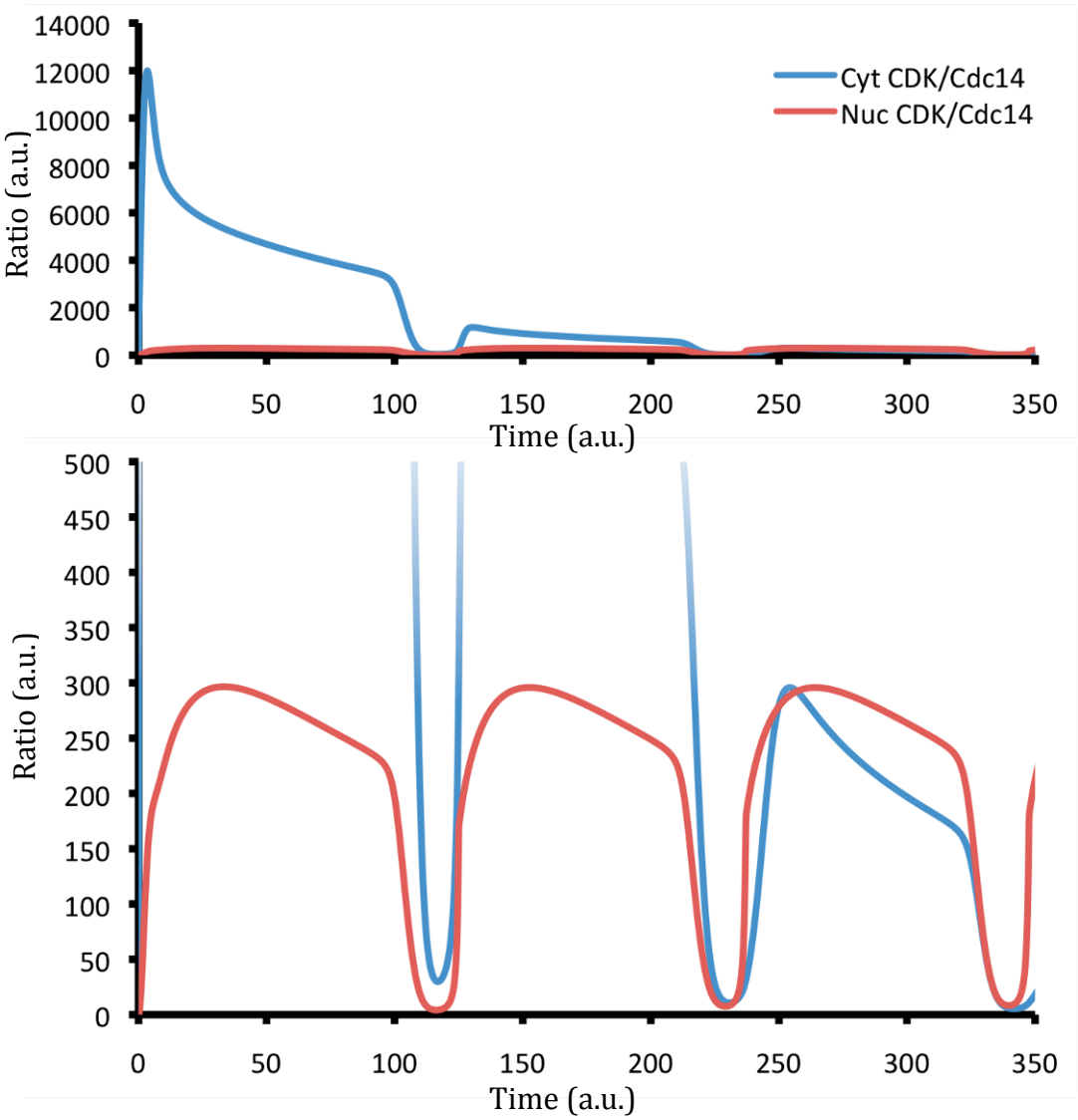

Figure 5-11 ***Clb1-CDK/Cdc14 phosphatase ration in cytoplasm and nucleus as predicted by Model 6 when the kexp$_{Clb1}$ = 0.1.*** *The values of Clb1 and Cdc14 for each compartment derived from the numerical simulation (Figure 5-10) were compared to produce the ratio of Clb1-CDK/Cdc14 phosphatase activity in each compartment. The ratio shows two cycles of CDK activity. CytCDK to Cdc14 ratio is very high in the first cycle before Clb1 import can trigger Cdc14 release.*

The cytoplasmic ratio rose very high, initially, as Y prevented export of Cdc14 so Clb1 was unchallenged. Y remained for two cycles here. As with the nuclear import scenario, Cdc20 activation, and hence the rate of Y degradation, was affected. The troughs correlating with the divisions were both delayed and narrower, showing the opposite effect to increased nuclear localisation. Cytoplasmic Clb1 was continuing to repress CKI without increasing the activation of FEAR.

This scenario may have similar limitations to the *CKIΔ* scenario considered in the Initial model (Section 4.2.3.3), in the translation of the result to

phenotypes. However, it was predicted that both divisions would be delayed and that Clb-CDK/Cdc14 ratio would not be as robustly decreased. In FEAR mutants, in which Cdc14 release is compromised, the spindle is not disassembled. In mutant strains where the CDK/Cdc14 ratio is not so effectively decreased during the division, a similar but weaker phenotype may be observed. For example, spindle disassembly may be delayed or disrupted.

5.3 Clb1 localisation during meiosis I

Imaging studies have shown that Clb1 is nuclear in meiosis, and appears to be degraded at anaphase I (Buonomo et al., 2003). Another study, in which the meiotic cultures were synchronised, found that Clb1 is not degraded in meiosis I, but persists until meiosis II (Carlile and Amon, 2008). A transient modification of Clb1 appears to correlate with the nuclear localisation, and with the activity of Clb1. The protein then remains, inactive and unmodified, until exit from meiosis II (Carlile and Amon, 2008). The apparent disappearance of Clb1-HA at anaphase I in the earlier results could be a consequence of dispersal and perhaps partial degradation leading to a lower detectable signal.

Nuclear localisation and modification of Clb1 are coincident with the active state (Carlile and Amon, 2008), and regulate Clb1 activity. We have seen that the modification is phosphorylation, specific to meiosis I, and dependent on Cdc5 and Cdc28 activity (Chapter 3). Nuclear localisation of Clb1 is not dependent on its phosphorylation: Clb1-Myc_9 appeared to concentrate to the nucleus in meiotic cells depleted of Cdc5, but was not phosphorylated. Nuclear localisation of Clb1 is not seen during mitosis in the SK1 yeast strain and could be a meiosis I-specific feature.

Nuclear localisation of Clb1 is likely to be important for regulating the meiotic cell cycle. What are the effects on meiosis of having Clb1 constitutively directed to the cytoplasm or nucleus? In order to determine the functional significance of Clb1 localisation, mutants were created to disrupt the localisation and examine the effects on meiotic cell cycle progression.

5.4 Disruption of the endogenous nuclear localisation sequence in Clb1

The Clb1 sequence bears both an endogenous nuclear localisation sequence (NLS) and an endogenous nuclear export sequence (NES). Nuclear

localisation could be directed by the NLS, controlled either by activating the NLS or by inhibiting the NES that counters it.

5.4.1 Creation of the NLS mutant

A mutant was created in which the endogenous NLS of Clb1 was mutated to alanine (*clb1-NLS6A-HA$_6$*) to inactivate it. The endogenous nuclear localisation site is found at K158 to K176 (Figure 4.4?). Instead of a terminal tag added by PCR, this mutant was created by generating the 5' end of the gene bearing the mutation, linked to a *LEU2* marker. This resulted in a truncated fragment of *CLB1* near the modified *CLB1* gene (Figure 5-12). This process was used due to the location of the nuclear localisation site being too far from the 3' end of the gene for the mutation and C-terminal tag to be added in the same step. An identical protocol was followed with an unmodified *CLB1* fragment, to generate a control containing *CLB1-HA$_6$* with an intact NLS sequence and the same truncated *CLB1* fragment. This allele will be referred to as *CLB1-NLScontrol-HA$_6$.*

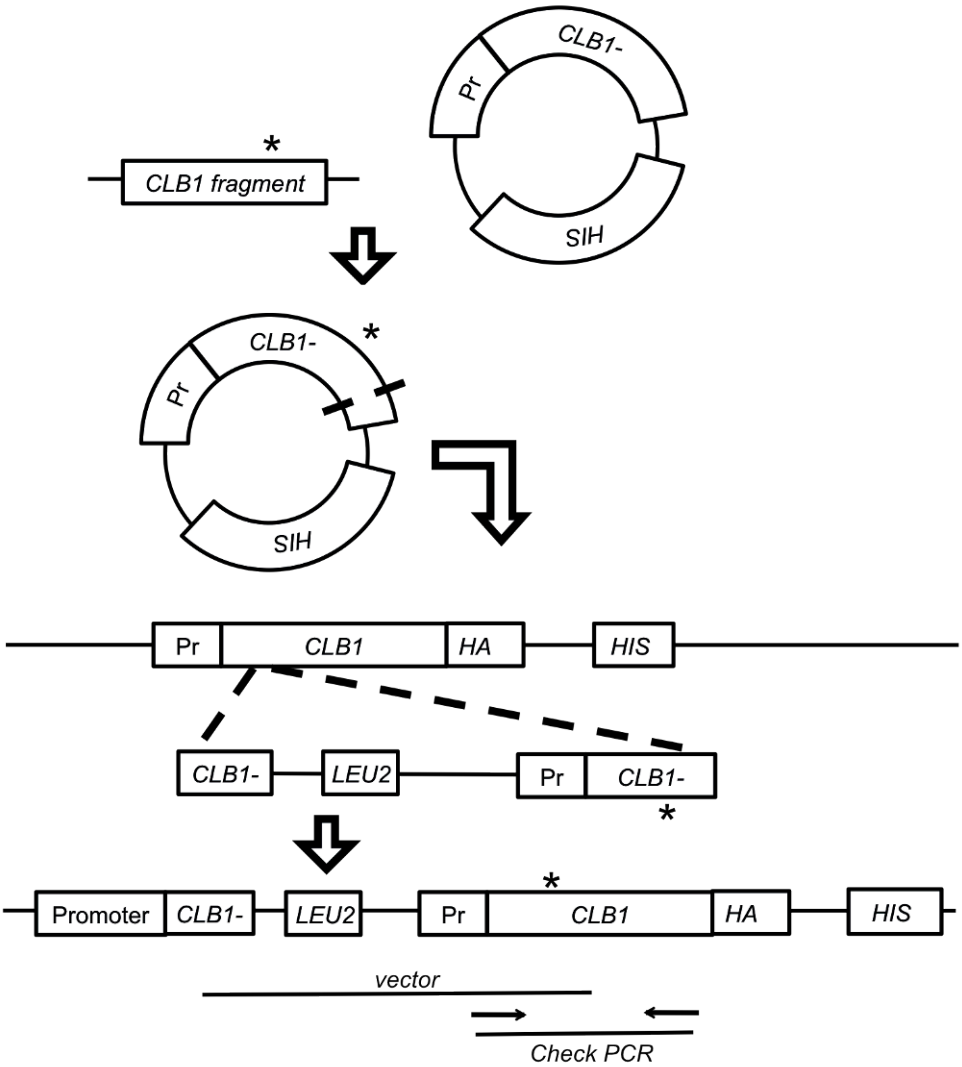

Figure 5-12 ***Construction of the Clb1 endogenous localisation sequence mutant and control*** *The Clb1 sequence was mutated so that the lysines of the nuclear localisation sequence (Figure 4-4) were replaced by alanines. This was incorporated into a plasmid bearing the Clb1 promoter and 3' end of the ORF. The plasmid was cut within the Clb1 sequence and transformed into a strain bearing Clb1-HA. Transformation and homologous recombination lead to the endogenous promoter and a truncated Clb1 fragment, followed by the plasmid Clb1 promoter, and complete Clb1 sequence with the mutation, followed by the HA tag.*

5.4.2 Effect of mutating the endogenous NLS of Clb1

Diploid strains expressing Clb1-NLS6A-HA_6 and Clb1-NLScontrol-HA_6 were induced to sporulate by incubating cells on SPO plates for 24 hours. Strains bearing *clb1-NLS6A-*HA_6 have poor sporulation efficiencies in comparison to the wild type strains, with triad/tetrad proportion dropping from 64% to approximately 47% (Figure 5-13). However, this effect was also seen in the

control *CLB1-NLScontrol-HA* bearing strains in which the proportion of triads/tetrads was 44% (Figure 5-13).

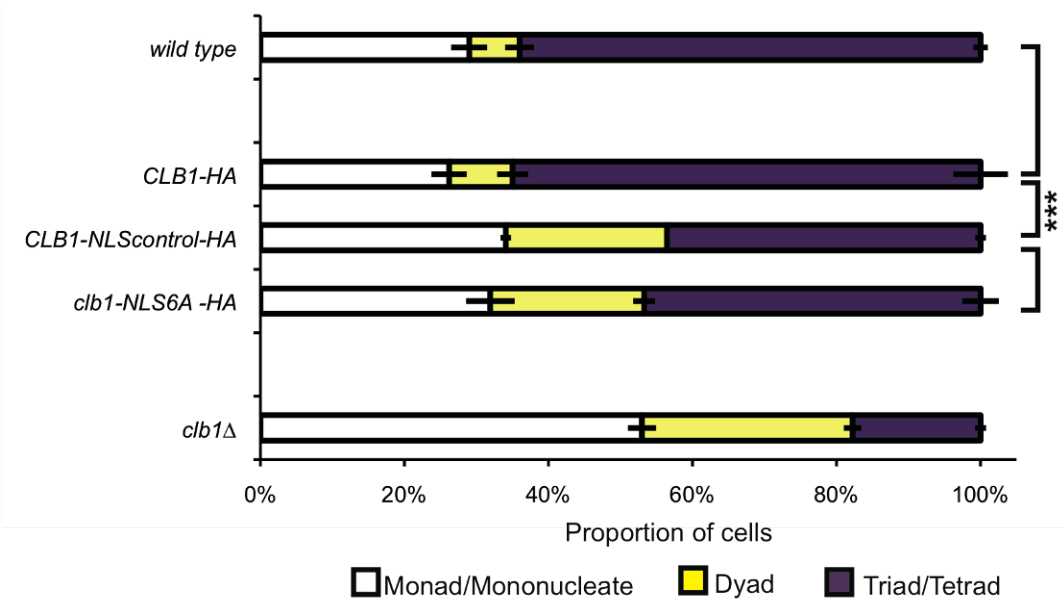

Figure 5-13 ***Sporulation efficiency of Clb1 NLS mutants****. Strains bearing HA-tagged endogenous localisation mutants, wild type and* clb1Δ *strains were allowed to sporulate on SPOVB plates at 30˚C for 48 hours. Three sets of 100 cells were examined for nuclear divisions using DAPI staining. Percentage of cells forming dyads, tetrads and monads or mononucleates were calculated. Asterisks show significance calculated using Mann Whitney U test. (* p<0.05, ** p<0.01, ***p<0.001).*

The decrease in the sporulation efficiency was not due to the HA tag as the *CLB1-HA*$_6$ strains sporulated well at 63%. Therefore, the phenotype cannot be construed to be an effect of the Clb1 nuclear localisation mutation, but may be an artefact from the method of production of the mutant, such as expression of the truncated Clb1 fragment. Heterozygous mutants were not tested so we cannot say whether the effect is dominant.

Strains bearing *CLB1-NLS6A-HA*$_6$ and *CLB1-NLScontrol-HA*$_6$ were induced to enter meiosis. Probing fixed samples for Clb1 demonstrated that Clb1-NLS6A-HA$_6$ was still nuclear, though not to the extent of Clb1-HA$_6$, or Clb1control-HA$_6$. Both strains bearing the truncated Clb1 showed a decreased amount of cells bearing detectable Clb1 (Figure 5-14), in comparison to the Clb1-HA$_6$ control. These localisation results, and others in this chapter, have to be considered with the fact that a control to detect non-specific binding of the antibodies was not performed. The mutants showed very little change in the rate of progress through meiosis (Figure 5-14). Both mutants were a little slower to enter

meiosis, with lower binucleate counts and later accumulation of tetranucleates, compared to the wild type.

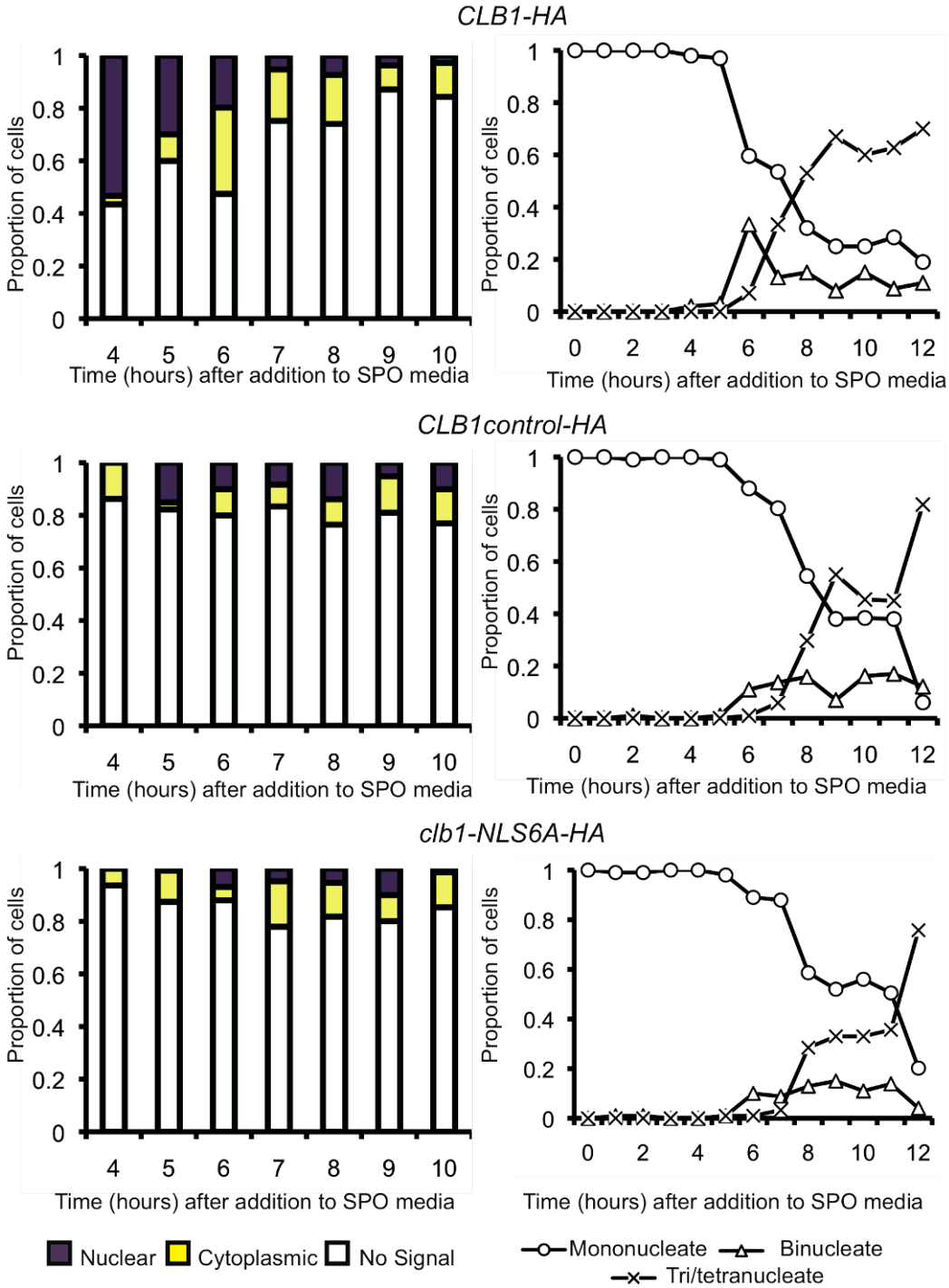

Figure 5-14 ***Clb1 localisation and nuclear division in Clb1 nuclear localisation site mutants.*** *Cultures of cells bearing* CLB1-NLScontrol-HA$_6$ *and* CLB1-NLS6A-HA$_6$ *and* CLB1-HA$_6$ *were induced to undergo meiosis by resuspension in sporulation media (SPO media).* ***A*** *Cells were fixed and examined for Clb1-HA$_6$ localisation by in situ immunofluorescence. 100 cells were scored for each time point. Example images are shown in Figure 5-17. Proportion of cells with nuclear Clb1*

(purple), cytoplasmic Clb1 (yellow) and no Clb1 signals (white) are indicated. ***B*** *Nuclear division is scored over the time course.*

There was a strong reduction in the number of cells with detectable Clb1, compared to the Clb1-HA_6 parent strain. The Clb1 fragment may have affected the stability of the tagged Clb protein independently of the mutation. Both Clb1-NLScontrol-HA_6 and Clb1-NLS6A-HA_6 showed the gel shift indicating phosphorylation. In the *CLB1-NLS6A-HA_6* strain, the modification appeared to be delayed by one hour and to last for a longer period.

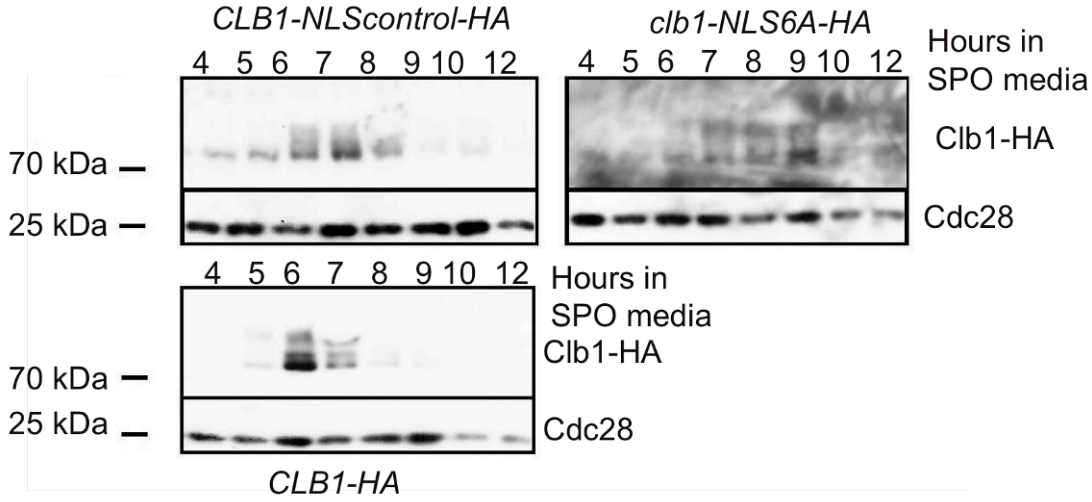

Figure 5-15 ***Clb1 modification in nuclear localisation site mutants.*** *Cultures of* CLB1-NLScontrol-HA_6 *and* CLB1-NLS6A-HA_6 *and* CLB1-HA_6 *cells were induced to undergo meiosis by resuspension in SPO media. Gel mobility of Clb1-HA_6 was assayed by subjecting whole cell extracts to SDS-PAGE followed by western blot analysis using anti-ha. Blots were also probed with anti-tubulin.*

The *clb1-NLS6A-HA_6* mutation had a partial effect on Clb1 nuclear localisation. However, as the control strain showed altered Clb1 expression and sporulation efficiency, these strains were not used to further investigate the effect of Clb1 localisation.

5.5 Ectopic localisation tags on Clb1

Mutating the endogenous localisation sequence did not allow us to alter the localisation of Clb1 effectively. It is improbable that mutating the nuclear export sequence (NES) would prevent nuclear localisation during meiosis I, and, if alternative localisation factors are involved in export, the mutation may not have any effect at all. In order to alter the localisation of Clb1, it was decided to tag the sequence with ectopic NLS and NES tags, as well as the HA tag. We

inserted two copies of the localisation sequences in tandem to overpower endogenous regulation.

5.5.1 Generation of *clb1* localisation mutants

The *CLB1* gene sequence was modified using PCR-tagging (Figure 5-16) to insert two localisation sequences followed by six copies of the HA tag, using the *HIS3MX6* marker for selection (Janke et al., 2004). The NLS tagged and NES tagged alleles of *CLB1* will be referred to as *CLB1-NLS$_2$-HA$_6$* and *CLB1-NES$_2$-HA$_6$*, respectively. These mutants were compared with a *CLB1-HA$_6$* strain.

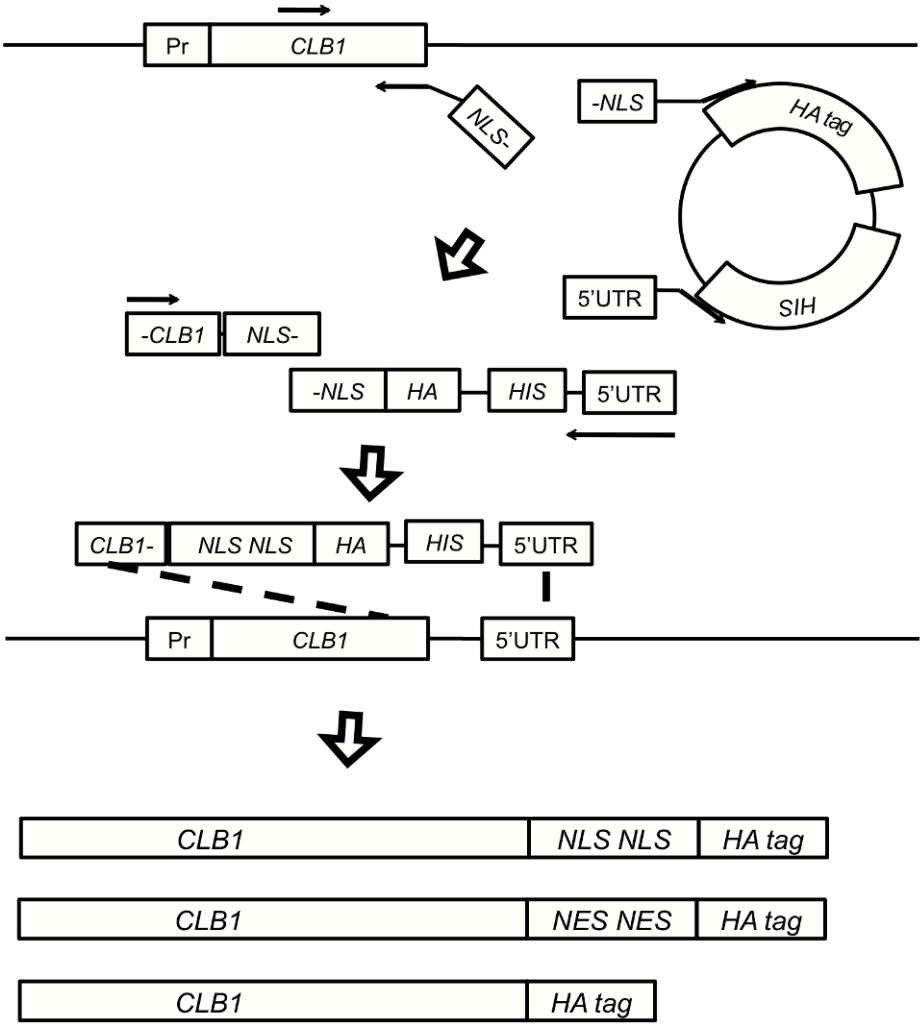

Figure 5-16 ***Construction of CLB1 genes tagged with ectopic localisation tags and 6xHA.*** *Clb endogenous sequence and tagged primers was used to generate a 5' fragment of Clb1 bearing part of the localisation tag. A plasmid was used to create a fragment bearing an overlapping part of the localisation sequence and HA tag, with the selective* HIS *marker. Overlapping fragments were combined by PCR and transformed into the wild type Clb1 sequence by homologous recombination, generating a wild-type Clb1 sequence followed by tandem localisation sequences and HA tags.*

5.5.1.1 Validation of the localisation mutants

To test whether the localisation tags cause the predicted effect, cells bearing the genes were arrested in metaphase of meiosis, and metaphase of mitosis. Mitotic cultures of P_{MET}*CDC20* cells bearing *CLB1-NLS*$_2$*-HA*$_6$*, CLB1-NES*$_2$*-HA*$_6$ or *CLB1-HA*$_6$, were arrested in metaphase of mitosis by growth in media containing methionine (Methods Section 2.2.1.3). Meiotic cultures of P_{Clb2}*CDC20* cells bearing *CLB1-NLS*$_2$*-HA*$_6$*, CLB1-NES*$_2$*-HA*$_6$ or *CLB1-HA*$_6$, were induced to enter meiosis by resuspension in sporulation media and arrested in metaphase of meiosis I due to Cdc20 depletion. Cell samples were taken for imaging 7 hours into sporulation media (SPO media) (Figure 5-17). These localisation results, and others in this chapter, have to be considered with the fact that a control to detect non-specific binding of the antibodies was not performed.

The Clb1-NES$_2$-HA$_6$ protein was largely cytoplasmic during meiosis I, but was not entirely expelled from the nucleus, as the nucleus did not appear as a darker region in meiotic cells (Figure 5-17). The Clb1-NLS2-HA$_6$ protein was concentrated in the nucleus during the mitotic metaphase arrest, unlike the wild type Clb1-HA$_6$ (Figure 5-17). This validated the localisation mutants. Sporulation efficiency was not strongly affected by these mutations. Strains bearing either *CLB1-NLS*$_2$*-HA*$_6$ or *CLB1-NES*$_2$*-HA*$_6$ were compared with the control strain bearing *CLB1-HA*$_6$ and with *clb1Δ* strains (Figure 5-18).

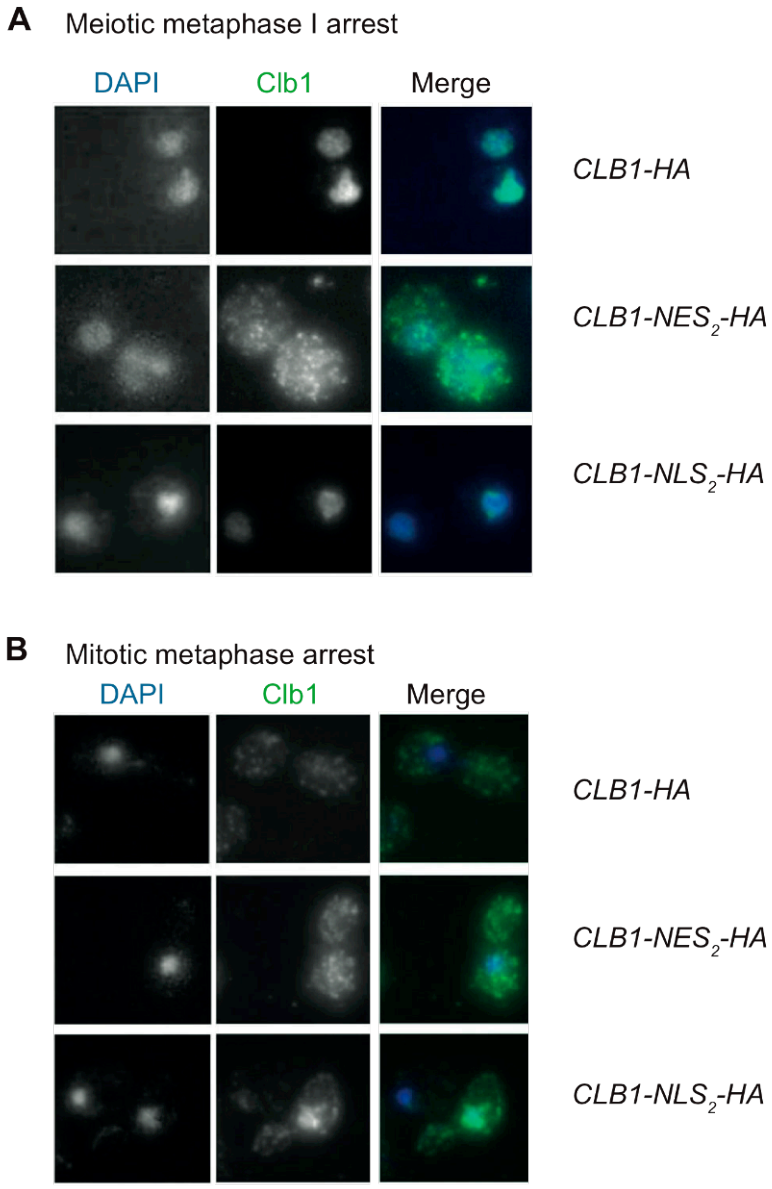

Figure 5-17 ***Images for Clb1 localisation in metaphase arrests. A*** *Cultures of* P_{CLB2}CDC20 CLB1-NLS_2-HA_6, P_{CLb2}CDC20 CLB1-NES_2-HA_6 *and* P_{CLb2}CDC20 CLB1-HA_6 *cells are induced to undergo meiosis by resuspension in SPO media. Samples taken at 7 hours into sporulation media are fixed and examined for Clb1-*HA_6 *localisation by in situ immunofluorescence.* ***B*** *Cultures of* P_{MET}CDC20 CLB1-NLS_2-HA_6, P_{MET}CDC20 CLB1-NES_2-HA_6 and P_{MET}CDC20 CLB1-HA_6 *cells are arrested in metaphase by methionine. Samples taken at 2 hours from addition of methionine are fixed and examined for Clb1-*HA_6 *localisation by in situ immunofluorescence.*

The former three shared similar sporulation efficiencies of 53% to 70%, while the *clb1Δ* strain had a tetrad proportion reduced to 18%, consistent with published results (Grandin and Reed, 1993). The *CLB1-*NES_2*-*HA_6 strain did not have a severe loss in sporulation efficiency, though the *clb1Δ* strain did show a severe loss. This indicates that Clb1-NES_2-HA_6 is partly functional, and might persist at low levels within the nucleus. This provides genetic evidence that the

mutant Clb1 proteins are still active and carrying out their function. A further implication is that the meiosis-specific nuclear localisation, and later export, are not as essential for the progression through meiosis as Clb1 activity.

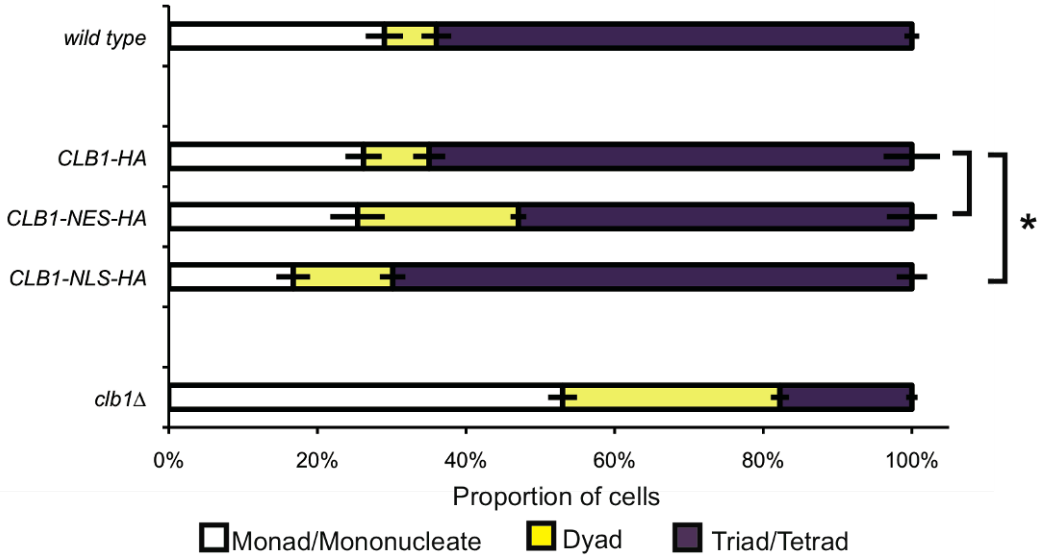

Figure 5-18 ***Sporulation efficiency of localisation tagged Clb1.*** *Strains bearing Clb1 localisation mutants, as well as wild type and* clb1Δ *strains, were allowed to sporulate on SPOVB plates at 30°C for 48 hours. Three sets of 100 cells were examined for nuclear divisions using DAPI staining. Percentage of cells forming dyads, tetrads and monads or mononucleates were calculated. Asterisks show significance calculated using Mann Whitney U test. (* p<0.05, ** p<0.01, ***p<0.001)*

Spore viability was also largely unaffected by the mutations: *CLB1-HA*$_6$ and *CLB1-NES*$_2$*-HA*$_6$ strains have viabilities of 97%, whereas the *CLB1-NLS*$_2$*-HA*$_6$ strain has a spore viability of 85%. To confirm the activity of the localisation tagged Clb1 proteins, the tagged proteins were purified and subjected to a kinase assay. Four strains were grown in to mid-log phase: *CLB1-NLS*$_2$*-HA*$_6$ *cdc28-as*, *CLB1-NES*$_2$*-HA*$_6$ *cdc28-as* and *CLB1-HA*$_6$ *cdc28-as* cells, with *CLB1-MYC*$_9$ *cdc28-as* cells as an untagged control. Clb1 was immunoprecipitated from the harvested cells using an anti-HA antibody. Immunoprecipitation was confirmed by SDS-PAGE followed by western blot analysis (Figure 5-19 A). A slight difference was seen consistently in gel mobility, between the two mutant proteins and the wild type protein.

The purified protein complexes were assayed for Cdc28-dependent kinase activity using two concentrations of the test substrate, histone H1. In one set of reactions, 1-NM-PP1 was added to test whether the kinase activity was CDK-dependent (Figure 5-19 B)

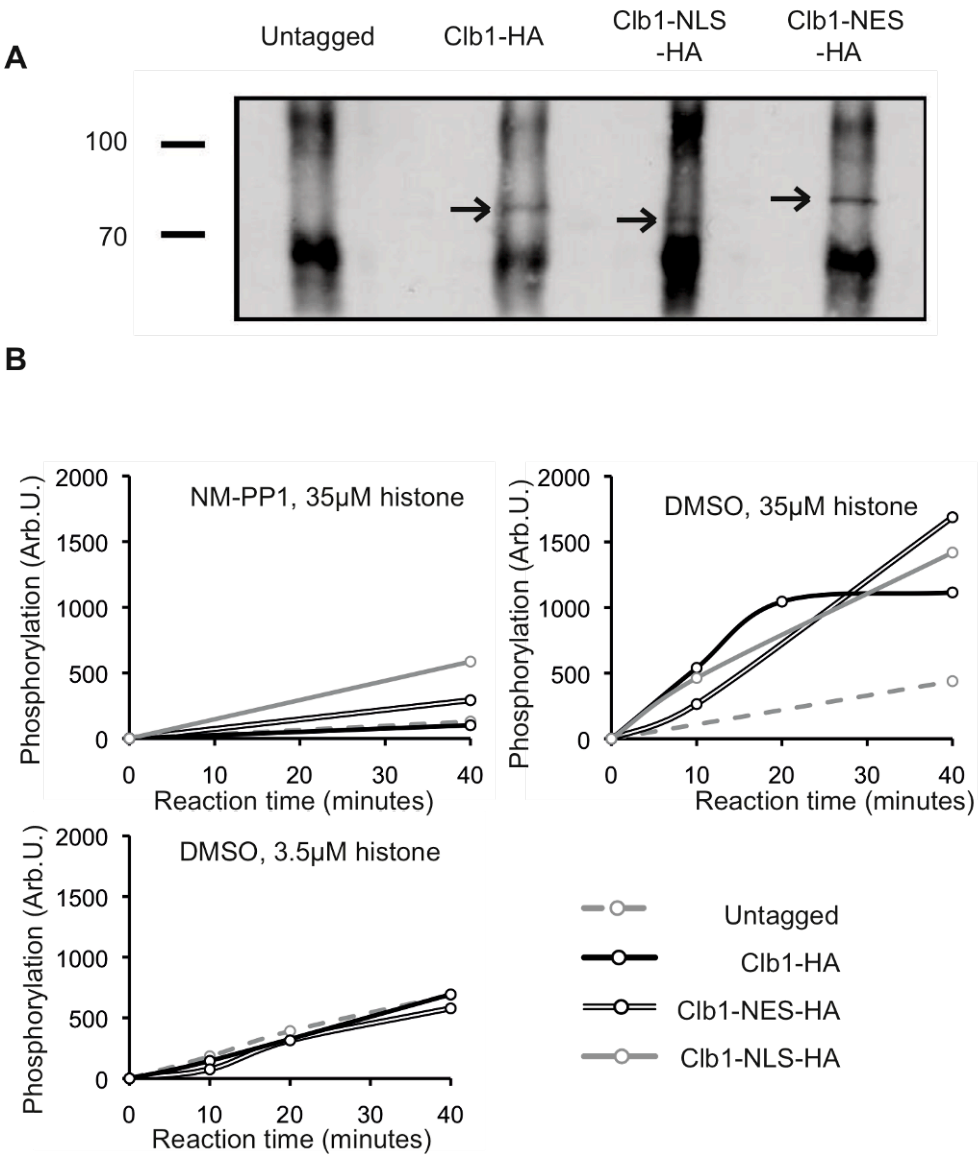

Figure 5-19 ***Activity of HA-tagged Clb1 from mitotic cultures. A.*** *Cultures of cells bearing* CLB1-NLS_2-HA_6 cdc28-as, CLB1-NES_2-HA_6 cdc28-as, CLB1-HA_6 cdc28-as *or* CLB1-MYC_9 cdc28-as *(Untagged) were grown in YEPD to an* OD_{600} *of 1, before cell harvesting. HA tagged protein was immunoprecipitated from the mitotic cultures.* ***B****: Immunoprecipitated Clb1 protein was incubated with histone substrate at two concentrations, 3.5μM and 35μM. Incubation with 1-NM-PP1 was performed as a control to confirm that detected kinase activity was CDK dependent.*

At the lower concentration there was little difference between the three strains. In the reaction with the higher histone concentration, the untagged control sample showed a weak kinase activity. However, the untagged strain showed similar kinase activity in the presence of the inhibitor. Since Cdc28-as activity was inhibited in this condition, the activity in the untagged control must result from non-specific binding including a protein with some kinase activity. The non-specific binding appeared to be out-competed by HA-tagged Clb1 in the

tagged strains, as these strains did not show kinase activity in the presence of the inhibitor.

5.5.2 Phenotypes of Clb1 localisation mutants

5.5.2.1 Effect of localisation mutants on sporulation

Cultures of *CLB1-NLS$_2$-HA$_6$ PDS1-MYC*, *CLB1-HA$_6$ PDS1-MYC*, and *CLB1-NES$_2$-HA$_6$ PDS1-MYC* cells were induced to undergo meiosis, and examined for changes in the timing of meiotic nuclear divisions and spindle assembly. Imaging confirmed that Clb1 was more nuclear in the *CLB1-NLS$_2$-HA$_6$ PDS1-MYC$_9$* strain than in the *CLB1-HA$_6$ PDS1-MYC$_9$* strain (Figure 5-17), although a small proportion of cells showed cytoplasmic Clb1, later in the time course (9 hours into SPO). All cells in the *CLB1-NES$_2$-HA$_6$ PDS1-MYC$_9$* culture that had Clb1 signal showed dispersed Clb1 localisation, so nuclear concentration of Clb1 was abolished.

Nevertheless, as demonstrated in Figure 5-17, Clb1 was not excluded from the nucleus in these cells; no dark area was seen to coincide with DAPI staining. The proportion of cells bearing Clb1 signal appeared one hour later in the *CLB1-NES$_2$-HA$_6$ PDS1-MYC$_9$* strain than the wild type (6-7 hours rather than 5-6 hours), and peaked later. This former observation could be explained by the difficulty detecting early lower levels of Clb1 when dispersed in the cytoplasm. These localisation results, and others in this chapter, have to be considered with the fact that a control to detect non-specific binding of the antibodies was not performed.

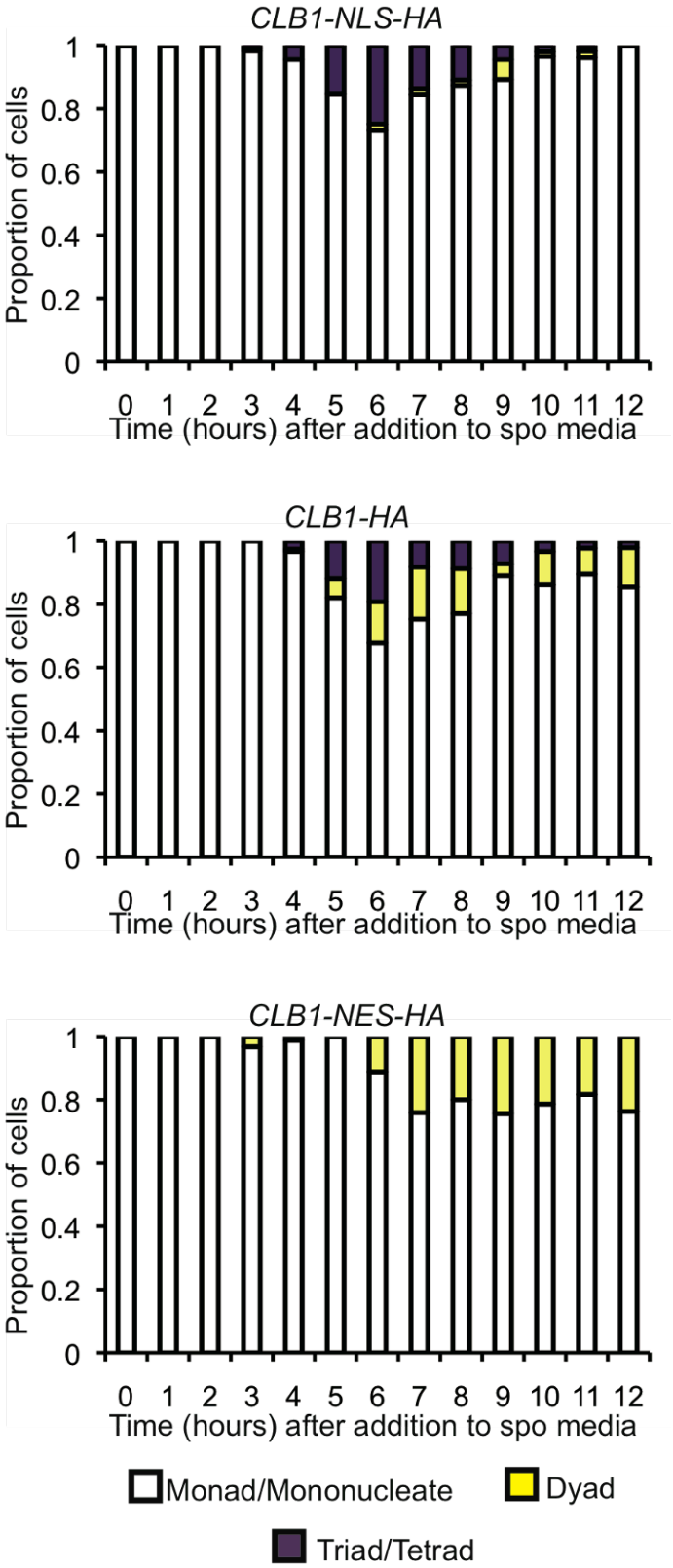

Figure 5-20 ***Localisation of Clb1 in NLS and NES tagged Clb1 mutants.*** *Cultures of CLB1-NLS$_2$-HA$_6$ PDS1-MYC$_9$, CLB1-HA$_6$ PDS1-MYC$_9$ and CLB1-NES$_2$-HA$_6$ PDS1-MYC$_9$ cells were induced to undergo meiosis by resuspension in SPO media. Cells were fixed and examined for Clb1-HA$_6$ localisation by in situ immunofluorescence. 100 cells were scored for each time point and examples*

are shown in Figure 5-17. Proportion of cells with nuclear Clb1 (purple), cytoplasmic Clb1 (yellow) and no Clb1 signals (white) are indicated.

Nuclear divisions were also delayed in the *CLB1-NES$_2$-HA$_6$ PDS1-MYC$_9$* strain (Figure 5-21), with binucleates appearing later than in the *CLB1-HA$_6$* strain. A similar number of tetrads was not reached in the 12-hour time course, despite the similar sporulation efficiencies seen after 48 hours on SPO plates (Figure 5-18). It is generally observed that sporulation on plates is more efficient than in liquid medium (Keeney, 2009) and the *CLB1-NES$_2$-HA$_6$ PDS1-MYC$_9$* strain showed a small decrease in tetrad proportion (Figure 5-21).

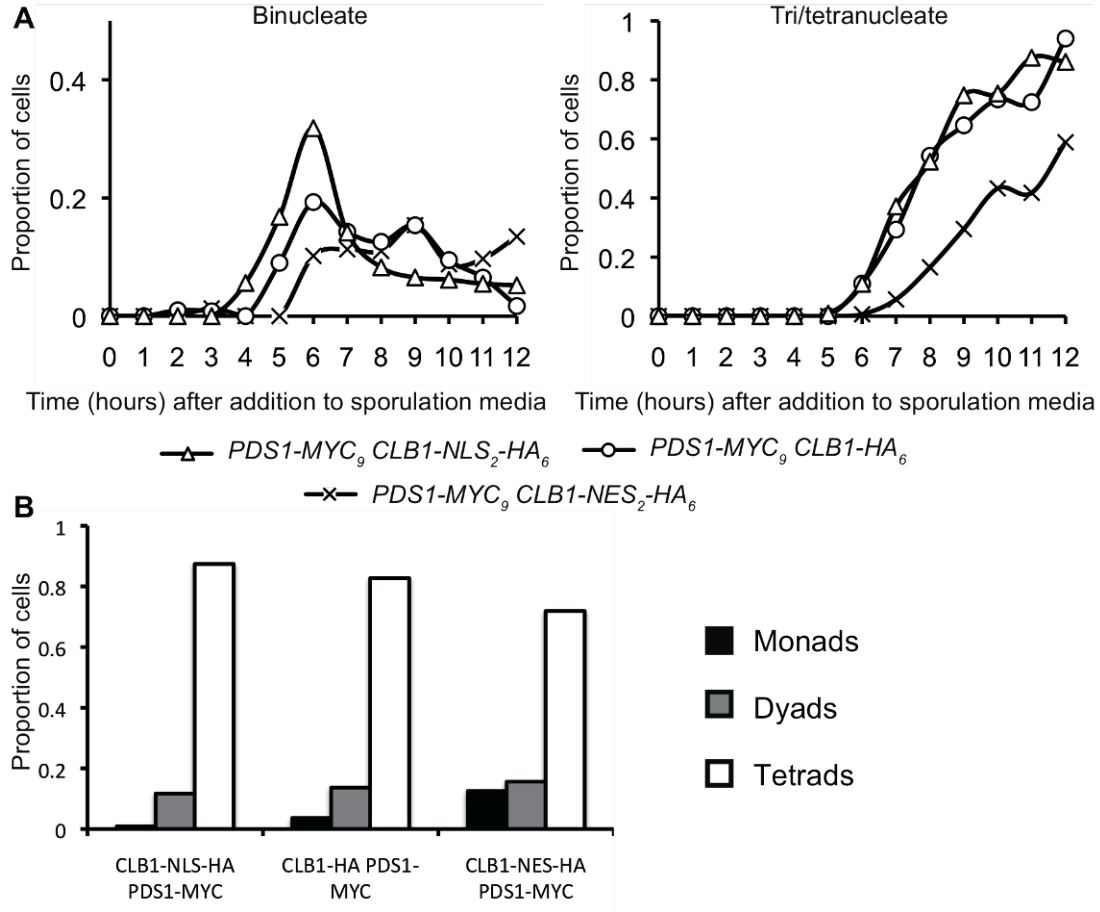

Figure 5-21 ***Nuclear division in NLS and NES tagged Clb1 mutants.*** *Cultures of CLB1-NLS$_2$-HA$_6$ PDS1-MYC$_9$, CLB1-HA$_6$ PDS1-MYC$_9$ and CLB1-NES$_2$-HA$_6$ PDS1-MYC$_9$ cells were induced to undergo meiosis by resuspension in SPO media.* ***A:*** *Samples were taken for in situ immunofluorescence hourly and nuclear division was scored by DAPI staining. 100 cells were scored for each time point.* ***B:*** *Samples were taken at 24 hours into sporulation media for final sporulation counts. 100 cells were scored for each time point. Difference between the final sporulation efficiency of the three cultures was found insignificant (p>0.05) by Mann Whitney U test.*

Interestingly, the *CLB1-NLS$_2$-HA$_6$ PDS1-MYC$_9$* strain showed the opposite effect (Figure 5-21), with an accelerated appearance of binucleates. The

timing of meiosis II was not altered in this case, as tri/tetranucleates appeared with similar kinetics to the wild type.

Fixed cells were examined for presence of Pds1 (Figure 5-22). The *CLB1-NES$_2$-HA$_6$ PDS1-MYC$_9$* strain did show a later peak of Pds1 bearing cells, possibly reflecting delayed entry into meiosis. However, asynchrony is such that the two peaks of Pds1 denoting the two divisions were not clearly differentiable, so levels of Pds1 would not be indicative as to the effects of these mutants on progress through meiosis. The use of synchronised cultures may have given more informative results.

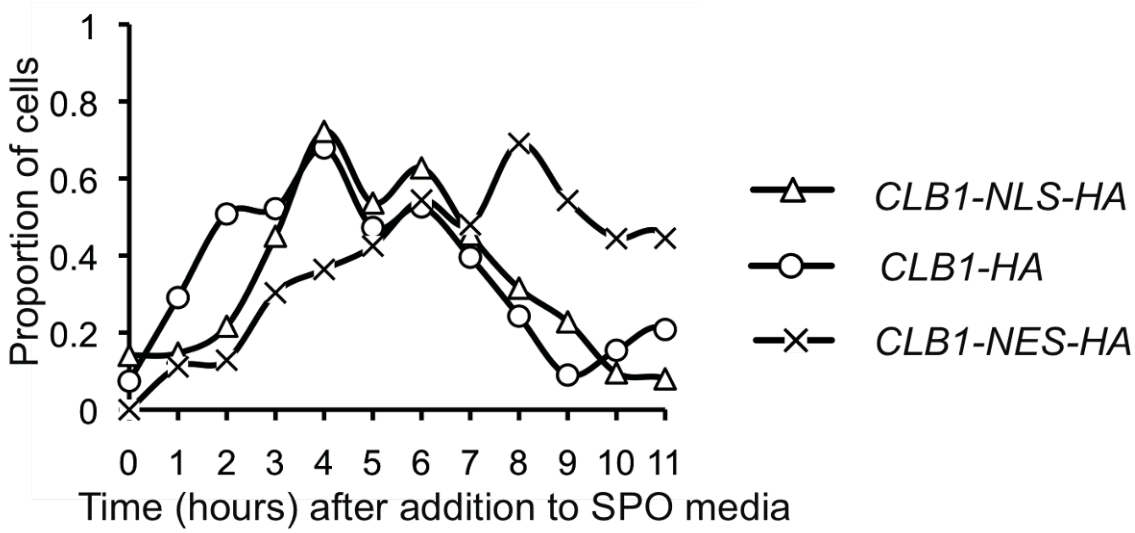

Figure 5-22 ***Presence of Pds1 in NLS and NES tagged Clb1 mutants.*** *Cultures of CLB1-NLS$_2$-HA$_6$ PDS1-MYC$_9$, CLB1-HA$_6$ PDS1-MYC$_9$ and CLB1-NES$_2$-HA$_6$ PDS1-MYC$_9$ cells were induced to undergo meiosis by resuspension in SPO media. Cells were fixed and examined for Pds1-Myc$_9$ by in situ immunofluorescence. 100 cells were counted in each time point.*

Similarly, the lack of synchrony made any differences in spindle timings difficult to detect. Spindle graphs are shown in Figure 5-23. There were low proportions of spindles at each time point, so variability between time points was large enough to disguise any peak, and made it difficult to assess whether the spindle dynamics had changed between strains. Spindle types were totalled over the time course as this provided an indication of the time spent at each stage (Figure 5-23). There was a reduced number of anaphase II spindle-containing cells in the *CLB1-NES$_2$-HA$_6$ PDS1-MYC$_9$* strain, reflecting the delay as the later spindle types were cut off by the end point of the time course. The *CLB1-NES$_2$-HA$_6$ PDS1-MYC$_9$* strain also showed a greater duration of the two

meiosis I spindle types. The totalled spindle types are not proportional, so this was not a consequence of the reduced later spindle types. *CLB1-NES$_2$-HA$_6$ PDS1-MYC$_9$* cells appear to be delayed, not just in entering meiosis I, but also in exiting meiosis I.

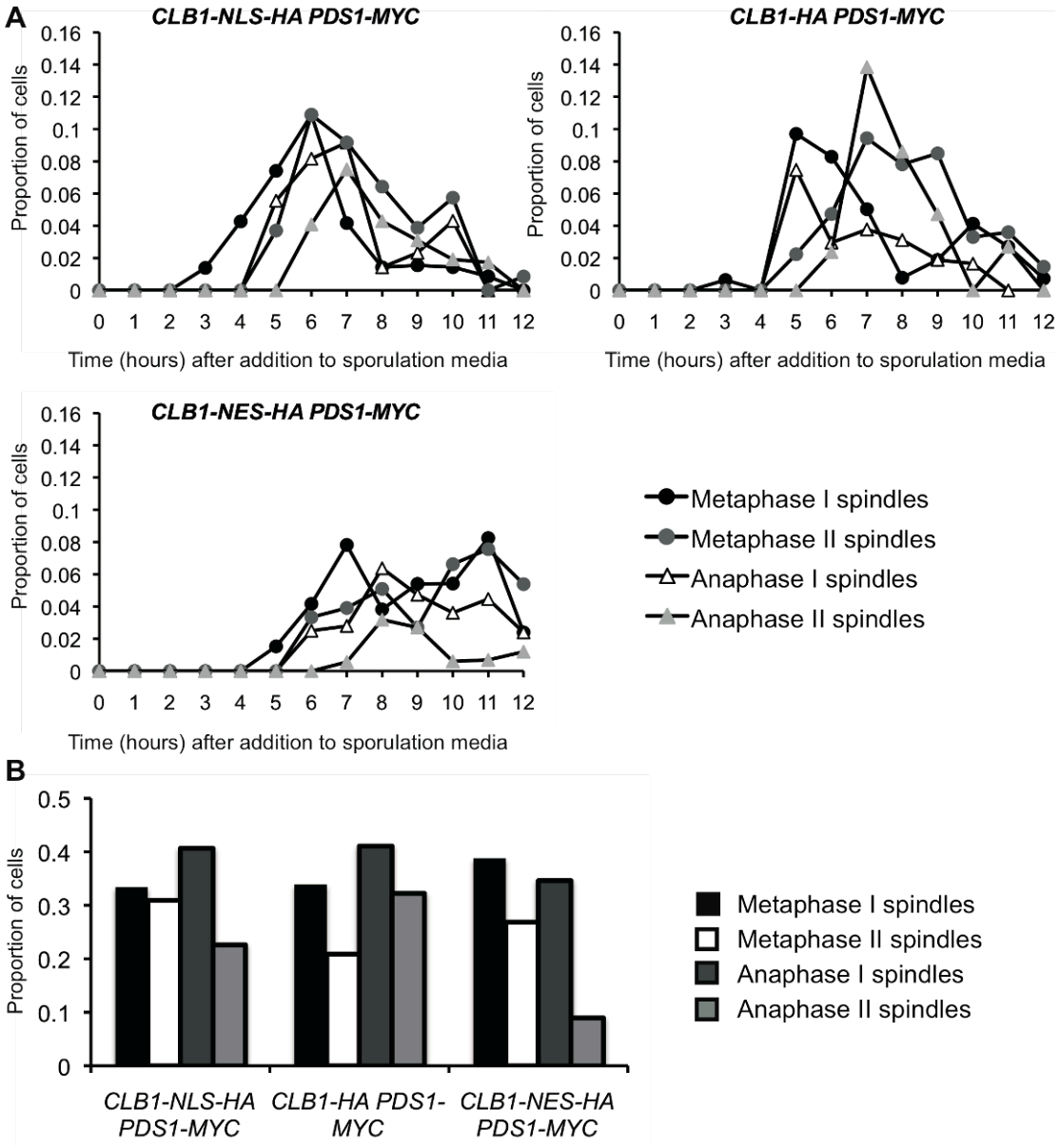

Figure 5-23 ***Spindle stages in NLS and NES tagged Clb1 mutants.*** *Cultures of CLB1-NLS$_2$-HA$_6$ PDS1-MYC$_9$, CLB1-HA$_6$ PDS1-MYC$_9$ and CLB1-NES$_2$-HA$_6$ PDS1-MYC$_9$ cells were induced to undergo meiosis by resuspension in SPO media.* ***A****: Cells were fixed and examined for spindle type by in situ immunofluorescence. 100 cells were counted in each sample.* ***B:*** *The time spent in each stage was estimated by summing the number of each spindle type – a greater number of a spindle type would indicate a greater amount of time spent at that stage.*

The *CLB1-NLS$_2$-HA$_6$ PDS1-MYC$_9$* strain showed a slightly increased proportion of cells in anaphase I. This could suggest that the delay between the accelerated entry into meiosis I and the normally timed meiosis II derived from a delay in exiting anaphase I, with an intact spindle. The inability to export Clb1 may have left too much CDK activity to be countered by FEAR-released Cdc14. The model in Section 5.2 suggested a similar effect on the timing and duration of the low CDK state during meiotic divisions. The model was highly simplified, and did not include regulated export of Clb1 in the "wild type" scenario. However, ectopic nuclear and cytoplasmic localisation of Clb1 were simulated. In the model in which Clb1 localisation was nuclear, the low CDK state was initiated earlier, but lasted longer. In the model in which Clb1 localisation was increasingly cytoplasmic, the low CDK state was initiated later. This parallels the observations of the localisation tagged mutants.

5.5.2.2 Effect of localisation mutants on Clb1 phosphorylation in meiosis

To examine the effect on the phosphorylation of Clb1, localisation-tagged Clb1 strains were induced to enter meiosis, and samples taken for whole cell extracts. Each mutant was compared with the *CLB1-HA* control. Clb1 gel mobility was analysed by western blot analysis (Figure 5-24)

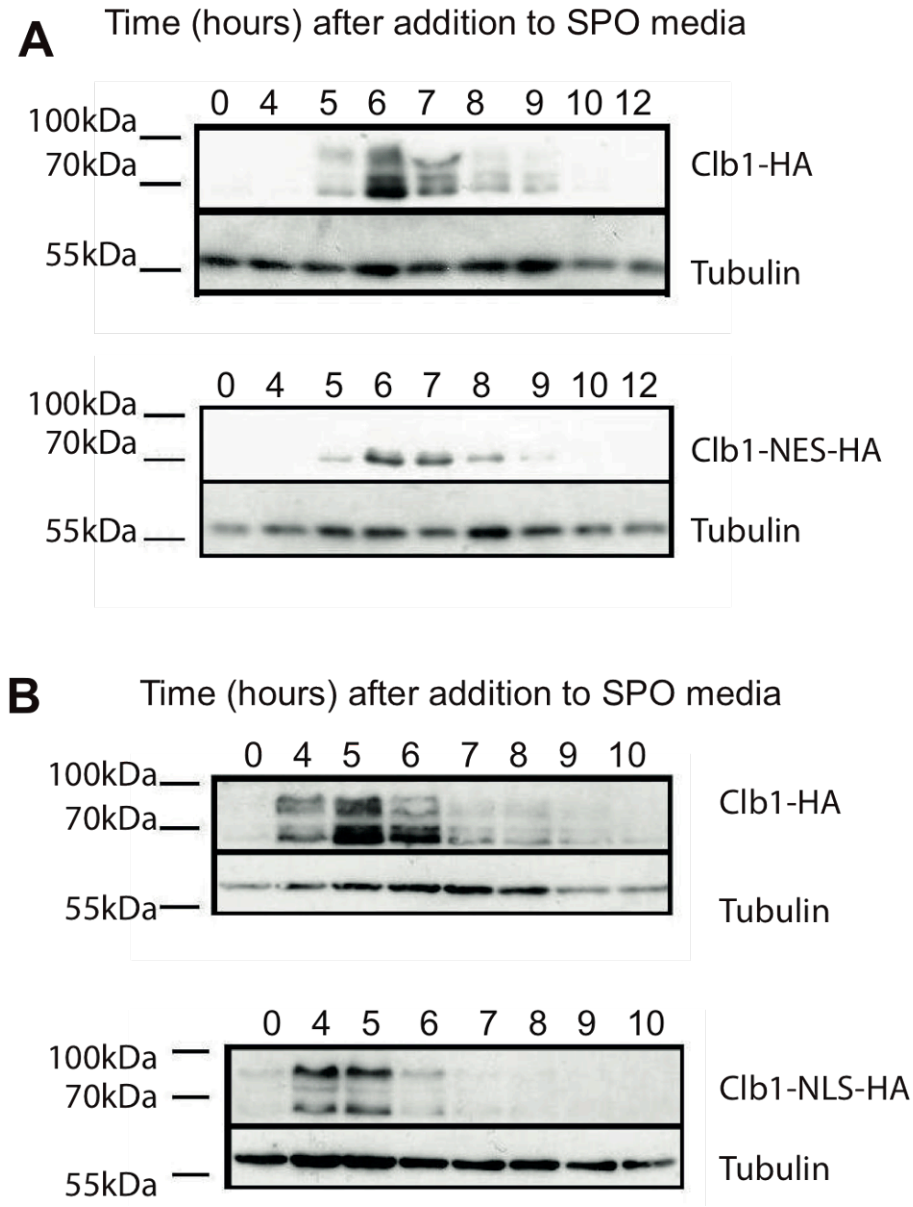

Figure 5-24 ***Gel mobility of NES and NLS tagged Clb1. A*** *Cultures of CLB1-NES$_2$-HA$_6$ PDS1-MYC$_9$, and CLB1-HA$_6$ PDS1-MYC$_9$ cells were induced to undergo meiosis by resuspension in SPO media.* ***B*** *Cultures of CLB1-NLS$_2$-HA$_6$ PDS1-MYC$_9$, and CLB1-HA$_6$ PDS1-MYC$_9$ cells were induced to undergo meiosis by resuspension in SPO media. Gel mobility of Clb1-HA$_6$ was assayed by subjecting whole cell extracts to SDS-PAGE followed by western blot analysis using anti-ha. Blots were also probed with anti-tubulin.*

In both *CLB1-NLS$_2$-HA$_6$* and *CLB1-HA$_6$* strains, the gel shift was clearly visible. In contrast, Clb1-NES$_2$-HA$_6$ phosphorylation was not detected (Figure 5-24). It is not possible to conclude with certainty from this that Clb1-NES$_2$-HA$_6$ is not phosphorylated. With freely sporulating cells, the synchronicity may be such that sampling could miss a transient phosphorylation. The *CLB1-HA$_6$* and *CLB1-NLS$_2$-HA$_6$* cultures, assayed in the same time course, displayed a long

duration of phosphorylation of Clb1 (two to three hours), so the Clb1-NES_2-HA_6 protein was likely to be resistant to phosphorylation. To confirm this, the mutants were combined with $P_{CLB2}CDC20$ to arrest the sporulating cells in metaphase I and maintain the phosphorylation should it occur.

Cultures of cells bearing $P_{CLB2}CDC20$ $CLB1\text{-}NLS_2\text{-}HA_6$, $P_{CLB2}CDC20$ $CLB1\text{-}NES_2\text{-}HA_6$ or $P_{CLB2}CDC20$ $CLB1\text{-}HA_6$ were induced to enter sporulation and samples were taken for western blot analysis of Clb1 gel mobility (Figure 5-25). In $P_{CLB2}CDC20$ $CLB1\text{-}NES_2\text{-}HA_6$ strains, Clb1 is not concentrated in the nucleus and is not modified. It seems that nuclear import is necessary for the phosphorylation and not vice versa. In $P_{CLB2}CDC20$ $P_{CLB2}CDC5$ $CLB1\text{-}MYC_9$ cells, Clb1 underwent nuclear import but no modification (Section 4.4.6) This suggests that the presence of Cdc5 is required, as well as nuclear import, to phosphorylate Clb1.

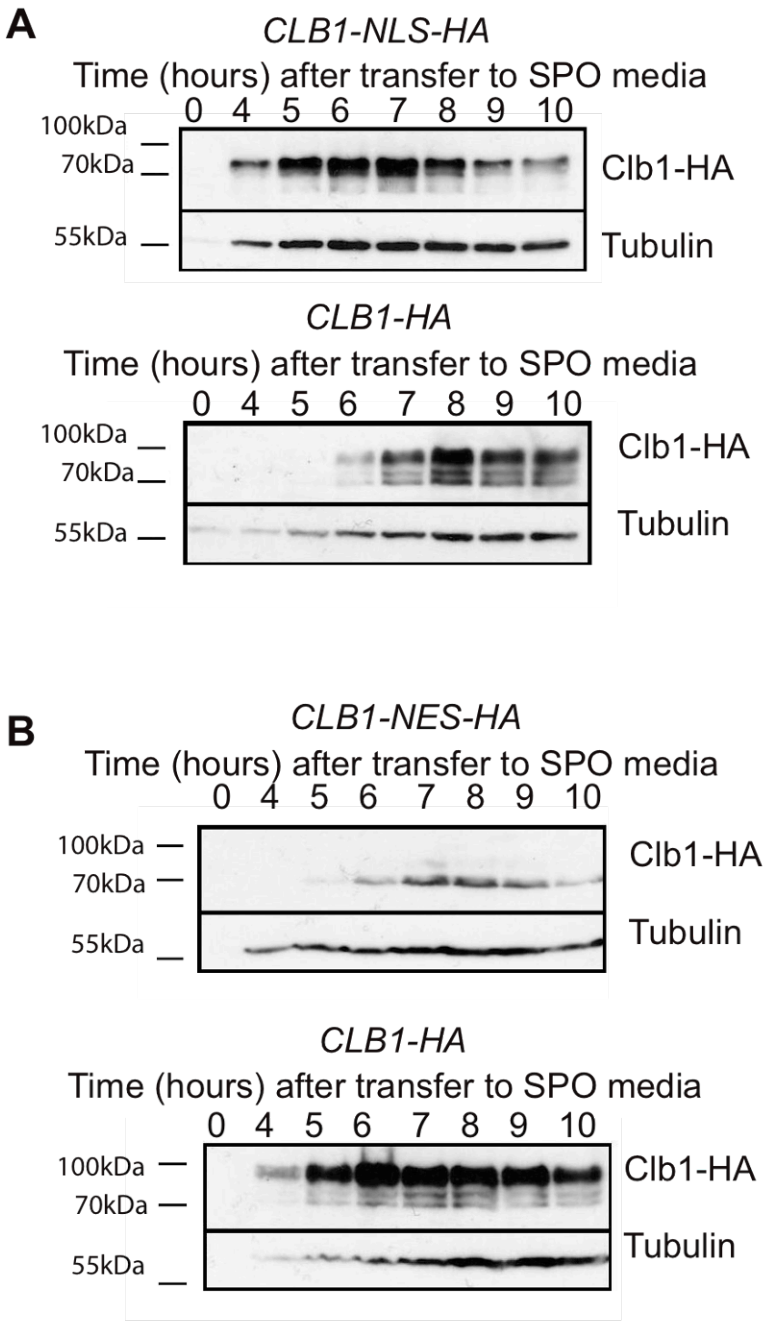

Figure 5-25 ***Gel mobility of NES and NLS tagged Clb1 in meiotic metaphase arrest A*** *Cultures of P_{CLB2}CDC20 CLB1-NES$_2$-HA$_6$, and P_{CLB2}CDC20 CLB1-HA$_6$ cells were induced to undergo meiosis by resuspension in SPO media.* ***B*** *Cultures of P_{CLB2}CDC20 CLB1-NLS$_2$-HA$_6$ and P_{CLB2}CDC20 CLB1-HA$_6$ cells were induced to undergo meiosis by resuspension in SPO media. Gel mobility of Clb1-HA$_6$ was assayed by subjecting whole cell extracts to SDS-PAGE followed by western blot analysis using anti-ha. Blots were also probed with anti-tubulin.*

5.5.2.3 Cyclin redundancy

The localisation mutations of Clb1 had very little effect on the sporulation efficiency of the cells (Figure 5-18). To determine whether cyclin redundancy was responsible for the insensitivity to Clb1 localisation, we examined the phenotypic consequences of altering nuclear localisation in *clb3Δ clb4Δ* strains.

CLB3 and *CLB4* deletions, on their own or in combination, did not have a strong effect on sporulation efficiency (Figure 5-26). However, if *clb3Δ* and *clb4Δ* were combined with *clb1Δ*, no tetrads and few dyads were seen (Grandin and Reed, 1993). Figure 5-26 shows a complete failure to sporulate for the *clb1Δ clb3Δ clb4Δ clb6Δ* strain, which would only be expressing one B-cyclin, *CLB5* (and *CLB2* in mitosis).

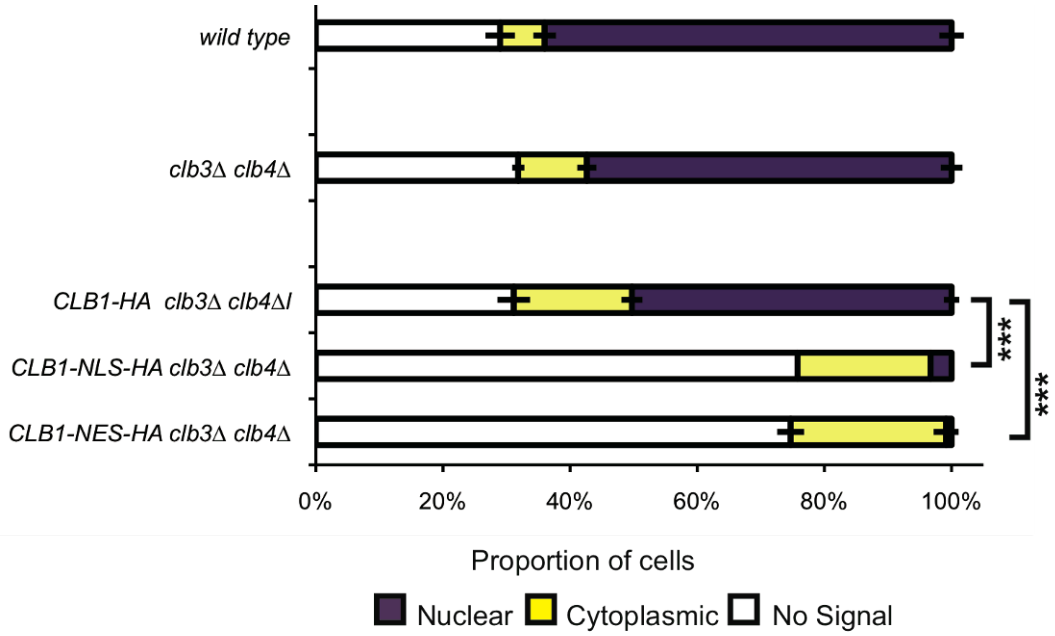

Figure 5-26 ***Sporulation efficiency of localisation mutants cyclin deletions.*** *Strains bearing HA-tagged endogenous localisation mutants and wild type CLB1 with cyclin deletions were allowed to sporulate at 30˚C on SpoVB plates for 48 hours. 3 x 100 cells were counted and the percentage of cells forming dyads and tetrads calculated. Asterisks show significance calculated using Mann Whitney U test (* p<0.05, ** p<0.01, ***p<0.001).*

Both *CLB1* localisation mutants, in combination with *clb3Δclb4Δ*, caused a reduction in sporulation efficiency, reducing triad/tetrads to 1% to 3% whilst producing dyads to 20% to 30%. This indicates that cyclin redundancy has some role in the insensitivity of cells to *CLB1* localisation mutants. As both strains failed to complete sporulation, it appears that CDK activity is required in both

cytoplasm and nucleus during meiosis. To examine the phenotypes further, we looked at the nuclear divisions over a 12-hour time course (Figure 5-27).

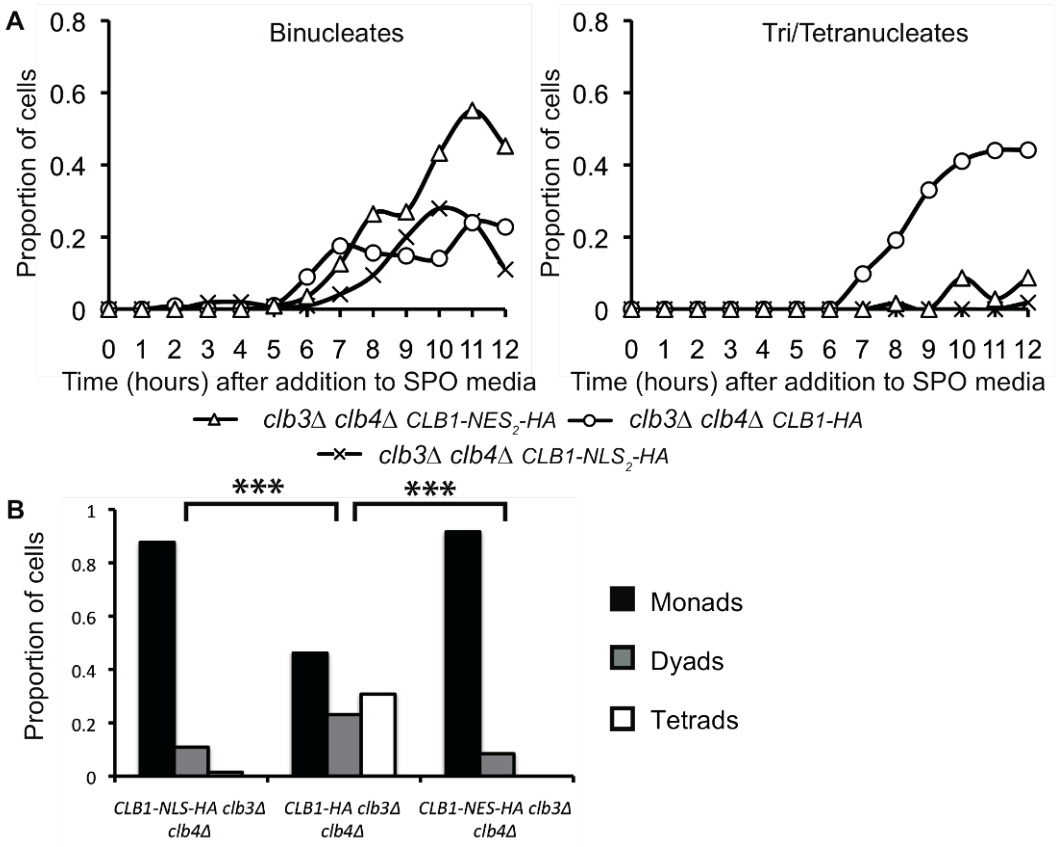

Figure 5-27 ***Nuclear divisions in Clb1 localisation mutants in clb3Δ clb4Δ backgrounds.*** *Cultures of clb3Δ, clb4Δ, CLB1-NES$_2$-HA, clb3Δ, clb4Δ, CLB1-HA, and clb3Δ, clb4Δ, CLB1-NLS$_2$-HA cells were induced to undergo meiosis by resuspension in SPO media.* ***A:*** *Samples were taken for in situ immunofluorescence hourly and nuclear division was scored by DAPI staining. 100 cells were scored for each time point.* ***B:*** *Samples were taken at 24 hours into sporulation media for final sporulation counts. 100 cells were scored for each time point.*

The *clb3Δ clb4Δ CLB1-HA$_6$* strain underwent nuclear divisions an hour later than *CLB3 CLB4 CLB1-HA$_6$* strain (Figure 5-21), and produced a lower proportion of tetranucleates after 12 hours. *clb3Δ clb4Δ CLB1-NES$_2$-HA$_6$* and *clb3Δ clb4Δ CLB1-NLS$_2$-HA$_6$* failed to form tetrads after 24 hours, but during the time course, both *clb3Δ clb4Δ CLB1-NES$_2$-HA$_6$* and *clb3Δ clb4Δ CLB1-NLS$_2$-HA$_6$* bearing cells formed a proportion of binucleates. Cells bearing *clb3Δ clb4Δ CLB1-NES$_2$-HA$_6$* formed binucleates with only a slight delay compared to cells bearing *clb3Δ clb4Δ*, while cells bearing *clb3Δ clb4Δ CLB1-NLS$_2$-HA$_6$* formed binucleates much later, and failed to form tetranucleates. *CLB1-NLS$_2$-HA$_6$* bearing cells formed a proportion of binucleates Surprisingly, the *clb3Δ clb4Δ CLB1-NES$_2$-HA$_6$* cells divided their nuclei better than the *clb3Δ clb4Δ CLB1-NLS$_2$-HA$_6$* cells,

forming a higher proportion of binucleates and even a few tetranucleates. In these cases, the mislocalisation of Clb1 must also be affecting the completion of sporulation.

A balance of nuclear and cytoplasmic CDK activity seems to be required for successful meiosis. In cells in which Clb3 and Clb4 were present, they were able to compensate for disrupted localisation of Clb1. In cells in which Clb3 and Clb4 were absent, nuclear-localised Clb1 was capable of inducing the first division but not the second. Cells bearing *clb3Δ, clb4Δ, CLB1-NES$_2$-HA$_6$* appeared to complete both divisions, but failed to package the divided nuclei in spores, resulting in a lower tetrad count after 48 hours (Figure 5-26). Clb1-NES$_2$-HA$_6$ is not entirely excluded from the nucleus but not concentrated there, so the lack of success in completing sporulation on plates in *clb3Δ, clb4Δ, CLB1-NES$_2$-HA$_6$* was presumably a result of insufficient CDK activity in the nucleus.

Samples taken for TCA preparation were analysed by western blot for Clb1 mobility (Figure 5-28). Clb1 modification was present in the *clb3Δ clb4Δ CLB1-NLS$_2$-HA$_6$* and *clb3Δ clb4Δ CLB1-HA$_6$* samples, and absent from the *clb3Δ clb4Δ CLB1-NES$_2$-HA$_6$* samples, consistent with the results obtained in the *P$_{CLB2}$CDC20* and wild type backgrounds.

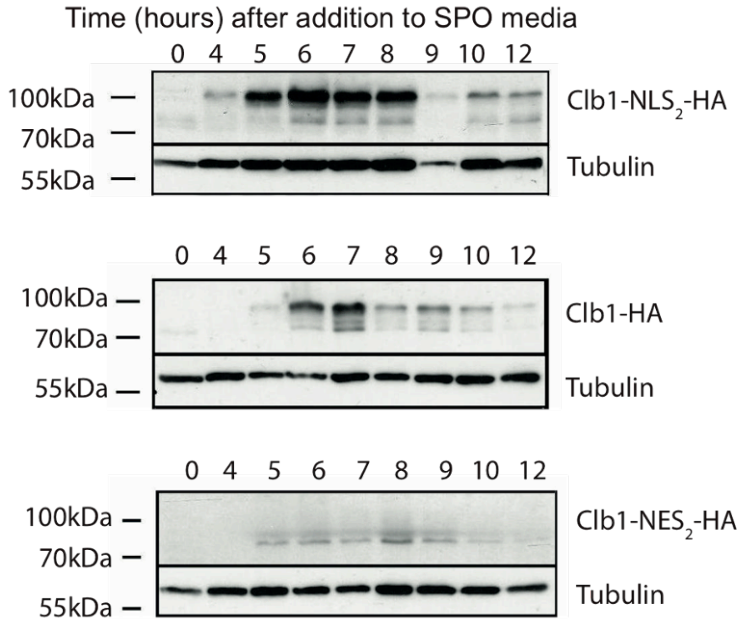

Figure 5-28 ***Clb1 gel mobility in Clb1 localisation mutants in clb3Δ clb4Δ backgrounds.*** *Cultures of clb3Δ clb4Δ CLB1-NES$_2$-HA, clb3Δ clb4Δ CLB1-HA, and clb3Δ clb4Δ CLB1-NLS$_2$-HA cells were induced to undergo meiosis by resuspension in SPO media. Gel mobility of Clb1-HA$_6$ was*

assayed by subjecting whole cell extracts to SDS-PAGE followed by western blot analysis using anti-ha. Blots were also probed with anti-tubulin.

5.5.2.4 Effect of nuclear localisation mutants on FEAR activation

We investigated whether Clb1 nuclear or cytoplasmic localisation altered the phenotypes of FEAR mutants, as this might indicate an effect on FEAR activation. We found that Clb1 localisation mutants had synthetic effects on spore formation with FEAR mutants (Figure 5-29).

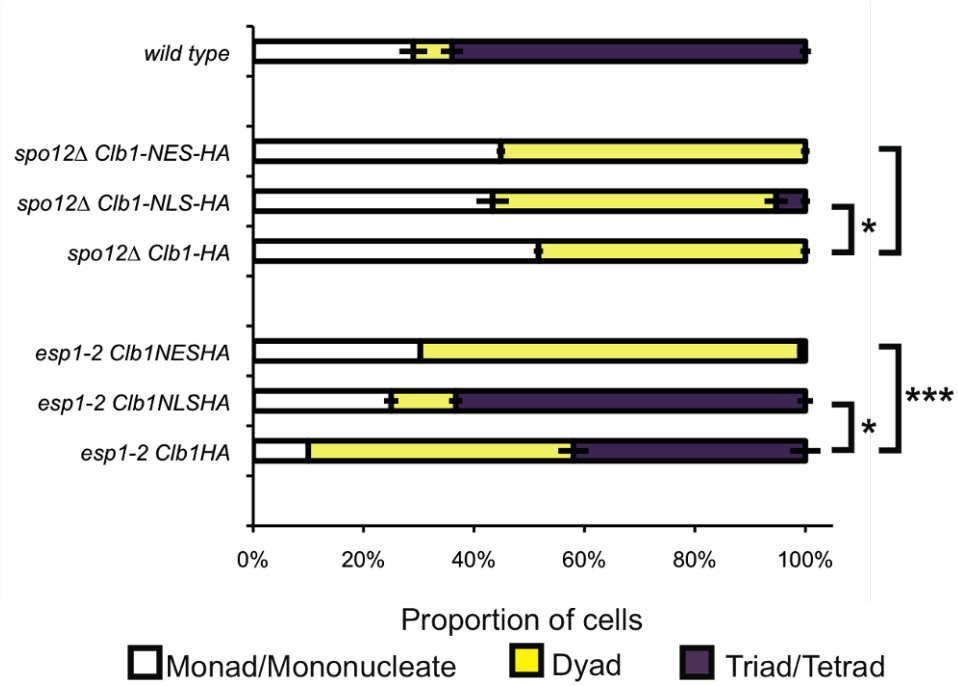

Figure 5-29 ***Sporulation efficiency of Clb1 localisation mutants in combination with FEAR mutants.*** CLB1-HA_6, CLB1-NES_2-HA_6 *and* CLB1-NLS_2-HA_6 *strains bearing* spo12Δ *and* esp1-2 *or their wild type alleles were allowed to sporulate on SpoVB plates for 48 hours at 30˚C. 5 x 100 cells were counted and the percentage of cells forming dyads, tetrads and monads were calculated after 48 h. Asterisks show significance calculated using Mann Whitney U test (* p<0.05, ** p<0.01, ***p<0.001).*

The *spo12Δ* strain forms dyads during meiosis, as the anaphase I spindle fails to disassemble after the first meiotic division, and the second division happens on the same spindle (Marston and Amon, 2004). The *CLB1-HA_6* tag did not change the *spo12* dyad phenotype (Figure 5-29). Interestingly, the nuclear localisation of Clb1 showed a partial suppression of the phenotype, and led to the production of approximately 5% tetrads. Cytoplasmic localisation of Clb1 did not

alter the phenotype. The effect of the *CLB1-NLS$_2$-HA$_6$* allele suggests that increased nuclear localisation of Clb1 amplifies FEAR activation.

esp1-2 is a temperature sensitive mutation in the gene encoding separase, which leads to an increased number of dyads and decreased number of tetrads compared to the wild type at 30˚C (Buonomo et al., 2000; Queralt and Uhlmann, 2008), but has a far weaker effect at 25˚C (Figure 5-29). *CLB1-NLS$_2$-HA$_6$* improved the ratio of tetrads produced from 42% to 63%, whereas *CLB1-NES$_2$-HA$_6$* caused almost complete loss of tetrads, confirming that the two mutations have opposing effects on FEAR activation.

If Clb1 localisation alters FEAR activation, we may see an effect on Cdc14 release. Although Cdc14 release in meiosis I is hard to detect by *in situ* immunofluorescence, released Cdc14 leads to the separation of nucleolar DNA (Sullivan et al., 2004) so we can use separation of Nop1 dots as a marker for the release of Cdc14. Nop1 separation was scored in cells having either a metaphase I or anaphase I spindle (Figure 5-30).

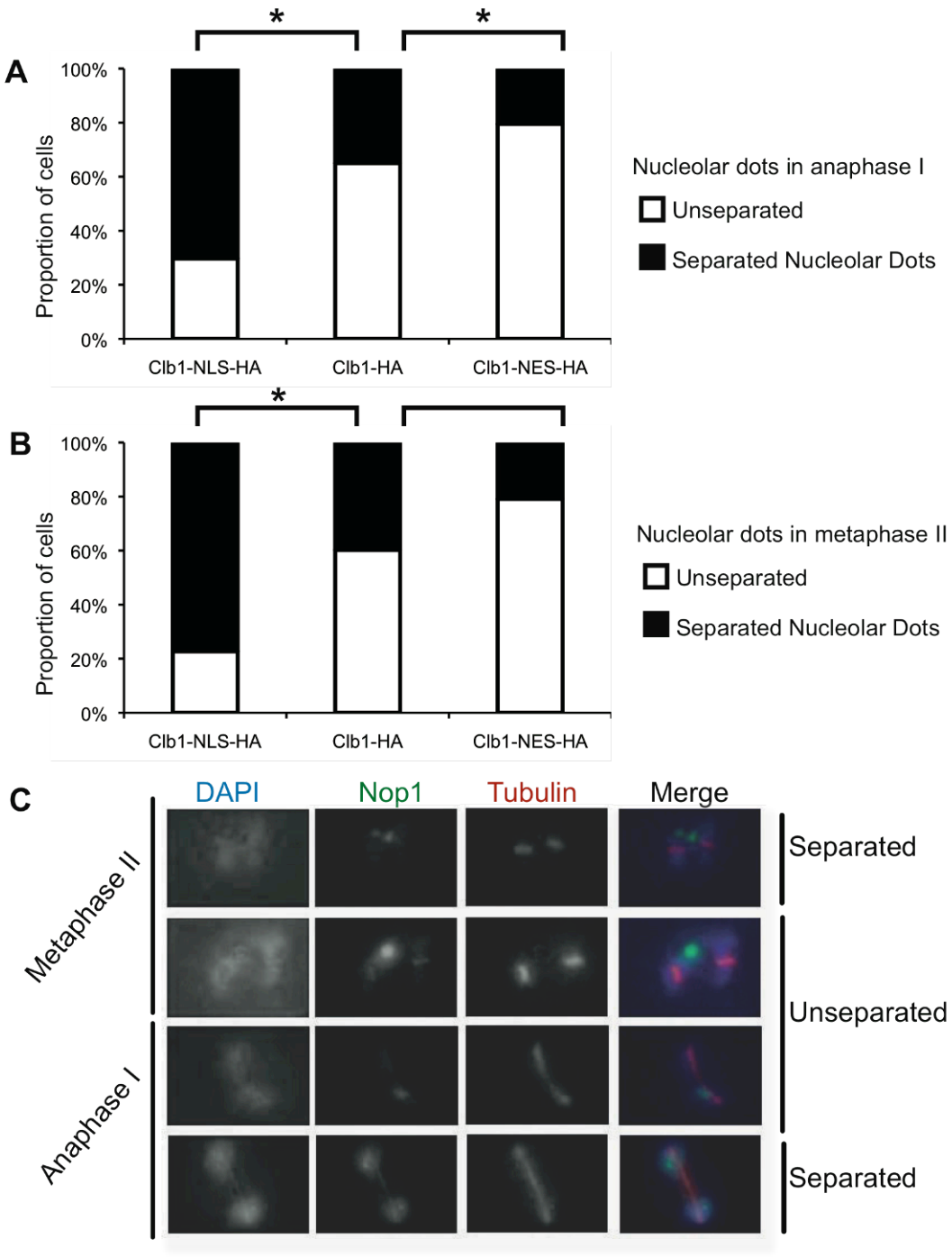

Figure 5-30 ***Nucleolar separation in Clb1 localisation mutant strains.*** *Cultures of CLB1-NES$_2$-HA, CLB1-HA, and CLB1-NLS$_2$-HA cells were induced to undergo meiosis by resuspension in SPO media. Cells were fixed and examined for separation of nucleolar dots in cells with anaphase I (**A**) or metaphase II (**B**) spindles. Asterisks show significance calculated using Mann Whitney U test (* p<0.05, ** p<0.01, ***p<0.001). Around 40 cells were counted per strain. Example images of separate and unseparated nuclear dots at different spindle stages (**C**)*

CLB1-NLS$_2$-HA$_6$ cells showed increased proportion of separated nucleolar dots in both anaphase I and metaphase II spindle-containing cells, whilst *CLB1-NES$_2$-HA$_6$* cells showed the opposite effect. At both cell cycle stages, Cdc14

release appeared to be accelerated or upregulated in *CLB1-NLS$_2$-HA$_6$* cells. An alternative explanation is that cytoplasmic Clb1 is required for onset of anaphase I. Combined with the effect of the localisation mutants on the sporulation efficiency on the FEAR mutants, the above results imply that increased nuclear concentration of Clb1 leads to accelerated and increased Cdc14 release.

5.5.2.5 Effect of altering Clb1 nuclear localisation on Net1 phosphorylation in a *P$_{CLB2}$CDC55 P$_{CLB2}$CDC20* background

An increase in FEAR activation could be indicated in an increase in Net1 phosphorylation, as well as an increase in nucleolar separation. To examine the effects of Clb1 localisation on Cdc14 release, cultures of *P$_{CLB2}$CDC20* cells, and *P$_{CLB2}$CDC20 P$_{CLB2}$CDC55* cells bearing one of *CLB1, CLB1-HA, CLB1-NES$_2$-HA,* or *CLB1-NLS$_2$-HA,* were induced to undergo meiosis by resuspension in sporulation media. Samples were taken hourly for whole cell analysis and for immunofluorescence analysis.

Net1 is phosphorylated by CDK and Cdc5 and dephosphorylated by PP2A^{Cdc55}, whose activity is downregulated during FEAR activation. This phosphorylation is strongly detectable by gel shift in *P$_{CLB2}$CDC20 P$_{CLB2}$CDC55* cultures, but is depleted in the *P$_{CLB2}$CDC20* cultures as PP2A^{Cdc55} remains active (Kerr et al., 2011). The effect of Clb1 localisation on phosphorylation of Net1 was examined in *P$_{CLB2}$CDC20 P$_{CLB2}$CDC55* strains, as PP2A^{Cdc55} would counter CDK activity in *P$_{CLB2}$CDC20* cells. As Cdc55 is depleted in these cells, the final extent of Net1 phosphorylation would be unlikely to change. However, there may be discernable differences in timing of the phosphorylation of Net1 as detected by the gel shift of Net1.

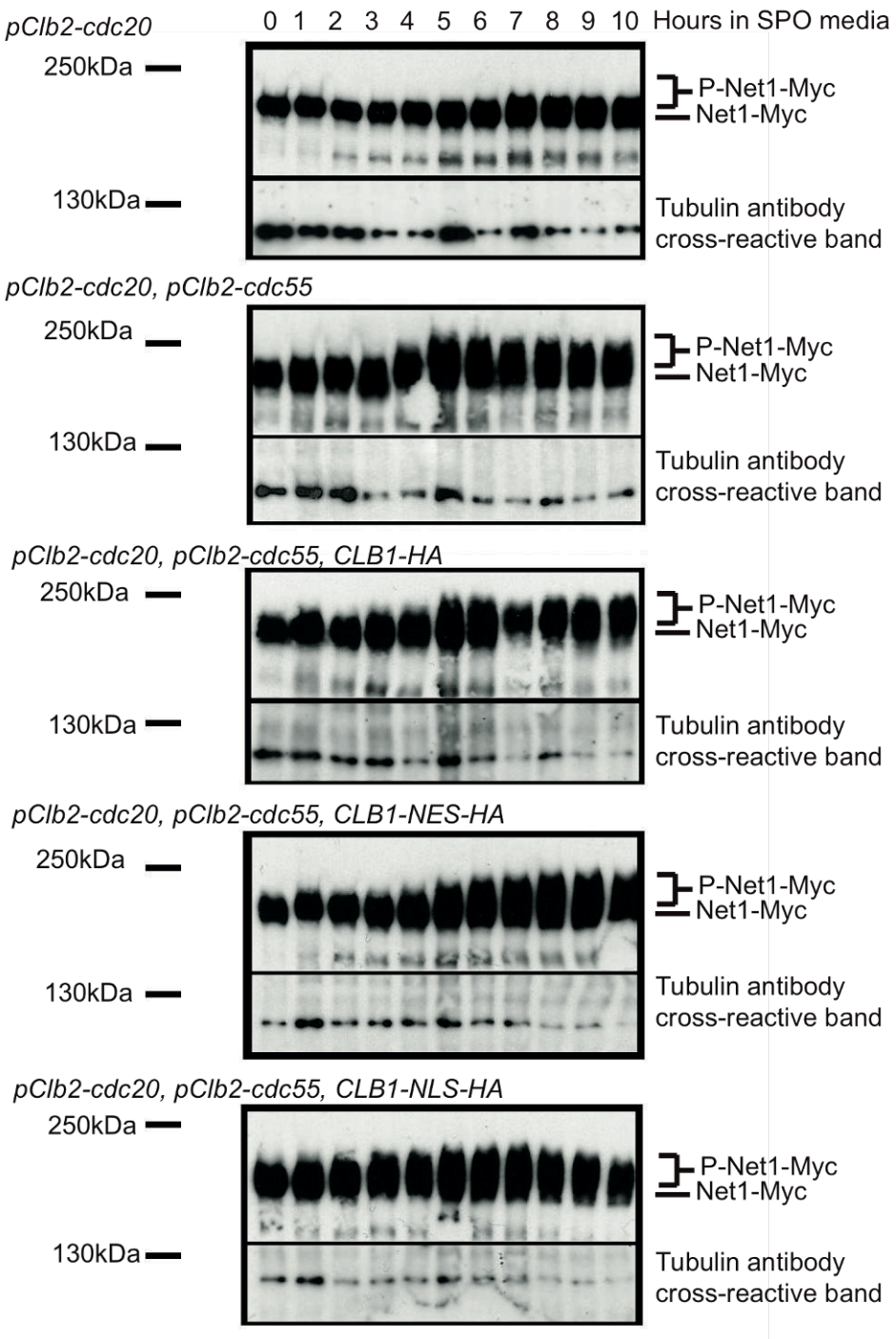

Figure 5-31 ***Net1 gel mobility in Clb1 localisation mutant strains in*** $\mathbf{P_{CLB2}}$**CDC20** $\mathbf{P_{CLB2}}$**CDC55** ***background.*** *Cultures of* P_{CLB2}*CDC20* P_{CLB2}*CDC55, and* P_{CLB2}*CDC20 cells and cultures of cells bearing CLB1-NLS*$_2$*-HA, CLB1-HA and CLB1-NES*$_2$*-HA in a* P_{CLB2}*CDC20* P_{CLB2}*CDC55 background were induced to enter sporulation by resuspension in sporulation media. Net1 phosphorylation in assayed by subjecting whole cell extracts to SDS-PAGE followed by western blot analysis using anti-ha. Blots were also probed with anti-tubulin.*

The results in Figure 5-31 reiterated the finding that $P_{CLB2}CDC20$ strains had reduced Net1 phosphorylation, as shown by a smaller gel shift, and that $P_{CLB2}CDC20$ $P_{CLB2}CDC55$ strains demonstrated a sustained Net1 phosphorylation.

P_{CLB2}CDC20 P_{CLB2}CDC55 Clb1-HA$_6$ showed similar Net1 phosphorylation to the *P_{CLB2}CDC20 P_{CLB2}CDC55* strain, confirming the HA tag did not affect Net phosphorylation. On comparing *P_{CLB2}CDC20 P_{CLB2}CDC55 CLB1-HA$_6$* and *P_{CLB2}CDC20 P_{CLB2}CDC55 CLB1-NES$_2$-HA$_6$*, a slight delay of between 1 and 2 hours in achieving the full phosphorylation was observed, turning the step-like change into a graduation. This delay was similar to that seen in the progress of *CLB1-NES$_2$-HA$_6$* strains undergoing wild-type meiosis (5.5.2.1).

The *P_{CLB2}CDC20 P_{CLB2}CDC55 CLB1-NLS$_2$-HA$_6$* culture appeared to show initial Net1 smearing from T0 and achieved similar extent of phosphorylation of Net1, again without the step-like change in mobility. However, if the early Net1 phosphorylation effect was true, it was observable before the time that Clb1 expression was detectable in other time-courses. The effect could possibly be due to a long-lasting result of mitotic nuclear Clb1, or due to the earliest expression in the fastest cells to enter meiosis. Expressing the nuclear localization mutant alleles of *CLB1* from a mitosis-specific promoter like *CLB2* could test this possibility. The samples from *P_{CLB2}CDC20 P_{CLB2}CDC55 CLB1-NLS$_2$-HA$_6$* cultures showed a decline in Net1 phosphorylation in later time-points. This probably reflected accumulation of dead cells. *P_{CLB2}CDC20 P_{CLB2}CDC55 CLB1-NLS$_2$-HA$_6$* cultures undergoing meiosis consistently accumulated dead cells faster than in any other strain used in this experiment.

The minor difference in timing of apparent Net phosphorylation was small compared to the variability of unsynchronised time course data. To summarise, it was not possible to draw a conclusion on the effect of Clb1 localisation on FEAR release from the gel shift of Net1.

5.5.2.6 Effect of altering Clb1 nuclear localisation on Cdc14 release in a *P_{CLB2}CDC55 P_{CLB2}CDC20* background

Nucleolar (Nop1) dot separation was used previously as a marker for Cdc14 release, as Cdc14 release is difficult to detect in meiosis I. Nop1 dot separation was analysed in the aforementioned strains.

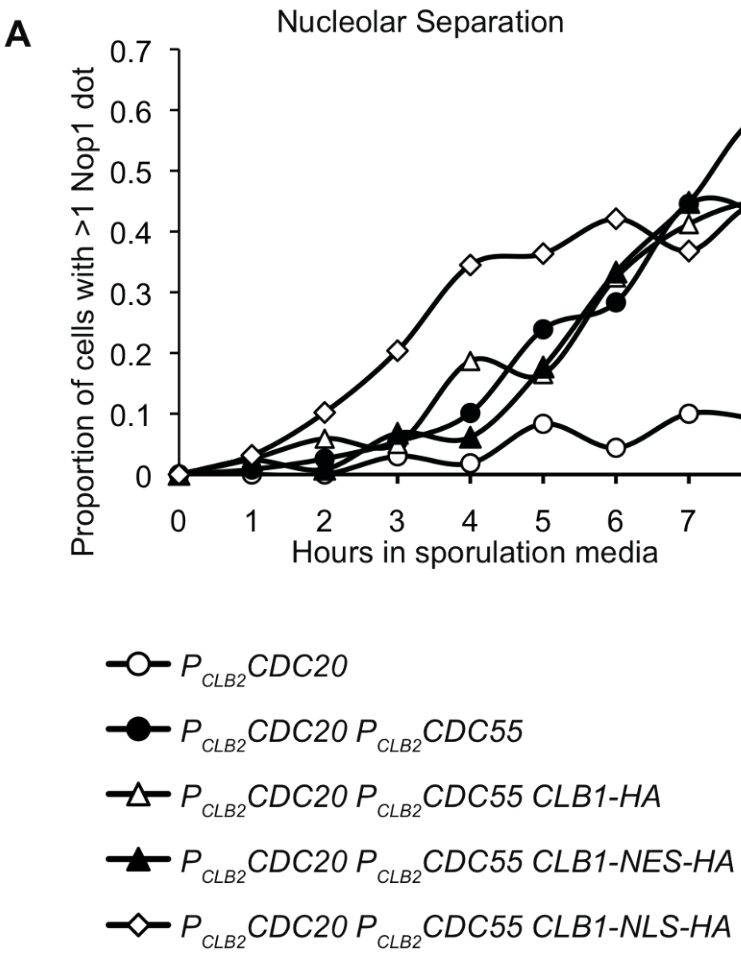

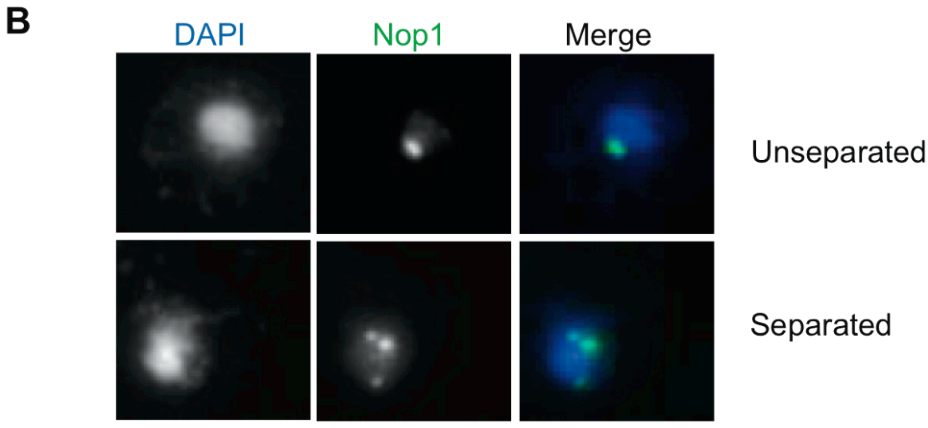

Figure 5-32 ***Nucleolar separation in Clb1 localisation mutant strains in*** **P_{CLB2}CDC20 P_{CLB2}CDC55** ***background.*** *Cultures of* P_{CLB2}CDC20 P_{CLB2}CDC55, *and* P_{CLB2}CDC20 *cells and cultures of cells bearing* CLB1-NLS_2-HA, CLB1-HA *and* CLB1-NES_2-HA *in a* P_{CLB2}CDC20 P_{CLB2}CDC55 *background were induced to enter sporulation by resuspension in sporulation media. Cells were fixed and examined for Cdc14 release and Nop1 separation by in situ immunofluorescence.*

In all three measures in the $P_{CLB2}CDC20\ P_{CLB2}CDC55$ background, the effect of $CLB1\text{-}NLS_2\text{-}HA_6$ occurred before Clb1 was detectable in western blots. This

could be caused by *CLB1-NLS$_2$-HA$_6$* expression in the preceding mitotic cycle. Alternatively, it could be due to initial expression of Clb1 to an extent too low to be detected by western blots, due to a small proportion of cells progressing more rapidly. With Cdc55 depleted, initial Clb1 expression would not be countered by PP2A and could initiate Cdc14 release immediately. Nuclear import of Clb1 may thus control the timing of Cdc14 release in meiosis I.

5.6 Summary

The first model introduced in this chapter does not incorporate Clb1 phosphorylation. Instead, Model 5 (Section 5.1) considers the possibility that Cdc14 nuclear retention during meiosis I prevents complete exit from meiosis. This model predicts that the cell may not enter the second division, should sufficient Cdc14 export be induced during meiosis I. Experiments in altering Cdc14 release in meiosis are recounted in Chapter 6.

Model 5 suggested the possibility of examining the Clb/Cdc14 ratios of the two compartments, nucleus and cytoplasm, separately. This was done in Model 6 (Section 5.2), in which the effects of localisation mutants on the kinase/phosphatase ratio were investigated, in anticipation of the work in Chapter 5. Clb1 nuclear localisation was proposed to increase the rate of FEAR release of Cdc14. Therefore, regulation of Clb1 localisation could play a role in altering the activation of FEAR, relative to cyclin levels. The model predicted that increased Clb1 import would increase the rate of progress through meiosis, speeding up both divisions, while decreased Clb1 export would have the opposite effect. We examined this by altering the localisation of Clb1 using ectopic NLS or NES sites.

Efficient nuclear import of Clb1 during meiosis was not necessary for successful meiosis. Cells with constitutive nuclear, or cytoplasmic, localisation of Clb1 underwent meiosis with similar efficiency to wild type. Enforced nuclear localisation of Clb1 accelerated entry into meiosis I and spindle elongation, as *CLB1-NLS$_2$-HA$_6$* cells accumulated binucleate cells at a faster rate than wild type. Entry into meiosis II was not similarly accelerated. However, it is hard to be certain due to asynchrony in the cultures. More information could be gained by looking at these localisation mutants in synchronised cultures, such as those

described in the Appendix Section 9.3.2. Decreased nuclear localisation delayed both meiosis I and meiosis II divisions. The model predicted that increased nuclear localisation of Clb1 would lead to accelerated divisions and decreased nuclear localisation would lead to decelerated nuclear divisions. This was seen in the experiments with the difference that the second division was not accelerated by increased nuclear localisation of Clb1.

Genotype	Phenotype
CLB1-HA	Sporulation efficiency is not significantly different from wild type Clb1.
CLB1-NLS$_2$-HA	Accelerated meiosis I.
CLB1-NES$_2$-HA	No phosphorylation of Clb1.
clb3Δ, clb4Δ, CLB1-HA	Sporulation efficiency is not significantly different from wild type Clb1.
clb3Δ, clb4Δ, CLB1-NLS$_2$-HA	Sporulation efficiency severely reduced.
clb3Δ, clb4Δ, CLB1-NES$_2$-HA	Sporulation efficiency severely reduced.
spo12Δ, CLB1-HA	Formation of monads and dyads only.
spo12Δ, CLB1-NLS$_2$-HA	Formation of monads, dyads and a few tetrads.
spo12Δ, CLB1-NES$_2$-HA	Formation of monads and dyads.
esp1-2, CLB1-HA	Sporulation efficiency not significantly different from wild type
esp1-2, CLB1-NLS$_2$-HA	Sporulation efficiency slightly improved – tetrads increased, dyads decreased
esp1-2, CLB1-NES$_2$-HA	Sporulation efficiency strongly decreased – almost no tetrad production

Table 5-5 ***Summary of phenotypes.*** *Genotypes covered in this chapter and associated phenotypes.*

The above results suggest that nuclear import of Clb1 both amplifies and accelerates Cdc14 release during meiosis I. The genetic interaction of the localisation alleles of Clb1 with the FEAR mutants, and the increased separation of nucleolar dots, suggest that increased nuclear localisation of Clb1 leads to increased Cdc14 release. FEAR activation in the *P_{CLB2}CDC20 P_{CLB2}CDC55* background and the timing of the nuclear divisions in the otherwise wild type background, also seem to suggest that FEAR activation occurs earlier in strains with increased nuclear Clb1.

Localisation of Clb1 to the nucleus would increase CDK activity around the targets that initiate FEAR activation, and increase access to the nucleolar protein Net1. Increased FEAR activation and increased Net1 phosphorylation

would result in a greater release of Cdc14. The extra Cdc14 phosphatase released would initially be opposing a high CDK activity background. Clb1 export around anaphase would decrease CDK activity and help the CDK/Cdc14 ratio to drop sufficiently to allow mitotic spindle disassembly.

6 Cdc14 release during meiosis I

6.1 Activation of MEN during meiosis

At the end of mitosis, two regulatory networks manage the Cdc14 release that triggers the sharp decline in CDK activity, required for mitotic exit; FEAR (Cdc14 early anaphase release) and MEN (mitotic exit network) (Dumitrescu and Saunders, 2002). The FEAR network alone is not sufficient to allow mitotic exit (Bardin and Amon, 2001). Cdc14 release is transient, and insufficient to cause spindle disassembly. MEN initiates the CDK inhibitors that stabilise the G1 state. During meiosis, the FEAR network alone is sufficient for spindle disassembly and exit from meiosis I (Kamieniecki et al., 2005; Stern, 2003).

A further consideration is that the drop in CDK activity, which happens during mitotic exit, allows DNA replication origins to be relicensed for the next round of DNA replication (Dahmann et al., 1995; Diffley, 2004). Also, if CDK activity drops sufficiently, and the CDK inhibitors become active, the balance between these two could cross the threshold of the bistable system (Lopez-Aviles et al., 2009; Novak et al., 2007), and the system could return to the low CDK stable state. During exit from meiosis I, the FEAR induced drop in CDK activity must be carefully balanced to allow the spindle to disassemble, but not to allow relicensing of replication origins or to trigger the system to switch states.

Ime2, the meiosis specific kinase, is active during the meiotic divisions and has overlapping substrate specificity to CDK (Holt et al., 2007). Ime2 phosphorylation consensus sites are resistant to Cdc14 dephosphorylation, unlike CDK consensus sites (Holt et al., 2007), which may prevent the relicensing of replication origins and activation of CKIs. Many CDK substrates have Ime2 sites, including Sic1 (Sedgwick et al., 2006), Cdh1 (Bolte et al., 2002) and

replication proteins (Clifford et al., 2004). If Cdc14 release is amplified during meiosis I, Ime2 phosphorylation of certain substrates could maintain their phosphorylation during decreasing CDK activity. Ime2 would keep the phosphorylation/phosphatase ratio high on the overlapping substrates. This would require that Ime2 phosphorylation has the same effect as CDK phosphorylation on the substrate, but this is not necessarily the case (Sedgwick et al., 2006).

MEN is involved in exit from meiosis II (Attner and Amon, 2012) but not in meiosis I (Kamieniecki et al., 2005). MEN components and even Cdc14 nuclear export are dispensable for both divisions, and Cdc15 is required for spore genesis rather than its role in the MEN (Pablo-Hernando et al., 2007). However, MEN is active in its role in triggering Cdc14 export and seems to be involved in regulating the timing of meiosis II (Attner and Amon, 2012). This raises the question as to whether MEN activation in meiosis I would lead to an increased release of Cdc14. If so, would increased Cdc14 release lead to complete meiotic exit and formation of dyads, or to the re-initiation of DNA replication?

6.1.1 Expression of cdc15-7A-HA$_3$

MEN activation in meiosis I was first attempted by expression of *cdc15-7A-HA$_3$* under the *GAL1-10* promoter. Cdc15 is repressed by high CDK activity by phosphorylation (Jaspersen and Morgan, 2000). Cdc15-7A-HA$_3$ has the repressive CDK phosphorylation sites converted to alanine, and is resistant to CDK inhibition and therefore constitutively active. Cells expressing Cdc15-7A-HA$_3$ under the Gal promoter are viable and capable of completing mitosis even if MEN genes are mutated (Jaspersen and Morgan, 2000). In our strains, expression of *cdc15-7A-HA$_3$* is driven by the P$_{GPD1}$GAL4-ER /P$_{GAL}$ system (Benjamin et al., 2003), triggered by the addition of estradiol to the sporulation media.

A plasmid bearing *cdc15-7A-HA$_3$* under the *GAL1-10* promoter was obtained as a gift from Prof. Morgan (UCSF, California). The allele was integrated at the *TRP1* locus in the wild-type strain, and then introduced into a strain expressing *P$_{GPD1}$GAL4-ER* by crossing the strains. A strain bearing only *P$_{GPD1}$GAL4-ER* was used as a negative control. Expression of Cdc15-7A-HA$_3$ was tracked in a meiotic culture. Results are shown for addition of estradiol to 1μM at

5 hours after resuspension in potassium acetate (Figure 6-1). Background expression was undetectable in uninduced cultures, and cultures of the *P_{GPD1}GAL4-ER* strain showed no detectable expression. Cdc15-7A-HA$_3$ was detectable at two hours after induction.

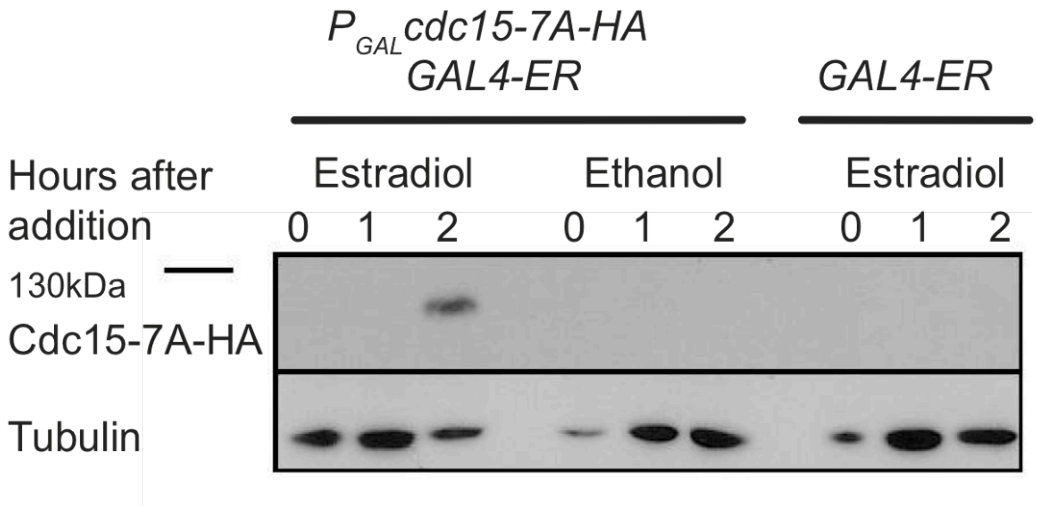

Figure 6-1 ***Induced Cdc15 expression.*** *Cultures of cells bearing* P_{GPD1}GAL4-ER P_{GAL}cdc15-7A-HA$_3$ *or* P_{GPD1}GAL4-ER *were induced to enter meiosis by resuspension in sporulation media (SPO media). Cultures were induced with 1μM estradiol, or 0.2μL of the solvent, ethanol, per ml of culture at 5 hours into SPO media. Presence of Cdc15-7A-HA$_3$ was assayed by subjecting whole cell extracts to SDS-PAGE followed by western blot analysis using anti-HA antibody. Blots were also probed with anti-tubulin.*

The meiotic culture was stressed by nutrient deprivation, and presumably had fewer resources to expend on protein production, so the delay was explicable. The results indicate that Cdc15-7A-HA$_3$ was expressed between 1 and 2 hours after induction in meiotic cultures. Cdc15-7A-HA was not placed under the Cdc15 promoter so endogenous expression levels were not available for comparison.

6.1.2 Effects of Cdc15-7A-HA$_3$ expression

A strain bearing *P_{GAL}cdc15-7A-HA$_3$ P_{GPD1}GAL4-ER* was tested to determine the effect of Cdc15 activation in meiosis I. The cells were resuspended in sporulation media. Expression of Cdc15-7A-HA$_3$ was induced at 5, 6 and 7 hours after resuspension in sporulation media, by addition of 1μM estradiol. Samples were taken half-hourly to follow nuclear divisions.

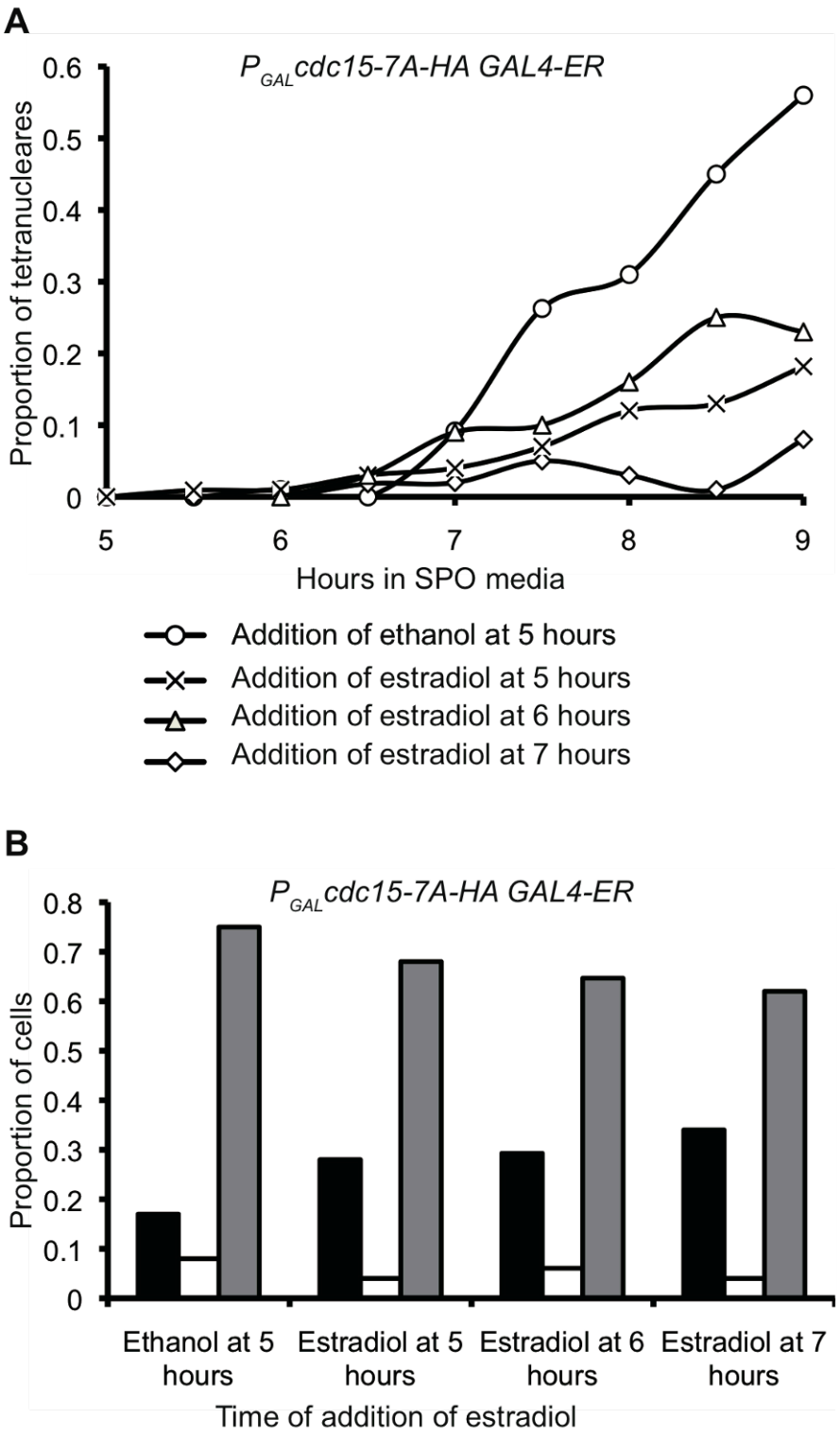

Figure 6-2 ***cdc15-7A-HA expression delays tetranucleate formation in a 9 hour time course.*** P_{GPD1}GAL4-ER P_{GAL}cdc15-7A-HA_3 *cells were induced to enter meiosis by resuspension in sporulation media (SPO media) and induced by induced by estradiol as described.* **A:** *Samples were taken for in situ immunofluorescence every half hour and nuclear division was scored by DAPI staining. 100 cells were scored at each time point.* ***B:*** *After 22 hours, the percentage of cells forming dyads, tetrads and monads were calculated. 100 cells were counted for each culture. Differences in sporulation*

efficiency between the mock addition culture and the treatment cultures were found insignificant (p>0.05) using Mann Whitney U test.

Estradiol expression reduced the number of tetranucleate cells produced in the 9-hour period (Figure 6-2 A). Earlier addition of estradiol caused a greater effect. However, the cultures were examined for tetrad formation after 22 hours and little difference was seen (Figure 6-2 B). A slight increase in mononucleates was seen with *cdc15-7A-HA$_3$* expression, with a concomitant decrease in tetranucleates. However, this was not strongly affected by the timing of Cdc15-7A-HA$_3$ expression and may have reflected the effect of Cdc15-7A-HA$_3$ overexpression on spore formation, in which Cdc15 is involved (Pablo-Hernando et al., 2007). Therefore, the Cdc15-7A-HA$_3$ expression appeared to delay, but not prevent, completion of meiosis, nor did it alter the final proportion of tetrads.

To examine the delay further, the experiment was repeated with hourly sample taking over a longer duration. The strain bearing *P$_{GPD1}$GAL4-ER,* but not *P$_{GAL}$cdc15-7A-HA$_3$* was included as a control. Cultures of *P$_{GPD1}$GAL4-ER P$_{GAL}$cdc15-7A-HA$_3$* and *P$_{GPD1}$GAL4-ER* cells were induced to enter meiosis by resuspension in SPO media. Aliquots of cultures of each strain were taken from the uninduced master cultures at 5, 6 and 7 hours into sporulation and 1μM estradiol or an equivalent volume of the solvent, ethanol, was added (Figure 6-3).

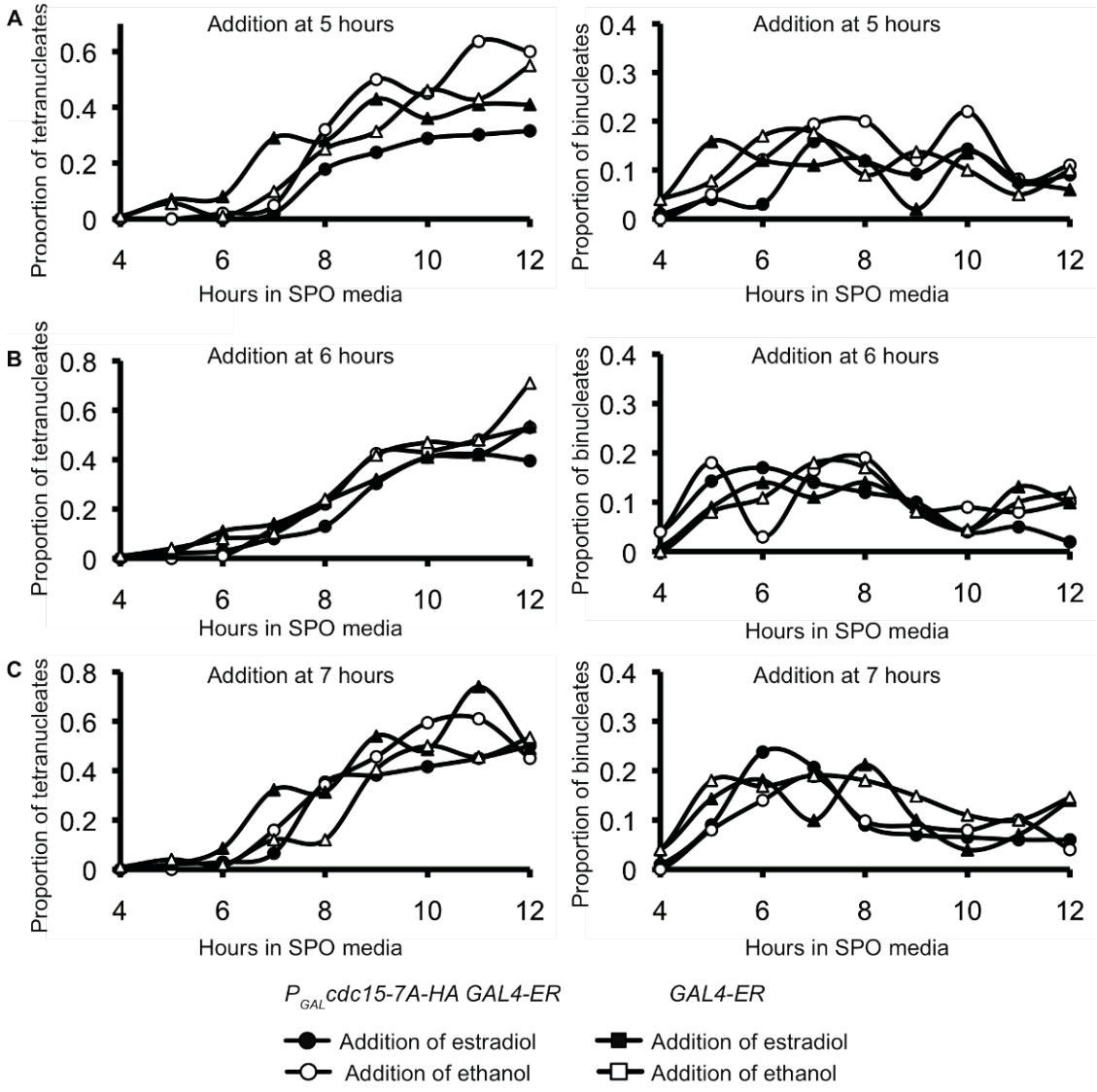

Figure 6-3 ***cdc15-7A-HA expression reduces tetranucleate formation in a 12 hour time course.*** *Cultures of P_{GPD1}GAL4-ER, P_{GAL}cdc15-7A-HA$_3$ cells and P_{GPD1}GAL4-ER cells were induced to enter meiosis by resuspension in SPO media and induced by estradiol induced by estradiol or mock induced by ethanol at (**A**) 5 (**B**) 6 or (**C**) 7 hours into sporulation media. Samples were taken for in situ immunofluorescence hourly and nuclear division was scored by DAPI staining. Tetranucleates (left) and binucleates (right) are shown. 100 cells were scored at each time point.*

Ectopic expression of *cdc15-7A-HA$_3$* in meiosis I caused a minor delay in the completion of meiosis, as measured by the production of tetranucleate cells (Figure 6-3). Addition of estradiol at 5 hours showed an effect on the formation of tetranucleates: tetranucleate production was decreased compared to ethanol addition or estradiol addition to the control *P_{GPD1}GAL4-ER* strain (Figure 6-3 A). In addition, the delay started between 1 and 2 hours after induction, in compliance with the above data on expression of *cdc15-7A-HA$_3$* during meiosis

(Figure 6-1). Addition of estradiol to the P_{GPD1}*GAL4-ER* strain did not affect the formation of tetranucleates. This delay was dependent on *cdc15-7A-HA* expression.

The delay may be explicable if Cdc15-7A-HA$_3$ production increased Cdc14 release in meiosis I. The cells may take longer to increase CDK activity sufficiently to enter meiosis II. However, Cdc14 release is difficult to assay in fixed meiotic cells (Kerr et al., 2011). Cdc14 release could have been examined indirectly by looking at nucleolar dot separation. However, we aimed to determine the stage of meiosis in which the delay occurred, before or between the divisions. The proportion of binucleate cells was examined (Figure 6-3). The results indicated a lack of synchrony in the cultures, as binucleate cells did not produce a single clear peak in each culture. However, in the culture at which estradiol was added at 5 hours, the level of binucleates rose later than in the uninduced cultures. This may indicate that the delay to meiosis caused by expression of Cdc15-7A-HA$_3$ occurred before anaphase of meiosis I.

The results may indicate a return-to-growth response to the induction of the Gal promoter. However, the delay is specific to the strain bearing P_{GAL}*CDC15-7A-HA* and the final proportion of tetranucleates is not strongly affected, indicating that cells continue to complete meiosis. Earlier expression of *cdc15-7A-HA*$_3$ may have induced release of Cdc14 and delayed entry into meiosis. Released Cdc14 would make it harder for the Clb-CDK to achieve a sufficient CDK/Cdc14 ratio for meiosis I compared to uninduced cells. This is supported by the fact that earlier expression had the greater effect. The earlier the Cdc15-7A-HA$_3$ expression occurred, the fewer cells would have passed the point at which ectopic Cdc15-7A-HA$_3$ could no longer delay them, leading to a greater effect when totalled over the population. This explanation also accounts for the initial appearance of the tetranucleates not being delayed. The earliest tetranucleates would result from the earliest cells to enter meiosis. These cells would have entered meiosis rapidly, and could have already passed the point at which the program would be delayed by Cdc15-7A-HA$_3$ expression. A more optimal experiment to determine this would be to use synchronous cultures, in which Ndt80 is under the control of another inducible promoter, such as P_{CUP1}*NDT80* strains (Sopko et al., 2002). Forcing expression of Ndt80 with synchronised

strains could also limit the possibility of a return to growth effect (Winter, 2012). However, expression of Cdc15-7A-HA_3 did not affect the proportion of tetrads and dyads produced after 22 hours in SPO media, and the effect on timing of entry to meiosis was small. Therefore this experiment was not pursued further.

Cdc15-7A-HA_3 expression is unable to affect the timing of progress through the meiotic divisions, which suggested that the MEN was inhibited during meiosis, and in a manner independent of Cdc15 phosphorylation. Since this work, Attner *et al.* (Attner and Amon, 2012) examined the regulation of MEN in meiosis. They confirmed that MEN was activated in meiosis II. They found a lack of dependence of activation on the localisation of MEN components to the SPB, contrary to mitosis in which this is a prerequisite (Bardin et al., 2000). They, similarly, could not cause MEN activation during meiosis I.

6.2 Ectopic Cdc14 release in meiosis I

cdc15-7A-HA expression would be insufficient to trigger Cdc14 release, if the MEN is repressed or if downstream proteins were absent in meiosis I. We considered expressing downstream proteins during meiosis. Since then, the results of Attner *et al* (Attner and Amon, 2012) have suggested that would have been unsuccessful. As the Mitotic Exit Network seemed to be resistant to activation in meiosis I, we considered ways of causing Cdc14 release more directly in meiosis I. For this purpose, we considered a number of mutants.

CDC14-TAB6 is an allele of *CDC14*, which rescues the telophase arrest caused by MEN defect (Shou et al., 2001). This suggests the allele could compensate the inability of MEN to become active in meiosis I. *CDC14-TAB6* has a point mutation which reduces the Cdc14-Net1 interaction (Shou et al., 2001).

6.2.1 Cdc14-TAB6 expression

CDC14-TAB6 was expressed under the galactose promoter using the same induction method as *cdc15-7A-*HA_3. Strains bearing P_{GAL}*CDC14-TAB6* P_{GPD1}*GAL4-ER* and P_{GPD1}*GAL4-ER* were induced to enter meiosis by resuspension in SPO media, and expression of *CDC14-TAB6* was induced by addition of 1μM estradiol at 5, 6 and 7 hours into SPO media. Samples were taken hourly through meiosis for analysis of the fixed cells by DAPI staining and immunofluorescent imaging.

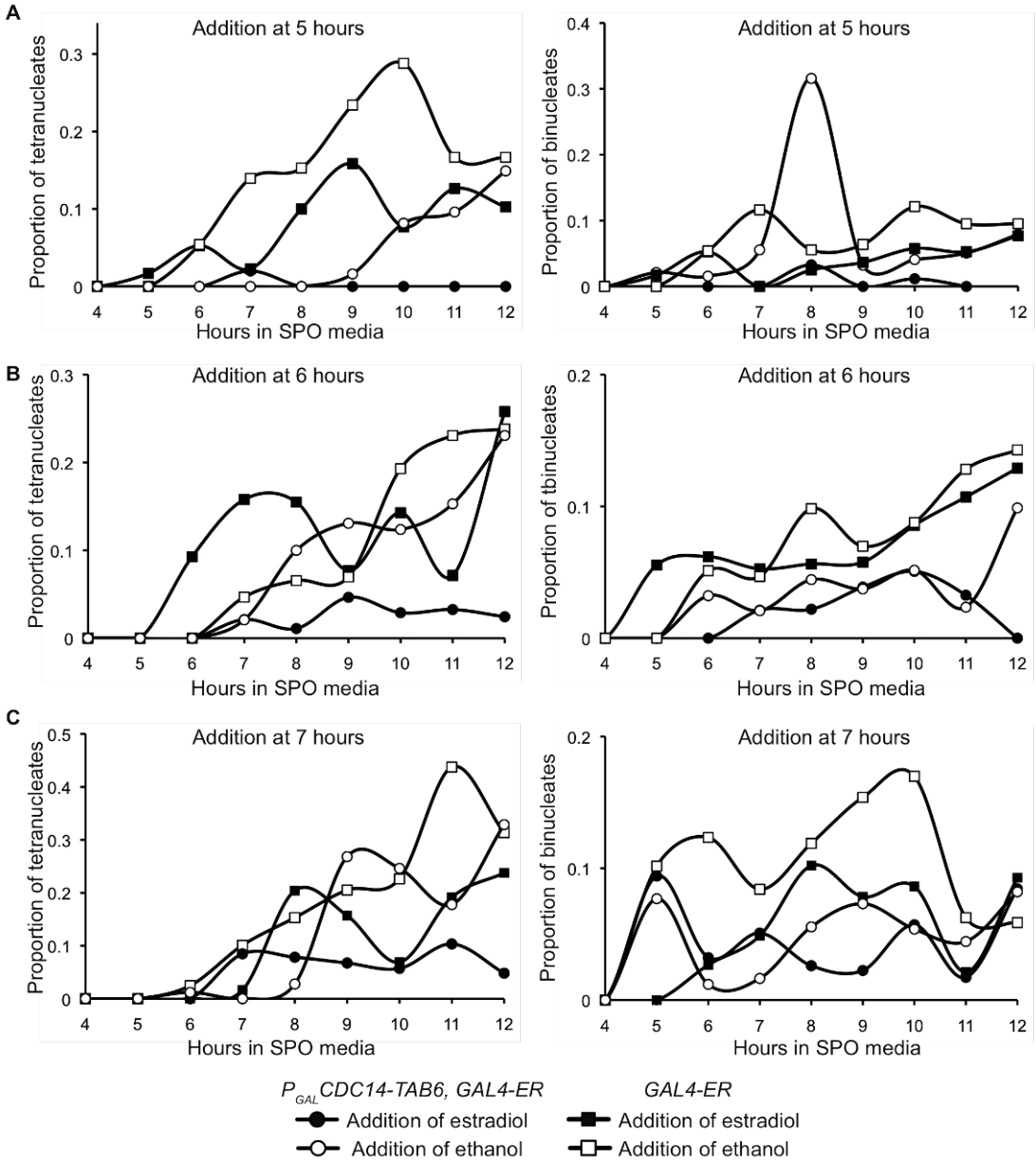

Figure 6-4 ***Effect of expression of Cdc14-Tab6 on nuclear division in a 12 hour time course.*** *Cultures of P_{GAL}CDC14-TAB6 P_{GPD1}GAL4-ER and P_{GPD1}GAL4-ER cells were induced to enter meiosis by resuspension in SPO media and induced by estradiol or mock induced by ethanol at (a) 5 (b) 6 or (c) 7 hours into sporulation media. Samples were taken for in situ immunofluorescence hourly and nuclear division was scored by DAPI staining. 100 cells are counted for each time point.*

Presence of the *CDC14-TAB6* gene under the Gal promoter led to a slight decrease in tetranucleate production over 12 hours (Figure 6-4, circular markers) compared to the P_{GPD1}*GAL4-ER* control strain (Figure 6-4, square markers). This decrease occurred independently of the presence of estradiol. P_{GAL} is known to be expressed at a low level under meiotic conditions, even in the absence of induction (Kaback and Feldberg, 1985), which may explain this result. Addition of the estradiol led to a clearer reduction in tetranucleate production

over a 12-hour time course (Figure 6-4, filled circular markers). Addition of estradiol to the control strain led to a less severe reduction in tetranucleate production apparent in the 5 and 7 hour additions (Figure 6-4, filled square markers). This may be a return-to-growth response to Gal induction. Binucleates were also counted over the 12 hour time course (Figure 6-4). Binucleate cells were highly variable, so an effect is hard to determine. The *GAL4-ER* P_{GAL}*CDC14-TAB6* strain appeared to have lower binucleate counts at all stages compared to the *GAL4-ER* strain. As this effect was also independent of estradiol addition, it may be due to the low level expression from the P_{GAL} promoter in meiosis.

We found Cdc14 release in meiosis I difficult to assess using immunofluorescent imaging. The results were not easily decipherable. A slight increase in apparent Cdc14 release in some induced samples could be detected, but could not be construed as significant, given the high variation in both induced and non-induced samples (Figure 6-5).

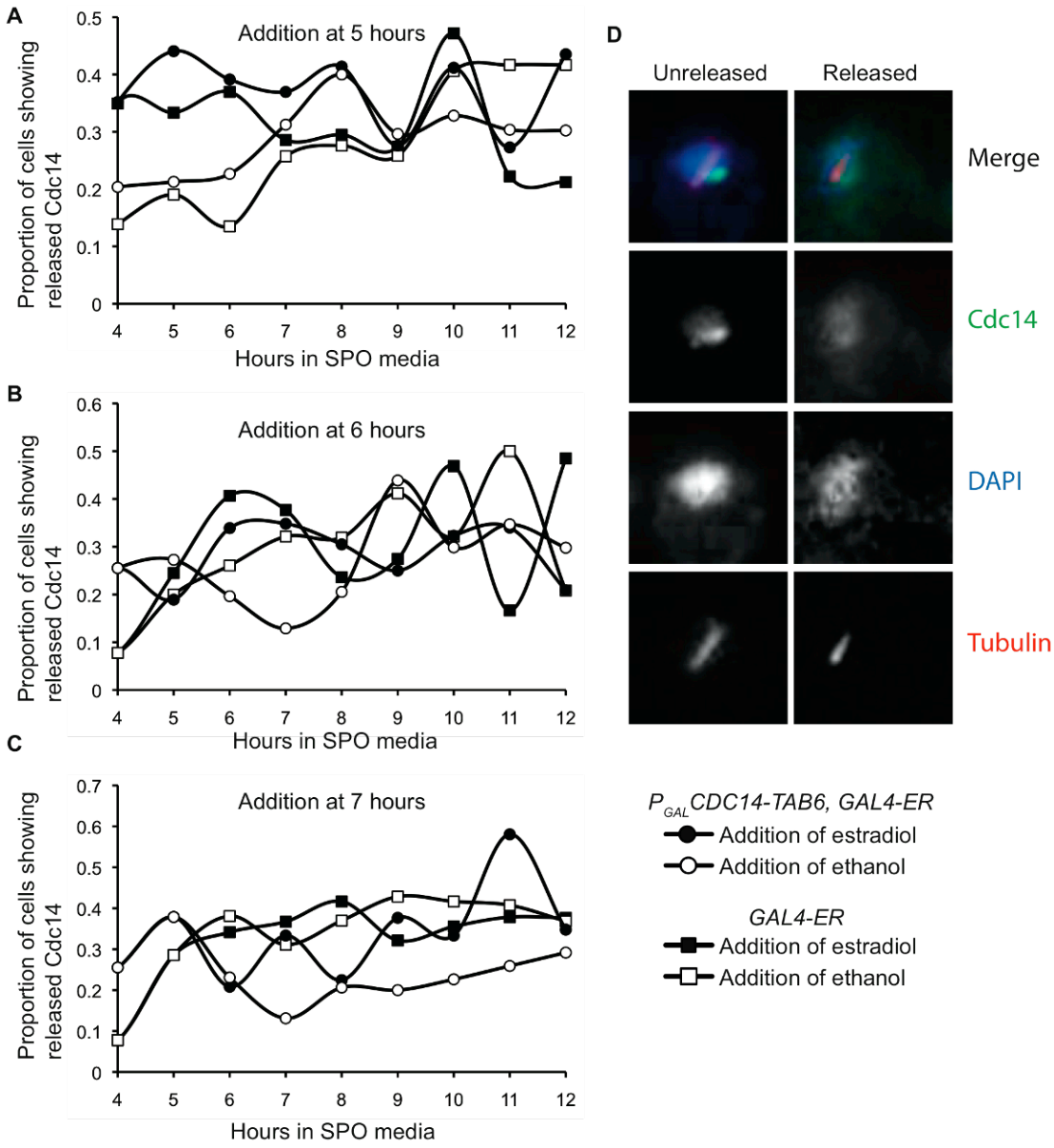

Figure 6-5 ***Effect of expression of Cdc14-Tab6 on Cdc14 release in a 12 hour time course.*** *Cultures of P_{GAL}CDC14-TAB6 P_{GPD1}GAL4-ER and P_{GPD1}GAL4-ER cells were induced to enter meiosis by resuspension in SPO media and induced by estradiol as described. Cells were fixed and examined for Cdc14 localisation by in situ immunofluorescence. 100 cells were counted in each time point.*

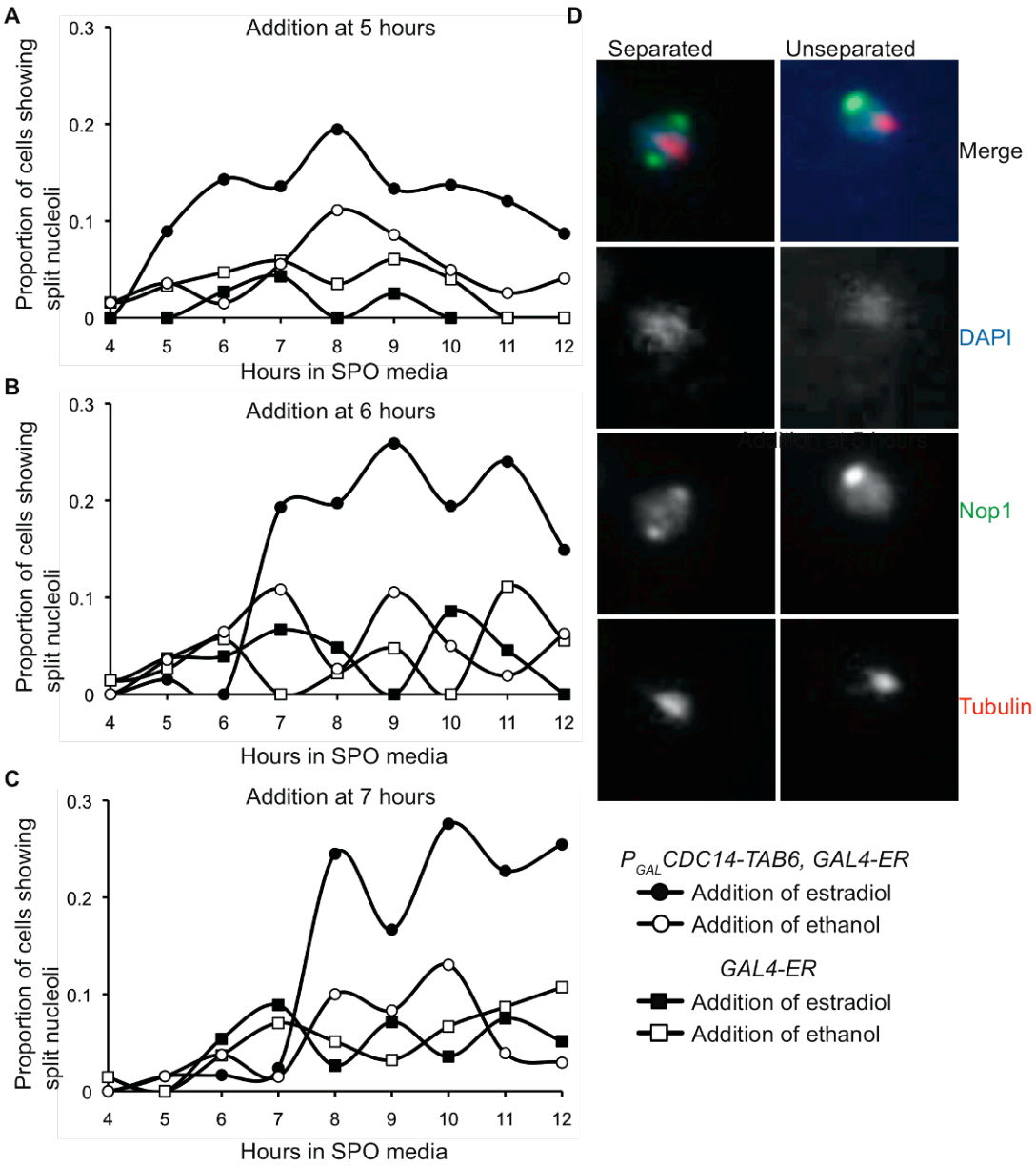

Figure 6-6 ***Effect of Cdc14Tab6 expression on Nop1*** *Cultures of P_{GAL}CDC14-TAB6 P_{GPD1}GAL4-ER and P_{GPD1}GAL4-ER cells were induced to enter meiosis by resuspension in SPO media and induced by estradiol as described. Cells were fixed and examined for Nop1 separation by in situ immunofluorescence. 100 cells were counted in each time point.*

Examination of the cultures after 22 hours into SPO media showed that, in this case, the effect of induction was not simply a delay. The 22-hour cultures showed a strong reduction in completed tetrads in response to *CDC14-TAB6* expression.

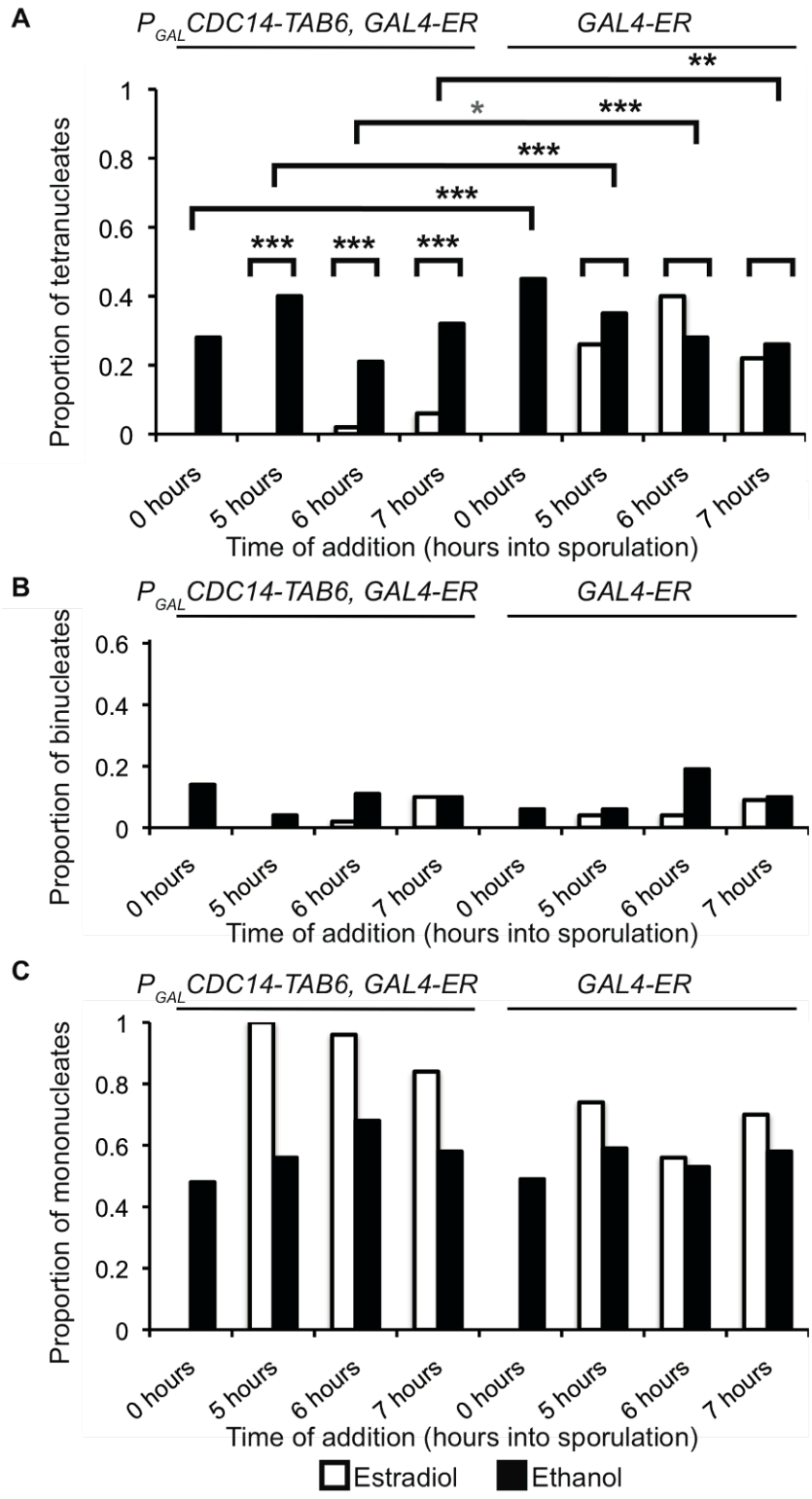

Figure 6-7 ***Effect of Cdc14-Tab6 expression on tetranucleate production.*** *Cultures of P_{GAL}CDC14-TAB6 P_{GPD1}GAL4-ER and P_{GPD1}GAL4-ER cells were induced to enter meiosis by resuspension in SPO media and induced by estradiol as described. After 24 hours, the proportion of cells forming tetrads (**A**), dyads (**B**) and monads (**C**) were calculated. Asterisks in upper graph show significance in difference in sporulation efficiency, calculated using Mann Whitney U test (* p<0.05, ** p<0.01, ***p<0.001). Upper brackets show comparisons between strains, for ethanol treated (grey*

asterisk) and estradiol treated (black asterisks) strains. Lower brackets show comparisons between addition and mock treatment.

The induction of Cdc14Tab6 at three different stages should have caught some cells during exit from meiosis I, in which case the ectopic Cdc14 release may have prevented entry into meiosis II and induced the production of dyads from singly-divided cells. However, none of the three induced cultures showed an increase in dyads. The loss of tetrads was matched by an increase of mononucleate cells.

This indicates that the extra Cdc14 activity from *CDC14-TAB6* induction affected the CDK activity required for progression through meiosis I. Given the difficulty in assaying Cdc14 release in these strains, we used an indirect method to confirm that the induction of *CDC14-TAB6* was increasing Cdc14 activity. We used nucleolar (Nop1) dot separation as a measure of Cdc14 release in P_{CLB2}*CDC20* strains. P_{CLB2}*CDC20* cultures undergoing meiosis do not release Cdc14, as the FEAR network is not activated. These cells arrest in metaphase I with short spindles and unseparated nucleoli. If induction of P_{GAL}*CDC14-TAB6* caused increased Cdc14 release, Nop1 separation would be observed.

P_{CLB2}*CDC20* P_{GPD1}*GAL4-ER* and P_{GAL}*CDC14-TAB6* P_{CLB2}*CDC20* P_{GPD1}*GAL4-ER* strains undergoing meiosis were examined for nucleolar (Nop1) dot separation and metaphase spindles at the 8-hour time point. At this point, the cells should be arrested in metaphase I. Figure 6-8(A) showed that around 1/3 of the cells were arrested in metaphase in the P_{CLB2}*CDC20* P_{GPD1}*GAL4-ER* cultures, and in uninduced P_{GAL}*CDC14-TAB6* P_{CLB2}*CDC20* P_{GPD1}*GAL4-ER* cultures, while estradiol-induced cultures showed much lower numbers of metaphase I spindles.

Figure 6-8 shows the proportion of split nucleoli. The proportion of split nucleoli remained low in P_{CLB2}*CDC20* P_{GPD1}*GAL4-ER* and uninduced P_{GAL}*CDC14-TAB6* P_{CLB2}*CDC20* P_{GPD1}*GAL4-ER* cultures. In P_{GAL}*CDC14-TAB6* P_{CLB2}*CDC20* P_{GPD1}*GAL4-ER* cultures induced at 4 and 6 hours, increased numbers of nucleoli were split. Nucleolar separation is indicative of Cdc14 release (Sullivan et al., 2004).

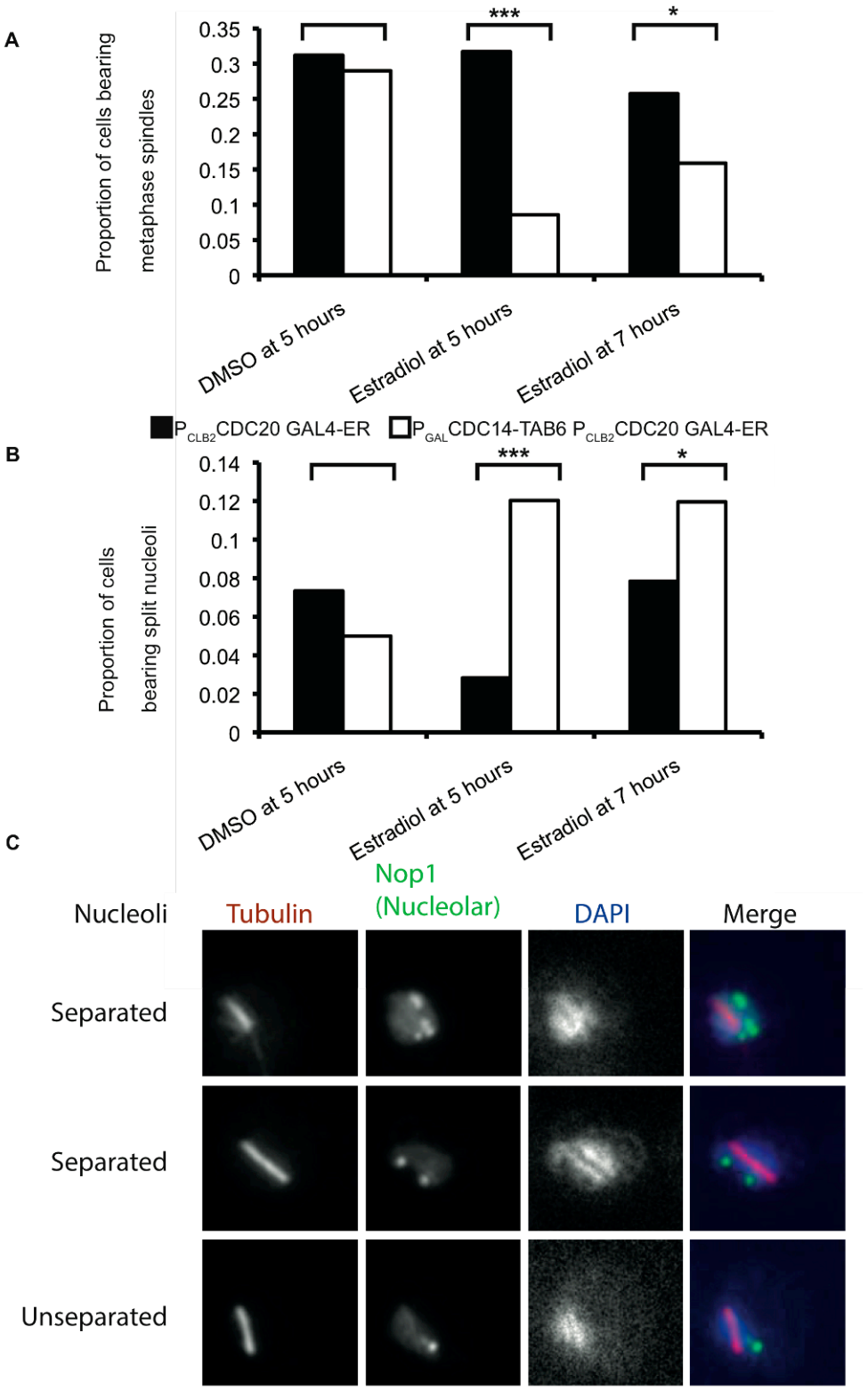

Figure 6-8 ***Nop1 separation in cultures expressing Cdc14-TAB6*** *Cultures of* P_{CLB2}CDC20 P_{GAL}CDC14-TAB6 P_{GPD1}GAL4-ER *and* P_{CLB2}CDC20 P_{GPD1}GAL4-ER *cells were induced to enter meiosis by resuspension in SPO media and induced by estradiol as described. Cells were fixed and examined by in situ immunofluorescence for the following:* ***A*** *Metaphase spindles and* ***B*** *Nop1 separation.* ***C*** *Example images of cells demonstrating separated or unseparated nucleolar dots. Asterisks show significance calculated using Chi Squared test (* p<0.05, ** p<0.01, ***p<0.005).*

6.3 Ime2 and FEAR

ime2-as is an analogue-sensitive allele of *IME2*. We found that *ime2-as*, in absence of the inhibitor, had a synthetic effect on spore formation with *net1-6CDK* (Figure 6-9, communication from Gary Kerr). This was interesting, as *net1-6CDK* encodes a mutant version of the nucleolar protein Net1, lacking 6 CDK sites (Azzam et al., 2004) and is partially defective in FEAR activation. This synthetic phenotype suggests that Ime2 contributes to the activation of FEAR in meiosis I. To investigate this relationship further, we combined *ime2-as* with two other FEAR mutants (Figure 6-9).

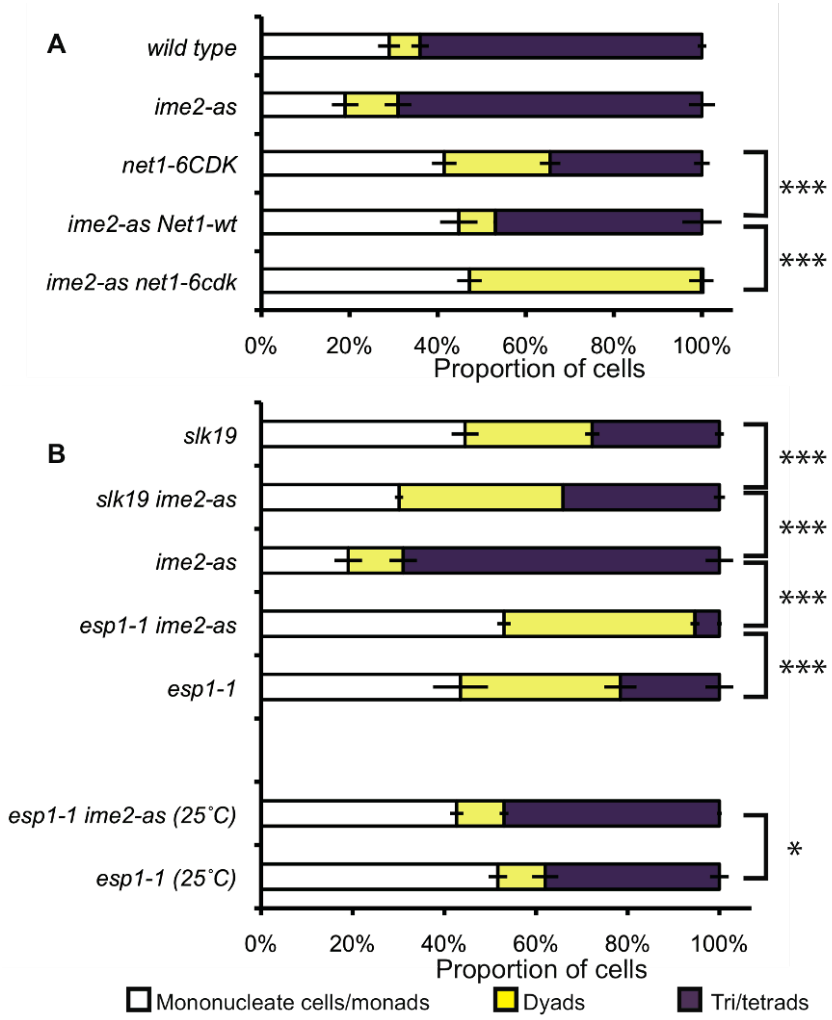

Figure 6-9 ***Interactions between ime2-as and FEAR.*** *Cells bearing the ime2-as-MYC$_9$ allele in combination with net1-6CDK, esp1-2 or slk19 or the wild type alleles were allowed to sporulate. All sporulations occurred at 30˚C unless otherwise stated. 3 sets of 100 cells were counted for each strain. Percentage of cells forming dyads, tetrads and monads were calculated after 48 h. Asterisks show significance calculated using Mann Whitney U test (* p<0.05, ** p<0.01, ***p<0.001).*

The synthetic effect of *ime2-as* and *net1-6CDK* was demonstrated (Figure 6-9 A). Both *slk19Δ* and the temperature sensitive *esp1-2* strain at the permissive temperature had no synthetic effect with *ime2-as.* However, the *esp1-2 ime2-as* strain undergoing meiosis at 30˚C produced only 7% tetrads compared to 24% for *esp1-2* strain (Figure 6-9 B). The synthetic effect of *ime2-as* and *net1-6CDK* was also demonstrated (Figure 6-9 A). These genetic interactions suggest that Ime2 might be a positive regulator of the FEAR pathway.

6.4 In Summary

In our experiment, the MEN was resistant to activation by Cdc15-7A-HA_3 expression during meiosis I. MEN may be inhibited, independently of Cdc15 phosphorylation, during meiosis I, a conclusion upheld by the findings of Attner *et al.* (Attner and Amon, 2012).

Ectopic Cdc14 release in meiosis I was insufficient to stabilise the lower CDK state in absence of MEN. The effect of Cdc14 may be restricted by additional factors that occur during meiosis I, but not in mitosis. Ime2 is likely to be involved in the restriction of Cdc14 activity (Holt et al., 2007).

Ime2 analogue sensitive allele interacted with some FEAR mutants during meiosis I, suggesting a role for Ime2 in FEAR activation.

7 Conclusion and Discussion

7.1 Background

The mitotic cell cycle can be envisaged as an oscillation between two stable states maintained by mutual inhibition. CDK and CDK inhibitors (CKIs) repress each other's activity, so if one is dominant, that state is able to maintain itself. Transition between the states is triggered by the Starter Kinase and by the Exit Phosphatase (Nasmyth, 1996; Novak et al., 2007) (Figure 7-1).

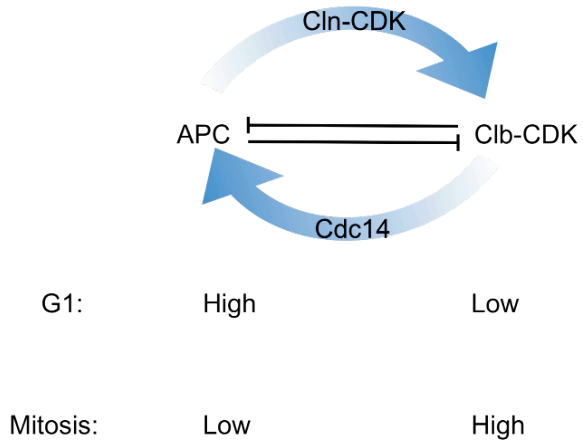

Figure 7-1 ***Mutual inhibition maintains the states of the mitotic cell cycle****. Cln-CDK and Cdc14 initiate transitions (see also Section 1.3.5).*

Meiosis requires that two nuclear divisions happen in sequence without an intervening round of DNA replication. Meiosis I has four specialisations in order to achieve this. These are monopolar attachment, crossovers between homologous chromosomes, protection of pericentric cohesion, and the transition to a second division without an intervening S-phase (Marston and Amon, 2004).

In the regulation of meiosis, the transition to the second division is key. In terms of the above representation of the mitotic cell cycle as an oscillation between two states, the meiotic program must initiate the transition from high

CDK activity to low activity. This allows CDK activity to drop sufficiently to exit the first division, however the cell must revert back to the high CDK state for the second division, without entering the low CDK stable state (Marston and Amon, 2004). One method by which this could be achieved is maintenance of the Starter Kinase activity during the first division to counter CKI activity even as CDK is inhibited. A second method is to limit the activity of Exit Phosphatases to prevent CKI activation.

The exit phosphatase of budding yeast, Cdc14, is maintained in an inactive state in the nucleolus by the inhibitor Net1. Two regulatory networks trigger activity of Cdc14: the FEAR network, triggering a transient nuclear release of Cdc14, and the MEN, triggering a sustained whole-cell release. In meiosis I, only the FEAR network is active, which suggests that the route by which budding yeast achieve a second division is limiting the Exit Phosphatase. However, FEAR release alone in mitosis is not sufficient to trigger spindle disassembly, while the FEAR dependent Cdc14 release in meiosis can achieve this. This suggests that FEAR release of Cdc14 is amplified in some way in meiosis I, or that the factors maintaining the spindle are reduced.

Cdc14 directly counters CDK activity by dephosphorylating its substrates, as well as its role in activating the CKIs. Therefore the CDK activity experienced by the substrates can more accurately be considered as CDK/EP ratio (Bouchoux and Uhlmann, 2011; Drapkin et al., 2009). Phosphorylation of CDK substrates controls the passage through the cell cycle: targets of CDK include cell cycle regulators (Gartner et al., 1998; Rudner and Murray, 2000; Verma et al., 1997; Zachariae et al., 1998). CDK substrates are also involved in cell cycle events such as DNA replication (Elsasser et al., 1999; Masumoto et al., 2002) and spindle assembly and kinetics (Juanes et al., 2011; Woodbury and Morgan, 2007). So the CDK/Cdc14 ratio experienced by these proteins directs passage through the cell cycle and drives the events of the cell cycle. The CDK/Cdc14 ratio leading to change in phosphorylation state appears to depend on the preference of the site for CDK or Cdc14 (Bouchoux and Uhlmann, 2011), giving a mechanism for controlling the timing of the phosphorylation and dephosphorylation.

The B-type cyclin Clb1, the most important cyclin for meiosis, is active during meiosis I (Fitch et al., 1992; Grandin and Reed, 1993). A gel shift in Clb1

occurs during meiosis I coinciding with Clb1 nuclear import and activity (Carlile and Amon, 2008). However, the functional significance of these events was unknown and despite the correlation, the causal relationship was not clear.

In this project, we aimed to discover the nature of this modification. We considered how Clb1 regulation might contribute to the regulation of meiosis I, as envisaged in a simple ODE model. We investigated the functional significance of Clb1 localisation. We also explored the regulation of MEN in meiosis I, and the effect of ectopically increasing Cdc14 in meiosis I.

7.2 Nature of the Clb1 modification

Our results indicated that modification of Clb1 is phosphorylation (Figure 3-5). We have confirmed that the phosphorylation is meiosis-specific. The nuclear localisation of Clb1 also appears to occur specifically during meiosis. However, the localisation results throughout have to be considered with the fact that a control to detect non-specific binding of the antibodies was not performed. Phosphorylation has been associated before with the nuclear import of cyclins so this information seemed to suggest that the meiosis-specific phosphorylation of Clb1 controlled its nuclear import. However, in further investigation of the potential kinases for the phosphorylation of Clb1, we discovered that this was not the case.

Attempts to purify the phosphorylated Clb1 for mass spectrometric analysis proved unsuccessful, and we moved on to investigating the phosphorylation and the functional significance of the nuclear localisation.

7.3 Incorporating Clb1 regulation in an ODE model of meiosis

Given the apparent concurrence of Clb1 phosphorylation with its activity, we considered the case that Clb1 may only be active when phosphorylated. This would be dependent on a meiosis-specific layer of regulation, as Clb1 is unphosphorylated and active in mitosis (Grandin and Reed, 1993). The phosphorylation may be a method of delaying Clb1 activity, as proposed in the models we considered in Chapter 4 (Initial model shown in Figure 4-1). Phosphorylated Clb1 activates Cdc20, which in turn degrades it, but the continued phosphorylation of the pool of unphosphorylated Clb1 acts to delay the effect of Cdc20 on Clb1P.

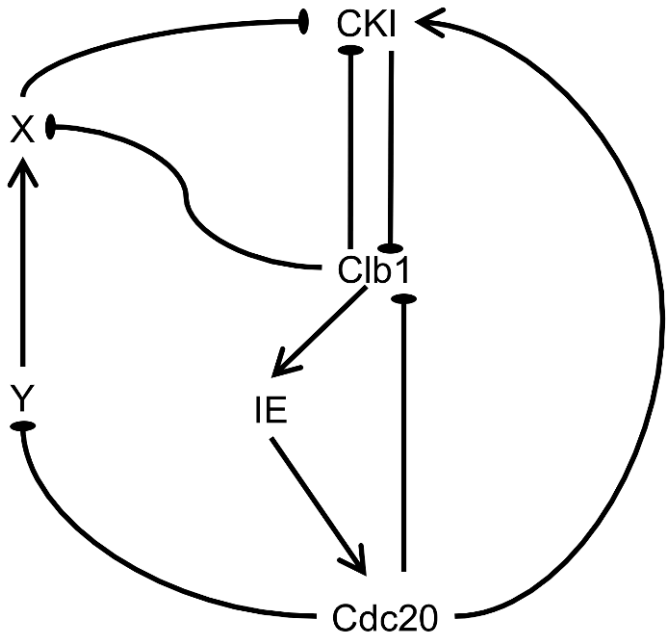

Figure 7-2 ***Proposed wiring diagram of the initial model for meiosis.*** *The reactions are described below. Justification of this diagram with references is Chapter 4. Arrow-headed interactions are positive interactions e.g. activation. Flat-ended interactions are negative interactions e.g. inhibition. Interacting partners of Clb1 and Cdc20, Cdc28 and APC, are not shown.*

Versions of the model were constructed in which three kinases were employed to phosphorylate Clb1. We found Clb1 phosphorylation to be a plausible method of delaying Clb1 activity on Cdc20. These models presuppose that only phosphorylated Clb1 is active, perhaps due to a specific inhibitor of Clb1, which may be prevented from binding by the phosphorylation. Therefore, these models predict that, if Clb1 phosphorylation is prevented, meiosis will fail before the first meiotic division, due to the inactivity of Clb1. The Ime2-dependent model was the least successful in producing distinct peaks of Clb1-CDK activity, as the activity did not fall close to 0 between the peaks. The Autophosphorylation and Alternative Kinase models produced two distinct peaks, followed by the CKI steady state.

We investigated three kinases that could possibly phosphorylate Clb1, by depleting or inhibiting them during meiosis. Ime2 activity was found to be dispensable in both the phosphorylation and nuclear import of Clb1 (Figure 4-8,Figure 4-9), while Cdc28 activity was found to be necessary for both the initial phosphorylation and for maintenance of the phosphorylation (Figure 4-12). Cdc28 activity was also necessary for the nuclear localisation of Clb1 (Figure 4-13). The meiotic depletion of Cdc5, however, demonstrated that

nuclear import was not dependent on phosphorylation, as P_{CLB2}*CDC5* P_{CLB2}*CDC20* strains appeared to concentrate Clb1 in the nucleus without modifying it. (Figure 4-16, Figure 4-17) This is the first separation of the two observations.

The results indicated that Clb1 is imported into the nucleus specifically during meiosis; this is dependent on Cdc28 activity. Clb1 is phosphorylated at the same time. This requires Cdc28 activity and presence of Cdc5. This may imply Cdc28-dependent import and a Cdc5-dependent phosphorylation once inside the nucleus.

Ime2 has been ruled out as a candidate kinase for Clb1 phosphorylation (Section 4.4.2) Autophosphorylation, and phosphorylation by a CDK-dependant kinase such as Cdc5, were found to be plausible for Clb1 phosphorylation. However, the link between Clb1 phosphorylation and activity that these models relied on was implied to be false by later results in Chapter 5. Here, *CLB1-NES$_2$-HA* strains did not give the same phenotype as *clb1Δ* strains, though phosphorylation of the Clb1 protein was not detected. Therefore, the unphosphorylated Clb1 was capable of performing the essential role of Clb1.

7.4 Clb1 Localisation

Clb1 phosphorylation was considered as a mechanism to protect Clb1 from degradation or inhibition by the CKIs during the first cycle. Rather than considering one of the three previously mentioned kinases for this role, hypothetical protein Y was proposed. This role for Clb1 phosphorylation was capable of permitting the system to achieve two cycles of Clb1-CDK activity, and this behaviour was dependent on Y. In this case, Clb1 phosphorylation is not required for Clb1 activity in the first cycle. This model predicts that, if Clb1 phosphorylation were prevented, the cell would undergo one successful division and form dyads. This prediction was also disproven by *CLB1-NES$_2$-HA* strains.

A similar model considered the possibility that Cdc14 export was prevented by Y. This model did not include Clb1 regulation, but introduced the separate nuclear and cytoplasmic fractions of Clb1. This model further predicted that Cdc14 export would permit the cell to exit meiosis in the first cycle.

Concentration of Clb1 activity in the nucleus may counter Cdc14 release by FEAR. Clb1 may act in this role to prevent Cdc14 from permitting relicensing

of DNA origins. However, Clb1 is reported to disappear or return to the cytoplasm at anaphase (Buonomo et al., 2003; Carlile and Amon, 2008; Marston et al., 2003), so the Cdc14 phosphatase would then be uncontested. In addition, FEAR released Cdc14 in mitosis is not sufficient to counter Clb-CDK activity sufficiently for complete exit, spindle disassembly and DNA relicensing, leading to the necessity of MEN activation. In meiosis I, spindle disassembly is achieved, so FEAR-released Cdc14 is sufficient here. Clb-CDK activity drives FEAR release of Cdc14. By concentrating Clb-CDK activity in the nucleus, and perhaps also by delaying its activity relative to the accumulation of the Clb1 protein, the Clb-CDK activity driving FEAR may be amplified, and cause increased Cdc14 release over that seen in mitosis.

Using the same ODE-based approach as before, we investigated whether Clb1 nuclear concentration was a plausible method of amplifying FEAR (Figure 5-4). Our model showed that nuclear accumulation of Clb1 accelerated the divisions, and altered the Cdc14/CDK ratio experienced by the cell during the cycle, and that decreasing nuclear localisation of Clb1 had the opposite effect. However, the lowest Cdc14/CDK ratio was unchanged. This was investigated experimentally when localisation of Clb1 was altered in Chapter 6.

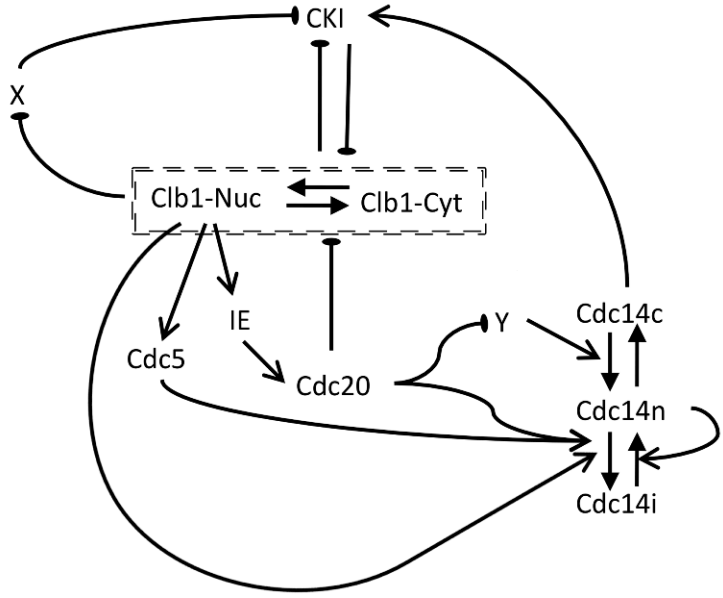

Figure 7-3 ***Proposed wiring diagram for the Clb1 Localisation model.*** *The model is similar to those in Chapter 4. Open-headed arrows indicate positive interactions such activation, flat ended arrows indicate negative interactions such as inhibition, and solid-headed arrows indicate transition of proteins between two states i.e. phosphorylation. However, Cdc14 is activated by*

parallel pathways from Clb1 activity. Clb1 is split into two subtypes and only nuclear Clb1 activity triggers FEAR activity.

We investigated the functional significance of the localisation of Clb1 by tagging the Clb1 gene with localisation sequences. By altering the localisation of Clb1, we were able to investigate the relationship between nuclear import and phosphorylation. Our NES-tagged Clb1 showed no gel shift, demonstrating that nuclear import is required for the phosphorylation (Figure 5-24). The strain bearing *CLB1-NES$_2$-HA* did not have a severe defect in sporulation efficiency, as seen in the *clb1Δ* strain (Figure 4-18), indicating that neither the modification nor nuclear concentration is required for passage through meiosis. However, the Clb1-NES$_2$-HA was not excluded from the nucleus entirely.

The constitutively nuclear Clb1 mutant demonstrated an accelerated entry into meiosis I and then progression to anaphase I, but did not progress to accelerated spindle disassembly (Figure 5-21). This implied that nuclear-concentrated Clb1 was triggering entry into meiosis and initial Cdc14 release. Continued nuclear-concentrated Clb1 may delay spindle disassembly. Entry into meiosis II occurred with normal timing. The second division of meiosis II is controlled by Clb3-CDK activity (Carlile and Amon, 2008).

Interestingly, Clb1 localisation mutants altered the sporulation efficiency in combination with FEAR mutants (Figure 5-29). Constitutively nuclear Clb1 partially rescued the phenotypes of both *spo12Δ* and *esp1-2* cells, and the cytoplasmic Clb1 mutant exacerbated the phenotype of *esp1-2* cells. Nuclear localisation of Clb1 appeared to partially compensate for impaired FEAR activation, suggesting a role in FEAR amplification.

The import and export of Clb1 appears to control the Cdc14/CDK ratio of meiosis I, an important factor in the specialisation of meiosis. However, both of the strains in which Clb1 localisation was altered, were found to sporulate efficiently, unlike the *clb1Δ* strain. This is genetic evidence that the non-phosphorylated NES-tagged Clb1 is active during meiosis, and repudiates the proposed relationship between Clb1 phosphorylation and Clb1-CDK activity.

7.5 MEN activation and Cdc14 release

Amplified FEAR, particularly when unchallenged by the exported or inactivated Clb1, would be capable of disassembling the spindle. However, the

DNA replication proteins must not become reactivated, risking partial or complete rereplication in the meiosis I – II transition. Similarly, the cell must inhibit CDK but avoid passing the threshold to the low CDK state. Amplified Cdc14 release must be carefully balanced with CDK activity, unless the activity of Cdc14 was restricted in some way, allowing Cdc14 release to be increased without negative consequences. Ime2 has been suggested in this role, being a kinase whose phosphorylation sites are relatively resistant to Cdc14. Ime2 substrate specificity may allow the kinase to limit Cdc14 activity in some areas and not others. Alternatively, Cdc14 release may be restricted. We attempted to disrupt this by artificially amplifying Cdc14 release, to see if we could force the cell over the threshold to the low CDK state during meiosis I.

We attempted to alter the Cdc14/CDK ratio ectopically by expressing a constitutively active MEN component *cdc15-7A-HA*$_3$ (Section 6.1). Our results suggested that Cdc15-7A-HA$_3$ was ineffective at activating the MEN once cells had entered meiosis, and could not cause increased Cdc14 release in meiosis I. An observed delay after early expression of Cdc15-7A-HA$_3$ was held to be the result of delayed entry to meiosis due to induced Cdc14 release. An investigation of MEN activation in meiosis I has since confirmed that MEN is resistant to activation at this stage (Attner and Amon, 2012).

We attempted to alter the Cdc14/CDK ratio more directly by expressing a telophase arrest-bypassing mutant of *CDC14* (Section 6.2). *CDC14TAB6* is capable of rescuing the inactivation of MEN in *cdc15* mutants (Shou and Deshaies, 2002), which suggested that the allele may be able to emulate the function of MEN in meiosis I. We found that early induction of *CDC14TAB6* during meiosis increased the proportion of mononucleate cells after sporulation. However, no increase of dyads was seen. Ectopic Cdc14 release from early meiosis is capable of preventing spindle production and resulting in monads (Kerr et al., 2011). Therefore, the results reiterate the inference that increased Cdc14 release has no effect after entry to meiosis.

The above data suggest a robust inhibition of MEN during meiosis, as confirmed by Attner *et al.* (Attner and Amon, 2012), and also that the effects of direct ectoptic Cdc14 release are curbed during meiosis I.

7.6 Discussion

Although we have identified the requirement for CDK activity and Cdc5 for the meiosis-specific Clb1 phosphorylation, we have been unable to identify the site and kinase for the modification. We have demonstrated that nuclear localisation of Clb1 is not dependent on the phosphorylation, and that the dependence is reversed: Clb1 phosphorylation appears to be dependent on the nuclear localisation.

Our results suggested that the meiosis-specific Clb1 phosphorylation and localisation are not necessary for successful meiosis in ideal conditions, but operate in controlling the timing of meiosis I, or in making the process more robust to perturbations, by amplifying FEAR-driven Cdc14 release.

Maintenance of a level of CDK activity during exit from meiosis I could fulfil this role. This has been seen in meiosis in *Xenopus* (Iwabuchi et al., 2000). CDK activity would have to be maintained against increased pressure from the Exit Phosphatase. Maintenance of CDK may be achieved by giving cyclins resistance to repression. Phosphorylation may play a role here, disguising binding sites and allowing Clb1 to partially escape inhibition by Cdc14 triggered CKIs until the high CDK state is established for meiosis II.

Alternatively, CKIs may continue to be repressed during the meiotic divisions by a mechanism resistant to the exit phosphatase. Ime2 is also a strong candidate for such a role. Ime2 is capable of Cdc14-resisitant phosphorylation (Holt et al., 2007) and has overlapping substrates with CDK (Bolte et al., 2002; Clifford et al., 2004). Ime2 has been proposed to take on the Starter Kinase role of the Clns, which are absent in meiosis (Dirick et al., 1998). However, in some cases the phosphorylations do not have the same effect on the substrates and this may not be sufficient (Sedgwick et al., 2006).

Ime2 is insufficient to maintain CDK activity and to allow the construction of a meiotic spindle against ectopically released Cdc14 in early meiosis(Kerr et al., 2011). This may indicate Ime2 is insufficient to maintain the spindle against Cdc14 release, which would work with the above theory. Spindle maintenance is one of the roles of CDK that must not be taken by Ime2 in the meiosis I to II transition. However, construction and maintenance of a spindle are different tasks, different factors may come into play.

A mechanism to prevent increased Cdc14 release from switching the system from CDK- to CKI-dominated steady states would give the cell a wider range in which to increase FEAR-driven Cdc14 release during meiosis I. Increased Cdc14 release could then achieve such purposes as spindle disassembly that would otherwise be incomplete.

Clb1 nuclear import could be a part of such regulation, increasing the force behind FEAR-driven release of Cdc14. Our results indicated that Clb1 import was not necessary for disassembly of the meiosis I spindle, so if an amplification of FEAR-dependent Cdc14 release is a genuine feature of meiosis I, then other factors must also be involved in its release.

7.7 Future work

There are a number of questions raised by this work. How is the nuclear localisation of Clb1 controlled during meiosis I? Clb1 phosphorylation is dependent on the nuclear localisation rather than vice versa, so the signals directing import of Clb1 during metaphase and Clb1 export in anaphase are as yet unknown. What are the sites of phosphorylation of Clb1 and how is Cdc5 involved? The use of the constitutively nuclear Clb1 mutant could show whether Cdc28 activity is required for Clb1 phosphorylation beyond the induction of Clb1 import. Identification of the Clb1 modification sites would help to identify the kinases responsible and may clarify the participation of Cdc5. Mass spectronomic analysis of modified Clb1 would clarify these relationships and may identify the purpose of the phosphorylation.

The functional significance of Clb1 localisation seemed related to the timing and extent of Cdc14 release in meiosis I. However, our ability to detect alterations in timing was limited. The use of live-cell imaging to follow single cells through meiosis would allow the precise measurement of the timing and duration of cell cycle events. Live cell imaging was attempted (Appendix Section 9.4) but optimisation was unsuccessful with the time and equipment available. Live cell imaging and fluorescence tagging could also be used to give quantitative time course data on the presence and activity of proteins (for example: the activity of Cdc20 may be indicated by monitoring levels of targets such as Pds1, which is degraded after Cdc20-dependent ubiquitinylation). Quantitative, single

cell data would be much more precise and accurate, rather than using protein levels detected by western blot analysis from whole-cell extracts in asynchronous cultures. Fluorescence imaging would also reveal data on the localisation of proteins. Detailed quantitative time course data would be useful for the testing and refining of models of meiosis, leading to more accurate predictions. The answers to these queries would help us to understand how the meiosis-specific regulation in yeast achieves its specialised aims.

8 Bibliography

Acosta, I., Ontoso, D., and San-Segundo, P.A. (2011). The budding yeast polo-like kinase Cdc5 regulates the Ndt80 branch of the meiotic recombination checkpoint pathway. Mol Biol Cell *22*, 3478-3490.

Allers, T., and Lichten, M. (2001). Differential timing and control of noncrossover and crossover recombination during meiosis. Cell *106*, 47-57.

Amon, A., Irniger, S., and Nasmyth, K. (1994). Closing the cell cycle circle in yeast: G2 cyclin proteolysis initiated at mitosis persists until the activation of G1 cyclins in the next cycle. Cell *77*, 1037-1050.

Amon, A., Tyers, M., Futcher, B., and Nasmyth, K. (1993). Mechanisms that help the yeast cell cycle clock tick: G2 cyclins transcriptionally activate G2 cyclins and repress G1 cyclins. Cell *74*, 993-1007.

Andersen, S.L., and Sekelsky, J. (2010). Meiotic versus mitotic recombination: two different routes for double-strand break repair: the different functions of meiotic versus mitotic DSB repair are reflected in different pathway usage and different outcomes. Bioessays *32*, 1058-1066.

Andrews, B., and Measday, V. (1998). The cyclin family of budding yeast: abundant use of a good idea. Trends Genet *14*, 66-72.

Archambault, V., Chang, E.J., Drapkin, B.J., Cross, F.R., Chait, B.T., and Rout, M.P. (2004). Targeted proteomic study of the cyclin-Cdk module. Mol Cell *14*, 699-711.

Asakawa, K., Yoshida, S., Otake, F., and Toh-e, A. (2001). A novel functional domain of Cdc15 kinase is required for its interaction with Tem1 GTPase in Saccharomyces cerevisiae. Genetics *157*, 1437-1450.

Ashton, T.M., Mankouri, H.W., Heidenblut, A., McHugh, P.J., and Hickson, I.D. (2011). Pathways for Holliday junction processing during homologous recombination in Saccharomyces cerevisiae. Mol Cell Biol *31*, 1921-1933.

Attner, M.A., and Amon, A. (2012). Control of the mitotic exit network during meiosis. Mol Biol Cell *23*, 3122-3132.

Azzam, R., Chen, S.L., Shou, W., Mah, A.S., Alexandru, G., Nasmyth, K., Annan, R.S., Carr, S.A., and Deshaies, R.J. (2004). Phosphorylation by cyclin B-Cdk underlies release of mitotic exit activator Cdc14 from the nucleolus. Science *305*, 516-519.

Bailly, E., Cabantous, S., Sondaz, D., Bernadac, A., and Simon, M.N. (2003). Differential cellular localization among mitotic cyclins from Saccharomyces cerevisiae: a new role for the axial budding protein Bud3 in targeting Clb2 to the mother-bud neck. J Cell Sci *116*, 4119-4130.

Bardin, A.J., and Amon, A. (2001). Men and sin: what's the difference? Nat Rev Mol Cell Biol *2*, 815-826.
Bardin, A.J., Visintin, R., and Amon, A. (2000). A mechanism for coupling exit from mitosis to partitioning of the nucleus. Cell *102*, 21-31.
Bembenek, J., Kang, J., Kurischko, C., Li, B., Raab, J.R., Belanger, K.D., Luca, F.C., and Yu, H. (2005). Crm1-mediated nuclear export of Cdc14 is required for the completion of cytokinesis in budding yeast. Cell Cycle *4*, 961-971.
Benjamin, K.R., Zhang, C., Shokat, K.M., and Herskowtiz, I. (2003). Control of landmark events in meiosis by the CDK cdc28 and the meiosis-specific kinase Ime2. Genes & Development *17*, 1524-1539.
Bertazzi, D.T., Kurtulmus, B., and Pereira, G. (2011). The cortical protein Lte1 promotes mitotic exit by inhibiting the spindle position checkpoint kinase Kin4. J Cell Biol *193*, 1033-1048.
Biggins, S., and Murray, A.W. (2001). The budding yeast protein kinase Ipl1/Aurora allows the absence of tension to activate the spindle checkpoint. Genes Dev *15*, 3118-3129.
Bishop, A.C., Ubersax, J.A., Petsch, D.T., Matheos, D.P., Gray, N.S., Blethrow, J., Shimizu, E., Tsien, J.Z., Schultz, P.G., Rose, M.D.*, et al.* (2000). A chemical switch for inhibitor-sensitive alleles of any protein kinase. Nature *407*, 395-401.
Bolte, M., Steigemann, P., Braus, G.H., and Irniger, S. (2002). Inhibition of APC-mediated proteolysis by the meiosis-specific protein kinase Ime2. Proc Natl Acad Sci U S A *99*, 4385-4390.
Bouchoux, C., and Uhlmann, F. (2011). A quantitative model for ordered Cdk substrate dephosphorylation during mitotic exit. Cell *147*, 803-814.
Brazhnik, P., and Tyson, J.J. (2006). Cell cycle control in bacteria and yeast: a case of convergent evolution? Cell Cycle *5*, 522-529.
Bremmer, S.C., Hall, H., Martinez, J.S., Eissler, C.L., Hinrichsen, T.H., Rossie, S., Parker, L.L., Hall, M.C., and Charbonneau, H. (2012). Cdc14 phosphatases preferentially dephosphorylate a subset of cyclin-dependent kinase (Cdk) sites containing phosphoserine. J Biol Chem *287*, 1662-1669.
Brush, G.S., Najor, N.A., Dombkowski, A.A., Cukovic, D., and Sawarynski, K.E. (2012). Yeast IME2 functions early in meiosis upstream of cell cycle-regulated SBF and MBF targets. PLoS ONE *7*, e31575.
Buonomo, S.B., Clyne, R.K., Fuchs, J., Loidl, J., Uhlmann, F., and Nasmyth, K. (2000). Disjunction of homologous chromosomes in meiosis I depends on proteolytic cleavage of the meiotic cohesin Rec8 by separin. Cell *103*, 387-398.
Buonomo, S.B., Rabitsch, K.P., Fuchs, J., Gruber, S., Sullivan, M., Uhlmann, F., Petronczki, M., Toth, A., and Nasmyth, K. (2003). Division of the nucleolus and its release of CDC14 during anaphase of meiosis I depends on separase, SPO12, and SLK19. Dev Cell *4*, 727-739.
Carey, L.B., Leatherwood, J.K., and Futcher, B. (2008). Huxley's revenge: cell-cycle entry, positive feedback, and the G1 cyclins. Mol Cell *31*, 307-308.
Carlile, T.M., and Amon, A. (2008). Meiosis I is established through division-specific translational control of a cyclin. Cell *133*, 280-291.
Caydasi, A.K., Lohel, M., Grunert, G., Dittrich, P., Pereira, G., and Ibrahim, B. (2012). A dynamical model of the spindle position checkpoint. Mol Syst Biol *8*, 582.
Caydasi, A.K., and Pereira, G. (2012). SPOC alert--when chromosomes get the wrong direction. Exp Cell Res *318*, 1421-1427.

Cenamor, R., Jimenez, J., Cid, V.J., Nombela, C., and Sanchez, M. (1999). The budding yeast Cdc15 localizes to the spindle pole body in a cell-cycle-dependent manner. Mol Cell Biol Res Commun *2*, 178-184.
Chan, L.Y., and Amon, A. (2010). Spindle position is coordinated with cell-cycle progression through establishment of mitotic exit-activating and -inhibitory zones. Mol Cell *39*, 444-454.
Charvin, G., Cross, F.R., and Siggia, E.D. (2009). Forced periodic expression of G1 cyclins phase-locks the budding yeast cell cycle. Proc Natl Acad Sci U S A *106*, 6632-6637.
Charvin, G., Oikonomou, C., Siggia, E.D., and Cross, F.R. (2010). Origin of irreversibility of cell cycle start in budding yeast. PLoS Biol *8*, e1000284.
Chen, K.C., Calzone, L., Csikasz-Nagy, A., Cross, F.R., Novak, B., and Tyson, J.J. (2004). Integrative analysis of cell cycle control in budding yeast. Mol Biol Cell *15*, 3841-3862.
Chen, K.C., Csikasz-Nagy, A., Gyorffy, B., Val, J., Novak, B., and Tyson, J.J. (2000). Kinetic analysis of a molecular model of the budding yeast cell cycle. Mol Biol Cell *11*, 369-391.
Chen, Y.C., and Weinreich, M. (2010). Dbf4 regulates the Cdc5 Polo-like kinase through a distinct non-canonical binding interaction. J Biol Chem *285*, 41244-41254.
Cheng, L., Hunke, L., and Hardy, C.F. (1998). Cell cycle regulation of the Saccharomyces cerevisiae polo-like kinase cdc5p. Mol Cell Biol *18*, 7360-7370.
Cherry, J.M., Adler, C., Ball, C., Chervitz, S.A., Dwight, S.S., Hester, E.T., Jia, Y., Juvik, G., Roe, T., Schroeder, M.*, et al.* (1998). SGD: Saccharomyces Genome Database. Nucleic Acids Res *26*, 73-79.
Chu, S., DeRisi, J., Eisen, M., Mulholland, J., Botstein, D., Brown, P.O., and Herskowitz, I. (1998). The transcriptional program of sporulation in budding yeast. Science *282*, 699-705.
Chu, S., and Herskowitz, I. (1998). Gametogenesis in yeast is regulated by a transcriptional cascade dependent on Ndt80. Mol Cell *1*, 685-696.
Clifford, D.M., Marinco, S.M., and Brush, G.S. (2004). The meiosis-specific protein kinase Ime2 directs phosphorylation of replication protein A. J Biol Chem *279*, 6163-6170.
Collins, I., and Newlon, C.S. (1994). Chromosomal DNA replication initiates at the same origins in meiosis and mitosis. Mol Cell Biol *14*, 3524-3534.
Colomina, N., Gari, E., Gallego, C., Herrero, E., and Aldea, M. (1999). G1 cyclins block the Ime1 pathway to make mitosis and meiosis incompatible in budding yeast. EMBO J *18*, 320-329.
Conant, G.C., and Wagner, A. (2003). Convergent evolution of gene circuits. Nat Genet *34*, 264-266.
Cooper, K.F., Mallory, M.J., Egeland, D.B., Jarnik, M., and Strich, R. (2000). Ama1p is a meiosis-specific regulator of the anaphase promoting complex/cyclosome in yeast. Proc Natl Acad Sci U S A *97*, 14548-14553.
Coudreuse, D., and Nurse, P. (2010). Driving the cell cycle with a minimal CDK control network. Nature *468*, 1074-1079.
Covitz, P.A., Herskowitz, I., and Mitchell, A.P. (1991). The yeast RME1 gene encodes a putative zinc finger protein that is directly repressed by a1-alpha 2. Genes Dev *5*, 1982-1989.

Cromie, G.A., and Smith, G.R. (2007). Branching out: meiotic recombination and its regulation. Trends Cell Biol *17*, 448-455.
Cross, F.R. (1988). DAF1, a mutant gene affecting size control, pheromone arrest, and cell cycle kinetics of Saccharomyces cerevisiae. Mol Cell Biol *8*, 4675-4684.
Cross, F.R. (1995). Starting the cell cycle: what's the point? Curr Opin Cell Biol *7*, 790-797.
Cross, F.R., Archambault, V., Miller, M., and Klovstad, M. (2002). Testing a mathematical model of the yeast cell cycle. Mol Biol Cell *13*, 52-70.
Cross, F.R., and Blake, C.M. (1993). The yeast Cln3 protein is an unstable activator of Cdc28. Mol Cell Biol *13*, 3266-3271.
Cross, F.R., Buchler, N.E., and Skotheim, J.M. (2011). Evolution of networks and sequences in eukaryotic cell cycle control. Philos Trans R Soc Lond B Biol Sci *366*, 3532-3544.
Cross, F.R., and Siggia, E.D. (2005). Mode locking the cell cycle. Phys Rev E Stat Nonlin Soft Matter Phys *72*, 021910.
Cross, F.R., and Tinkelenberg, A.H. (1991). A potential positive feedback loop controlling CLN1 and CLN2 gene expression at the start of the yeast cell cycle. Cell *65*, 875-883.
Cross, F.R., Yuste-Rojas, M., Gray, S., and Jacobson, M.D. (1999). Specialization and targeting of B-type cyclins. Mol Cell *4*, 11-19.
Cvrckova, F., and Nasmyth, K. (1993). Yeast G1 cyclins CLN1 and CLN2 and a GAP-like protein have a role in bud formation. EMBO J *12*, 5277-5286.
D'Aquino, K.E., Monje-Casas, F., Paulson, J., Reiser, V., Charles, G.M., Lai, L., Shokat, K.M., and Amon, A. (2005). The protein kinase Kin4 inhibits exit from mitosis in response to spindle position defects. Mol Cell *19*, 223-234.
Dahmann, C., Diffley, J.F., and Nasmyth, K.A. (1995). S-phase-promoting cyclin-dependent kinases prevent re-replication by inhibiting the transition of replication origins to a pre-replicative state. Curr Biol *5*, 1257-1269.
Dahmann, C., and Futcher, B. (1995). Specialization of B-Type Cyclins for Mitosis or Meiosis in Saccharomyces-Cerevisiae. Genetics *140*, 957-963.
DeCesare, J.M., and Stuart, D.T. (2012). Among B-type cyclins only CLB5 and CLB6 promote premeiotic S phase in Saccharomyces cerevisiae. Genetics *190*, 1001-1016.
Diamond, A.E., Park, J.S., Inoue, I., Tachikawa, H., and Neiman, A.M. (2009). The anaphase promoting complex targeting subunit Ama1 links meiotic exit to cytokinesis during sporulation in Saccharomyces cerevisiae. Mol Biol Cell *20*, 134-145.
Diffley, J.F. (2004). Regulation of early events in chromosome replication. Curr Biol *14*, R778-786.
Diffley, J.F., Cocker, J.H., Dowell, S.J., and Rowley, A. (1994). Two steps in the assembly of complexes at yeast replication origins in vivo. Cell *78*, 303-316.
Dirick, L., Bohm, T., and Nasmyth, K. (1995). Roles and regulation of Cln-Cdc28 kinases at the start of the cell cycle of Saccharomyces cerevisiae. EMBO J *14*, 4803-4813.
Dirick, L., Goetsch, L., Ammerer, G., and Byers, B. (1998). Regulation of meiotic S phase by Ime2 and a Clb5,6-associated kinase in Saccharomyces cerevisiae. Science *281*, 1854-1857.

Drapkin, B.J., Lu, Y., Procko, A.L., Timney, B.L., and Cross, F.R. (2009). Analysis of the mitotic exit control system using locked levels of stable mitotic cyclin. Mol Syst Biol *5*, 328.
Dumitrescu, T.P., and Saunders, W.S. (2002). The FEAR Before MEN: networks of mitotic exit. Cell Cycle *1*, 304-307.
Edgington, N.P., and Futcher, B. (2001). Relationship between the function and the location of G1 cyclins in S. cerevisiae. J Cell Sci *114*, 4599-4611.
Elia, A.E., Rellos, P., Haire, L.F., Chao, J.W., Ivins, F.J., Hoepker, K., Mohammad, D., Cantley, L.C., Smerdon, S.J., and Yaffe, M.B. (2003). The molecular basis for phosphodependent substrate targeting and regulation of Plks by the Polo-box domain. Cell *115*, 83-95.
Elsasser, S., Chi, Y., Yang, P., and Campbell, J.L. (1999). Phosphorylation controls timing of Cdc6p destruction: A biochemical analysis. Mol Biol Cell *10*, 3263-3277.
Eluere, R., Offner, N., Varlet, I., Motteux, O., Signon, L., Picard, A., Bailly, E., and Simon, M.N. (2007). Compartmentalization of the functions and regulation of the mitotic cyclin Clb2 in S. cerevisiae. J Cell Sci *120*, 702-711.
Engel, S.R., Dietrich, F.S., Fisk, D.G., Binkley, G., Balakrishnan, R., Costanzo, M.C., Dwight, S.S., Hitz, B.C., Karra, K., Nash, R.S.*, et al.* (2013). The Reference Genome Sequence of Saccharomyces cerevisiae: Then and Now. G3 (Bethesda).
Epstein, C.B., and Cross, F.R. (1992). CLB5: a novel B cyclin from budding yeast with a role in S phase. Genes Dev *6*, 1695-1706.
Evans, T., Rosenthal, E.T., Youngblom, J., Distel, D., and Hunt, T. (1983). Cyclin: a protein specified by maternal mRNA in sea urchin eggs that is destroyed at each cleavage division. Cell *33*, 389-396.
Falk, J.E., Chan, L.Y., and Amon, A. (2011). Lte1 promotes mitotic exit by controlling the localization of the spindle position checkpoint kinase Kin4. Proc Natl Acad Sci U S A *108*, 12584-12590.
Ferrell, J.E., Jr. (2002). Self-perpetuating states in signal transduction: positive feedback, double-negative feedback and bistability. Curr Opin Cell Biol *14*, 140-148.
Ferrell, J.E., Jr., Tsai, T.Y., and Yang, Q. (2011). Modeling the cell cycle: why do certain circuits oscillate? Cell *144*, 874-885.
Fitch, I., Dahmann, C., Surana, U., Amon, A., Nasmyth, K., Goetsch, L., Byers, B., and Futcher, B. (1992). Characterization of four B-type cyclin genes of the budding yeast Saccharomyces cerevisiae. Mol Biol Cell *3*, 805-818.
Foiani, M., Nadjar-Boger, E., Capone, R., Sagee, S., Hashimshoni, T., and Kassir, Y. (1996). A meiosis-specific protein kinase, Ime2, is required for the correct timing of DNA replication and for spore formation in yeast meiosis. Mol Gen Genet *253*, 278-288.
Friedlander, G., Joseph-Strauss, D., Carmi, M., Zenvirth, D., Simchen, G., and Barkai, N. (2006). Modulation of the transcription regulatory program in yeast cells committed to sporulation. Genome Biol *7*, R20.
Ganesan, A.T., Holter, H., and Roberts, C. (1958). Some observations on sporulation in Saccharomyces. C R Trav Lab Carlsberg Chim *31*, 1-6.
Gartner, A., Jovanovic, A., Jeoung, D.I., Bourlat, S., Cross, F.R., and Ammerer, G. (1998). Pheromone-dependent G1 cell cycle arrest requires Far1 phosphorylation, but may not involve inhibition of Cdc28-Cln2 kinase, in vivo. Mol Cell Biol *18*, 3681-3691.

Geil, C., Schwab, M., and Seufert, W. (2008). A nucleolus-localized activator of Cdc14 phosphatase supports rDNA segregation in yeast mitosis. Curr Biol *18*, 1001-1005.
Geymonat, M., Jensen, S., and Johnston, L.H. (2002a). Mitotic exit: The Cdc14 double cross. Current Biology *12*, R482-R484.
Geymonat, M., Spanos, A., de Bettignies, G., and Sedgwick, S.G. (2009). Lte1 contributes to Bfa1 localization rather than stimulating nucleotide exchange by Tem1. J Cell Biol *187*, 497-511.
Geymonat, M., Spanos, A., Smith, S.J., Wheatley, E., Rittinger, K., Johnston, L.H., and Sedgwick, S.G. (2002b). Control of mitotic exit in budding yeast. In vitro regulation of Tem1 GTPase by Bub2 and Bfa1. J Biol Chem *277*, 28439-28445.
Gladfelter, A.S., Hungerbuehler, A.K., and Philippsen, P. (2006). Asynchronous nuclear division cycles in multinucleated cells. J Cell Biol *172*, 347-362.
Goldbeter, A. (1991). A minimal cascade model for the mitotic oscillator involving cyclin and cdc2 kinase. Proc Natl Acad Sci U S A *88*, 9107-9111.
Goulev, Y., and Charvin, G. (2011). Ultrasensitivity and positive feedback to promote sharp mitotic entry. Mol Cell *41*, 243-244.
Grandin, N., and Reed, S.I. (1993). Differential function and expression of Saccharomyces cerevisiae B-type cyclins in mitosis and meiosis. Mol Cell Biol *13*, 2113-2125.
Guttmann-Raviv, N., Boger-Nadjar, E., Edri, I., and Kassir, Y. (2001). Cdc28 and Ime2 possess redundant functions in promoting entry into premeiotic DNA replication in Saccharomyces cerevisiae. Genetics *159*, 1547-1558.
Haase, S.B., and Reed, S.I. (1999). Evidence that a free-running oscillator drives G1 events in the budding yeast cell cycle. Nature *401*, 394-397.
Hagting, A., Jackman, M., Simpson, K., and Pines, J. (1999). Translocation of cyclin B1 to the nucleus at prophase requires a phosphorylation-dependent nuclear import signal. Curr Biol *9*, 680-689.
Hancioglu, B., and Tyson, J.J. (2012). A mathematical model of mitotic exit in budding yeast: the role of Polo kinase. PLoS ONE *7*, e30810.
Hartwell, L.H., Culotti, J., Pringle, J.R., and Reid, B.J. (1974). Genetic control of the cell division cycle in yeast. Science *183*, 46-51.
Hartwell, L.H., and Weinert, T.A. (1989). Checkpoints: controls that ensure the order of cell cycle events. Science *246*, 629-634.
Hassold, T., and Hunt, P. (2001). To err (meiotically) is human: the genesis of human aneuploidy. Nat Rev Genet *2*, 280-291.
He, E., Kapuy, O., Oliveira, R.A., Uhlmann, F., Tyson, J.J., and Novak, B. (2011). System-level feedbacks make the anaphase switch irreversible. Proc Natl Acad Sci U S A *108*, 10016-10021.
Henderson, K.A., Kee, K., Maleki, S., Santini, P.A., and Keeney, S. (2006). Cyclin-dependent kinase directly regulates initiation of meiotic recombination. Cell *125*, 1321-1332.
Hepworth, S.R., Friesen, H., and Segall, J. (1998). NDT80 and the meiotic recombination checkpoint regulate expression of middle sporulation-specific genes in Saccharomyces cerevisiae. Mol Cell Biol *18*, 5750-5761.
Hereford, L.M., and Hartwell, L.H. (1974). Sequential gene function in the initiation of Saccharomyces cerevisiae DNA synthesis. J Mol Biol *84*, 445-461.
Higuchi, T., and Uhlmann, F. (2005). Stabilization of microtubule dynamics at anaphase onset promotes chromosome segregation. Nature *433*, 171-176.

Hirschberg, J., and Simchen, G. (1977). Commitment to the mitotic cell cycle in yeast in relation to meiosis. Exp Cell Res *105*, 245-252.
Holt, L.J., Hutti, J.E., Cantley, L.C., and Morgan, D.O. (2007). Evolution of Ime2 phosphorylation sites on Cdk1 substrates provides a mechanism to limit the effects of the phosphatase Cdc14 in meiosis. Mol Cell *25*, 689-702.
Holt, L.J., Krutchinsky, A.N., and Morgan, D.O. (2008). Positive feedback sharpens the anaphase switch. Nature *454*, 353-357.
Honigberg, S.M., and Purnapatre, K. (2003). Signal pathway integration in the switch from the mitotic cell cycle to meiosis in yeast. J Cell Sci *116*, 2137-2147.
Hu, F., and Aparicio, O.M. (2005). Swe1 regulation and transcriptional control restrict the activity of mitotic cyclins toward replication proteins in Saccharomyces cerevisiae. Proc Natl Acad Sci U S A *102*, 8910-8915.
Hu, F., Wang, Y., Liu, D., Li, Y., Qin, J., and Elledge, S.J. (2001). Regulation of the Bub2/Bfa1 GAP complex by Cdc5 and cell cycle checkpoints. Cell *107*, 655-665.
Hua, H., Namdar, M., Ganier, O., Gregan, J., Mechali, M., and Kearsey, S.E. (2013). Sequential steps in DNA replication are inhibited to ensure reduction of ploidy in meiosis. Mol Biol Cell *24*, 578-587.
Hwang, L.H., Lau, L.F., Smith, D.L., Mistrot, C.A., Hardwick, K.G., Hwang, E.S., Amon, A., and Murray, A.W. (1998). Budding yeast Cdc20: a target of the spindle checkpoint. Science *279*, 1041-1044.
Iwabuchi, M., Ohsumi, K., Yamamoto, T.M., Sawada, W., and Kishimoto, T. (2000). Residual Cdc2 activity remaining at meiosis I exit is essential for meiotic M-M transition in Xenopus oocyte extracts. EMBO J *19*, 4513-4523.
Jambhekar, A., and Amon, A. (2008). Control of meiosis by respiration. Curr Biol *18*, 969-975.
Janke, C., Magiera, M.M., Rathfelder, N., Taxis, C., Reber, S., Maekawa, H., Moreno-Borchart, A., Doenges, G., Schwob, E., Schiebel, E.*, et al.* (2004). A versatile toolbox for PCR-based tagging of yeast genes: new fluorescent proteins, more markers and promoter substitution cassettes. Yeast *21*, 947-962.
Jaquenoud, M., van Drogen, F., and Peter, M. (2002). Cell cycle-dependent nuclear export of Cdh1p may contribute to the inactivation of APC/C(Cdh1). EMBO J *21*, 6515-6526.
Jaspersen, S.L., Charles, J.F., and Morgan, D.O. (1999). Inhibitory phosphorylation of the APC regulator Hct1 is controlled by the kinase Cdc28 and the phosphatase Cdc14. Curr Biol *9*, 227-236.
Jaspersen, S.L., Charles, J.F., Tinker-Kulberg, R.L., and Morgan, D.O. (1998). A late mitotic regulatory network controlling cyclin destruction in Saccharomyces cerevisiae. Mol Biol Cell *9*, 2803-2817.
Jaspersen, S.L., and Morgan, D.O. (2000). Cdc14 activates cdc15 to promote mitotic exit in budding yeast. Curr Biol *10*, 615-618.
Jensen, S., Geymonat, M., and Johnston, L.H. (2002). Mitotic exit: delaying the end without FEAR. Curr Biol *12*, R221-223.
Johnston, G.C., Pringle, J.R., and Hartwell, L.H. (1977). Coordination of growth with cell division in the yeast Saccharomyces cerevisiae. Exp Cell Res *105*, 79-98.
Juanes, M.A., ten Hoopen, R., and Segal, M. (2011). Ase1p phosphorylation by cyclin-dependent kinase promotes correct spindle assembly in S. cerevisiae. Cell Cycle *10*, 1988-1997.

Kaback, D.B., and Feldberg, L.R. (1985). Saccharomyces cerevisiae exhibits a sporulation-specific temporal pattern of transcript accumulation. Mol Cell Biol *5*, 751-761.
Kamieniecki, R.J., Liu, L., and Dawson, D.S. (2005). FEAR but not MEN genes are required for exit from meiosis I. Cell Cycle *4*, 1093-1098.
Kapuy, O., He, E., Uhlmann, F., and Novak, B. (2009). Mitotic exit in mammalian cells. Mol Syst Biol *5*, 324.
Karpenshif, Y., and Bernstein, K.A. (2012). From yeast to mammals: recent advances in genetic control of homologous recombination. DNA Repair (Amst) *11*, 781-788.
Kassir, Y., Adir, N., Boger-Nadjar, E., Raviv, N.G., Rubin-Bejerano, I., Sagee, S., and Shenhar, G. (2003). Transcriptional regulation of meiosis in budding yeast. International Review of Cytology - a Survey of Cell Biology, Vol 224 *224*, 111-171.
Kassir, Y., and Simchen, G. (1991). Monitoring meiosis and sporulation in Saccharomyces cerevisiae. Methods Enzymol *194*, 94-110.
Katis, V.L., Galova, M., Rabitsch, K.P., Gregan, J., and Nasmyth, K. (2004a). Maintenance of cohesin at centromeres after meiosis I in budding yeast requires a kinetochore-associated protein related to MEI-S332. Curr Biol *14*, 560-572.
Katis, V.L., Lipp, J.J., Imre, R., Bogdanova, A., Okaz, E., Habermann, B., Mechtler, K., Nasmyth, K., and Zachariae, W. (2010). Rec8 phosphorylation by casein kinase 1 and Cdc7-Dbf4 kinase regulates cohesin cleavage by separase during meiosis. Dev Cell *18*, 397-409.
Katis, V.L., Matos, J., Mori, S., Shirahige, K., Zachariae, W., and Nasmyth, K. (2004b). Spo13 facilitates monopolin recruitment to kinetochores and regulates maintenance of centromeric cohesion during yeast meiosis. Curr Biol *14*, 2183-2196.
Keeney, S. (2009). Meiosis. Volume 1, molecular and genetic methods. Preface. Methods Mol Biol *557*, v-vi.
Keeney, S., Giroux, C.N., and Kleckner, N. (1997). Meiosis-specific DNA double-strand breaks are catalyzed by Spo11, a member of a widely conserved protein family. Cell *88*, 375-384.
Keeney, S., and Neale, M.J. (2006). Initiation of meiotic recombination by formation of DNA double-strand breaks: mechanism and regulation. Biochem Soc Trans *34*, 523-525.
Kerr, G.W., Sarkar, S., Tibbles, K.L., Petronczki, M., Millar, J.B., and Arumugam, P. (2011). Meiotic nuclear divisions in budding yeast require PP2A(Cdc55)-mediated antagonism of Net1 phosphorylation by Cdk. J Cell Biol *193*, 1157-1166.
Kim, K.P., Weiner, B.M., Zhang, L., Jordan, A., Dekker, J., and Kleckner, N. (2010). Sister cohesion and structural axis components mediate homolog bias of meiotic recombination. Cell *143*, 924-937.
Kitajima, T.S., Kawashima, S.A., and Watanabe, Y. (2004). The conserved kinetochore protein shugoshin protects centromeric cohesion during meiosis. Nature *427*, 510-517.
Klapholz, S., and Esposito, R.E. (1980a). Isolation of SPO12-1 and SPO13-1 from a natural variant of yeast that undergoes a single meiotic division. Genetics *96*, 567-588.

Klapholz, S., and Esposito, R.E. (1980b). Recombination and chromosome segregation during the single division meiosis in SPO12-1 and SPO13-1 diploids. Genetics *96*, 589-611.
Klein, F., Mahr, P., Galova, M., Buonomo, S.B., Michaelis, C., Nairz, K., and Nasmyth, K. (1999). A central role for cohesins in sister chromatid cohesion, formation of axial elements, and recombination during yeast meiosis. Cell *98*, 91-103.
Knapp, D., Bhoite, L., Stillman, D.J., and Nasmyth, K. (1996). The transcription factor Swi5 regulates expression of the cyclin kinase inhibitor p40SIC1. Mol Cell Biol *16*, 5701-5707.
Koivomagi, M., Valk, E., Venta, R., Iofik, A., Lepiku, M., Morgan, D.O., and Loog, M. (2011). Dynamics of Cdk1 substrate specificity during the cell cycle. Mol Cell *42*, 610-623.
Kominami, K., Sakata, Y., Sakai, M., and Yamashita, I. (1993). Protein kinase activity associated with the IME2 gene product, a meiotic inducer in the yeast Saccharomyces cerevisiae. Biosci Biotechnol Biochem *57*, 1731-1735.
Kramer, E.R., Scheuringer, N., Podtelejnikov, A.V., Mann, M., and Peters, J.M. (2000). Mitotic regulation of the APC activator proteins CDC20 and CDH1. Mol Biol Cell *11*, 1555-1569.
Kuhne, C., and Linder, P. (1993). A new pair of B-type cyclins from Saccharomyces cerevisiae that function early in the cell cycle. EMBO J *12*, 3437-3447.
Labbe, J.C., Picard, A., Peaucellier, G., Cavadore, J.C., Nurse, P., and Doree, M. (1989). Purification of MPF from starfish: identification as the H1 histone kinase p34cdc2 and a possible mechanism for its periodic activation. Cell *57*, 253-263.
Lew, D.J., and Reed, S.I. (1993). Morphogenesis in the yeast cell cycle: regulation by Cdc28 and cyclins. J Cell Biol *120*, 1305-1320.
Li, J., Meyer, A.N., and Donoghue, D.J. (1997). Nuclear localization of cyclin B1 mediates its biological activity and is regulated by phosphorylation. Proc Natl Acad Sci U S A *94*, 502-507.
Liang, F.S., Jin, F.Z., Liu, H., and Wang, Y.C. (2009). The Molecular Function of the Yeast Polo-like Kinase Cdc5 in Cdc14 Release during Early Anaphase. Molecular Biology of the Cell *20*, 3671-3679.
Lindner, K., Gregan, J., Montgomery, S., and Kearsey, S.E. (2002). Essential role of MCM proteins in premeiotic DNA replication. Mol Biol Cell *13*, 435-444.
Lohka, M.J., Hayes, M.K., and Maller, J.L. (1988). Purification of maturation-promoting factor, an intracellular regulator of early mitotic events. Proc Natl Acad Sci U S A *85*, 3009-3013.
Longhese, M.P., Foiani, M., Muzi-Falconi, M., Lucchini, G., and Plevani, P. (1998). DNA damage checkpoint in budding yeast. EMBO J *17*, 5525-5528.
Loog, M., and Morgan, D.O. (2005). Cyclin specificity in the phosphorylation of cyclin-dependent kinase substrates. Nature *434*, 104-108.
Lopez-Aviles, S., Kapuy, O., Novak, B., and Uhlmann, F. (2009). Irreversibility of mitotic exit is the consequence of systems-level feedback. Nature *459*, 592-595.
Lowery, D.M., Mohammad, D.H., Elia, A.E., and Yaffe, M.B. (2004). The Polo-box domain: a molecular integrator of mitotic kinase cascades and Polo-like kinase function. Cell Cycle *3*, 128-131.
Lu, Y., and Cross, F. (2009). Mitotic exit in the absence of separase activity. Molecular Biology of the Cell *20*, 1576-1579.

Lu, Y., and Cross, F. (2010). Periodic Cyclin-CDK activity entrains an autonomous Cdc14 release Oscillator. Cell *141*, 268-279.
Lydall, D., Nikolsky, Y., Bishop, D.K., and Weinert, T. (1996). A meiotic recombination checkpoint controlled by mitotic checkpoint genes. Nature *383*, 840-843.
Maekawa, H., Priest, C., Lechner, J., Pereira, G., and Schiebel, E. (2007). The yeast centrosome translates the positional information of the anaphase spindle into a cell cycle signal. J Cell Biol *179*, 423-436.
Mah, A.S., Jang, J., and Deshaies, R.J. (2001). Protein kinase Cdc15 activates the Dbf2-Mob1 kinase complex. Proc Natl Acad Sci U S A *98*, 7325-7330.
Malmanche, N., Maia, A., and Sunkel, C.E. (2006). The spindle assembly checkpoint: preventing chromosome mis-segregation during mitosis and meiosis. FEBS Lett *580*, 2888-2895.
Manfrini, N., Guerini, I., Citterio, A., Lucchini, G., and Longhese, M.P. (2010). Processing of meiotic DNA double strand breaks requires cyclin-dependent kinase and multiple nucleases. J Biol Chem *285*, 11628-11637.
Marston, A.L., and Amon, A. (2004). Meiosis: cell-cycle controls shuffle and deal. Nat Rev Mol Cell Biol *5*, 983-997.
Marston, A.L., Lee, B.H., and Amon, A. (2003). The Cdc14 phosphatase and the FEAR network control meiotic spindle disassembly and chromosome segregation. Dev Cell *4*, 711-726.
Masui, Y., and Markert, C.L. (1971). Cytoplasmic control of nuclear behavior during meiotic maturation of frog oocytes. J Exp Zool *177*, 129-145.
Masumoto, H., Muramatsu, S., Kamimura, Y., and Araki, H. (2002). S-Cdk-dependent phosphorylation of Sld2 essential for chromosomal DNA replication in budding yeast. Nature *415*, 651-655.
Matos, J., Lipp, J.J., Bogdanova, A., Guillot, S., Okaz, E., Junqueira, M., Shevchenko, A., and Zachariae, W. (2008). Dbf4-dependent CDC7 kinase links DNA replication to the segregation of homologous chromosomes in meiosis I. Cell *135*, 662-678.
Mendenhall, M.D., and Hodge, A.E. (1998). Regulation of Cdc28 cyclin-dependent protein kinase activity during the cell cycle of the yeast Saccharomyces cerevisiae. Microbiol Mol Biol Rev *62*, 1191-1243.
Michaelis, C., Ciosk, R., and Nasmyth, K. (1997). Cohesins: chromosomal proteins that prevent premature separation of sister chromatids. Cell *91*, 35-45.
Miller, M.E., and Cross, F.R. (2000). Distinct subcellular localization patterns contribute to functional specificity of the Cln2 and Cln3 cyclins of Saccharomyces cerevisiae. Mol Cell Biol *20*, 542-555.
Moffat, J., and Andrews, B. (2004). Late-G1 cyclin-CDK activity is essential for control of cell morphogenesis in budding yeast. Nat Cell Biol *6*, 59-66.
Mohl, D.A., Huddleston, M.J., Collingwood, T.S., Annan, R.S., and Deshaies, R.J. (2009). Dbf2-Mob1 drives relocalization of protein phosphatase Cdc14 to the cytoplasm during exit from mitosis. J Cell Biol *184*, 527-539.
Moore, M., Shin, M.E., Bruning, A., Schindler, K., Vershon, A., and Winter, E. (2007). Arg-Pro-X-Ser/Thr is a consensus phosphoacceptor sequence for the meiosis-specific Ime2 protein kinase in Saccharomyces cerevisiae. Biochemistry *46*, 271-278.
Morgan, D. (2007). The Cell Cycle: Principles of Control. Oxford University Press.
Morgan, D.O. (1995). Principles of CDK regulation. Nature *374*, 131-134.

Mortensen, E.M., Haas, W., Gygi, M., Gygi, S.P., and Kellogg, D.R. (2005). Cdc28-dependent regulation of the Cdc5/Polo kinase. Curr Biol *15*, 2033-2037.
Murray, A.W., and Kirschner, M.W. (1989). Dominoes and clocks: the union of two views of the cell cycle. Science *246*, 614-621.
Nachman, I., Regev, A., and Ramanathan, S. (2007). Dissecting timing variability in yeast meiosis. Cell *131*, 544-556.
Nasmyth, K. (1993). Control of the yeast cell cycle by the Cdc28 protein kinase. Curr Opin Cell Biol *5*, 166-179.
Nasmyth, K. (1995). Evolution of the cell cycle. Philos Trans R Soc Lond B Biol Sci *349*, 271-281.
Nasmyth, K. (1996). At the heart of the budding yeast cell cycle. Trends Genet *12*, 405-412.
Neale, M.J., and Keeney, S. (2006). Clarifying the mechanics of DNA strand exchange in meiotic recombination. Nature *442*, 153-158.
Neiman, A.M. (2011). Sporulation in the budding yeast Saccharomyces cerevisiae. Genetics *189*, 737-765.
Nicklas, R.B., and Koch, C.A. (1969). Chromosome micromanipulation. 3. Spindle fiber tension and the reorientation of mal-oriented chromosomes. J Cell Biol *43*, 40-50.
Novak, B., and Tyson, J.J. (1993). Numerical analysis of a comprehensive model of M-phase control in Xenopus oocyte extracts and intact embryos. J Cell Sci *106 (Pt 4)*, 1153-1168.
Novak, B., Tyson, J.J., Gyorffy, B., and Csikasz-Nagy, A. (2007). Irreversible cell-cycle transitions are due to systems-level feedback. Nature Cell Biology *9*, 724-728.
Nowak, M.A., Komarova, N.L., Sengupta, A., Jallepalli, P.V., Shih Ie, M., Vogelstein, B., and Lengauer, C. (2002). The role of chromosomal instability in tumor initiation. Proc Natl Acad Sci U S A *99*, 16226-16231.
Nurse, P. (1990). Universal control mechanism regulating onset of M-phase. Nature *344*, 503-508.
Nurse, P., Thuriaux, P., and Nasmyth, K. (1976). Genetic control of the cell division cycle in the fission yeast Schizosaccharomyces pombe. Mol Gen Genet *146*, 167-178.
Oelschlaegel, T., Schwickart, M., Matos, J., Bogdanova, A., Camasses, A., Havlis, J., Shevchenko, A., and Zachariae, W. (2005). The yeast APC/C subunit Mnd2 prevents premature sister chromatid separation triggered by the meiosis-specific APC/C-Ama1. Cell *120*, 773-788.
Ofir, Y., Sagee, S., Guttmann-Raviv, N., Pnueli, L., and Kassir, Y. (2004). The role and regulation of the preRC component Cdc6 in the initiation of premeiotic DNA replication. Mol Biol Cell *15*, 2230-2242.
Okaz, E., Arguello-Miranda, O., Bogdanova, A., Vinod, P.K., Lipp, J.J., Markova, Z., Zagoriy, I., Novak, B., and Zachariae, W. (2012). Meiotic prophase requires proteolysis of M phase regulators mediated by the meiosis-specific APC/CAma1. Cell *151*, 603-618.
Orlando, D.A., Lin, C.Y., Bernard, A., Wang, J.Y., Socolar, J.E., Iversen, E.S., Hartemink, A.J., and Haase, S.B. (2008). Global control of cell-cycle transcription by coupled CDK and network oscillators. Nature *453*, 944-947.
Pablo-Hernando, M.E., Arnaiz-Pita, Y., Nakanishi, H., Dawson, D.S., del Rey, F., Neiman, A.M., and Vasquez de Aldana, C.R. (2007). Cdc15 is required for Spore

Morphogenesis Independently of Cdc14 in Saccharomyces cerevisiae. Genetics *177*, 281-293.
Padmore, R., Cao, L., and Kleckner, N. (1991). Temporal comparison of recombination and synaptonemal complex formation during meiosis in S. cerevisiae. Cell *66*, 1239-1256.
Pak, J., and Segall, J. (2002a). Regulation of the premiddle and middle phases of expression of the NDT80 gene during sporulation of Saccharomyces cerevisiae. Mol Cell Biol *22*, 6417-6429.
Pak, J., and Segall, J. (2002b). Role of Ndt80, Sum1, and Swe1 as targets of the meiotic recombination checkpoint that control exit from pachytene and spore formation in Saccharomyces cerevisiae. Mol Cell Biol *22*, 6430-6440.
Paweletz, N. (2001). Walther Flemming: pioneer of mitosis research. Nat Rev Mol Cell Biol *2*, 72-75.
Pellman, D. (2007). Cell biology: aneuploidy and cancer. Nature *446*, 38-39.
Pereira, G., Hofken, T., Grindlay, J., Manson, C., and Schiebel, E. (2000). The Bub2p spindle checkpoint links nuclear migration with mitotic exit. Mol Cell *6*, 1-10.
Pereira, G., Manson, C., Grindlay, J., and Schiebel, E. (2002). Regulation of the Bfa1p-Bub2p complex at spindle pole bodies by the cell cycle phosphatase Cdc14p. J Cell Biol *157*, 367-379.
Pereira, G., and Schiebel, E. (2003). Separase regulates INCENP-Aurora B anaphase spindle function through Cdc14. Science *302*, 2120-2124.
Perez-Hidalgo, L., Moreno, S., and C., M.-C. (2007). Modified Cell Cycle Regulation in Meiosis. Genome Dynamics and Stability *Recombination and meiosis, 2*, 307-353.
Peters, J.M. (1998). SCF and APC: the Yin and Yang of cell cycle regulated proteolysis. Curr Opin Cell Biol *10*, 759-768.
Peters, J.M. (2002). The anaphase-promoting complex: proteolysis in mitosis and beyond. Mol Cell *9*, 931-943.
Peterson, J.B., and Ris, H. (1976). Electron-microscopic study of the spindle and chromosome movement in the yeast Saccharomyces cerevisiae. J Cell Sci *22*, 219-242.
Petronczki, M., Matos, J., Mori, S., Gregan, J., Bogdanova, A., Schwickart, M., Mechtler, K., Shirahige, K., Zachariae, W., and Nasmyth, K. (2006). Monopolar attachment of sister kinetochores at meiosis I requires casein kinase 1. Cell *126*, 1049-1064.
Pierce, M., Benjamin, K.R., Montano, S.P., Georgiadis, M.M., Winter, E., and Vershon, A.K. (2003). Sum1 and Ndt80 proteins compete for binding to middle sporulation element sequences that control meiotic gene expression. Mol Cell Biol *23*, 4814-4825.
Pomerening, J.R., Sontag, E.D., and Ferrell, J.E., Jr. (2003). Building a cell cycle oscillator: hysteresis and bistability in the activation of Cdc2. Nat Cell Biol *5*, 346-351.
Potapova, T.A., Daum, J.R., Pittman, B.D., Hudson, J.R., Jones, T.N., Satinover, D.L., Stukenberg, P.T., and Gorbsky, G.J. (2006). The reversibility of mitotic exit in vertebrate cells. Nature *440*, 954-958.
Queralt, E., Lehane, C., Novak, B., and Uhlmann, F. (2006). Downregulation of PP2A(Cdc55) phosphatase by separase initiates mitotic exit in budding yeast. Cell *125*, 719-732.

Queralt, E., and Uhlmann, F. (2008). Separase cooperates with Zds1 and Zds2 to activate Cdc14 phosphatase in early anaphase. Journal of Cell Biology *182*, 873-883.
Rabitsch, K.P., Petronczki, M., Javerzat, J.P., Genier, S., Chwalla, B., Schleiffer, A., Tanaka, T.U., and Nasmyth, K. (2003). Kinetochore recruitment of two nucleolar proteins is required for homolog segregation in meiosis I. Developmental Cell *4*, 535-548.
Rahal, R., and Amon, A. (2008a). Mitotic CDKs control the metaphase-anaphase transition and trigger spindle elongation. Genes Dev *22*, 1534-1548.
Rahal, R., and Amon, A. (2008b). The Polo-like kinase Cdc5 interacts with FEAR network components and Cdc14. Cell Cycle *7*, 3262-3272.
Ray, D., Su, Y., and Ye, P. (2013). Dynamic modeling of yeast meiotic initiation. BMC Syst Biol *7*, 37.
Reed, S.I. (2003). Ratchets and clocks: the cell cycle, ubiquitylation and protein turnover. Nat Rev Mol Cell Biol *4*, 855-864.
Rice, L.M., Plakas, C., and Nickels, J.T., Jr. (2005). Loss of meiotic rereplication block in Saccharomyces cerevisiae cells defective in Cdc28p regulation. Eukaryot Cell *4*, 55-62.
Richardson, H., Lew, D.J., Henze, M., Sugimoto, K., and Reed, S.I. (1992). Cyclin-B homologs in Saccharomyces cerevisiae function in S phase and in G2. Genes Dev *6*, 2021-2034.
Richardson, H.E., Wittenberg, C., Cross, F., and Reed, S.I. (1989). An essential G1 function for cyclin-like proteins in yeast. Cell *59*, 1127-1133.
Riedel, C.G., Katis, V.L., Katou, Y., Mori, S., Itoh, T., Helmhart, W., Galova, M., Petronczki, M., Gregan, J., Cetin, B.*, et al.* (2006). Protein phosphatase 2A protects centromeric sister chromatid cohesion during meiosis I. Nature *441*, 53-61.
Roeder, G.S., and Bailis, J.M. (2000). The pachytene checkpoint. Trends Genet *16*, 395-403.
Rudner, A.D., and Murray, A.W. (1996). The spindle assembly checkpoint. Curr Opin Cell Biol *8*, 773-780.
Rudner, A.D., and Murray, A.W. (2000). Phosphorylation by Cdc28 activates the Cdc20-dependent activity of the anaphase-promoting complex. J Cell Biol *149*, 1377-1390.
Satyanarayana, A., and Kaldis, P. (2009). Mammalian cell-cycle regulation: several Cdks, numerous cyclins and diverse compensatory mechanisms. Oncogene *28*, 2925-2939.
Sawarynski, K.E., Najor, N.A., Kepsel, A.C., and Brush, G.S. (2009). Sic1-induced DNA rereplication during meiosis. Proc Natl Acad Sci U S A *106*, 232-237.
Schindler, K., and Winter, E. (2006). Phosphorylation of Ime2 regulates meiotic progression in Saccharomyces cerevisiae. J Biol Chem *281*, 18307-18316.
Schwab, M., Lutum, A.S., and Seufert, W. (1997). Yeast Hct1 is a regulator of Clb2 cyclin proteolysis. Cell *90*, 683-693.
Schwartz, E.K., and Heyer, W.D. (2011). Processing of joint molecule intermediates by structure-selective endonucleases during homologous recombination in eukaryotes. Chromosoma *120*, 109-127.
Schwob, E., and Nasmyth, K. (1993). CLB5 and CLB6, a new pair of B cyclins involved in DNA replication in Saccharomyces cerevisiae. Genes Dev *7*, 1160-1175.

Sedgwick, C., Rawluk, M., Decesare, J., Raithatha, S., Wohlschlegel, J., Semchuk, P., Ellison, M., Yates, J., 3rd, and Stuart, D. (2006). Saccharomyces cerevisiae Ime2 phosphorylates Sic1 at multiple PXS/T sites but is insufficient to trigger Sic1 degradation. Biochem J *399*, 151-160.
Sha, W., Moore, J., Chen, K., Lassaletta, A.D., Yi, C.S., Tyson, J.J., and Sible, J.C. (2003). Hysteresis drives cell-cycle transitions in Xenopus laevis egg extracts. Proc Natl Acad Sci U S A *100*, 975-980.
Sheu, Y.J., and Stillman, B. (2006). Cdc7-Dbf4 phosphorylates MCM proteins via a docking site-mediated mechanism to promote S phase progression. Mol Cell *24*, 101-113.
Shin, M.E., Skokotas, A., and Winter, E. (2010). The Cdk1 and Ime2 protein kinases trigger exit from meiotic prophase in Saccharomyces cerevisiae by inhibiting the Sum1 transcriptional repressor. Mol Cell Biol *30*, 2996-3003.
Shirayama, M., Toth, A., Galova, M., and Nasmyth, K. (1999). APC(Cdc20) promotes exit from mitosis by destroying the anaphase inhibitor Pds1 and cyclin Clb5. Nature *402*, 203-207.
Shou, W., Azzam, R., Chen, S.L., Huddleston, M.J., Baskerville, C., Charbonneau, H., Annan, R.S., Carr, S.A., and Deshaies, R.J. (2002). Cdc5 influences phosphorylation of Net1 and disassembly of the RENT complex. BMC Mol Biol *3*, 3.
Shou, W., and Deshaies, R.J. (2002). Multiple telophase arrest bypassed (tab) mutants alleviate the essential requirement for Cdc15 in exit from mitosis in S.cerevisiae. BMC Genetics *3*.
Shou, W., Sakamoto, K.M., Keener, J., Morimoto, K.W., Traverso, E.E., Azzam, R., Hoppe, G.J., Feldman, R.M., DeModena, J., Moazed, D*., et al.* (2001). Net1 stimulates RNA polymerase I transcription and regulates nucleolar structure independently of controlling mitotic exit. Mol Cell *8*, 45-55.
Shou, W., Seol, J.H., Shevchenko, A., Baskerville, C., Moazed, D., Chen, Z.W., Jang, J., Charbonneau, H., and Deshaies, R.J. (1999). Exit from mitosis is triggered by Tem1-dependent release of the protein phosphatase Cdc14 from nucleolar RENT complex. Cell *97*, 233-244.
Simchen, G. (2009). Commitment to meiosis: what determines the mode of division in budding yeast? Bioessays *31*, 169-177.
Skotheim, J.M., Di Talia, S., Siggia, E.D., and Cross, F.R. (2008). Positive feedback of G1 cyclins ensures coherent cell cycle entry. Nature *454*, 291-296.
Smeets, M.F., and Segal, M. (2002). Spindle polarity in S. cerevisiae: MEN can tell. Cell Cycle *1*, 308-311.
Smith, K.N., Penkner, A., Ohta, K., Klein, F., and Nicolas, A. (2001). B-type cyclins CLB5 and CLB6 control the initiation of recombination and synaptonemal complex formation in yeast meiosis. Curr Biol *11*, 88-97.
Sopko, R., Raithatha, S., and Stuart, D. (2002). Phosphorylation and maximal activity of Saccharomyces cerevisiae meiosis-specific transcription factor Ndt80 is dependent on Ime2. Mol Cell Biol *22*, 7024-7040.
Sourirajan, A., and Lichten, M. (2008). Polo-like kinase Cdc5 drives exit from pachytene during budding yeast meiosis. Genes Dev *22*, 2627-2632.
Stegmeier, F., and Amon, A. (2004). Closing mitosis: the functions of the Cdc14 phosphatase and its regulation. Annu Rev Genet *38*, 203-232.
Stegmeier, F., Huang, J., Rahal, R., Zmolik, J., Moazed, D., and Amon, A. (2004). The replication fork block protein Fob1 functions as a negative regulator of the FEAR network. Current Biology *14*, 467-480.

Stegmeier, F., Visintin, R., and Amon, A. (2002). Separase, polo kinase, the kinetochore protein Slk19 and Spo12 function in a network that controls Cdc14 localization during early anaphase. Cell *108*, 207-220.
Stern, B.M. (2003). Fearless in Meiosis. Molecular Cell *11*, 1123-1125.
Strich, R., Mallory, M.J., Jarnik, M., and Cooper, K.F. (2004). Cyclin B-cdk activity stimulates meiotic rereplication in budding yeast. Genetics *167*, 1621-1628.
Stuart, D., and Wittenberg, C. (1995). CLN3, not positive feedback, determines the timing of CLN2 transcription in cycling cells. Genes Dev *9*, 2780-2794.
Stuart, D., and Wittenberg, C. (1998). CLB5 and CLB6 are required for premeiotic DNA replication and activation of the meiotic S/M checkpoint. Genes Dev *12*, 2698-2710.
Sullivan, M., Higuchi, T., Katis, V.L., and Uhlmann, F. (2004). Cdc14 phosphatase induces rDNA condensation and resolves cohesin-independent cohesion during budding yeast anaphase. Cell *117*, 471-482.
Sullivan, M., and Uhlmann, F. (2003). A non-proteolytic function of separase links the onset of anaphase to mitotic exit. Nature Cell Biology *5*, 249-254.
Takeda, D.Y., Wohlschlegel, J.A., and Dutta, A. (2001). A bipartite substrate recognition motif for cyclin-dependent kinases. J Biol Chem *276*, 1993-1997.
Thornton, B.R., and Toczyski, D.P. (2003). Securin and B-cyclin/CDK are the only essential targets of the APC. Nat Cell Biol *5*, 1090-1094.
Tomson, B.N., Rahal, R., Reiser, V., Monje-Casas, F., Mekhail, K., Moazed, D., and Amon, A. (2009). Regulation of Spo12 Phosphorylation and Its Essential Role in the FEAR Network. Current Biology *19*, 449-460.
Toth, A., Rabitsch, K.P., Galova, M., Schleiffer, A., Buonomo, S.B., and Nasmyth, K. (2000). Functional genomics identifies monopolin: a kinetochore protein required for segregation of homologs during meiosis i. Cell *103*, 1155-1168.
Tyers, M. (1996). The cyclin-dependent kinase inhibitor p40SIC1 imposes the requirement for Cln G1 cyclin function at Start. Proc Natl Acad Sci U S A *93*, 7772-7776.
Tyers, M., Fitch, I., Tokiwa, G., Dahmann, C., Nash, R., Linskens, M., and Futcher, B. (1991). Characterization of G1 and mitotic cyclins of budding yeast. Cold Spring Harb Symp Quant Biol *56*, 21-32.
Tyson, J.J., Chen, K.C., and Novak, B. (2003). Sniffers, buzzers, toggles and blinkers: dynamics of regulatory and signaling pathways in the cell. Current Opinion in Cell Biology *15*, 221-231.
Tyson, J.J., and Novak, B. (2008). Temporal organization of the cell cycle. Current Biology *18*, R759-R768.
Uhlmann, F., Lottspeich, F., and Nasmyth, K. (1999). Sister-chromatid separation at anaphase onset is promoted by cleavage of the cohesin subunit Scc1. Nature *400*, 37-42.
Uhlmann, F., Wernic, D., Poupart, M.A., Koonin, E.V., and Nasmyth, K. (2000). Cleavage of cohesin by the CD clan protease separin triggers anaphase in yeast. Cell *103*, 375-386.
Valerio-Santiago, M., and Monje-Casas, F. (2011). Tem1 localization to the spindle pole bodies is essential for mitotic exit and impairs spindle checkpoint function. J Cell Biol *192*, 599-614.
Varetti, G., and Musacchio, A. (2008). The spindle assembly checkpoint. Curr Biol *18*, R591-595.

Verma, R., Annan, R.S., Huddleston, M.J., Carr, S.A., Reynard, G., and Deshaies, R.J. (1997). Phosphorylation of Sic1p by G1 Cdk required for its degradation and entry into S phase. Science *278*, 455-460.
Vinod, P.K., Freire, P., Rattani, A., Ciliberto, A., Uhlmann, F., and Novak, B. (2011). Computational modelling of mitotic exit in budding yeast: the role of separase and Cdc14 endocycles. J R Soc Interface *8*, 1128-1141.
Visintin, R., and Amon, A. (2001). Regulation of the mitotic exit protein kinases Cdc15 and Dbf2. Mol Biol Cell *12*, 2961-2974.
Visintin, R., Craig, K., Hwang, E.S., Prinz, S., Tyers, M., and Amon, A. (1998). The phosphatase Cdc14 triggers mitotic exit by reversal of Cdk-dependent phosphorylation. Mol Cell *2*, 709-718.
Visintin, R., Hwang, E.S., and Amon, A. (1999). Cfi1 prevents premature exit from mitosis by anchoring Cdc14 phosphatase in the nucleolus. Nature *398*, 818-823.
Visintin, R., Prinz, S., and Amon, A. (1997). CDC20 and CDH1: a family of substrate-specific activators of APC-dependent proteolysis. Science *278*, 460-463.
Wan, L., Niu, H., Futcher, B., Zhang, C., Shokat, K.M., Boulton, S.J., and Hollingsworth, N.M. (2008). Cdc28-Clb5 (CDK-S) and Cdc7-Dbf4 (DDK) collaborate to initiate meiotic recombination in yeast. Genes Dev *22*, 386-397.
Wang, Y., and Burke, D.J. (1997). Cdc55p, the B-type regulatory subunit of protein phosphatase 2A, has multiple functions in mitosis and is required for the kinetochore/spindle checkpoint in Saccharomyces cerevisiae. Mol Cell Biol *17*, 620-626.
Wang, Y., and Ng, T.Y. (2006). Phosphatase 2A negatively regulates mitotic exit in Saccharomyces cerevisiae. Mol Biol Cell *17*, 80-89.
Weinert, T.A., Kiser, G.L., and Hartwell, L.H. (1994). Mitotic checkpoint genes in budding yeast and the dependence of mitosis on DNA replication and repair. Genes Dev *8*, 652-665.
Williamson, D.H., Johnston, L.H., Fennell, D.J., and Simchen, G. (1983). The timing of the S phase and other nuclear events in yeast meiosis. Exp Cell Res *145*, 209-217.
Winey, M., and O'Toole, E.T. (2001). The spindle cycle in budding yeast. Nat Cell Biol *3*, E23-27.
Winter, E. (2012). The Sum1/Ndt80 transcriptional switch and commitment to meiosis in Saccharomyces cerevisiae. Microbiol Mol Biol Rev *76*, 1-15.
Woodbury, E.L., and Morgan, D.O. (2007). Cdk and APC activities limit the spindle-stabilizing function of Fin1 to anaphase. Nat Cell Biol *9*, 106-112.
Xu, L., Ajimura, M., Padmore, R., Klein, C., and Kleckner, N. (1995). NDT80, a meiosis-specific gene required for exit from pachytene in Saccharomyces cerevisiae. Mol Cell Biol *15*, 6572-6581.
Yellman, C.M., and Burke, D.J. (2006). The role of Cdc55 in the spindle checkpoint is through regulation of mitotic exit in Saccharomyces cerevisiae. Mol Biol Cell *17*, 658-666.
Yokobayashi, S., and Watanabe, Y. (2005). The kinetochore protein Moa1 enables cohesion-mediated monopolar attachment at meiosis I. Cell *123*, 803-817.
Yoshida, S., and Toh-e, A. (2001). Regulation of the localization of Dbf2 and mob1 during cell division of saccharomyces cerevisiae. Genes Genet Syst *76*, 141-147.

Yoshida, S., and Toh-e, A. (2002). Budding yeast Cdc5 phosphorylates Net1 and assists Cdc14 release from the nucleolus. Biochem Biophys Res Commun *294*, 687-691.
Zachariae, W., and Nasmyth, K. (1999). Whose end is destruction: cell division and the anaphase-promoting complex. Genes & Development *13*, 2039-2058.
Zachariae, W., Schwab, M., Nasmyth, K., and Seufert, W. (1998). Control of cyclin ubiquitination by CDK-regulated binding of Hct1 to the anaphase promoting complex. Science *282*, 1721-1724.
Zhou, Y., Ching, Y.P., Chun, A.C., and Jin, D.Y. (2003). Nuclear localization of the cell cycle regulator CDH1 and its regulation by phosphorylation. J Biol Chem *278*, 12530-12536.
Zou, L., and Stillman, B. (1998). Formation of a preinitiation complex by S-phase cyclin CDK-dependent loading of Cdc45p onto chromatin. Science *280*, 593-596.

9 Appendix

9.1 Modification of Clb1-Myc is not Ama1-dependent

Before the gel shift was shown to be removed by phosphatase (Section 3.4), we examined the possibility of ubiquitinylation. The large, discrete change in gel mobility, rather than smearing or multiple closer bands, seemed to indicate a larger, single modification, such as an ubiquitinylation. The timing of the modification may indicate that Clb1 is ubiquitinylated in meiosis I, but protected from subsequent recognition and degradation by another modification, explaining its continued presence during anaphase (Carlile and Amon, 2008). As the gel shift is apparent in strains depleted of Cdc20, it cannot be caused by Cdc20 dependent ubiquitinylation, and Cdh1 is expected to be inhibited by high CDK activity (Zachariae et al., 1998) during metaphase I. A more likely candidate is Ama1, a meiosis-specific APC activator, known to be capable of ubiquitinylating Clb1 (Cooper et al., 2000). As Ama1 is meiosis specific, this would explain the meiosis specificity of the modification. Ama1 is, like Cdh1, inhibited by CDK phosphorylation (Diamond et al., 2009), and would be unlikely to become active in a strain arrested in metaphase, where CDK activity would remain high. However, changes in Pds1 degradation have been noted in *mnd2Δ* cells before metaphase I of meiosis (Oelschlaegel et al., 2005). This suggests that Ama1 can become active earlier in meiosis I despite the CDK activity, and that the repressive subunit Mnd2 is required for complete inhibition (Oelschlaegel et al., 2005). This leaves open the possibility that Ama1-APC activity could ubiquitinate Clb1 during meiosis I.

To determine if Ama1-dependent ubiquitinylation is involved in the modification, Clb1 gel mobility was monitored in *ama1Δ* cells. P_{CLB2}*CDC20 AMA1*

CLB1-MYC$_9$ and *P*$_{CLB2}$*CDC20 ama1Δ CLB1-MYC*$_9$ cells were induced to go through meiosis by resuspension in SPO media, and samples taken for *in situ* immunofluorescent imaging hourly, and for protein extracts between 5 and 7 hours.

The gel shift was maintained in both strains, appearing at the 7-hour time point (Figure 9-1).

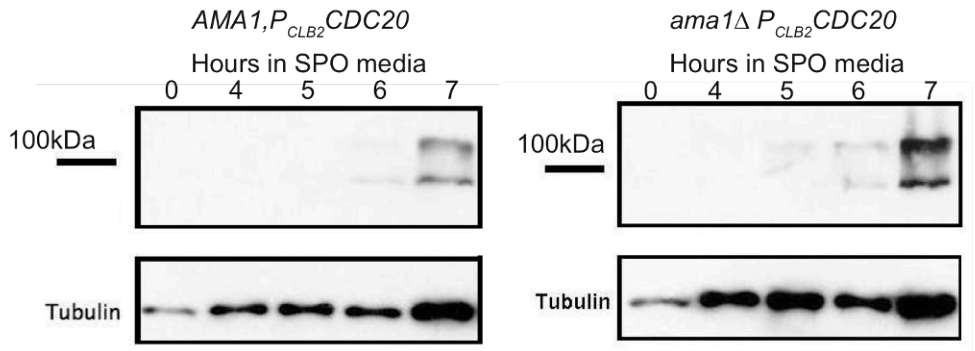

Figure 9-1 ***Clb1 is modified in the nucleus in Ama1-depleted cells arrested in metaphase I.*** *Cultures of cells bearing* AMA1 P$_{CLB2}$CDC20 CLB1-MYC *and* ama1Δ P$_{CLB2}$CDC20 CLB1-MYC *were induced to undergo meiosis by resuspension in SPO media. Samples were taken hourly. Gel mobility of Clb1-Myc*$_9$ *was assayed by subjecting whole cell extracts to SDS-PAGE followed by western blot analysis using anti-myc. Blots were also probed with anti-tubulin.*

Clb1 localisation was examined in fixed cells from samples taken through the time course(Figure 9-2). Both strains showed mostly-nuclear Clb1, although in the case of *ama1*Δ fewer cells have detectable Clb1 signal leading to reduced levels of cells bearing nuclear Clb1. There is no increase in cells bearing dispersed or cytoplamsic Clb1, so we conclude that Ama1 is not required for nuclear concentration of Clb1.

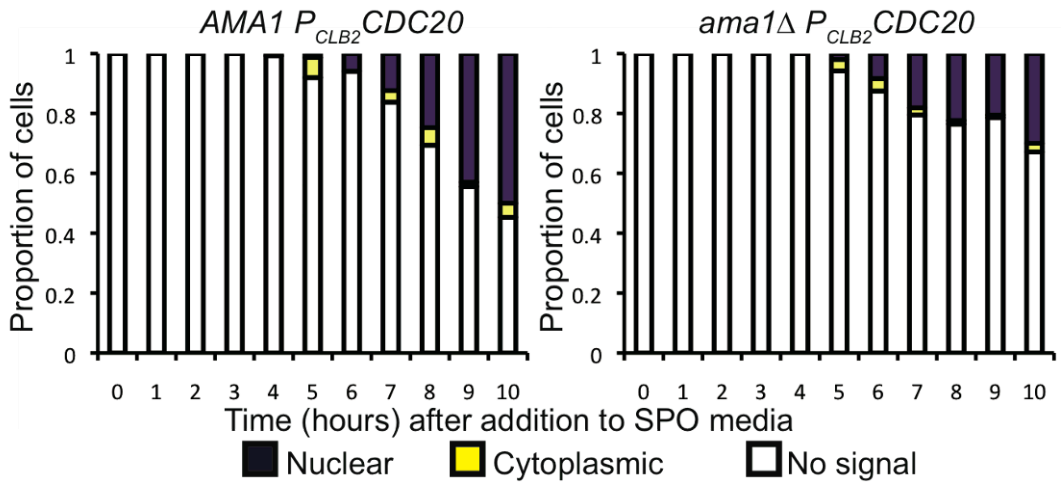

Figure 9-2 ***Clb1 is concentrated in the nucleus in Ama1-depleted cells arrested in metaphase I.*** *Cultures of cells bearing* AMA1 P_{CLB2}CDC20 CLB1-MYC *and* ama1Δ P_{CLB2}CDC20 CLB1-MYC *were induced to undergo meiosis by resuspension in SPO media. Samples were taken hourly and cells were fixed and examined for Clb1-Myc$_9$ localisation by* in situ *immunofluorescence. Proportion of cells with nuclear Clb1 (purple), cytoplasmic Clb1 (yellow) and no Clb1 signals (white) are indicated.*

The modification of Clb1 is not Ama1-dependent. Cdc20 dependent ubiquitinylation is not possible as Cdc20 is under the *CLB2* promoter. Cdh1-dependent ubiquitinylation would be possible as Cdh1 is present in meiosis, but Cdh1 should be inhibited by CDK activity during metaphase. We next considered phosphorylation (Section 3.4).

9.1.1 Attempt to purify Clb1-TAP

Phosphorylation has been shown to be dependent on CDK activity and the presence of Cdc5. However, it hasn't been shown that direct Clb1 phosphorylation by these kinases is responsible for the gel shift. They may activate other kinases, deactivate phosphatases, or they may directly phosphorylate Clb1, creating sites for further phosphorylation by other kinases.

To identify modified sites on Clb1, we attempted to purify Clb1 for mass spectrometric analysis. Cultures of P_{CLB2}*CDC20 CLB1-TAP* cells were induced to enter meiosis and cells pelleted at 7 hours, in order to purify TAP tagged Clb1 from the cell extract. P_{CLB2}*CDC20* strain was used as an untagged control.

The initial attempt was made using mitotic cultures, as it was quicker and easier to grow sufficient cells for optimisation. This resulted in a faint tag-dependent band on silver-stained gels, seen in TCA-concentrated sample of the eluate (Figure 9-3). The untagged strain had no equivalent band, despite heavier non-specific staining. The band was presumed to be faint due to lower expression of Clb1 in mitosis, and the protocol was applied to meiotic cells.

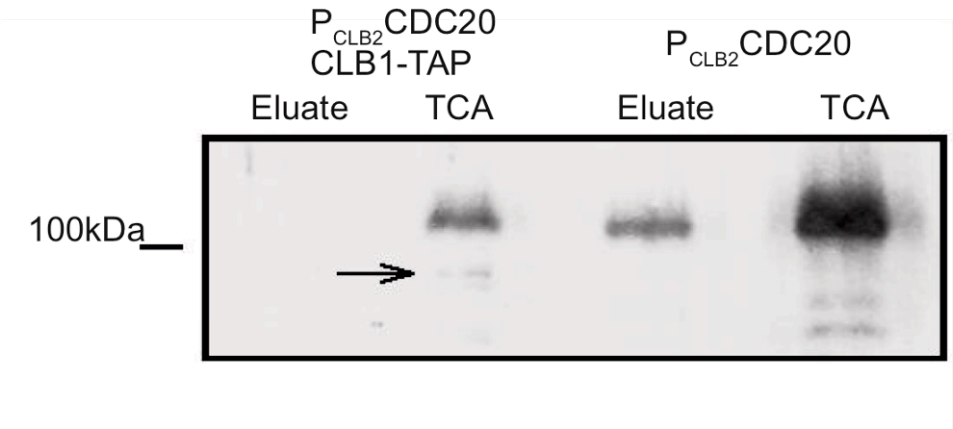

Figure 9-3 ***TAP purification of Clb1-HA.*** *Silver-stained gel showing Clb1-TAP purification from mitotic cultures of* CLB-TAP P_{CLB2}CDC20 *cells. Arrow indicates Tag specific band. Other bars are non-specific binding.*

Repeated attempts using meiotic cultures found that Clb1-TAP was undetectable by western blot after TEV protease treatment, and that the cell extracts showed no upper band after bead-beating. TCA-treated whole cell extracts from the same cultures showed the upper band, confirming that meiotic cultures were in the right stage for assaying Clb1 phosphorylation. Silver stained gels of the final extract also showed no tag-specific bands. Optimisation of the TAP procedure would be time consuming and, as the immunoprecipitation attempts for the phosphatase assay has shown (Section 3.4), could result in a compromise on the amount of retained phosphorylation. Therefore, this avenue of investigation was not pursued.

9.1.2 Effect of localisation mutants on Clb1 phosphorylation in mitosis

The dependence of the phosphorylation on Clb1 nuclear localisation suggests an explanation for its meiosis specificity. The kinase no longer needs to be meiosis-specific itself, if its access to the substrate is controlled in a meiosis-specific manner. To examine this, the phosphorylation status of Clb1-NLS_2-HA_6 in *P_{MET}CDC20* strains arrested in mitotic metaphase was analysed.

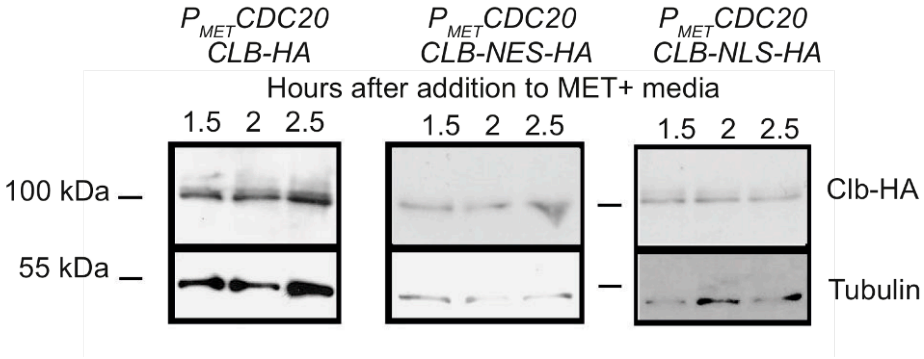

Figure 9-4 ***Nuclear localisation is not sufficient for Clb1 phosphorylation.*** *Cultures of P_{MET}CDC20 CLB1-NLS$_2$-HA$_6$ and P_{MET}CDC20 CLB1-HA$_6$ cells were arrested in metaphase by resuspension in high methionine media. Gel mobility of Clb1-HA$_6$ was assayed by subjecting whole cell extracts to SDS-PAGE followed by western blot analysis using anti-HA. Blots were also probed with anti-tubulin.*

No large gel shift was seen in mitotic metaphase arrest in any strain (Figure 9-4), confirming that nuclear localisation of Clb1-HA$_6$ was not sufficient to induce phosphorylation, but that some meiosis-specific step must be involved. A faint band was seen near to the Clb1 band, turning it into a couplet. The bands were seen in the wild-type Clb1-HA$_6$ strain and NLS-tagged Clb1.

9.2 Models of meiosis

Files are listed for use in winpp or xpp. Parameter names differ slightly from those listed in the paper due to string length limits in winpp, by character removal of non-distinguishing characters i.e. $ka_{cdc20clb1P}$ becomes $ka_{c20clb1P}$.

9.2.1 Initial_Model.ode

```
init Clb1=0, CKIA=1, Cdc20A=0, IEa=0, X=1, Y=1
Clb1' = ksclb1 - (kdclb1+kdclb1CKI*CKIA+kdclb1c20*Cdc20A)*Clb1
CKIA' = (kaCKI+kaCKIc20*Cdc20A)*(CKIt-CKIA)/(JaCKI+CKIt-CKIA)-
        (kiCKIx*X+kiCKIclb*Clb1)*CKIA/(JiCKI+CKIA)
IEa' = kaieclb1*(IEt-IEa)*Clb1/(Jaie+IEt-IEa)-kiie*IEa/(Jiie+IEa)
Cdc20A' = kacdc20ie*IEa*(Cdc20t-Cdc20A)/(Jacdc20+Cdc20t-Cdc20A)-
        kicdc20*Cdc20A/(Jicdc20+Cdc20A)
X' = -kpx*Clb1*X/(Jpx+X)+kdpx*Y*(Xt-X)/(Jdpx+Xt-X)
Y' = -kdy*Cdc20A*Y
p ksclb1=0.01,kdclb1=0.01,kdclb1CKI=1,kdclb1c20=0.2
p kaCKI=0.2,kaCKIc20=0.8,kiCKIx=2,kiCKIclb=15,JaCKI=0.02,JiCKI=0.02
p kacdc20ie=1,kicdc20=0.5,Jacdc20=0.001,Jicdc20=0.001
p kaieclb1=0.1,kiie=0.02, Jaie=0.01, Jiie=0.01
p kpx=0.2,Jpx=0.04,kdpx=0.1,Jdpx=0.04,kdy=0.2
p CKIt=1,IEt=1,Cdc20t=1,Xt=1
@ YP=M, TOTAL=300, DT=0.1, METH=stiff, XHI=300, YLO=0, YHI=1, BOUND=1000
done
```

9.2.2 Ime2_Clb1P.ode

```
init Clb1=0,Clb1P=0, CKIA=1, Cdc20A=0, X=0.99999, XP=0, Y=1,
Clb1' = ksclb1+kdpclb1*Clb1P/(Jdpclb1+Clb1P)-
    (kdclb1+kdclb1CKI*CKIA+kdclb1c20*Cdc20A+kpclb1x*(Xt-X)/(Jpclb1+Clb1))*Clb1
Clb1P' = kpclb1x*(Xt-X)*Clb1/(Jpclb1+Clb1)-
    (kdclb1+kdclb1CKI*CKIA+kdclb1c20*Cdc20A+kdpclb1/(Jdpclb1+Clb1P))*Clb1P
CKIA' = (kaCKI+kaCKIc20*Cdc20A)*(CKIt-CKIA)/(JaCKI+CKIt-CKIA)-
    (kiCKIx*(X+XP)+kiCKIclb*Clb1P)*CKIA/(JiCKI+CKIA)
Cdc20A' = ka20clb1p*Clb1P*(Cdc20t-Cdc20A)/(Jacdc20+Cdc20t-Cdc20A)-
    kicdc20*Cdc20A/(Jicdc20+Cdc20A)
X' = kdpxpy*Y*(XP)/(Jdpxp+XP)-kpxclb1*(Clb1+Clb1P)*X/(Jpx+X)
XP' = kpxclb1*(Clb1+Clb1P)*X/(Jpx+X)+kdpxp2y*Y*(Xt-(X+XP))/(Jdpxp2+(Xt-(X+XP)))-
    (kdpxpy*Y/(Jdpxp+XP)+kpxpclb1*(Clb1+Clb1P)/(Jpxp+XP))*XP
Y' = -kdycdc20*Cdc20A*Y
p ksclb1=0.015, kdclb1=0.001, kdclb1CKI=0.1, kdclb1c20=0.1,
p kdpclb1=0.5, Jdpclb1=0.01, kpclb1x=0.7, Jpclb1=0.01,
p kaCKI=0.8, kaCKIc20=2, kiCKIx=20, kiCKIclb=3, JaCKI=0.04, JiCKI=0.04,
p ka20clb1p=0.25, kicdc20=0.1, Jacdc20=0.001,Jicdc20=0.001,
p kpxclb1=0.1, Jpx=0.04, kdpxpy=0.05, Jdpxp=0.04,
p kpxpclb1=0.2, Jpxp=0.04, kdpxp2y=3.5, Jdpxp2=0.04,
p kdycdc20=0.2
p CKIt=1, Cdc20t=1, Xt=1
@ YP=M, TOTAL=300, DT=0.1, METH=stiff, XHI=300, YLO=0, YHI=1, BOUND=1000
done
```

9.2.3 AutoClb1P_Model.ode

```
 init Clb1=0, Clb1P=0, CKIA=1, Cdc20A=0, X=1, Y=1
Clb1' = ksclb1+kdpclb1p*Clb1P/(Jdpclb1p+CLb1P)-
    (kdclb1+kdclb1CKI*CKIA+kdclb1c20*Cdc20A+(kpclb1+kpclbclb1*Clb1P)/(Jpclb1+Clb1)
    )*Clb1
Clb1P' = (kpclb1+kpclbclb1*Clb1P)*Clb1/(Jpclb1+Clb1)-
    (kdclb1+kdclb1CKI*CKIA+kdclb1c20*Cdc20A+kdpclb1p)/(Jdpclb1p+Clb1P)*Clb1P
CKIA' = (kaCKI+kaCKIc20*Cdc20A)*(CKIt-CKIA)/(JaCKI+CKIt-CKIA)-
    (kiCKIx*X+kiCKIclb*Clb1P)*CKIA/(JiCKI+CKIA)
Cdc20A' = ka20clb1p*Clb1P*(Cdc20t-Cdc20A)/(Jacdc20+Cdc20t-Cdc20A)-
    kicdc20*Cdc20A/(Jicdc20+Cdc20A)
X' = -kpxclb1*Clb1P*X/(Jpx+X)+kdpxy*Y*(Xt-X)/(Jdpx+Xt-X)
Y' = -kdycdc20*Cdc20A*Y
p ksclb1=0.015, kdclb1=0.005, kdclb1CKI=0.08, kdclb1c20=0.08,
p kdpclb1p=0.01, jdpclb1p=0.01, kpclb1=0.01, kpclbclb1=0.08, jpclb1=0.01,
p kaCKI=0.4, kaCKIc20=0.1, kiCKIx=6, kiCKIclb=0.2, JaCKI=0.01, JiCKI=0.01,
p ka20clb1p=0.5, kicdc20=0.2, Jacdc20=0.001, Jicdc20=0.001,
p kpxclb1=0.07, Jpx=0.04, kdpxy=0.1, Jdpx=0.04,
p kdycdc20=0.8,
p CKIt=1,Cdc20t=1, Xt=1,
@ YP=M, TOTAL=300, DT=0.1, METH=stiff, XHI=300, YLO=0, YHI=1, BOUND=1000
done
```

9.2.4 AltKClb1P_Model.ode

```
init Clb1=0, Clb1P=0, Cdh1A=1, Cdc20A=0, X=1, Y=1, ZP=0
Clb1' = ksclb1+kdpclb1p*Clb1P/(Jdpclb1p+CLb1P)-
    (kdclb1+kdclb1dh1*Cdh1A+kdclb1c20*Cdc20A+kpclb1zp*ZP/(Jpclb1+Clb1))*Clb1
Clb1P' = kpclb1zp*ZP*Clb1/(Jpclb1+Clb1)-
    (kdclb1+kdclb1dh1*Cdh1A+kdclb1c20*Cdc20A+kdpclb1p/(Jdpclb1p+Clb1P))*Clb1P
Cdh1A' = (kacdh1+kacdh1c20*Cdc20A)*(Cdh1t-Cdh1A)/(Jacdh1+Cdh1t-Cdh1A)-
    (kicdh1x*X+kicdh1clb*Clb1P)*Cdh1A/(Jicdh1+Cdh1A)
```

```
Cdc20A'          =          ka20clb1p*Clb1P*(Cdc20t-Cdc20A)/(Jacdc20+Cdc20t-Cdc20A)-
        kicdc20*Cdc20A/(Jicdc20+Cdc20A)
X'  = -kpxclb1*Clb1P*X/(Jpx+X)+kdpxy*Y*(Xt-X)/(Jdpx+Xt-X)
Y'  = -kdycdc20*Cdc20A*Y
ZP'  = (kpz+kpzclb1*Clb1P)*(Zt-ZP)/(Jpz+(Zt-ZP))-kdpz*ZP/Jdpz*ZP
p ksclb1=0.01, kdclb1=0.005, kdclb1dh1=0.1, kdclb1c20=0.06
p kdpclb1p=0.12, jdpclb1p=0.01, kpclb1zp=0.8, jpclb1=0.01
p kacdh1=0.3, kacdh1c20=0.8, kicdh1x=10, kicdh1clb=4.4, Jacdh1=0.04, Jicdh1=0.04
p ka20clb1p=0.5, kicdc20=0.12, Jacdc20=0.001, Jicdc20=0.001
p kpxclb1=0.2, Jpx=0.04, kdpxy=0.1, Jdpx=0.04
p kdycdc20=0.1,
p kpz=0.02, kpzclb1=0.15, Jpz=0.04, kdpz=0.06, Jdpz=0.04,
p cdh1t=1, Cdc20t=1, Xt=1, Zt=1
@ YP=M, TOTAL=300, DT=0.1, METH=stiff, XHI=300, YLO=0, YHI=1, BOUND=1000
done
```

9.2.5 Degradation_Model.ode

```
init Clb1=0, Clb1P=0, CKIA=1, IEa=0, Cdc20A=0, X=1, Y=1
Clb1'          =          ksclb1+kdpclb1p*Clb1P/(Jdpclb1p+CLb1P)-
        (kdclb1+kdclb1c20*Cdc20A+kdclb1CKI*CKIA+(kpclby*Y)/(Jpclb1+Clb1))*Clb1
Clb1P'          =          (kpclby*Y)*Clb1/(Jpclb1+Clb1)-
        (kdclb1+kdclb1c20*Cdc20A+kdpclb1p/(Jdpclb1p+Clb1P))*Clb1P
CKIA'          =          (kaCKI+kaCKIc20*Cdc20A)*(CKIt-CKIA)/(JaCKI+CKIt-CKIA)-
        (kiCKIx*X+kiCKIclb*(Clb1P+Clb1))*CKIA/(JiCKI+CKIA)
IEa' = kaieclb1*(IEt-IEa)*(Clb1+Clb1P)/(Jaie+IEt-IEa)-kiie*IEa/(Jiie+IEa)
Cdc20A'          =          kacdc20ie*IEa*(Cdc20t-Cdc20A)/(Jacdc20+Cdc20t-Cdc20A)-
        kicdc20*Cdc20A/(Jicdc20+Cdc20A)
X'  = -kpx*(Clb1+Clb1P)*X/(Jpx+X)
Y'  = -kdycdc20*Cdc20A*Y
p ksclb1=0.01, kdclb1=0.005, kdclb1CKI=1, kdclb1c20=0.15,
p kdpclb1p=0.01, jdpclb1p=0.04, kpclby=0.7, Jpclb1=0.04,
p kaCKI=0.5, kaCKIc20=0.5, kiCKIx=2, kiCKIclb=15, JaCKI=0.04, JiCKI=0.04,
p kacdc20ie=1,kicdc20=0.5,Jacdc20=0.001,Jicdc20=0.001
p kaieclb1=0.1,kiie=0.02, Jaie=0.01, Jiie=0.01
p kpx=0.2, Jpx=0.04, kdpxy=0.1, Jdpx=0.04,
p kdycdc20=0.2,
p CKIt=1, IEt=1, Cdc20t=1, Xt=1,
@ YP=M, TOTAL=300, DT=0.1, METH=stiff, XHI=300, YLO=0, YHI=1, BOUND=1000
done
```

9.2.6 Degradation_FEAR.ode

```
init Clb1=0, CKIA=1, IEa=0, Cdc20A=0, Cdc14n=0, Cdc14c=0, X=1, Y=1
Clb1'     = ksclb1 - (kdclb1+kdclb1CKI*CKIA+kdclb1c20*Cdc20A)*Clb1
CKIA'          =          (kaCKI+kaCKIc14*Cdc14c)*(CKIt-CKIA)/(JaCKI+CKIt-CKIA)-
        (kiCKIx*X+kiCKIclb*Clb1)*CKIA/(JiCKI+CKIA)
IEa'      = kaieclb1*(IEt-IEa)*Clb1/(Jaie+IEt-IEa)-kiie*IEa/(Jiie+IEa)
Cdc20A'          =          kacdc20ie*IEa*(Cdc20t-Cdc20A)/(Jacdc20+Cdc20t-Cdc20A)-
        kicdc20*Cdc20A/(Jicdc20+Cdc20A)
Cdc14n'=(kaCdc14n+kaC14nC20*Cdc20A)*(Cdc14t-Cdc14n-Cdc14c)/(JaCdc14n+(Cdc14t-
        Cdc14n-Cdc14c))+(kiCdc14+kiCdc14Y*Y)*Cdc14c-
        (kiCdc14n/(JiCdc14n+Cdc14n)+kaCdc14c)*Cdc14n
Cdc14c' = kaCdc14c*Cdc14n - (kiCdc14 + kiCdc14Y*Y)*Cdc14c
X'        = -kpx*Clb1*X/(Jpx+X)
Y'        = -kdy*Cdc20A*Y
p ksclb1=0.01,kdclb1=0.01,kdclb1CKI=1,kdclb1c20=0.2,
p kaCKI=0.03,kaCKIc14=0.5,JaCKI=0.001, kiCKIx=2,kiCKIclb=2,JiCKI=0.001
p kaieclb1=0.1,Jaie=0.01,kiie=0.02,Jiie=0.01,
p kacdc20ie=1,Jacdc20=0.001,kicdc20=0.5,Jicdc20=0.001,
```

```
p kaCdc14n=0.01,kaC14nC20=1,JaCdc14n=0.01,kiCdc14=0.1,
p kiCdc14Y=4,kiCdc14n=1,JiCdc14n=0.1,kaCdc14c=0.1,
p kpx=0.2,Jpx=0.04,kdpx=0.1,Jdpx=0.04,
p kdy=0.12,
p CKIt=1, IEt=1, Cdc20t=1, Cdc14t=0.5, Xt=1,
@ YP=M, TOTAL=300, DT=0.1, METH=stiff, XHI=300, YLO=0, YHI=1, BOUND=1000
done
```

9.2.7 Location_Model.ode

```
init Clb1Cyt=0, Clb1Nuc=0, CKIA=1, IEa=0, Cdc20A=0, Cdc14n=0, Cdc14c=0, X=1, Y=1, Cdc5A=0,
Clb1Cyt' = ksclb1+kdpclb1p*Clb1Nuc-
        (kdclb1+kdclb1c20*Cdc20A+kdclb1CKI*CKIA+kpclb1)*Clb1Cyt
Clb1Nuc' = (kpclb1)*Clb1Cyt-(kdclb1+kdclb1c20*Cdc20A+kdclb1CKI*CKIA+kdpclb1p)*Clb1Nuc
CKIA' = (kaCKI+kaCKIc14*Cdc14c)*(CKIt-CKIA)/(JaCKI+CKIt-CKIA)-
        (kiCKIx*X+kiCKIclb*(Clb1Cyt+Clb1Nuc))*CKIA/(JiCKI+CKIA)
IEa' = kaieclb1*(IEt-IEa)*Clb1Nuc/(Jaie+IEt-IEa)-kiie*IEa/(Jiie+IEa)
Cdc20A' = kacdc20ie*IEa*(Cdc20t-Cdc20A)/(Jacdc20+Cdc20t-Cdc20A)-
        kicdc20*Cdc20A/(Jicdc20+Cdc20A)
Cdc14n'=(kaCdc14n+kaC14nC20*Cdc20A+kaC14nC5*Cdc5A+kaC14Clb1*Clb1Nuc)*(Cdc14t-
        Cdc14n-Cdc14c)/(JaCdc14n+(Cdc14t-Cdc14n-
        Cdc14c))+(kimpCdc14+kimpC14Y*Y)*Cdc14c-
        (kiCdc14/(JiCdc14n+Cdc14n)+kexpC14n)*Cdc14n
Cdc14c' = kexpC14n*Cdc14n -(kimpCdc14+kimpC14Y*Y)*Cdc14c
Cdc5A' = kpc5cb1*(Clb1Nuc)*(Cdc5t-Cdc5A)/(Jpcdc5+(Cdc5t-Cdc5A))-
        kdpcdc5*Cdc5A/Jdpcdc5*Cdc5A
X' = -kpx*Clb1Nuc*X/(Jpx+X)
Y' = -kdy*Cdc20A*Y
p ksclb1=0.01,kdclb1=0.01,kdclb1c20=0.5,kdclb1CKI=0.8,kpclb1=0.1,kdpclb1p=0.01,
p kaCKI=0.08,kaCKIc14=0.3,kiCKIx=2,kiCKIclb=4,JaCKI=0.001,JiCKI=0.001,
p kaieclb1=0.1,Jaie=0.01,kiie=0.015,Jiie=0.01,
p kacdc20ie=1,Jacdc20=0.01,kicdc20=0.5,Jicdc20=0.001,
p kaCdc14n=0.01, kaC14nC20=0.6, kaC14nC5=0.6, kaC14Clb1=0.6, JaCdc14n=0.01,
p kimpCdc14=0.1, kimpC14Y=5,kiCdc14=0.5, JiCdc14n=0.001,kexpC14n=0.4
p kpc5cb1=1,Jpcdc5=0.01, kdpcdc5=0.1,Jdpcdc5=0.01,
p kpx=0.2,Jpx=0.04,
p kdy=0.2,
p CKIt=1, IEt=1, Cdc20t=1, Cdc14t=0.5, Xt=1,Cdc5t=1,
@ YP=M, TOTAL=300, DT=0.1, METH=stiff, XHI=300, YLO=0, YHI=1, BOUND=1000
done
```

9.3 Synchronised Sporulation

9.3.1 Synchronous sporulation protocol

The effects of mutations on meiotic progression can be detected more effectively using synchronous meiotic cultures. To optimise protocol for synchronous meiosis protocol, a number of sporulation protocols were considered. Figure 9-5 tracks the nuclear divisions of uninduced P_{GPD1}*GAL4-ER* P_{GAL}*cdc15-7A-HA*$_3$ cells undergoing meiosis after preparation by the three different methods detailed in 2.2.1.2.

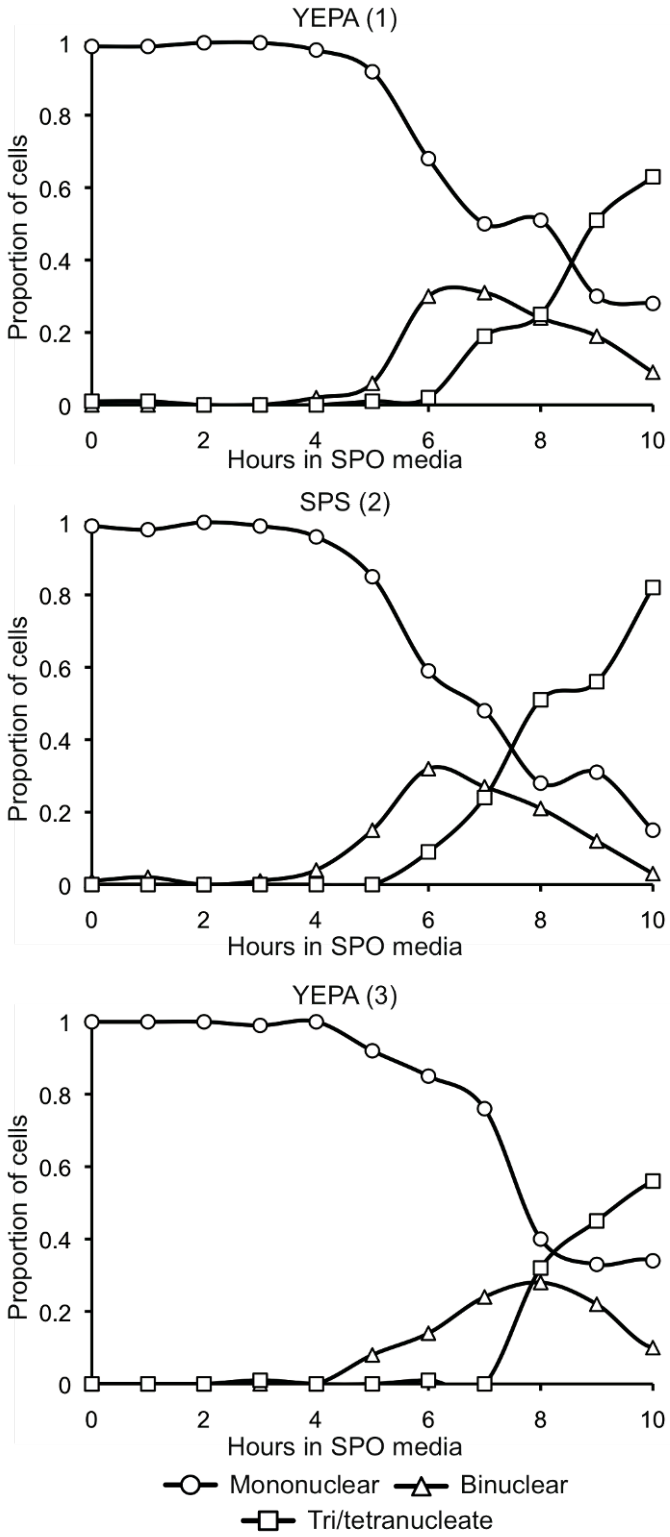

Figure 9-5 ***Sporulation methods.*** *Cultures of P_{GPD1}GAL4-ER P_{GAL}cdc15-7A-HA_3 cultures were induced to undergo meiosis by resuspension in SPO media, under the three sporulation protocols used throughout this work (with no addition of estradiol). Samples were taken for in situ immunofluorescence hourly and nuclear division was scored by DAPI staining.*

Initially, we used YEPA(1) (Padmore et al., 1991), which could result in high sporulation efficiency, and was fairly synchronous (Figure 9-5). This

method was used for the initial live cell imaging cultures, for the Cdc15-7A-HA_3 expression and for the Cdc14 mutant time courses in this chapter. However, YEPA(1) was unreliable, sometimes resulting in sporulation efficiencies as low as 30%. In addition, using this method, cells were sometimes found to have sporulated early, forming completed tetrads by 6 hours into sporulation media. YEPA(1) includes an early step to streak out the cells on glycerol media. This step removes respiration-incompetent cells, which can't sporulate. However, we found better results and avoided early sporulation using YEPA(3) which omitted this step, and had a shorter duration of incubation in YEPA media before resuspension. An SPS-grown method was also considered. However, YEPA(3) provided a consistent method to induce meiosis and was used to prepare cells for meiosis in chapters 0 and 0.

9.3.2 Synchrony by induction

All three methods produced a degree of synchrony: the majority of cells were in G1 after slow growth in less optimal media. Slow growth extends the G1 phase and delays START. However, cell size variation led to asynchrony (Nachman et al., 2007).

An alternative protocol for synchronous meiosis involves arrest in prophase I followed by induction of Ndt80 to trigger exit from prophase (Carlile and Amon, 2008). Most variability in entering meiosis, from cell size, takes effect in the timing of meiotic entry (Nachman et al., 2007). Therefore, cells in which *NDT80* is induced should undergo meiosis in a highly synchronised fashion.

Initially we used P_{GAL}-*NDT80* P_{GPD1}*GAL4-ER* bearing strains (Figure 9-6). This was compared with a wild type strain undergoing meiosis. Both strains were induced to enter meiosis by resuspension in sporulation media, then estradiol was added at 6 hours into meiosis, when most cells should have arrested in prophase in the P_{GAL}-*NDT80* P_{GPD1}*GAL4-ER* strain.

In comparison to the wild type strain, the P_{GAL}-*NDT80* P_{GPD1}*GAL4-ER* strain underwent meiosis in a more synchronised fashion, with a distinct peak in binucleates and steeper increase in tetranucleates. However we did not see the level of synchrony in the original report (Carlile and Amon, 2008).

The P_{GAL}-*NDT80* P_{GPD1}*GAL4-ER* system was used to synchronise the cells used in live cell imaging below (Figure 9-9).

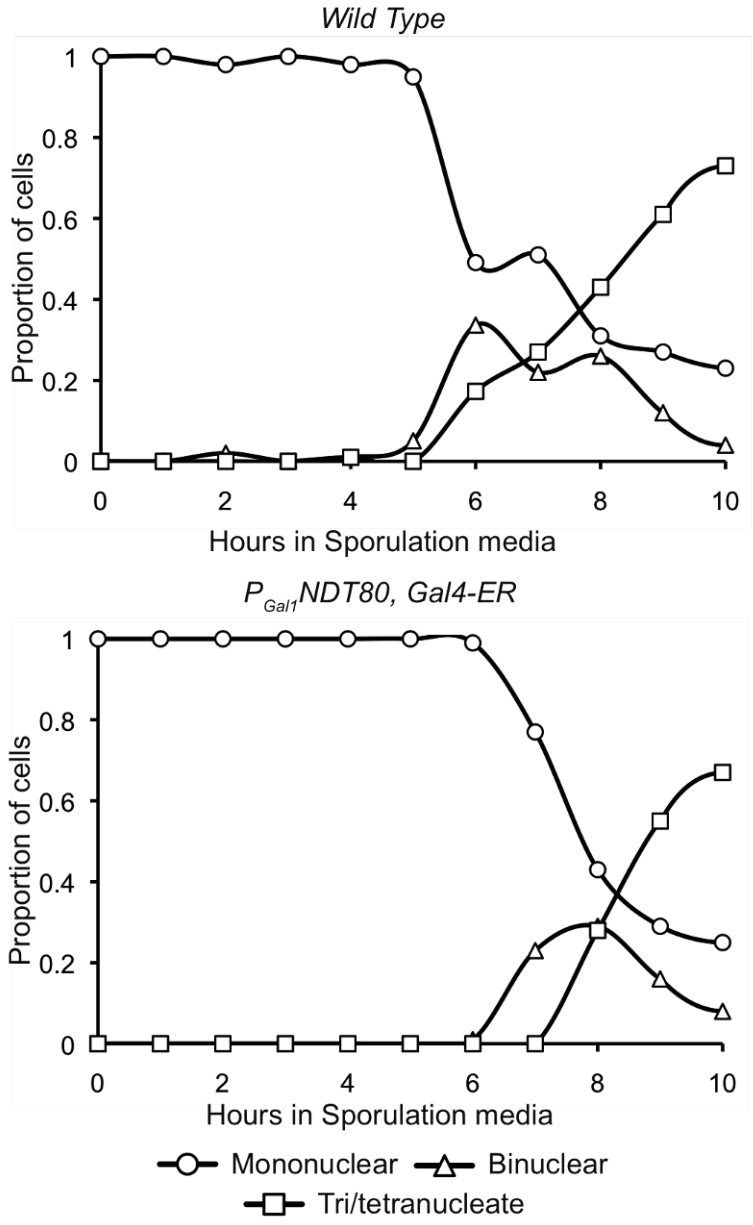

Figure 9-6 ***Synchronous meiosis using arrest and release.*** *Cultures of wild type and* P_{GAL}*NDT80* P_{GPD1}*GAL4-ER cells were induced to undergo meiosis by resuspension in SPO media, induced with estradiol at 6 hours. Samples were taken for in situ immunofluorescence hourly and nuclear division was scored by DAPI staining.*

The P_{GPD1}*GAL4-ER* plus P_{GAL} combination is useful to induce expression in meiosis as P_{GAL} and galactose alone would disrupt meiosis. This was why the same combination of P_{GAL} and P_{GPD1}GAL4-ER was used for Cdc15-7A-HA_3 expression and Cdc14-Tab6 expression. However this would mean we could only use estradiol to induce these proteins during prophase in synchronised cultures.

In anticipation of the need to induce proteins at other stages than prophase in synchronised cultures, we tried a P_{CUP1}-*NDT80* system, inducible by copper expression. This system was not used for this purpose as Cdc15-7A-HA_3 and Cdc14Tab6 results were unfavourable. The P_{CUP}-*NDT80* strain was used as a prophase-arrested strain in Section 4.4.6.3.

The P_{CUP}-*NDT80* strain was compared with the P_{GAL}-*NDT80*,P_{GPD1}*GAL4-ER* strain in Figure 9-7.

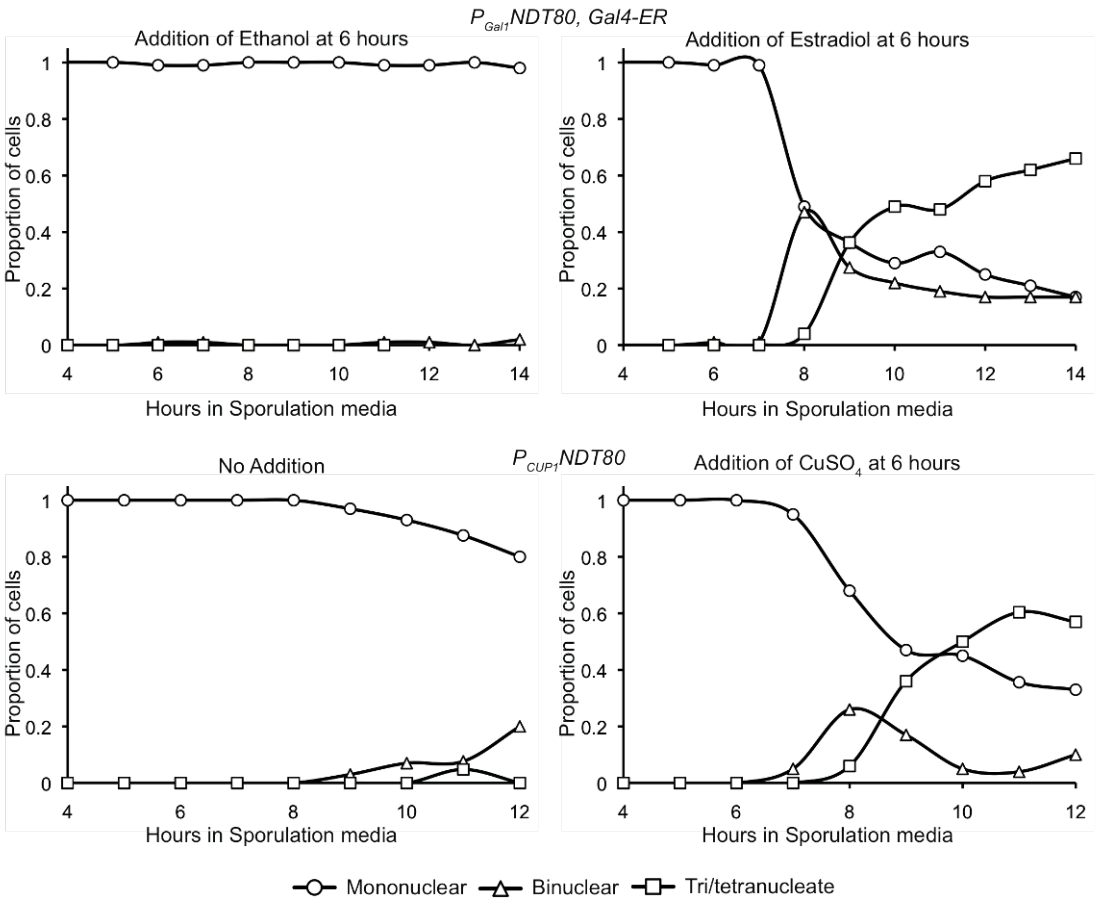

Figure 9-7 ***Synchronous meiosis by arrest and release.*** *Cultures of P_{GAL}-NDT80,P_{GPD1}GAL4-ER and P_{CUP}NDT80 cells were induced to undergo meiosis by resuspension in SPO media. Cultures were induced as described at 6 hours. Samples were taken for in situ immunofluorescence hourly and nuclear division was scored by DAPI staining.*

The P_{GAL}-*NDT80* P_{GPD1}*GAL4-ER* system achieved a higher level of synchrony in this experiment compared to the last (Figure 9-6). Despite both being induced at 6 hours, it seemed more cells were arrested at prophase at this point in the second example, than in the first. This could indicate that slightly later induction would improve synchrony with this system, as day-to-day variation could lead to slower-running cultures not being fully arrested by 6 hours.

The P_{CUP}-*NDT80* system resulted in a similar sporulation efficiency, and synchrony, as the earlier P_{GAL}-*NDT80* P_{GPD1}*GAL4-ER* experiment. However, the uninduced culture showed some low levels of binucleates and even tetranucleates at later time points, indicating slightly leaky expression from the CUP1 promoter during meiosis. This leaky expression was also indicated by results in Section 4.4.6.3.

9.3.3 cdc14-PS1,2E and cdc14-BP1,3A

White attempting to induce increased Cdc14 release during meiosis (Section 6.2), we also considered two further Cdc14 mutants in which a) phosphorylation sites near basic patches on Cdc14 were mutated to be phosphomimetic (*cdc14-PS1,2E*), b) the basic patches that comprise the nuclear localisation sequence were mutated (*cdc14-BP1,3A*) (Mohl et al., 2009). Cdc14 phosphorylation, by Cdc15, leads to released Cdc14 being exported from the nucleus and allowed access to cytoplasmic substrates. *cdc14-PS1,2E* and *cdc14-BP1,3A* cause increased export of Cdc14-GFP to the cytoplasm (Mohl et al., 2009). These mutants, therefore, imitate the effect of MEN on Cdc14 and should compensate for an inability to activate MEN. The *cdc14-PS1,2E* and *cdc14-BP1,3A* alleles tagged with GFP were donated by Professor R. Deshaies (Mohl et al., 2009). The *cdc14-PS1,2E* and *cdc14-BP1,3A* alleles were inserted in the *his3* locus and crossed with a strain in which the endogenous *CDC14* sequence was placed under the control of the *CLB2* promoter, to inhibit its expression in meiosis. This was to ensure that only the mutant Cdc14 proteins were present in meiosis. Neither mutation caused an appreciable difference in the sporulation efficiency of the strain (Figure 9-8).

The lack of effect may suggest that cytoplasmic inhibitors, such as Cdh1, are effectively inhibited by Ime2 alone. Ime2 phosphorylation is not removed by Cdc14 (Holt et al., 2007) and Ime2 is known to phosphorylate some of the same targets as CDK (Bolte et al., 2002; Clifford et al., 2004; Sedgwick et al., 2006), although not always to the same effect (Sedgwick et al., 2006). Alternatively, the inhibitors may be prevented from becoming active by another factor that is resistant to Cdc14 release. These strains were not followed through time courses due to the lack of effect on sporulation efficiency.

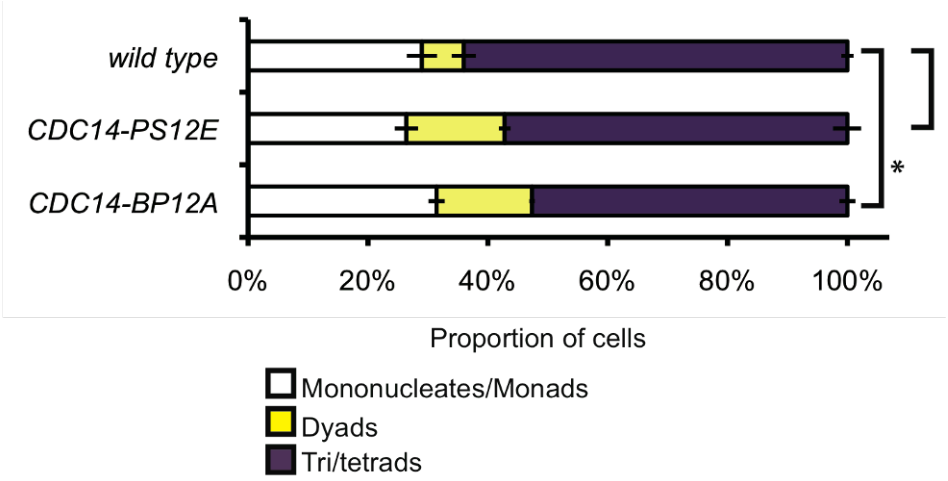

Figure 9-8 ***Sporulation efficiency in mutants bearing Cdc14 localisation mutants:*** *Cells bearing the two mutant cdc14 alleles or the wild type allele were allowed to sporulate on SpoVB plates at 30˚C for 48 hours. Percentage of cells forming dyads, tetrads and mononucleate cells were calculated. Three sets of 100 cells were counted for each strain. Asterisks show significance calculated using Mann Whitney U test. (* p<0.05, ** p<0.01, ***p<0.001)*

9.4 Live Cell Imaging

Single cell studies would be useful in assessing the effects of mutants. Live cell imaging requires tagging proteins with fluorescent tags, then following sporulating cells through meiosis on a slide. Images were taken at regular time points through meiosis. The live cell imaging protocol must be optimised with respect to light exposure, temperature, oxygen availability and other environmental factors in order to maximise the sporulation efficiency and the information available.

Considerations in optimising the protocol for light cell imaging:

- Cells will inevitably undergo a less successful meiosis under live cell imaging conditions. To maximise the success, as many cells as possible must be passing through meiosis during the imaging interval. This can be achieved with a reliable protocol that gives a high level of synchrony and sporulation efficiency.
- Conditions experienced by the cells on the slide must remain as close as possible to the optimum for meiosis, ideally at 30˚C, in well-aerated sporulation media.

- Light exposure is a major consideration due to the sensitivity of meiotic cells. Also, as meiosis is a long process, cumulative exposure can lead to bleaching of the fluorescent tags and loss of information. Exposure can be minimised by increasing intervals between steps, reducing the number of z steps required, decreasing the duration of each exposure, and using filters. However, each of these steps leads to a loss of information, so a compromise must be reached.

9.4.1 Live cell imaging optimisation

Live cell imaging was undertaken using an adapted method (Matos et al., 2008). The cells were prepared using the YEPA(1) protocol. Sporulating cells were taken at 3.5 hours, or after induction for inducible strains, and set on MatTek glass-bottomed dishes prepared with Concanavalin-A. Media requirements were met by the addition of a small amount of sporulation media to the dish. Aeration was assumed sufficient due to the shallow media. The dish was placed on the microscope stage, which was kept at 30˚C for the duration. This could potentially have lead to evaporation from the small amount of media - however, after 6 hours, the slide was not observed to have dried out.

During each attempt at live cell imaging, an extra slide was prepared and placed in a 30˚C incubator to mimic the microscope conditions without the light stress, while the culture was returned to the incubator to complete sporulation. In this way, the effect of light stress, and the stress of the other conditions on the slide, could be separated.

The following methods were undertaken to minimise cell damage:

- To minimise exposure, intervals between time points were increased to 10 minutes rather than 5, leading to a total of 37 time points over 6 hours.
- Exposure times were reduced to 300ms in both wavelengths (FITC and Cy3) at 10 minute intervals.
- Neutral density filters were added to the laser to reduce the intensity of the light exposure.
- Inducible strains were used to improve synchrony and increase the number of cells undergoing meiosis in the field of view.

After multiple attempts, cells were observed to undertake meiosis in the field of view (Figure 9-9).

Three cells successfully underwent meiosis out of the 22 in the field of view, a proportion of ~14%. However, the quality of the images deteriorated throughout the process. Due to the poor quality of the images and low sporulation efficiency, these results were not considered for follow up. Mutations that disrupt the process of meiosis would further lower successful sporulation and result in time-consuming experiments with little or no data.

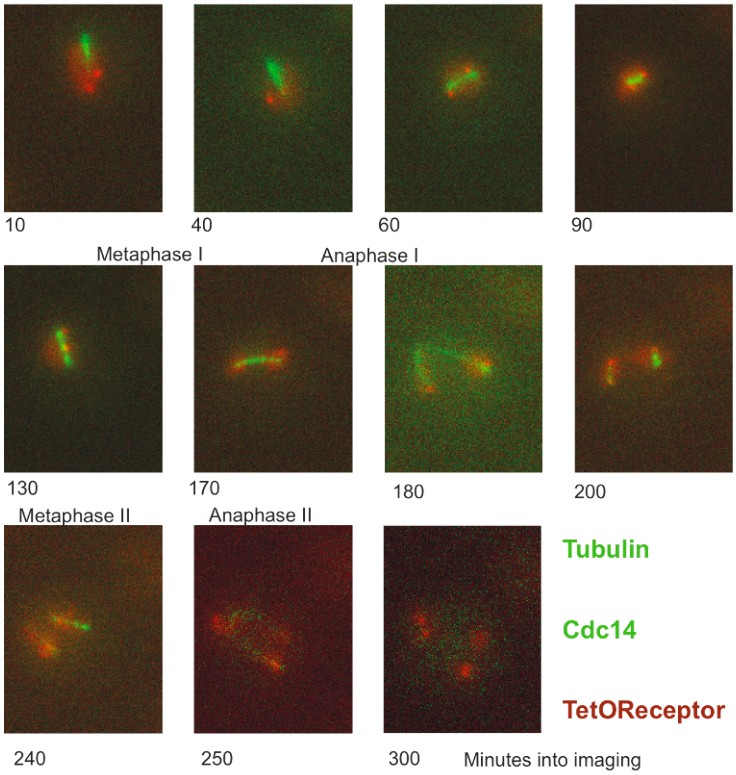

Figure 9-9 ***Live cell imaging of meiosis*** *A culture of P_{GAL}NDT80 GAL4ER TUB1-GFP CDC14-GFP tetR-Tomato tetOx cells were induced to enter meiosis by resuspension in SPO media. The culture was induced at 6 hours into SPO media and the cells were taken after induction for preparation and viewing.*

For successful live-cell imaging, more success could have been achieved with a flow cell to maintain greater control of the conditions under the microscope. The above experiment used YEPA(1) method. A more reliable sporulation protocol, such as that used in Chapters 3 and 5, may have permitted greater success. In the above case, relatively poor sporulation (39%) was seen in cultures in the shaker as well as in the microscope dish outside of the microscope (36%). However, the difference between the dish under the light and

the dish kept in the dark clearly suggests the exposure the light is causing the low sporulation.

9.5 List of primers

ID	Sequence 5-3	Use
KT7	GAGACCGAGTTAGGGACAGTTAGA	check insertion at *TRP1*, upstream
KT8	AAAAACTTGATTAGGGTGATGGTTC	check insertion of *CDC15* downstream
KT9	TTCGGTGATGACGGTGAAAACCTCT	check insertion of *CDC15* upstream
KT10	GTCATTGTAGCGTATGCGCCTGTG	check insertion at *TRP1* downstream
KT11	CAAGGTGTAGTGGCTATAAAGACAATG	*IME2*, upstream, for sequencing
KT12	ACAAAGGGCCAAATTATTACGAATTT	*IME2* sequence, downstream for sequencing
KT13	TTTGACAGTGTTATCAGCACTCAGC	Forward inside *CDC15*
KT14	GTAATACGCTTAACTGCTCATTGCT	Reverse in Gal promoter
KT15	GTAGGAGTGTATACCTCGAC	*CDC14* check near start
KT16	CGTTGGCCCTCAACAGCATTG	*CDC14* check middle and end
KT17	CCCTTTCTCGGCTGACCAG	*CDC14* check middle
KT18	CTTCATCGTCCCGAATGGAA	*CDC14* check sequence near end
KT19	TGTTCCCTCCACCAAAGGTG	insertion at *HIS3*, genome, pair with 3' (PA189 or 190)
KT20	GAAGGTAAGGAAAAATGGATATGATATTATGACATT GCATGAGTCCATGGAAAAGAGAAG	TAP tagging *CLB1* gene: *CLB1* seq – tag, pl155
KT21	TTGGTTTTCTGTGTAGGCTAGCACCTTCACTCATGCA ATGTCATACGACTCACTATAGGG	TAP tagging *CLB1* gene rc of tag - genome after *CLB1*
KT22	CAGTCTAGGACGTTAGCGAAGTTCCTAATG	checking insertion Start (inside *CLB1* gene forward)– ~640bp product
KT23	GGGTCATCTTTTAAACTTTGGATGAAGGCG	checking insertion Start (inside TAP) ~640bp product
KT24	CTATTATACAAAAATAAAGAATAAAGGATTTG	checking insertion End (inside TAP)– ~640bp product
KT25	CGTTTAAGGATTTTATCAGTGAACTAGTTG	checking insertion End (after *CLB1* gene sequence)– ~640bp product
KT26	CCCGTTTGCCAATTACTGATGGATTATC	Forward primer *CLB1* - 200bp upstream of stop
KT27	GCCATTAATATGTTACCAAATGCG	binds to *TRP1*, amplify TAP tag fusion (pair w fwd)
KT31	TGCTCTACAAGAGTTGATATTGGTGCTGCTGCTGCGG AATCTTCTCTCAT	Ala mutation of *CLB1* nls
KT32	CTCTTGTAGAGCAGGATGACCAGGCAGCATTCGCACT CCATGAATTGACT	Ala mutation of *CLB1* nls
KT33	GTGGACTTCAAGTTCATCGGGATATTACCGTCATTAT GTG	300bp upstream of *CLB1* stop
KT34	AAGTAAGGAAGTGAGATTTTGGTTTTCTGTGTAGGC TAGCACCTTCAATCGATGAATTCGAGCTCG	downstream utr of CL*B1* + tag end
KT35	GAAAAGTTGGTGCCGCCGCCCCTAAGAAGAAGCGTAA GGTCGGCCGTACGCTGCAGGTCGAC	Cterm of *CLB1-NLS-NLS*-start of tag

KT36	GGGGCGGCGGCACCAACTTTTCTTTTTTTTTTTGGAG CAGCAGCCTCATGCAATGTCATAATAT	Cterm of *CLB1-NLS-NLS*-start of tag
KT39	CTGGTTTGGATATTGCCGCCGCCCTAGCTCTAAAGCT AGCCGGCCTAGACATCCGTACGCTGCAGGTCGAC	Cterm of *CLB1-NES-NES*-start of tag
KT40	CTAGGGCGGCGGCAATATCCAAACCAGCCAATTTCAA AGCCAAAGCAGCAGCCTCATGCAATGTCATAATAT	Cterm of *CLB1-NES-NES*-start of tag
KT43	ATTTTCGTCCGTTATATCAACCATCAAAGCGGATCCC CGGGTTAATTAA	Upstream of *CLB1* sequence – marker sequence
KT44	TGATAAAGTAAGGAAGTGAGATTTTGGTTGATTCGA GCTCGTTTAAAC	Marker sequence - Downstream of *CLB1* sequence RC
KT45	TTACATTCGGCCAAACTTGAGCAGGCTGCA	Check primer 200bp upstream of *CLB1*
KT46	CAAATTTTTCGCGTTTGAAAATTTATGC	300bp upstream of *SCC1*, in promoter
KT47	CCTCTTGTTTTGATTAATGAAGGTGGTG	200bp downstream of start in *CDC5*
KT48	GATATGATATTATGACATTGCATGAGCGTACGCTGCA GGTCGAC	final 26bp of *CLB1* and start of TAG
KT49	GTCGACCTGCAGCGTACGCTCATGCAATGTCATAATA TCATATC	rc of KT48
KT51	CTATATATACTCTCTTTCATTCATCGATAAACGTTAC ATTTGTTATTCATAGGAATTCGAGCTCGTTTAAAC	promoter replacement for *CDC5*, p*CLB2*, 50bp upstream of *CDC5* plus end of tag
KT53	GAACGGGTATTCAATTGCTTATCATTGATAGCTTTAA GAGGACCCAACGACATGCACTGAGCAGCGTAATCTG	promoter replacement for *CDC5, pCLB2*. first 50 bp of ORF rc, then end of tag (CATG-)
KT54	GCTTTTTTTCCTATTTTTTCATCCTTCAATTTTGTGG CATATAC	Check primer 200bp upstream of *CDC5*
KT55	GTGCAGCTGTTTAGATCACAAAAGCGTAATTAAGAA TAAGATCTACCAACGAATTCGAGCTCGTTTAAAC	promoter replacement for *CLB1,* pgal. 50bp from upstream of *CLB1* plus end of tag (GAAT-)
KT56	CTTCATTACTATTAATGGTTCTACTATTCTCTACCAA AAGGGATCGTGACATGCACTGAGCAGCGTAATCTG	promoter replacement for *CLB1*, pgel. first 50 bp of ORF minus ATG, rc, then end of tag (CATG-)
KT57	CCTTATTGTTTAGTACTTCTTGTTTCACCCCCTGTCT AC	~260 downstream of ATG in *CLB1* for checking promoter
KT58	GAGAAGAAAGAACAGAGTAAGATCAAGTCGAATAAA GATGCGTACGCTGCAGGTCGAC	Replace primer of *CDC5* using Euroscarf
KT59	GGTATTCAATTGCTTATCATTGATAGCTTTAAGAGG ACCCAACGACATCGATGAATTCTCTGTCG	Replace primer of *CDC5* using Euroscarf
KT60	CGCTCAGGCGAAAAAAAACGCTATATG	3' utr of *CDC5*
PA53	GGGGTAATTAATCAGCGAAG	forward primer in the Gal promoter
PA55	CCCAGTCACGACGTTGTAAAACG	M13 forward primer
PA57	GGAAACAGCTATGACCATG	M13 reverse primer
PA99	GAAGCGGTTCTTTGATTGAGCATCTG	*CLB2* promoter forward primer
PA181	GCGGCGTTAGCACGTTGTCTGGTC	*CDC14* reverse primer after start for sequence checking
PA212	CCAAAAAAAAAAGGCCAATAGCTGCACTTGTAGAGC AGGATGACC	forward primer to mutate Ime2 site in *CLB1* alanine mutant

PA213	CCAAAAAAAAAAGGCCAATAGATGAACTTGTAGAGCAGGATGACC	forward primer to mutate Ime2 site in *CLB1* Aspartate/glutamate mutant
PA214	GGATATCATAGTCATCCGCTTTTGATATTCTCCTTAAGA	reverse primer to mutate Ime2 site in *CLB1*
PA215	TTCCACTCAAATGGAATGGCAGA	upcheck oligo in *CLB1*
PA216	CATTCGATAGAAATTATGGAAGCC	downcheck oligo in *CLB1*

Table 9-1 ***List of oligonucleotides used in this project***